GRANT NO: DAMD17-90-Z-0038

TITLE: THE MULTILEVELED REGULATION OF THE HUMAN CHOLINESTERASE GENES AND THEIR PROTEIN PRODUCTS

PRINCIPAL INVESTIGATOR: Hermona Soreq, Ph.D.

CONTRACTING ORGANIZATION: The Life Sciences Institute
Department of Biological Chemistry
The Hebrew University of Jerusalem
Jerusalem, Israel 91904

REPORT DATE: September 30, 1993

TYPE OF REPORT: Final Report

PREPARED FOR: U.S. Army Medical Research, Development, Acquisition, and Logistics Command (Provisional), ATTN: SGRD-RMI-S
Fort Detrick, Frederick, MD 21702-5012

DISTRIBUTION STATEMENT: Approved for public release; distribution unlimited

DISCLAIMER NOTICE

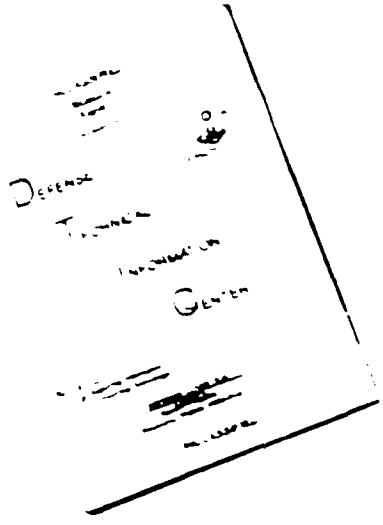

THIS DOCUMENT IS BEST QUALITY AVAILABLE. THE COPY FURNISHED TO DTIC CONTAINED A SIGNIFICANT NUMBER OF PAGES WHICH DO NOT REPRODUCE LEGIBLY.

SECURITY CLASSIFICATION OF THIS PAGE

REPORT DOCUMENTATION PAGE

Form Approved OMB No. 0704-0188

1a. REPORT SECURITY CLASSIFICATION Unclassified	1b. RESTRICTIVE MARKINGS
2a. SECURITY CLASSIFICATION AUTHORITY	3 DISTRIBUTION/AVAILABILITY OF REPORT Approved for public release, distribution unlimited.
2b. DECLASSIFICATION/DOWNGRADING SCHEDULE	
4. PERFORMING ORGANIZATION REPORT NUMBER(S)	5. MONITORING ORGANIZATION REPORT NUMBER(S)
6a. NAME OF PERFORMING ORGANIZATION The Hebrew University of Jerusalem 6b. OFFICE SYMBOL (If applicable)	7a. NAME OF MONITORING ORGANIZATION
6c. ADDRESS (City, State, and ZIP Code) Givat Ram Jerusalem 91904, Israel	7b. ADDRESS (City, State, and ZIP Code)
8a. NAME OF FUNDING/SPONSORING U.S. Army Medical Research, Development, Acquisition, and Logistics Command (Provisional), ATTN: SGRD-RMI-S Fort Detrick, Frederick, MD 21702-5012 8b. OFFICE SYMBOL	9. PROCUREMENT INSTRUMENT IDENTIFICATION NUMBER DAMD17-90-Z-0038 10. SOURCE OF FUNDING NUMBERS

PROGRAM ELEMENT NO.	PROJECT NO.	TASK NO.	WORK UNIT ACCESSION NO
61102A	61102BS12	AA	DA 335407

11. TITLE (Include Security Classification)
The Multileveled Regulation of Human Cholinesterase Genes and their Protein Products.

12. PERSONAL AUTHOR(S)
Hermona Soreq, Ph.D.

13a. TYPE OF REPORT	13b. TIME COVERED	14. DATE OF REPORT (Year, Month, Day)	15. PAGE COUNT
Final	FROM 7/30/90 TO _____	1993, September 30	xi + 165

16. SUPPLEMENTARY NOTATION

17. COSATI CODES			18. SUBJECT TERMS (Continue on reverse if necessary and identify by block number)
FIELD	GROUP	SUB-GROUP	Acetylcholinesterase/Butyrylcholinesterase/DNA sequencing/ alternative splicing/natural variants/Xenopus expression/ site-directed mutagenesis
06	01		
06	13		

19. ABSTRACT (Continue on reverse if necessary and identify by block number)

The human ACHE and BCHE genes encoding the acetylcholine hydrolyzing enzymes acetyl- and butyrylcholinesterase (AChE, BuChE) were molecularly cloned and their chromosomal positions determined to be 7q22 and 3q26, respectively. Several point mutations were found in these two genes and their frequency determined within ethnically distinct populations of Israeli residents. Xenopus oocyte expression studies revealed the BuChE mutations variably alter sensitivity to inhibitors, including organophosphorous poisons. The promoter controlling ACHE gene expression was characterized and shown to direct the expression of human AChE in developing myotomes from transiently transgenic Xenopus laevis embryos, where the transgenic enzyme faithfully accumulated in neuromuscular junctions. Alternative splicing in ACHEmRNA transcripts was found to lead to 3 distinct enzyme forms, 2 of which are abundant in tumors. Antisense phosphorothioate oligodeoxynucleotide-targetted destruction of ACHEmRNA in mice was found to cause transient hematopoietic alterations, notably reduced erythrocyte counts.

20. DISTRIBUTION/AVAILABILITY OF ABSTRACT	21. ABSTRACT SECURITY CLASSIFICATION
☐ UNCLASSIFIED/UNLIMITED ☒ SAME AS RPT. ☐ DTIC USERS	Unclassified

22a. NAME OF RESPONSIBLE INDIVIDUAL	22b. TELEPHONE (Include Area Code)	22c. OFFICE SYMBOL
Virginia M. Miller	(301) 619-7328	SGRD-RMI-S

DD Form 1473, JUN 86 Previous editions are obsolete. SECURITY CLASSIFICATION OF THIS PAGE

SUMMARY

Architecture of the human ACHE gene: The human ACHE gene encoding the acetylcholine-hydrolyzing enzyme acetylcholinesterase (AChE; acetylcholine acetyl hydrolase, E.C. 3.1.1.7), was found to be physically distinct from the related BCHE gene, encoding the less substrate-specific enzyme butyrylcholinesterase (BuChE, acylcholine acyl hydrolase, E.C. 3.1.1.8). Chromosomal mapping by polymerase chain reaction (PCR) amplification of genomic DNA fragments from somatic cell hybrids carrying different human chromosomes revealed that the ACHE gene resides on chromosome 7, and *in situ* hybridization demonstrated a single location at the 7q22 position for this gene. Construction and screening of complementary DNA libraries enabled the isolation of AChEcDNA, encoding the hydrophilic, brain AChE protein. To complete the 5'-end of the coding sequence, which was missing in the cDNA libraries, we screened a genomic DNA library and constructed a recombinant ACHE DNA expression vector, which encoded, in microinjected *Xenopus* oocytes, a catalytically active AChE having the characteristic biochemical properties of the authentic human enzyme. This sequence was subsequently transferred to A. Shafferman and colleagues at the Israel Biological Research Institute, where it was used to transfect human 293 cells for large-scale production of recombinant human AChE.

The promoter sequence controlling AChE production was further cloned and sequenced. When combined with the ACHE coding sequence, it directed expression of the human enzyme in developing myotomes of transiently transgenic *Xenopus* embryos, providing a convenient *in vivo* expression system amenable to analysis of the effects of AChE overexpression at the cellular, molecular and physiological levels. Several point mutations in the ACHE and BCHE genes were detected in Israeli residents of different ethnic origins and their incidences were found to vary considerably within the Israeli population and between this and other populations, e.g., Caucasian Americans. Phenotypic effects of natural genomic variants can thus be expected to vary according to ethnic origin.

Gene expression: The human ACHE gene was found to include 6 exons and 4 introns and to be subject to 3 distinct patterns of alternative splicing at its 3'-end, which potentially leads to 3 distinct forms of AChE, differing at their C-termini. The alternative AChEmRNA forms were found to be abundant in tumor cell lines of various tissue origins. In microinjected *Xenopus* oocytes and embryos, monomers of the hydrophilic form of AChE were found to accumulate efficiently at neuromuscular junctions (NMJs), where the transgenic enzyme caused ultrastructural alterations, increased length and enhanced NMJ foldings, suggesting developmental effects of ChE overexpression. This may be clinically significant, as the ACHE and BCHE genes were found to be subject to incomplete amplification and mutability in ovarian and bone marrow tumors, as well as in blood cell proliferation disorders, including polycythemia vera and lupus erythematosus-associated platelet deficiency. Indeed, *in vivo* administration to mice of antisense phosphorothioate oligodeoxynucleotide inducing targeted destruction of AChEmRNA caused transient hematopoietic alterations and hampered erythropoiesis and megakaryocytopoiesis in the treated animals, suggesting that AChE inhibition may cause hematopoietic disorders in poisoned individuals.

Structure-function relationships: Recombinant variants of human BuChE were expressed in microinjected *Xenopus* oocytes, and their biochemical properties were analyzed. These included natural variants, having the point mutations described above, a number of site-directed mutants of BuChE and a chimeric human AChE-BuChE enzyme constructed by engineered ligation of PCR fragments from both cDNAs. The examined mutations included nontolerated ones, which totally abolished catalytic activity, as well as mutations affecting the Michaelis constant and/or sensitivity to inhibition of the resultant enzyme products by different inhibitors. Thus the frequent alteration of Asp70 by Gly in human BuChE (8% heterozygotes in the Israeli population) was shown to decrease succinylcholine hydrolyzing activity and hence the post-anaesthetic prolonged apnea syndrome, and to induce extreme sensitivity to organophosphorus poisons and resistance to oxime reactivation in affected individuals. This mutation further causes resistance to natural glycoalkaloid poisons from *Solanum* plants, i.e., solanidine, which potentially explains the evolutionary persistence of the mutation. The apparent phenotype of Gly70 BuChE indicated involvement of peptides surrounding the rim area and the catalytic site groove in cholinesterases in the attraction of ligands and inhibitors. As this notion was further supported by analyses of several site-directed mutants of BuChE, we proceeded to construct a chimeric AChE-BuChE enzyme in which a peptide of 80 residues from this area in BuChE was introduced into AChE. The resultant chimeric enzyme displayed pronounced differences in its inhibitor interactions, suggesting that it might provide improved protection against organophosphorus poisons as compared with the native AChE and/or BuChE.

Thus genomic, posttranscriptional, cellular and biochemical approaches were combined to investigate the biogenesis of human cholinesterases and their biological functions and therapeutic implications.

FOREWORD

Opinions, interpretations, conclusions and recommendations are those of the author and are not necessarily endorsed by the US Army.

_____ Where copyrighted material is quoted, permission has been obtained to use such material.

_____ Where material from documents designated for limited distribution is quoted, permission has been obtained to use the material.

__X__ Citations of commercial organizations and trade names in this report do not constitute an official Department of Army endorsement or approval of the products or services of these organizations.

__X__ In conducting research using animals, the investigator(s) adhered to the "Guide for the Care and Use of Laboratory Animals," prepared by the committee on Care and Use of Laboratory Animals of the Institute of Laboratory Resources, National Research Council (NIH Publication No. 86-23, Revised 1985).

__X__ For the protection of human subjects, the investigator(s) adhered to policies of applicable Federal Law 45 CFR 46.

__X__ In conducting research utilizing recombinant DNA technology, the investigator(s) adhered to current guidelines promulgated by the National Institutes of Health.

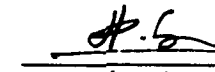

9/30/93

PI - Signature Date

ABBREVIATIONS, SYNONYMS AND TERMINOLOGY

ACh	acetyl choline
AChE	acetylcholinesterase
ACHE	acetylcholinesterase gene
AS-ACHE	oligonucleotide anti-sense to an ACHE coding sequence
ATCh	acetyl thiocholine
BCHE	butyrylcholinesterase gene
bp	base pairs
BuChE	butyrylcholinesterase
BTCh	butyryl thiocholine
BzCh	benzoyl choline
ChE	cholinesterase
CHE	cholinesterase gene
DFP	diisopropylfluorophosphonate
ds	double-stranded
echothiophate	diethoxyphosphinylthiocholine iodide
EDTA	ethylenediamine tetraacetic acid
EGTA	ethylene glycol-bis(beta-aminoethyl ether) tetraacetic acid
h	human
HpAChE	hydrophobic form of AChE
iso-OMPA	tetraisopropylpyrophosphoramide
kb	kilobases
mAb	monoclonal antibody
NMJ	neuromuscular junction
ORF	open reading frame
2-PAM	2-pyridinylaldoxime methiodide
PF	post-fertilization
PI	phosphitidyl inositol
PIP_2	inositol triphosphate
PrCh	propionyl choline
RFLP	restriction fragment length polymorphism
RNase	ribonuclease
r	recombinant human
S-ACHE	oligonucleotide from ACHE coding sequence (see AS-ACHE)
ss	single-stranded
SSB	single strand DNA-binding protein
SSC	standard saline-citrate
SuccCh	succinyl choline

Unless otherwise specified, numbering of the amino acid residues and bases is according to the sequences of hAChE and hACHE (Soreq et al., 1990), or for hBuChE and hBCHE (Prody et al., 1987). Mutants are designated by the wild-type residue and its replacement; thus, Leu286Asp is a replacement of the leucine at position 286 by an aspartate residue.

TABLE OF CONTENTS

I. INTRODUCTION

A. Overview and goals

Chemical warfare agents are aimed at inhibition of human acetylcholinesterase (hAChE), whereas the closely related agricultural insecticides are mostly designed for inhibition of the insect enzyme, with particular emphasis on low toxicity to humans. In addition, cholinesterase (ChE) inhibitors are employed clinically in the treatment of common syndromes, including Parkinson's disease, myasthenia gravis and multiple sclerosis; and attempts at restoration of cholinergic defects in Alzheimer's disease patients involve the use of various drugs that inhibit ChEs. The efficacy and specificity of such drugs on the one hand, and their toxicity factors on the other, largely depend on inhibition of ChEs in the treated individuals. For all these reasons, updated evaluation methods for these parameters should be valuable to chemical defense as well as pharmacological research focused on the development and use of cholinergic agents.

hChEs are classified mechanistically as carboxylesterase type B enzymes, and functionally are capable of rapidly terminating neurotransmission at cholinergic synapses and neuromuscular junctions. The ChEs are further classified according to substrate specificity and sensitivity to selective inhibitors into AChE and butyrylcholinesterase (BuChE). Subclassifications of ChEs are based on their hydrophobicity, interaction with membranes and multisubunit assembly.

AChE exists in several structurally distinct forms that can be differentiated on the basis of physical properties. These include the number and types of subunits of which they are composed, the molecular weight of these catalytic subunits, their sedimentation rate and hydrophobicity or hydrophilicity. All of the AChE forms are monomers or oligomers of a catalytic glycoprotein, the molecular weight of which is in the range of 70-80 kDa for mammals (Rotundo, 1984). Fig. 1 presents these forms schematically.

The different catalytic subunits of the polymorphic AChE forms are generally considered to share common biochemical and pharmacological properties. Thus, the significance of this polymorphism is usually assumed to reflect the extracellular distribution of these forms. The asymmetric form in muscle is characterized by the presence of a collagen-like tail. One catalytic tetramer can bind a collagenic subunit by disulfide bonds (Massoulie et al., 1993). Molecules containing one, two or three catalytic tetramers are named A_4, A_8 or A_{12} forms, respectively. Asymmetric forms of ChEs appear to be attached to extracellular matrices, e.g., the neuromuscular basal lamina. They are specifically expressed in nervous and muscular tissues and may be regulated according to the physiological state of the individual. The characteristic properties designating the asymmetric forms are reversible aggregation at low ionic strength, large Stokes radius (>8 nm), and a specific sensitivity to collagenase.

The second class of ChE, the globular forms, may be defined in a negative fashion by the absence of a collagen-like tail.

In the central nervous system, the principal form of AChE is a tetramer, and is membrane-bound. It has the same amino acid sequence as the asymmetric form, but is anchored differently. Amphiphilic dimers of AChE

from a number of sources (mammalian erythrocytes, *Xenopus* muscle, *Torpedo* electric organ and *Drosophila* nervous system) have been shown to possess an ethanolamine-glycan-phosphatidylinositol anchor, linked by an amide bond to the C-terminal amino acid residue of the catalytic subunits (for reviews see Silman & Futerman, 1987; Ferguson & Williams, 1988). Such molecules are called glycophosphatidylinositol-anchored (GPI-anchored). GPI anchors may be removed by a phosphatidylinositol-specific phospholipase C (PI-PLC), and an anchor-specific phospholipase D (PLD) from serum, except when the inositol ring is acylated. In addition to the catalytic subunits, this form includes a hydrophobic proteolipid subunit of 20 kDa associated by disulfide bridges to one of the dimers (Gennari et al., 1987; Inestrosa et al., 1987).

These different forms of AChE may vary in their sensitivity to specific cholinergic drugs. Certainly, whatever their *in vitro* sensitivity, *in vivo*, their different tissue, cellular and subcellular localization exposes them differently to OP agents.

Alternative splicing is known to control the generation of proteins with diverse properties from single genes (Maniatis, 1991), through the alternative excision of intronic sequences from the nuclear precursors of the relevant mRNA (pre-mRNA). It is known to be cell type-, tissue- and/or developmental stage-specific (Smith et al., 1989) and is considered as the principal mechanism controlling the site(s) and timing of expression and the properties of the resultant protein products from various genes (Baker, 1989). We have shown that alternative splicing is responsible for the expression from a single gene of those forms of AChE that possess the "optional" C-terminal domain and those that don't, and may also account for a yet-to-be-described third form.

In man, the existence of a separate BuChE was established over 50 years ago based upon the distinct substrate and inhibitor specificities (Alles & Hawes, 1940), which distinguish it from the closely related enzyme AChE. Apart from its possible role in supporting AChE in terminating cholinergic neurotransmission (Massoulie & Toutant, 1988), the intensive expression of BuChE in fetal tissues (Zakut et al., 1985, 1991; Layer & Sporns, 1987) and bone-marrow stem cells (Patinkin et al., 1990), together with its gene amplification in germ cells (Prody et al., 1989) as well as in blood cells (Lapidot-Lifson, 1989) and ovarian carcinomas (Zakut et al., 1990), indicate a probable growth-related role for BuChE (Soreq & Zakut, 1990a). Even if in this role its action is not dependent on its catalytic properties, its function in regulation of cellular development (*allo*function) must depend upon structure-*allo*function relations.

Serum BuChE exerts a key clinical role in the degradation of drugs such as succinylcholine (SuccCh) (Hodgkins et al., 1965), heroin (Valentino et al., 1990), physostigmine and ecothiophate (Silver, 1974), and activates prodrugs such as bambuterol (Olsson & Svensson, 1984). Ecologically, BuChE serves in the scavenging and subsequent detoxification of both naturally occurring (e.g., *Solanum* alkaloids or quinoline compounds) and synthetic (e.g., paraoxon) ChE inhibitors (Silver, 1974; Whittaker, 1986). On the other hand, the susceptibility of wild-type enzyme, unlike the "atypical" mutant, to inhibition by naturally occurring inhibitors, may in some environments confer a selective advantage on individuals who are at least heterozygous for the mutation.

In contrast to AChE, BuChE in man appears to be encoded by a single mRNA species, but displays biochemical variation due to its mutability. Over 20 different point mutations have been discovered so far in the coding sequence of the human gene encoding BuChE, BCHE. In several cases, these mutations bring about considerable changes in the sensitivity of allelic BuChE variants to selective inhibitors. The potential pharmacotherapeutic value of anti-ChE drugs may hence be improved by application of a deeper understanding of their mechanism of action on variable AChE and BuChE subtypes, which may be designed according to results of structure-function relationship studies using recombinant ChEs of human origin. This should also deepen our understanding of the variable response patterns to prophylactic AChE inhibition employed under threat of organophosphate (OP) poisoning.

The human cholinesterase genes (hCHEs) and their protein products have been the focus of intensive research for many years because of the physiologic[illegible] function attributed to these enzymes, both of which are capable of hydrolyzing the neurotransmitter ACh. Genetic linkage evidence indicates that two distinct genes, designated ACHE and BCHE, encode their respective enzymes, AChE and BuChE. The toxic effects of OP poisons, such as common insecticides or nerve gases, are generally attributed to their specific inhibition of the ChEs, particularly AChE, interfering with cholinergic neurotransmissions. OP inhibition of ChEs occurs through a covalent interaction of the OP compound with a serine residue at the catalytic site. However, detailed study of structure-function relationships in this family of enzymes has been hampered by the difficulties in purifying mammalian ChEs.

The specific goals set forth in our work were:

1. First and foremost, we wished to determine the detailed architecture of the ACHE gene, its exon-intron organization and its alternative splicing options as they related to the biochemical properties of the enzyme product. In addition, promoter element(s) were sought which would help explain the gene's properties and tissue specificitiy.

2. A second major goal of the work has been to further our understanding of the physiological roles of the ChEs. The role of AChE in terminating cholinergic neurotransmission has been very well recognized for decades. The role of BuChE has been a matter of some speculation, but no one would claim certain knowledge of it. Indeed, that humans without any active BuChE at all can lead apparently normal lives seems to deny BuChE any physiological role whatsoever. We thought, however, that as full a description as possible of the range of activities and susceptibilities to inhibition of natural variant BuChEs, combined with an analysis of human populati[illegible]ns that preserve these variants, would be informative of the role this [illegible]e might play, at least in some extreme conditions, such as under th[illegible]s of anti-ChE poisoning. Extending this line of inquiry to BuChEs d[illegible]ely mutated in the laboratory, we felt, could give information on the sub[illegible]olecular details of the enzymes that contribute to their characteristic activity and specificity toward substrates and inhibitors.

Several lines of evidence have indicated that ChEs may have a role in cellular growth and development, and this activity may be independent of their catalytic roles. As a model system, we have selected hematopoiesis, in which one may observe proliferation or development of stem cells. As a method for preventing AChE synthesis in the cells, we have used antisense

oligonucleotides, and have tested our hypothesis in mouse bone-marrow cells.

3. Our studies and other information have indicated that whatever role BuChE may play in normal physiology, it serves as a decoy to react with and inactivate anti-ChEs that normally are found in the diet, or to which individuals are exposed accidentally (agricultural insecticides) or deliberately (warfare nerve agents). In applying this information, we have sought to amplify the natural protective effect of human BuChE. With a knowledge of what controls expression of the ACHE and BCHE genes, we may be able to increase the steady-state levels, to counteract the action of anti-ChEs. With a knowledge of the roles of individual amino acid residues of BuChE, we may be able to extend our use of the techniques of molecular biology to design a more effective BuChE, one that would offer enhanced protection.

B. Allelic variants of hBuChE

Individual variations in the response to the clinical use of SuccCh led to the recognition of variant BuChEs. BuChE normally clears SuccCh from the circulation when administered at surgery to induce muscle relaxation. Following intravenous administration of SuccCh, a desired and brief, minutes-long neuromuscular blockade is induced; serum BuChE rapidly hydrolyses the bulk of the drug into the monocholine derivative, which is finally completely metabolized by both BuChE and AChE to succinate and choline. However, in some individuals (1:1,000 to 1:2,500, in different populations), serum BuChE displays a defective, homozygous "atypical" phenotype, in that it is incapable of hydrolyzing SuccCh. This causes a prolonged neuromuscular block, often of hours duration, termed "post-anaesthetic apnea". In addition to this characteristic inability to hydrolyze SuccCh, "atypical" BuChE is resistant to inhibition by solanidine, which has been proposed to be a selective advantage favoring this particular variant over the "normal", solanidine-sensitive enzyme in some environments. (Solanidine and related glycosteroid inhibitors of ChEs are prominent in most of the *Solanum* species, which include the potato, tomato and eggplant.) Another parameter, routinely employed for distinguishing the "atypical" phenotype from its "normal" counterpart, is its resistance to inhibition by dibucaine, which otherwise potently and irreversibly inhibits normal BuChE. Solanidine, SuccCh and dibucaine are all assumed to interact electrostatically with BuChE, suggesting that the mutation creating the "atypical" phenotype disrupts charge-dependent interactions in BuChE.

There are numerous variant alleles of BCHE (Whittaker, 1986; Soreq & Zakut, 1990a), 10 of which reflect amino acid substitutions that alter catalytic activity. Another 12 point mutations, insertions or deletions result in absence of enzyme activity ("silent" mutations) in serum, or even of the protein itself (summarized in Soreq & Zakut, 1993). A prominent mutation of BCHE, often used in population genetic studies, is the "atypical" BuChE. It is present with an allele frequency under 5% of the population of Europe and a far higher incidence in the Middle East (Whittaker, 1986). This phenotype is caused by substitution of aspartate 70 by glycine (Asp70Gly, GAT to GGT) (McGuire et al., 1989; Neville et al., 1990a). Resistance of "atypical" BuChE to natural alkaloid poisons prevalent in the Middle East (Neville et al., 1990b) raised the possibility that it confers selective advantage (Neville et al., 1992). It is also possible that the low level or absence of active BuChE in the serum that is characteristic of the

"atypical" and "silent" phenotypes, respectively, results in a reduced scavenging activity and therefore higher vulnerability to OP poisons, including warfare nerve agents.

Other BCHE mutations were associated with known BuChE phenotypes, among them the J variant (Glu497Val, GAA to GTA) and the K variant (Ala539Thr, GCA to ACA) (Bartels et al., 1992a,b), both of which cause reduced activity of the serum enzyme, and a corresponding increase in sensitivity to SuccCh during anaesthesia (Bartels et al, 1992b). In Americans Ala539Thr was reported to be closely linked to the Gly70 mutation, and Glu497Val was always found in the presence of Ala539Thr. A dA replacement by dG, less-tightly linked to the above-mentioned mutations, was also reported (Bartels et al., 1992b, referred to there as nucleotide 1914) at nucleotide position 2073 in the noncoding region of BuChEcDNA (Prody et al., 1987).

Perhaps due to the more vital nature of AChE as compared with BuChE, there is only one known natural mutation of ACHE that affects the mature protein (His322Asn, CAC to AAC), common to all AChE forms, including that on erythrocyte membranes. This mutation was first recognized as the basis of the Yt blood group system (Zelinski et al., 1991; Spring et al., 1992; Lockridge et al., 1992) and has no known phenotype except as this serological marker (Soreq & Zakut, 1993). The rare Yt^b allele has a frequency of ca. 5% in Europe (Giles et al., 1967), but is much more abundant (10 to 20%) in Middle East populations (Levene et al., 1984). More recently, additional phenotypically innocuous mutations of ACHE have been reported (Bartels et al., 1993): a change in the codon for Pro446, CCC to CCT, found in Americans in 100% linkage to the Asn322 mutation, and Pro561Arg, CCG to CGG, in the precursor polypeptide of hydrophobic AChE; this mutation was found not to be linked to the former two in Americans.

Contemporary Israel is well suited for exploration of genetic diversity, as there still exist relatively distinct communities, especially of older individuals, from the waves of immigration of the 19th and 20th Centuries. As it happens, there is an even greater variability of the ACHE and BCHE genes in some of these populations than has been reported for other populations. The Yt^b allele frequency, for instance, is over 15% among Jews from India and Pakistan, as was determined serologically (Levene et al., 1987), and the "atypical" BCHE allele frequency is 7.5% among Jews from Iran, as was determined biochemically (calculated from Szeinberg et al., 1972). As we have access to these unique communities, we saw the opportunity to compare patterns of genetic diversity in selected communities with their known historical (geographic and ethnic) origins. Furthermore, the recent reports of additional ACHE and BCHE mutations provided the impetus to observe, for the first time, mutations of both these genes in the same individuals. Earlier studies have identified the trans-Caucasian Georgian Jewish population as one that has been particularly insulated from admixture (Levene et al., 1984) since it was founded at least 1,500 years ago. Hence, it was interesting to compare allele frequencies for the phenotypically evident ACHE and BCHE mutations in Georgian Jews to reported incidence values of corresponding phenotypes in control populations.

C. Intramolecular relationships in ChEs

The availability of these compatible-with-life variants makes BuChE an appropriate model for structure-function relationship studies in ChEs. This has been achieved in the present study by engineering and expressing

plasmid vectors containing various human-derived allelic coding regions for BuChE or combined fragments from such alleles. Once modified domains within BuChE were correlated with distinctly altered enzyme properties, rational site-directed mutagenesis (Russell & Fersht, 1987) was devised to further modify key residues in the enzyme. The resultant series of naturally occurring and site-directed mutants was employed to pursue the roles of particular loops included in the BuChE polypeptide, to correlate individual amino acids or domains within the molecule with the binding of specific substrates and inhibitors, and to shed new light on intramolecular interactions in ChEs. Furthermore, the close sequence homology of BuChE with AChE has permitted construction of a credible 3-dimensional BuChE model by replacement of the AChE residues by the BuChE residues in the x-ray crystallography model of *Torpedo* AChE. The near superimposability of the two models assures the success of replacement of a region of one enzyme by the corresponding region of the other.

Several regions of ChEs were inferred on the basis of functional properties of ChEs. First identified were the catalytic site serine, which is phosphorylated by OP agents, and a histidine residue which gives the reaction its characteristic pH-dependence. When the x-ray crystallography model became available, these residues were seen as Ser200 and His440. Glu325 was also identified, in part by analogy with the catalytic triad of the serine proteases, which use Asp rather than Glu as the ultimate proton sink in making Ser200 an effective nucleophile. The part of the binding site that held the acetyl (AChE) or the butyryl moiety (BuChE), was defined as the acyl-binding site. The fact that substrates are choline esters indicated a cation-binding site, and several lines of evidence, including substrate inhibition (AChE) and activation (BuChE) suggested a peripheral anionic site. This site has been tentatively identified on the basis of chemical modification of specific residues, site-directed mutagenesis, and docking experiments.

The x-ray crystallography model reveals a globular molecule with a narrow 20-Å-deep depression leading to the catalytic site, deep within the molecule. Choline esters, which bear a positive charge, must be accommodated in the interior of a protein molecule. Therefore, one would expect a compensating charge at the cation-binding site. The early literature, long before any x-ray crystallography model was available, referred to this site as an anionic site, in anticipation of an acidic group to accommodate the substrate's quaternary amine. Unfortunately, this prejudiced the issue, so that when the x-ray crystallography model failed to show the predicted aspartate or glutamate at the right place, it was assumed that no coulombic force contribute to binding of the choline moiety. In fact, a tyrosine residue, number 438 in the hBuChE sequence, is strategically located near the choline-binding site, and may very well function as a cryptic anion, being protonated and neutral in the absence of the substrate, being deprotonated and acidic in its presence. Consistent with this hypothesis is the fact that the only known natural mutation at this position (in *Drosophila*) places an acidic aspartate residue there. The lining of the active site gorge is the passage through which substrates and inhibitors must pass to reach the catalytic site. Not unexpectedly, therefore, these residues, along with those of the acyl binding site, were found by site-directed mutagenesis to contribute to the specificities that define AChE and BuChE.

The only common natural mutation of AChE substitutes Asp for His322 on the surface of the molecule, well out of the way of the binding and catalytic sites. The fact that the only known phenotype of this mutation is an altered serotype, giving rise to the Yt blood group system, is consistent with the absence of any catalytic role for a residue in this position. The most common "atypical" BuChE mutation, however, replaces the Asp70 with glycine. The site of this residue is on the rim of the active site gorge, so this substitution has a well-understood consequence for the binding of substrates.

D. hAChE and hBuChE are encoded by two distinct genes

The covalent binding of OPs to the catalytic site serine in ChEs assisted microsequencing of the radioactively labeled active site peptide (Lockridge, 1984). Oligodeoxynucleotide mixtures were thereafter synthesized with the potential to encode this peptide, and cDNA libraries from various human tissues were screened with these radioactively labeled oligonucleotide probes (Prody et al., 1986). The first human cDNA clone which was thus isolated encoded BuChE, as became evident from comparison with peptide sequencing data (Prody et al., 1987). The cDNA was A,T rich, as expected from a tissue-specific gene. It encoded seven glycosylation sites and a signal sequence reflecting the known properties of the two enzymes and secretory nature of its protein product (Soreq & Gnatt, 1987). The same cDNA was found in brain, muscle, lymphocytes and liver libraries, suggesting that a single mRNA transcript encodes BuChE in all tissues (Dreyfus et al., 1988).

To isolate the DNA sequence encoding ACHE, oligodeoxynucleotides were synthesized which would recognize areas in *Torpedo* AChEcDNA (Schumacher et al., 1986), yet did not appear in hBuChEcDNA. The first clones which were thus found (Soreq & Prody, 1989), served to search for others until a diverse collection of hAChEcDNA clones of various origins and lengths had been assembled. These clones all encoded a protein with >50% homologies to both hBuChE and *Torpedo* AChE. All of the clones terminated within a short domain of approximately 100 nucleotides, downstream from the expected 5' end of the coding sequence. To reveal the complete coding region, a genomic DNA fragment encoding the missing 5' domain was isolated. This was combined with the cDNA by enzymatic restriction and ligation to yield an AChE-coding DNA (Soreq et al., 1990). In striking contrast to BuChEcDNA, the AChEcDNA sequence was found to be extremely rich in G,C residues (Ben-Aziz & Soreq, 1990).

In order to find an explanation for the premature termination of the various AChEcDNA clones, the ACHE coding sequence was subjected to secondary structure analysis by the Wisconsin Program. Tightly folded stems and loops structures spanning the common termination domain of the isolated AChE cDNAs (ΔG° = -117 kcal) were revealed. In other systems, for example in the adenovirus genome (Kessler et al., 1989), structures with free energy of the same order of magnitude were shown to attenuate transcription *in vivo*. It is currently assumed that the attenuator sequence was responsible for the incomplete synthesis of AChEcDNAs and that is capable of controlling AChE mRNA synthesis *in vivo*.

AChE and possibly BuChE are involved in the regulation of cholinergic signaling, together with the neurotransmitter acetylcholine (ACh) and the various ACh receptors. Tightly coordinated expression of the BCHE and ACHE genes has been observed in several biosystems. In addition to tissues

where cholinergic innervation is to be expected, like brain and muscle, hChEs are intensively expressed in various developing and tumor cells where no cholinergic function so far has been recognized (for recent examples, see Malinger et al., 1989; Prody et al., 1989). Furthermore, inhibition of the two ChE activities appears to affect cellular differentiation in bone marrow cells, where carbamylcholine or physostigmine administration induces promegakaryocytopoiesis, AChE production and platelet formation (Burstein et al., 1980, 1985). Other examples include sperm cells, in which OP poisons interfere with motility (Rama Sastry & Sadavongvivad, 1979). To approach the biochemical as well as the biological questions related to these enzymes, a search for the human BCHE and ACHE genes and their modes of expression was initiated.

The highly efficient catalytic activity of ChEs led to the development of very sensitive assays for these enzymes, including gel activity staining (Brock & Bader, 1983) based on the precipitation of ferrous-copper-thiocholine complexes (Koelle, 1972). When human serum is thus analyzed, various electrophoretic bands of BuChE activity may be observed. The more abundant C_{1-4} bands were all genetically linked to one locus, designated CHE1, and were found to appear in all humans (Whittaker, 1986). In contrast, the faster migrating C_5 band is expressed in only about 8% of the Caucasian population and is linked to a separate locus, designated CHE2 (Whittaker, 1986). It is currently believed that neither locus is linked to the ACHE locus, controlling AChE production (reviewed by Soreq & Zakut, 1990).

Molecular cloning studies have revealed the complete nucleotide sequences encoding hBuChE (Prody et al., 1986, 1987; McTiernan et al., 1986) and AChE (Soreq & Prody, 1989; Soreq & Zakut, 1990a), making *Homo sapiens* the first species in which both CHE coding sequences have been cloned. This study demonstrated that the genomic sequences encoding AChE and BuChE in humans do not display a high sequence homology (Lapidot-Lifson et al., 1989), in spite of the considerable similarity between the protein sequences encoded by these two genes.

The lack of sequence homology between AChEcDNA and BuChEcDNA proved beyond doubt that, in humans, AChE and BuChE are produced from two distinct mRNA transcripts. However, it could not answer the question of whether these two transcripts are produced from two independent genes or from one, perhaps by complex posttranscriptional processing. This question became particularly urgent in view of the findings that the BCHE and the ACHE genes are co-amplified in leukemias (Lapidot-Lifson et al., 1989) and ovarian carcinomas (Zakut et al., 1990). One approach to determine whether the BCHE and ACHE coding regions are included in a single complex gene would be to isolate the complete DNA sequence encompassing the regions coding for one of these enzymes and determine whether intron sequences included in this DNA contain the coding regions for the other. To this end we have performed cosmid recombination experiments aimed at selecting CHEDNA cosmid clones containing the complete BCHE coding region and their use for such analysis.

Genetic linkage evidence accumulated over the years suggests that the BCHE gene resides on the long arm of chromosome 3 (Sparkes et al., 1984; Arias et al., 1985; Whittaker, 1986). Significant, although considerably weaker, linkage with genes on the long arm of chromosome 16 (Lovrien, 1978) was also observed. *In situ* hybridization with spread mitotic chromosomes

revealed sequences complementary to BuChEcDNA on three sites, designated CHEL1, CHEL2 and CHEL3 at the respective positions 3q21, 3q26 and 16q21 (Soreq et al., 1987; Zakut et al., 1989). Recently, the isolation and mapping of 3'-extended BuChEcDNA clones from brain tumor libraries demonstrated that the 3'-additional fragment on these clones, which was designated Gb5, originates from the unique chromosomal position 3q26-ter (Gnatt et al., 1990). We therefore employed this unique Gb5 probe to further assess the chromosomal origin of the CHEDNA cosmids, used chromosomal blots from human/hamster hybrid cells to confirm our assessment, and performed *in situ* hybridization under stringent washing conditions to compare the hybridization results in blots to those obtained with chromosomes. Our findings support the notion of a single BCHE gene, localized to chromosomal position 3q26-ter, which does not include AChE-coding sequences, and indicate the possibility of differences between individuals in the content of BuChEcDNA-hybridizing sequences. To complete this aspect of the research, we undertook to map the ACHE gene as well.

E. CHE gene amplification in OP-exposed individuals

The same powerful biochemical methodology that expressed variants of the BCHE gene after *in vivo* microinjection of *Xenopus* oocytes, has enabled a search for yet more mutations. It happens that the frequency of variant BuChE alleles in Israel is twofold that found in Europe (Szeinberg et al., 1972), probably due to a founder effect characterizing size-limited populations. In addition, intensive agriculture in Israel is responsible for a relatively high exposure to OP insecticides. The combination of a variant BuChE phenotype and prolonged OP exposure was exemplified in the H family (Prody et al., 1989), where one brother was brought to intensive care following parathion, spraying in a cotton field, and his sister suffered from prolonged apnea following SuccCh administration at the surgical removal of oocytes for *in vitro* fertilization. The serum BuChE activities in this family were very low, which explained their vulnerability to OP poisoning and SuccCh administration. Moreover, 100 copies of the BCHE gene were found in peripheral blood DNA from the family member poisoned by parathion as well as in one of his sons. The amplification was most intense in central sequences within the coding region, and was, to the best of our knowledge, unique to this gene. Gene mapping by *in situ* hybridization revealed labeling 10-fold higher than usual, which mapped to chromosomal position 3q26-ter in lymphocyte chromosomes from the affected individual. This implied that the amplified DNA was probably inherited, although we could not exclude the possibility that the amplification occurred independently in the son as a result of a parallel insult (i.e., exposure to OP poisons at a critical developmental stage; for further discussion of this point see Soreq & Zakut, 1990a).

The findings in this family of linkage of a defective enzyme and exposure to OP agents on the one hand, and heritable gene amplification that appears in all tissues on the other, indicated that this multielement phenomenon should occur in germ cells, oocytes, or more likely, because of their large numbers, sperm. This, in turn, is in agreement with early observations that OP agents decrease sperm motility and, therefore, fertility (Rama Sastry & Sadavongvivad, 1979).

F. CHE gene amplifications in tumors

When and why do genes amplify? The H family presented the first case of an inherited gene amplification in apparently healthy human individuals. There is, however, ample precedent for gene amplification in tumors. For

example, genes encoding target proteins of toxic inhibitors amplify under exposure to such inhibitors (i.e., dihydrofolate reductase in leukemias, (Schimke, 1990)). Many oncogenes, either homologous to growth factors or to their receptors, amplify in rapidly developing cells (i.e. epidermal growth factor receptor in gliomas (Libermann et al., 1984)). In insects and amphibia, developmentally essential genes amplify when high expression is needed (i.e., chorion genes in *Drosophila* (Spralding, 1987)). In all these cases, the amplified genes confer a selection advantage to the cells and are subjected to frequent mutagenesis. However, not all of the amplified copies are expressed.

It is not yet certain that BCHE gene amplification in the H family reflected a response to OP exposure. Even if this was the cause of that event, it could be a unique phenomenon caused by the combination of chronic OP exposure and a variant BuChE phenotype. To examine whether this is the case, various tumor types were screened in search for BCHE and/or ACHE gene amplifications and mutability. Gene amplification frequently coincides with chromosome breakage in tumors. Therefore, evidence of CHE gene amplification was sought in tumors or disorders related to the chromosomal 3q26-ter region, which is known to frequently break. This occurs in leukemias and platelet disorders (Pintado et al., 1985). Furthermore, ChE inhibitors such as physostigmine induce platelet production in the mouse (Burstein et al., 1980), which indicates that the BCHE gene is actively involved in megakaryocytopoiesis. DNA hybridization revealed that in leukemias and platelet disorders, both the BCHE and the ACHE genes are amplified. Co-amplification probably occurs in response to a single stimulus, as it was observed in a large fraction of the cases examined (Lapidot-Lifson et al., 1989).

Another tissue type where CHE gene amplification was sought was the ovarian tumor, where cytochemical staining demonstrated overexpression (Drews, 1975). Here again, both BCHE and ACHE genes were amplified (Zakut et al., 1990). There was good correlation between the levels of CHE gene amplifications in ovarian tumors and the parallel amplification of several oncogenes. However, there was neither BCHE nor ACHE gene amplification in gall bladder tumors (unpublished observations), demonstrating that the phenomenon of gene amplification also depends on the nature of cells where it occurs.

The abnormalities in ChE expression observed in tumors, as well as a previously unforeseen peptide motif present in ChEs which makes them potential substrates for phosphorylation by CDC2 kinases, suggest a molecular mechanism that may link these enzymes to the cell division process.

G. The role of ChEs in hematopoiesis

Besides its activity in terminating neurotransmission (Taylor, 1990), accumulated evidence associates acetylcholinesterase (AChE) with growth of several cell types (Bartus et al., 1982; Soreq & Zakut, 1990a; Soreq et al., 1990), including hematopoietic cells (Dreyfus et al., 1991; La Du, 1989). Furthermore, exposure to AChE-inhibitory insecticides increases the risk of leukemia (Brown et al., 1990).

Mammalian hematopoiesis is a continuous process which includes cell proliferation, differentiation and programmed cell death (apoptotic) events characteristic for each of the hematopoietic cell lineages (for reviews see

Metcalf, 1992; Koury, 1992). Following bleeding or hypertransfusion, normal hematopoietic cell composition can be restored by changing this balance (Koury, 1990). However, the mechanisms responsible for such adjustment are not yet fully understood and candidate proteins involved in the maintenance of the fine hematopoietic balance are sought. The acetylcholine hydrolyzing enzymes acetyl- and butyrylcholinesterase (AChE, BuChE) may be considered for such hematopoietic role since both these enzymes are expressed in mammalian hematopoietic cell lineages (Burstein et al., 1980; Toutant et al., 1990; Soreq & Zakut, 1990a). Moreover, a growth regulatory role has been recently postulated for ACHE in hematopoiesis (Paoletti et al., 1992) and a high risk to develop leukemia was correlated with exposure to ChE inhibitory insecticides (Brown et al., 1990); in addition, the ACHE and BCHE genes reside on chromosomal domains which break frequently in hematopoietic malignancies (Gnatt, 1990; Ehrlich et al., 1992) and are subject to gene amplification and mutability in leukemias (Lapidot-Lifson et al., 1989) and in other blood cell abnormality syndromes, including platelet deficiency associated with Lupus erythematosus (Zakut et al., 1989). Morover, acetylcholine analogs and ACHE inhibitors were found to induce murine platelet production *in vivo* (Burstein & Harker, 1983) and AS-oligo inhibition of BCHE mRNA interfered with production of megakaryocytes (MK), the platelet progenitors, in interleukin 3-treated murine bone-marrow cultures (Patinkin et al., 1990; Lapidot-Lifson et al., 1992).

The large, polynucleated MK survive in the circulation for about 10 days and then are destroyed by the reticuloendothelial system (Mazur, 1987). Understanding of the biochemical mechanisms controlling megakaryocytopoiesis and platelet levels may hence lead to the development of selective treatment paradigms to platelet deficiencies (thrombocytopenias), which may cause bleeding, and excess (thrombocytosis), which may lead to blood vessel clotting (Handin, 1991). Malignancies, autoimmune diseases, chronic infection, irradiation, chemotherapy, and various drugs all perturb the balance of platelet counts (see Zakut et al., 1992, for a recent example). Many, if not all of these etiologies may develop through the distortion of specific signaling processes. Here, we report the *in vivo* use of AS-oligo inhibition of ACHE mRNA (AS-ACHE) to study this issue.

Antisense oligodeoxynucleotides (AS-oligo) are short, 15-20 mer synthetic DNA sequences which are actively taken up by living cells (Loke et al., 1989) where they hybridize with their target complementary mRNAs to create double-stranded DNA-mRNA hybrids (Ghosh et al., 1992). This can expose these cellular mRNAs to nucleolytic degradation by RNase H (Woolf et al., 1990), prevent correct splicing (Chiang, et al., 1991; Kole et al., 1991) and interfere with mRNA translation (Boiziau et al., 1991). AS-oligos may be protected from nucleolytic degradation by the insertion of internucleotide phosphorothioate groups (Eckstein, 1985; Spitzer & Ekstein, 1988; Matsukura et al., 1987). This turns them into stable, long-duration drugs (Shaw et al., 1991; Agrawal et al., 1991; Hoke et al., 1991), of potential importance for basic research as well as for clinical use, particularly when their target mRNAs are essential for crucial biochemical pathways or developmental processes (Bielinska et al., 1990). AS-oligos targeted against several oncogenes were shown to arrest hematopoietic cell proliferation (Szczylik et al., 1991; Wickstrom et al., 1988), growth (Calabretta et al., 1991), entry into the S phase of the cell cycle (Heikkila et al., 1987) and cell survival (Reed et al., 1990). Moreover,

AS-oligo to c-myb was shown to arrest leukemia *in vivo* (Ratajczak et al., 1992).

To examine whether ACHE is involved in controlling hematopoietic composition in general and MK development in particular, we treated mature female mice with phosphorothioate AS-ACHE. To monitor the effects of this treatment, we combined differential cell counts with a kinetic followup of polymerase chain reaction products (RNA-PCR). *In situ* hybridization with [^{35}S]-labeled ACHE and BuChEcRNA probes, followed by computerized quantification of the hybridization data, was used to associate mRNA levels with specific cell types. Our findings demonstrate involvement of the ACHE gene in maintenance of hematopoietic balance and foreshadow the use of AS-ACHE to transiently modulate hematopoietic cell composition by selective suppression of its target mRNA.

II. MATERIALS AND METHODS

A. MATERIALS

Diisopropylfluorophosphonate (DFP) was purchased from Aldrich Chemical Co. (Milwaukee, WI), and ecothiophate was a product of Ayerst Laboratories (Montreal, PQ, Canada). Restriction enzymes, T_4 polynucleotide kinase, T_4 DNA ligase and double-stranded (ds) M13 cloning vector M13mp18RF were from Boehringer/Mannheim (Mannheim, Germany). *In vitro* transcription kits were from Amersham International (Amersham, UK), and the reactions performed as detailed elsewhere (Ben-Aziz & Soreq, 1990) using CAP analogue (P'-5'-(7-methyl) guanosine-P3-5'-guanosine triphosphate) from Pharmacia (Uppsala, Sweden). *E. coli* strains MV1190 and CJ236 were from International Biotechnologies Inc. (New Haven, CT). Radiochemicals were purchased from Amersham International, and unless otherwise noted, all other chemicals were from Sigma Chemical Co. (St. Louis, MO), of the highest grade available.

BCHE mutagenic primer oligonucleotides supplied by Microsynth (Windisch, Switzerland) were:

pCC TAT GGG ACT CCT GAC TCA GTA AAC TTC GGT-OH	for Leu286 to Asp;
pCC TAT GGG ACT CCT AAG TCA GTA AAC TTT GG-OH	Lys;
pCC TAT GGG ACT CCT CAG TCA GTA AAC TTT GG-OH	Gln;
pCC TAT GGG ACT CCT CGG TCA GTA AAC TTT GG-OH	Arg;
pAA GGG ACA GCT TGT TTA GTC TAT GGT-OH	Phe329 to Cys;
pAT GAA GGG ACA GCT GAT TTA GTC TAT GGT GC-OH	Asp;
pAT GAA GGG ACA GCT CTT TTA GTC TAT GGT GC-OH	Leu;
pAT GAA GGG ACA GCT CAG TTA GTC TAT GGT GCT-OH	Gln:
pTC TTT GGA GAA TGT GCA GGA GCA-OH	Ser198 to Cys;
pC TTT GGA GAA ACT GCA GGA GCA G-OH	Thr;
pACT CTC TTT GGA GAA GAT GCA GGA GCA GCT TC-OH	Asp;
pA ACT CTC TTT GGA GAA CAG GCA GGA GCA GCT TCA-OH	Gln;
pACT CTC TTT GGA GAA CAT GCA GGA GCA GCT TC-OH	His.

Underlining indicates mismatched bases, as compared with wild-type BuChEcDNA, and the substituted amino acids are shown in parentheses. The homologous (-) strands were also synthesized for use as mutagenic primers.

External primers for PCR mutagenesis were pAAT GCT CCT TGG GCG CTA AC-OH (+841 to +860) and pTC CAG AGG TAA ACC AAA GAC-OH (-1511 to -1492) for use with the restriction nucleases XbaI and *StuI* in the mutagenesis of Leu286 and Phe329; and pGCC ACT GTA TTG ATA TGG A-OH (+478 to +496) and pTC AGT CTC ATT CTC TCT AG-OH (-935 to -917) for use with *AvaI* and *BamHI* in the mutagenesis of Ser198. *In vitro* transcription kits were from Amersham International.

B. Biochemical (enzyme) measurements

1. Preparation of enzyme

Expression in and extraction of enzyme from oocytes has been detailed elsewhere (Neville et al., 1990a,b) and is described below under "Expression, synthetic RNA preparation and microinjection."

Xenopus embryos were harvested in groups of 3 to 5 apparently normal individuals and stored frozen until used. Homogenates were prepared in a high salt/detergent buffer (0.01 M Tris, 1 M NaCl, 1% Triton X-100, 1 mM EGTA, pH 7.4; 150 µl/embryo), microcentrifuged for 20 min in the cold and assayed for enzymatic activity using the colorimetric assay employing

acetylthiocholine (ATCh) as substrate, as detailed elsewhere (Neville et al., 1992). A 30 to 40 min preincubation with specific inhibitors was performed prior to inhibition tests.

For assay of subcellular fractions, groups of 3 embryos were homogenized in LS buffer (0.02 M Tris-HCl, pH 7.5, 0.01 M $MgCl_2$, 0.05 M NaCl; 100 µl/embryo) and centrifuged at 100,000 rpm for 10 min in a Beckman TL100 tabletop ultracentrifuge. The supernatant fluid was defined as the low salt-soluble fraction. The sediment was resuspended in LSD buffer (0.01 M phosphate buffer, pH 7.4. 1% Triton X-100), incubated on ice for 1 hr, and centrifuged as above for 5 min. This supernatant fluid was defined as the membrane-associated fraction. This sediment was resuspended in HS buffer (0.1 M phosphate, pH 7.4, 1 M NaCl, 1 mM EGTA) and the supernatant fluid following centrifugation was defined as the high salt-soluble fraction and was considered to represent extracellular matrix associated AChE.

2. Spectrophotometric determination of enzyme activities and inhibitor studies

These assays were performed using the Ellman method (Ellman et al., 1961) with the modifications previously described (Neville et al., 1990a). Briefly 5, 10 or 20 µl aliquots of oocyte supernatant fluids were added to 170 µl of 0.1 M phosphate buffer at pH 7.4 containing 0.5 mM 5,5'-dithionitrobenzoic acid in 96-well microtiter plates. Reactions were initiated by the addition of 20 µl of butyrylthiocholine (BTCh) (final concentration 1 mM or 10 mM) and activities monitored by following the appearance of colored reaction product at 405 nm in a Vmax Kinetic Microplate Reader (Molecular Devices) equipped with the Softmax program for automated determination of hydrolysis rates.

For inhibitor studies, a preincubation period of 30 min was employed prior to the addition of substrate. Solanidine was initially dissolved in dimethylsulfoxide (DMSO) and then diluted to 16% (v/v) with H_2O to a stock concentration of 10 mM. alpha-Solanine and alpha-chaconine were each dissolved in 400 µl 0.1 M HCl and made up to 2 ml with double-distilled H_2O. Stock solutions of all *Solanum* alkaloids were 10 mM. Reaction mixtures subsequently contained 0.16% DMSO which by itself failed to influence BuChE activities. Final BTCh concentrations were 10 mM in dibucaine and solanidine experiments, and 1 mM in SuccCh and 2-PAM experiments. For Km determinations, the substrate concentration range was 0.1 mM to 20 mM. For reactivation experiments, 2-PAM was dissolved in 0.1 M NaCl at a stock concentration of 100 mM and pH adjusted to 7.4. Since 2-PAM itself causes hydrolysis of thiocholine ester substrates (Karlog & Peterson, 1963), a modified assay was required in the reactivation experiments. Briefly, 20 µl oocyte homogenates were added to 30 µl of 0.1 M phosphate buffer containing either 0.5 µM DFP or 10 mM 2-PAM. For reactivation analyses, a 30 min preincubation with DFP was followed by the addition of 2-PAM for a further 2 hr period. Subsequently, 10 µl aliquots were removed for BuChE activity measurements as detailed above. Determinations of K_m and IC_{50} values were performed as previously described (Neville et al., 1992).

3. Enzyme-antigen immunoassay (EAIA)

Mouse anti-human serum BuChE or anti-human erythrocyte AChE mAbs (53-8 and 101-2, respectively, from Dr. J. Liao) are bound to microtiter plates (Nunc, Roskilde, Denmark) at 0.5 µg/ml in 0.1 M carbonate buffer, pH 9.6, for 4 hr at room temperature. The plate is then washed three times in PBS-T buffer (144 mM NaCl, 20 mM phosphate, pH 7.4, 0.5% Tween-20). Free

binding sites at the well surface of the microtiter plate are blocked by addition of 1% bovine serum albumin in PBS-T for 1 h at 37 °C. After washing three times with PBS-T, enzyme is added at a concentration of 100 mIU/ml in PBS-T for 3 hr at room temperature with agitation. The plate is washed three times with PBS-T before use.

4. Rates of reaction with OPs

Enzymes were immobilized in the wells of microtiter plates which had been coated with anti-BuChE antibodies (Liao et al., 1992), then exposed to DFP for varying times. The DFP was washed away and assay of remaining activity was performed in 20 mM BTCh. Linear regression analysis of plots of the logarithms of remaining activity *vs.* time of exposure to DFP yielded pseudo-first order rate constants for the inactivation reaction.

5. Sucrose gradient analysis of AChE subunit assembly

Freshly prepared, high salt/detergent extracts from 1 to 2 embryos or 5 to 10 oocytes were applied to 12 ml 5 to 25% linear sucrose density gradients and centrifuged overnight at 4 °C ($\omega^2 t = 1.06 \times 10^{12}$). Fractions of 270 µl were collected into 96-well microtiter plates and assayed for AChE activity as previously described. To distinguish between endogenous *Xenopus* AChE and recombinant hAChE (rhAChE) in gradient fractions, enzyme antigen immunoassay (EAIA) was employed (see Liao et al., 1992). Gradient fractions were divided to generate two replicate plates for each sample. Aliquots of 100 µl were transferred to a Maxisorp immunoplate (Nunc) coated with a monoclonal antibody (mAb 101-1) that recognizes human but not frog AChE, and diluted 1:1 with double-distilled water to reduce the high salt and sucrose concentrations. Following overnight incubation, the plates were washed 3 times with PBS containing 0.05% Tween 20 and each well was assayed for AChE activity. Another 100 µl was transferred to a Nuclon Microwell polystyrene microtiter plate (Nunc) and assayed for total AChE activity, including both that contributed by rhAChE and the endogenous *Xenopus* enzyme.

C. Molecular biology

The following standard methods were performed as detailed in Sambrook et al. (1989), or according to the recommended procedures in the noted commercial kits:

Plasmid mini/large preparations; restriction endonuclease digestions
DNA fragment electroelution/Geneclean
DNA ligations
Bacterial transformation
Labeling of DNA probes (oligodeoxynucleotide end-labeling, random prime labeling of DNA fragments)
Total RNA extraction from human tissues and preparation of poly(A)+RNA samples; DNA and RNA blot hybridization analyses.

1. Libraries

Libraries screened included: FEB (fetal brain); NBG (neonatal basal ganglia, donated to the American Type Culture collection by RA Lazzarini), FEL (fetal liver, Prody et al., 1987); ABG (adult basal ganglia, constructed during the course of this study); and a human genomic DNA library (BRL, Gaithersburg).

Human tissues were dissected from the following adult and fetal sources:

Adult, 70 years old - basal nuclei, cerebellum, brain stem
Fetal, 18 weeks gestation - hippocampus, basal nuclei, heart, cells

K562-human erythroleukemia cell line was received from E. Kedar, Jerusalem.

2. Screening procedures

Tissues expressing translatable AChEmRNA were identified by a *Xenopus* oocyte bioassay (Soreq et al., 1984). Complementary DNA libraries were then constructed from polyAmRNA from fetal human muscle and from total RNA from adult basal brain nuclei in the lambda gt10 and lambda ZapII phage vectors (Stratagene, Heidelberg), respectively. Additional cDNA libraries which were screened are detailed under Results.

Oligodeoxynucleotides were 5'-end-labeled and differential library screening was performed by plaque hybridization (Prody et al., 1987), using the 35-mer-oligodeoxynucleotide CTACHE, 5'ATG TAC TAC GTG ACC TTC TTG GTC AAG CTG GTG AT3', complementary to the sequence that encodes the peptide sequence Tyr-Met-Met-His-Trp-Lys-Asn-Gln-Phe-Asp-His-Tyr present in the C'-terminal region of *Torpedo* AChE (Schumacher et al., 1986), and in which G or C residues were inserted in positions where codon ambiguity presented a choice between G and T or between C and A. This probe was designed not to hybridize with BuChEcDNA, as the parallel peptide of hBuChE differs in 3 of these 12 amino acids (Prody et al., 1987; McTiernan et al., 1987). Exclusion of false positives was then accomplished with OPSYNO (Prody et al., 1987), a mixed oligonucleotide probe expected to hybridize with both BuChEcDNA and AChEcDNA since it encodes the peptide Phe-Gly-Glu-Ser-Ala-Gly-Ala-Ala-Ser-Val found in the active esteratic site peptide of hBuChE (Prody et al., 1987; McTiernan et al., 1987) and differing from the parallel peptide of *Torpedo* AChE by only one amino acid, tryptophan in the above sequence, glycine in *Torpedo* AChE (Schumacher et al., 1986)].

3. DNA sequencing reactions

Sequencing reactions were performed using a commercial kit (Sequenase version 2, United States Biochemical Corp., Cleveland, OH). To maximize reliability in sequencing the G,C-rich fragments obtained in the screening, both strands were sequenced using multiple adjacent sequencing primers (Fig. 1A). In addition, reduced nucleoside triphosphate concentrations, replacement of guanosine nucleotides by inosine, and the inclusion of Mn^{2+} in sequencing reactions, all according to producers' recommendations, were found to be useful. Also, sequencing was repeatedly performed on the same DNA regions using the single-stranded (ss) phage M13 and the double-stranded (ds) pGEM and PUC118 plasmids. Finally, the combination of Sequenase DNA polymerase with single-strand binding protein (SSB) (United States Biochemical Corp.) resolved densely packed sequence domains. Wherever noted, annealing of ACHE-specific sequencing primers was performed at 72 °C, to circumvent the high G,C-rich content of the analyzed sequences. Also, reading included comparison of sequence data from both directions and with variable distances from the primers employed.

4. *In vitro* transcription

The construct encoding human ACHE was subcloned into the pSP64 transcription vector (Promega) essentially according to Krieg & Melton (1984). *In vitro* transcription and concomitant 5' capping of 5 µg plasmid DNA samples were carried out using commercially available kits from Amersham International at 40 °C following the enclosed manuals, except where mentioned otherwise. The G,C-rich ACHE DNA transcribed inefficiently by SP_6 RNA polymerase, far less than the related A,T-rich cDNA encoding BuChE (Soreq et al., 1989). To reduce the level of DNA folding and increase initiation rates from this G,C-rich DNA, SSB was employed. SSB is known to improve the quality of DNA sequencing from G,C-rich domains (Williams et al., 1983), and in our hands it significantly enhanced

transcription as well, as indicated by agarose gel electrophoresis (Ben-Aziz & Soreq, 1990). Unfolding of tight DNA structures was further ensured by retaining the G,C-rich insert within its circular plasmid DNA rather than transcribing it in a linear form.

The generally recommended protection of *in vitro* transcribed mRNAs by the addition of 5' m_7G(5')ppp(5')G cap analog presents a third technical difficulty in transcription of G,C-rich genes, as it involves reduced concentrations of GTP (1/8 of the level of other NTPs). This, in turn, interferes severely with the correct elongation of G,C-rich transcripts. However, *post-facto* capping was, in our hands, much less efficient than capping done concomitantly with transcription. The "capping" reaction was hence performed in the presence of fourfold higher GTP levels than those we use for A,T-rich transcripts. Together, the addition of SSB, the use of circular plasmids and the elevation of GTP levels resulted in an approximate 10-fold increase in the amount of G,C-rich transcripts produced *in vitro*, yielding an equal transcription efficiency for the G,C- and the A,T-rich sequences (Ben-Aziz & Soreq, 1990).

5. RNA-PCR procedure

For RNA-PCR analyses, total RNA was extracted by the guanidine thiocyanate method (Cinna/Biotecx, Houston, TX). Random hexamer primers (Boehringer/ Mannheim) were employed for cDNA preparation (0.4 µg RNA/sample) using the MMLV reverse transcriptase (Gibco, BRL, Gaithersburg, MD), essentially as described elsewhere (Lapidot-Lifson et al., 1992). PCR amplification in the 9600 Thermal Controller (Perkin-Elmer/Cetus, Norwalk, CT) (35 cycles) was performed using the noted primer pairs as follows: denaturation 94 °C, 1 min (first step 2 min); annealing 65 °C, 1 min; synthesis 72 °C, 1 min (last cycle 5 min). Amplification products (20%) were electrophoresed (7 V/cm, 60 min) on 1.6% agarose (International Biotechnology, Inc., New Haven, CT) gel containing ethidium bromide (1 µg/ml) with TAE (0.04 M Tris-acetate, 2 mM EDTA) as electrophoresis buffer, and were photographed under 320 nm illumination. Control reactions, without reverse transcriptase, remained negative, proving the absence of contaminating DNA sequences complementary to the relevant AChEmRNA.

The following ACHE primers (nos. 1-12, numbered according to their position in the hAChE upstream and coding sequence, and noted as upstream (+) or downstream (-) according to their orientation (all are 5' to 3') were used:

(1) 555+: CTGTGAGGCCCGGAGGACGCCG
(2) 670+: GCTCGGCCGCCTCAGACGCCG
(3) 705+: GGGACTCTCCTTAAGGCCCGGACGCC
(4) 739+: TGCGCTCCCCGAGGGACGCC
(5) 1000+: TACCCGAGCTGCGCAGACGCCG
(6) 614+: CAGCCTGCGCCGGGGAACATC
(7) 623+: GGGAACATCGGCCGCCTCCAG
(8) 664+: GGCCCGGCTCGGCCGCCTCA
(9) 590+: CGGCGGCTGTCAGAGTCGGCT
(10) 2623-: TCCTCGCTCAGCTCACGGTTGGG
(11) 1522+: CGGGTCTACGCCTACGTCTTTGAACACCGTGCTTC
(12) 1797-: CAGGTCCAGACTAACGTACTGCTGAGCCCCCGCCG

Amplification products (20%) were electrophoresed as described and were UV photographed (320 nm). Control reactions, without reverse transcriptase, remained negative, proving the absence of contaminating complementary DNA sequences.

6. Construction of variant transcription vectors

For AChE expression studies, contiguous DNA fragments from cDNA and genomic clones were ligated following digestion with appropriate restriction enzymes. Sequence continuity in the chimeric DNA product was confirmed by repeated sequencing across the ligation point, after which it was subcloned into the pGEM transcription vector behind the SP6 RNA polymerase binding site (Promega, Madison, WI).

Three naturally occurring variants of hBuChEcDNA were used to engineer mutated BCHE plasmids. Clone I: wild-type BuChEcDNA including Asp70, Tyr114, Ser425, Glu441, Ile442, Glu443 and Phe561 (Prody et al., 1987). Clone II: double-mutated Gly70/Pro425 BuChEcDNA derived from neuroblastoma and glioblastoma tumors (Gnatt et al., 1990). Clone III: a BuChEcDNA encoding the amino acid substitutions Asp70Gly, Tyr114His and Phe561Tyr (Gnatt, 1990). *PstI* and *BamHI* restrictions were employed to derive two fragments from each of these clones; 800 bp from the coding region and 4.6 kb consisting of the remaining 1600 bp from the BuChE coding region plus the 3 kb pSP64-41 plasmid. Fragments were isolated by gel electrophoresis and electroelution or Geneclean II Kit (Bio 101 Inc., La Jolla, CA) and were religated in various combinations to generate nine constructs. Briefly, the ligation mixtures contained 20 ng of the larger 4.6 kb fragment and 100 ng of the 800 bp *PstI/BamHI* fragment. To these, 2 µl of 10X ligation buffer, 10 mM ATP and 50 mM dithiothreitol were added followed by the addition of 2 µl of T4 DNA ligase (1 U/µl) in a total reaction mixture of 20 µl and overnight incubation at 4 °C. To prepare Clone IV, the 800 bp *BamHI/HindII* fragment of Clone I, which encoded the tripeptide Glu441-Ile442-Glu443 (EIE) of interest, was ligated into the *BamHI/HindII* restricted M13mp18RF vector and subjected to site-directed mutagenesis according to the method of Kunkel et al. (1987) with minor modifications. Recombinants were identified via formation of beta-galactosidase-negative colorless plaques and were used to infect *E. coli* MV1190 cells and prepare single-stranded (ss) phage DNA, which was used to subsequently infect *E. coli* CJ236 (*dut-/ung-*) bacteria for 18 hr growth in 100 ml of LB-Mg medium supplemented with 0.25 µg/ml of uridine. Uracil enriched phages were precipitated by adding 5.5 ml of 20% PEG/2.5 M NaCl to 22 ml aliquots of the overnight culture; kept on ice for 1 hr and centrifuged at 5,000 x g for 15 min. Sediment from the 88 ml culture was dissolved in 6 ml TE buffer and 1.5 ml aliquots transferred to microcentrifuge tubes, placed on ice for 60 min and centrifuged at 5,000 x g for 15 min. Supernatant fluids were extracted twice with phenol and once with chloroform, and the uracil-enriched ssDNA precipitated overnight at -20 °C with 1/10 vol 3 M NaCl and 2.5 vol ice-cold ethanol.

7. Site-directed mutagenesis of BuChE transcription vectors

A 26-mer minus strand oligonucleotide (30 ng), 5'-AAGACAAATTGAATTCCATAGCCATG-3', spanning nucleotides 1471-1496 of the hBuChEcDNA coding sequence (Prody et al., 1987) containing two mismatches directed at the Glu441-Ile442-Glu443 coding sequence, was phosphorylated using polynucleotide kinase and hybridized to 1 µg uracil-enriched ssDNA template according to the protocol of Kunkel et al. (1987). *In vitro* DNA synthesis was performed with T4 DNA polymerase in conjunction with T4 DNA ligase and 20 µl of the 100 µl reaction analyzed by 1% agarose gel electrophoresis in the presence of 0.5 µg/ml ethidium bromide.

Twenty microliter samples of the resultant double-stranded DNA (dsDNA) were used for transformation into competent *E. coli* MV1190 cells (Sambrook et

al., 1989) and kept on ice for 2 hr, after which time 200 µl of log growth *E. coli* MV1190 cells and 3 ml top agarose were added. The entire suspension was mixed thoroughly and immediately plated out on prewarmed LB-Mg plates and plaques grown overnight at 37 °C. Positive plaques were identified by hybridization to the [^{32}P]-labeled oligonucleotide, picked and grown for 6 hr in 4 ml LB-Mg containing 1:100 of an overnight culture of *E. coli* MV1190 cells. The ds RF form of M13 was then isolated by the lysozyme extraction technique as is used for plasmid minipreparations (Sambrook et al., 1989), and the isolated DNA was restricted with *EcoRI* to reconfirm that these were true positives. Phage supernatant fluids saved from these minipreparations were added to 500 ml LB-Mg containing 5 ml of an overnight culture of *E. coli* MV1190 cells and the dsM13 replicating form (RF) DNA prepared according to the Triton lysis method (Sambrook et al., 1989). Mutated DNA encoding the resultant Gly441-Ile442-Gln443 sequence was then restricted with *BamHI/HindII* and the resultant 800 bp fragment isolated by either electroelution following 1% agarose gel electrophoresis or by the use of Geneclean II Kit and religation into the pSP64-41 expression plasmids encoding either Asp70 or Gly70 to generate constructs No. 10 and 11. Plasmid minipreparations of colonies successfully grown on LB Ampicillin (50 µg/ml) plates were performed using the boiling minipreparation technique and the resultant plasmid DNA restricted separately with *EcoRI* or *BamHI/HindII* to isolate positive clones encoding the Gly441-Ile442-Gln443 sequence. Large plasmid DNA preps of these recombinant clones were then performed by the Triton lysis method, and DNA sequence confirmed across the mutagenesis site prior to its use for *in vitro* transcription.

Further mutagenesis of the wild-type hBuChEcDNA SP6 transcription vector (Prody et al., 1987) was performed in one of two ways. Met437Asp and Tyr440Asp were constructed by the method of Kunkel et al. (1987), as detailed (Neville et al., 1992). All other mutants were constructed using PCR mutagenesis as described by Higuchi (1990). Briefly, complementary pairs of internal, mutagenic oligonucleotides were synthesized for each mutation. These primers were identical to the wild-type BuChEcDNA sequence except for base substitutions in the primer encoding the desired amino acid alteration. Each was employed as one of the primers in separate PCR reactions with the nonmutated BuChE sequence template. The other, external primer lay beyond a unique restriction site. Purification of the PCR products by gel electrophoresis and QIAEX gel extraction kit (Qiagen Inc., Chatsworth, CA) resulted in two fragments with only the mutagenic primer sequence in common. These were then mixed, denatured and annealed, producing some hybrids in which only the mutagenic primer sequence was double-stranded. This mixture was then amplified by PCR, using the external primers to construct a fragment that included the mutant and was bracketed by the two restriction sites. The resultant DNA was restricted with *XbaI* and *StuI* (or *AvaI* and *BamHI*) and ligated into the similarly restricted BuChE transcription vector. To confirm the outcome of this process, the region generated by PCR amplification was subjected to sequencing, employing the external primers and Circumvent sequencing kit (New England Biolabs, Beverley, MA) or the Sequenase system (United States Biochemical Corp.).

8. Construction of a BuChE/AChE chimera

A 232 bp fragment was deleted from the BuChE coding sequence (nt333 through nt564, Prody et al., 1987) by restriction with *AvaI* and *BsmI*. The parallel fragment in the AChE coding sequence (nt438 through nt666, Soreq et al.,

1990) was PCR amplified, using oligodeoxynucleotide primers designed to introduce novel *AvaI* and *BsmI* restriction sites. The primers were:

(+) 438 (-) 666

* *

5'-TTGGAATGCCACAACCTTCCAGAGTGTCTGC-3' 5'-TGACCCGAGCCAAGAAGCGGCCATCGTACAC-3'

The signs (+) and (-) denote upstream and downstream orientations, respectively, and the starred residues, the site where the AChEcDNA sequence was diverted into the customized *AvaI* and *BsmI* restriction sites. Digestion of the PCR product with these enzymes, followed by ligation with the appropriate 3' and 5' BuChEcDNA fragments, completed the chimeric coding sequence. This sequence was propagated in the SP6 transcription vector (Neville et al., 1992). Accuracy of the replaced fragment was verified by DNA sequencing.

D. Expression

1. Synthetic RNA preparation and oocyte microinjection

Transcription *in vitro* from each of the above constructs was performed with the SP6 RNA polymerase essentially as detailed elsewhere (Soreq et al., 1989), and concomitantly with 5'-capping of the produced mRNA transcripts (Zakut et al., 1988). The efficiency of transcription was estimated by analytical agarose gel electrophoresis. Equal amounts of each of the transcripts were injected into mature (stage 5-6) *Xenopus laevis* oocytes essentially as previously detailed (Soreq et al., 1989). Briefly, frogs were anaesthetized on ice and oocytes dissected and gently dispersed in Barth's medium -- 80 mM NaCl, 1 mM KCl, 0.3 mM $Ca(NO3)_2$, 1.6 mM $MgSO_4$, 2.4 mM $NaHCO_3$, 0.4 mM $CaCl_2$, 2 mM Tris HCl, pH 7.4 -- supplemented with 400 mg/l streptomycin sulfate and penicillin G. At least 30 oocytes were injected with each mRNA preparation in several independent experiments (2 ng mRNA in 50 nl H_2O per oocyte). Parallel groups of oocytes were injected with Barth's medium and these served as controls. Incubation was in 96 well microtiter plates for 18 h at 19 °C in groups of 10 oocytes, each group incubated in 200 µl Barth's medium.

Following incubation, oocytes were removed from wells and were homogenized in 1 ml/30 oocytes of 10 mM Tris HCl buffer pH 7.4 containing 1 M NaCl, 1% Triton X-100 and 1 mM EGTA. Homogenates were centrifuged at $4x10^5$ x g for 5 min in a Beckman TL100 tabletop centrifuge (TLA.100.2 fixed angle rotor). Clear supernatant fluids were gently removed and either used immediately for enzymatic analyses or frozen at -20 °C for later use.

Generally, nonlinearized plasmid DNA (5 µg) was transcribed *in vitro*, except for some constructs which were linearized by *SacI* prior to transcription. In these microinjection experiments, the normal BCHE clone (I) was also linearized by *SacI* prior to transcription. In these cases, 150 nl RNA (0.2 µg/µl) was injected. Also, parallel amounts of control RNA were injected into each control oocyte.

2. DNA microinjection into *Xenopus* oocytes and embryos

DNA microinjections into *Xenopus* oocytes were essentially as described for RNA, except that oocytes were subjected to a 10 min centrifugation (600 x g) prior to injection (50 ng/oocyte). To produce embryos, female *Xenopus laevis* were induced to spawn by injection with human chorionic gonadotropin (hCG) 24 hr prior to the experiment. *In vitro* fertilization was accomplished with macerated testis from hCG-treated males in 0.1 X MMR

buffer (MMR = 100 mM NaCl, 2 mM KCl, 1 mM $MgSO_4$, 2 mM $CaCl_2$, 0.5 mM HEPES, 0.1 mM EDTA, pH 7.4) (Ruiz i Altaba et al., 1989). Fertilized eggs were dejellied for 2 hr in 2% cysteine and incubated in 0.3 X MMR containing 5% Ficoll. Cleaving eggs were injected with 2 to 5 ng DNA within the first 2 cleavage cycles and cultured overnight at 17 °C in 0.3 X MMR buffer. One-day-old embryos were transferred through successive dilutions to 0.1 X MMR, and after 2 days to aged tap water. Embryos were harvested by freezing groups in liquid nitrogen and stored frozen until used.

3. Protein blot analyses

rhAChE was purified from approx. 180 day 1 CMVACHE-injected embryos by affinity chromatography, using a modified procedure for the purification of native hAChE (Gennari & Brodbeck, 1985). Briefly, AChE from embryos homogenized in LSD buffer was bound to Sepharose beads carrying N-(1-aminohexyl)-3-dimethylethyl-aminobenzoic amide by shaking overnight at room temperature. Elution was with 0.02 M edrophonium chloride (Tensilon, Hoffmann-LaRoche, Switzerland). Embryonic *Xenopus* AChE was similarly purified from 1-week-old tadpoles, but had to be eluted by boiling in 0.1% SDS. Denaturing SDS polyacrylamide gel electrophoresis and blotting were essentially as described elsewhere (Liao et al., 1992) using a pool of monoclonal antibodies (mAbs; 132-1,2,3; 6 µg/ml each) raised against denatured human brain AChE (Brodbeck & Liao, 1992).

4. SDS-PAGE and immunoblot of oocyte proteins

Following oocyte microinjections and overnight incubation at 16 °C, some of the microinjected oocytes were homogenized in 15 µl/oocyte of a low salt/detergent buffer (0.1 M Na_2HPO_4 containing 1% Triton-X 100, pH 7.0) and sedimented in a microcentrifuge. Clear supernatant fluids corresponding to 2/3 oocyte were loaded onto 0.75 mm thick 10% discontinuous SDS-polyacrylamide gels in parallel with high MW markers and were electrophoresed for 3 to 5 hr at 120 V. Proteins were electroeluted onto nitrocellulose filters overnight in 20 mM Tris, 150 mM glycine, 20% methanol and 0.1% SDS at 50 mA constant current. Immunoreactive BuChE proteins were subsequently detected using the enhanced chemiluminescence (ECL) blotting detection system (Amersham International) using a 1:1000 dilution of the Dako (Glostrup, Denmark) rabbit anti-human serum BuChE as primary antibody and a 1:300 dilution of HRP-linked donkey anti-rabbit Igb Fab' fragment for labeling.

E. Genetics

1. DNA probes and oligonucleotides

Three cDNA probes from the BCHE gene were employed. These were a 2.4 kb hBuChEcDNA encoding the complete BuChE protein (Soreq & Gnatt, 1987), a genomic *EcoRI* fragment containing 190 bp from the 5' end of this sequence (Gnatt & Soreq, 1987) and a 0.7 kb 3'-extension of this cDNA that is expressed in brain tumors (Gnatt, 1990). Oligonucleotide probes synthesized according to the BuChEcDNA sequences were as described (Prody et al., 1986, 1987). To search for AChE-coding regions, a 1.5 kb hAChEcDNA fragment encoding 90% of the AChE protein was employed (Soreq & Prody, 1989; Lapidot-Lifson et al., 1989).

2. Cosmid recombination

Human cosmid libraries, constructed from male peripheral blood DNA in the pcos2 cosmid vector, providing kanamycin resistance, and cloned in DH1 *E. coli* cells, were generously provided by H. Lehrach (Imperial Cancer Research Fund, London), as well as the BHB3169 bacterial strain. Other

bacterial strains employed were AG1, mv1190 and BHB3175. Cosmid recombination was performed according to detailed published procedures (Poustka et al., 1984) with several modifications. Briefly, the 190 bp 5' BuChEcDNA fragment was inserted into the puc118 ampicillin-resistant plasmid (Stratagene), which does not display any sequence homology with the pcos2 vector, and transfected into BHB3175 bacteria. In order to rescue the cosmid library in the form of lambda bacteriophages, Lambda 3169 rescue phages were prepared by prophage induction at 42 °C from concentrated prophage-carrying BHB3169 bacteria grown at 30 °C. Rescue phages at a multiplicity of infection of 50 were added to DH1 cells carrying the cosmid library, and packaging was induced at 42 °C.

Approximately 10^9 colony-forming units of the packaged phages were employed to infect 10^7 BHB3175 cells containing the probe plasmid (carrying the 5'-190 bp BuChEcDNA fragment). Natural recombination was allowed to occur between the probe BuChEcDNA fragment in the plasmid and the genomic BCHEDNA sequences in the cosmids. Recombinants stable to both kanamycin and ampicillin, which implies the presence of recombined pcos2 and puc118 sequences, were selected for dual antibiotic plates. Packaging performed on these recombinants resulted in the formation of cosmid-phage recombinants in transfected AG1 cells. These were tested by colony hybridization with [^{32}P]-BuChEcDNA probe. Large-scale preparation of cosmid DNAs was then performed by the alkaline plasmid method (Sambrook et al., 1989).

3. DNA blot hybridizations and gene mapping experiments

Cosmid or genomic DNA was digested to completion by restriction endonucleases, separated by agarose gel electrophoresis, blotted under 0.5 M NaOH onto nylon Genescreen membranes (NEN, Boston, MA) and UV-cross-linked. Hybridization was in 35% formamide, 6X SSC and 1X Denhardt's solution. When nitrocellulose filters were employed, they were denatured, neutralized, baked *in vacuo* for 2 hr at 80 °C and hybridized in 6X SSC, 5X Denhardt's solution and 5 mM EDTA. Chromosomal blots were donated by Bios Corp. (New Haven, CT) and included DNA from 27 different hybrid human/hamster cell lines carrying hamster chromosomes as well as one or more human chromosomes or fragments thereof, all restricted with *HindIII*. Hybridization was performed as recommended for the Bios Corp. Timeframe System using the large hybridization cassette. Experiments were performed at 65 °C in an incubator with 2.4 kb BuChEcDNA at 10 ng/ml. Probe DNA was multiprime-labeled (Eiberg et al., 1989) yielding a specific activity of $6x10^8$ cpm/µg. Hybridization was for 60 to 90 min. Washes were at 65 °C in 1/10X SSC.

4. Isolation of genomic DNA from peripheral blood.

Peripheral blood cells were separated from 4 ml whole blood drawn into 13.3 mM EDTA, pH 7.5, by density gradient centrifugation in UNI-SEP tubes containing a 1.077 g/ml, 280 mOsm solution of 5.6% polysucrose and 9.6% sodium metrizoate (Eldan Technologies Co., Ltd., Jerusalem, Israel) according to the manufacturer's instructions. White cells were stored at -70 °C. For DNA extraction, cells were thawed and lysed in 3 ml lysis buffer (10 mM Tris-HCl, 400 mM NaCl, 2 mM EDTA, pH 8.2). Cell lysates were digested at 37 °C for 12 to 16 hr with 1 mg proteinase K in the presence of 0.15% SDS. Proteins and polypeptides were removed from the digests by sedimentation with 6 ml of 50% saturated NaCl (ca. 3 M) in a swinging bucket rotor at 1,500 x g for 30 min. Supernatant fluids were transferred to a clean tube to which 2 volumes of ethanol (room temp.) were added. DNA

was spooled out with a glass rod, washed with 70% ethanol (-20 °C) and dissolved in 0.5 ml TE buffer (10 mM Tris-HCl, 1 mM EDTA, pH 8.0). DNA samples were allowed to dissolve at room temperature for 12 to 16 h before determination of their concentrations (A_{260}) and purities ($A_{260}/A_{280} \geq 1.8$). DNA samples were stored at 4 °C.

5. PCR amplification and direct DNA sequencing.

Genomic DNA (ca. 0.1 µg) was PCR-amplified in buffer supplied by Boehringer/Mannheim, supplemented with all four deoxynucleoside triphosphates (dA, dC, dG and dT, 200 µM each), 50 pmol of an oligonucleotide primer and 10 units of *Taq* DNA polymerase in a final volume of 100 µl. Cycling conditions were: denaturation, 94 °C, 1 min (first cycle 3 min); annealing, 50 to 65 °C, 1 min; and elongation, 72 °C, 1 min (last cycle 5 min); 30 to 40 cycles were performed in a GeneAmp PCR System 9600 (Perkin-Elmer/Cetus). PCR products were stored at 4 °C. For DNA sequencing, PCR fragments were purified from agarose gels using the QIAEX gel extraction kit, and were subjected to direct DNA sequencing with the Sequenase kit, version II (United States Biochemical Corp.) according to the manufacturer's instructions, except for the annealing step, which included boiling for 3 min, freezing in liquid nitrogen and annealing at 4 °C for 20 min. [^{33}P]-alpha-dATP was used for labeling. Electrophoresis was on 6% polyacrylamide/7 M urea gels prepared in a SequiGen unit (Bio-Rad, Richmond, CA) according to the manufacturer's instructions.

6. Genomic *SauIIIA* and *RsaI* restriction fragment length polymorphism (RFLP) analyses

PCR fragments spanning the Asp70Gly ("atypical") and the Glu497Val (J variant) substitution regions in the BCHE gene were generated from sampled genomic DNA as described above, and 5 µl were digested directly as recommended by the supplier (Boehringer/Mannheim) in 8 mM spermidine and 50 units of the restriction endonuclease, *SauIIIA* for the Asp70Gly and *RsaI* for the Glu497Val analyses, in final volumes of 25 µl. Incubation was for 4 h at 37 °C. Due to the small DNA fragment sizes, both 10% native polyacrylamide gels and 4% SepRate-SDF gels (Amersham International) were used for the Asp70Gly *SauIIIA* and the Glu497Val *RsaI* RFLP analyses, respectively. Gels were stained after (acrylamide) or during (SepRate-SDF) electrophoresis with ethidium bromide and photographed.

7. RG-PCR introduced *DraI* and *NsiI* RFLP analyses.

Mutagenic PCR primers 13 and 14 (Table 1, in which lower case letters represent deliberately mismatched bases) were designed so that their incorporation into PCR products derived from an allele containing the Thr539 mutation and/or dA at nt2073 would generate a new restriction endonuclease recognition sequence for *DraI* and/or *NsiI*, respectively.

F. Cytology and hematology

1. PCR amplification of genomic DNA sequences

Oligonucleotide primer pairs from the ACHE and BCHE genes were computer-designed to avoid secondary structure interactions (Rychlik & Rhoades, 1989). Primer pairs from the ACHE gene included

(1) P340 (+) 5'-GCTTTCCTGGGCATCCCCTTTGCGGAGCCA-3' and
P790 (-) 5'-CAGGGCCAGCCTCTGATCCAGGAGACCCAG-3';
(2) P1241 (+) 5'-TGAAGGATGAGGGCTCGTATTTTCTGGTTT-3' and
P1695 (-) 5'-GTTGGCCCAGTATCGCATCAGTCGC-3';
(3) P1522 (+) 5'-CGGGTCTACGCCTACGTCTTTGAACACCGTGCTTC-3' and
P1695 (-);

(4) P1712 (+) 5'-ATCCCAATGAGCCCCGAGACCCCAA-3' and
P1869 (-) 5'-GAGCAATTTGGGGAGGAAGCGGTTCCAG-3'.
For BCHE we used
P271 (+) 5'-CTTGGTAGACTTCGATTCAAAAAGCCACAGTCT-3' and
P1588 (-) 5'-ATTTTGCAAAATTTGCCCACCGTTTCACTATGGA-3'.
Primers were marked as (+) for downstream or (-) for upstream, according to their 5' to 3' orientations; numbers indicate the position of the 5'-end residues in these primers within the relevant cDNA sequences (Soreq et al., 1990 for ACHE; Prody et al., 1987 for BCHE).

Distinct 451-, 455-, 174-, 158- and 1318-bp fragments were derived by these primers from the ACHE and BCHE genes, respectively, using the PCR at differential annealing temperatures (72 °C for ACHE and 65 °C for BCHE).

DNA samples (50 to 100 ng) from 19 human-hamster somatic cell hybrids (Bios Corp., New Haven, CT; see Gnatt et al., 1991 for details) and total human or hamster genomic DNA were subjected to PCR amplifiction with the human-specific ACHE and BCHE primer pairs. Cycling conditions: denaturation at 94 °C for 30 sec (first cycle 2 min); annealing at 72 °C (ACHE) and 65 °C (BCHE), 1.5 min; elongation at 72 °C, 1 min (last cycle 6.5 min). Fifty cycles were performed in the presence of 2.5 units of *Taq* DNA polymerase (Boehringer/Mannheim) added prior to the first cycle and following the 25th cycle, 50 pmol of each primer, 200 µM of each deoxynucleoside triphosphate (Pharmacia), 1.5 mM $MgCl_2$, 50 mM KCl, 10 mM Tris-HCl (pH 8.3), 0.01 % gelatin in the final volume of 100 µl, and 100 µl paraffin oil to avoid evaporation, all in 0.6 ml microtubes, using the Programmable Automated Thermal Controller (MJ Research, Boston, MA).

PCR amplification products (10%) were analyzed by agarose gel electrophoresis and compared with known size markers, and their identities vere verified by hybridization to the relevant probes and direct DNA sequencing.

Genomic DNA libraries (Deaven et al., 1986), each composed of fragments from sorted human chromosome 7 or 3 (ATTC, Rockville, MD), were used for direct PCR amplification with the ACHE and BCHE primer pairs. In both cases we ensured that the genomic sequences to be amplified would not include the restriction sites for the enzymes employed in the construction and cloning of these libraries (*HindIII* and *EcoRI* for chromosomes 3 and 7, respectively). Phages (1 x 10^8 PFU in 1 µl SM (Sambrook et al., 1989) were lysed in 50 µl double-distilled water by heating to 70 °C for 5 min, followed by two treatments of freezing in liquid nitrogen and then thawing. The resultant lysates were directly employed for PCR amplification and analysis.

Following gel electrophoresis, amplification products were hybridized as detailed (Soreq et al., 1990) in a hybridization oven (HyBaid, Teddington, UK) with a 2.2 kb fragment of ACHE DNA (clone GNACHE; Soreq et al., 1990) or a 2.4 kb BuChEcDNA (Gnatt et al., 1991).

2. Chromosomal gene mapping by *in situ* hybridization

Radioactive *in situ* hybridization to spread mitotic chromosomes was performed essentially as described elsewhere (Zakut et al., 1989; Soreq et al., 1987) except that an additional two 15 min washes were performed at 60 °C in 1/10X SSC. Following the hybridization, chromosomes were Giemsa stained and covered by a thin Optilux (0.75%, Becton Dickinson, Lincoln

Park, NJ) layer prior to emulsion autoradiography, to prevent interaction between the photographic emulsion and the Giemsa stain.

Fluorescent *in situ* hybridization (FISH) was applied to spread mitotic chromosomes, using cesium-purified biotinylated AChE DNA probes and fluorescence-intensified digital imaging microscopy (Viegas-Pequignot et al., 1989). The probes employed were electrophoretically separated and electroeluted 2.2- and 5.5-kb AChE DNA inserts (Soreq et al., 1990).

3. Cytochemical staining and electron microscope examination of *Xenopus* embryos

Two- or 3-day-old embryos were fixed for 1 h in 1% paraformaldehyde, 2.5% glutaraldehyde in 0.1 M phosphate buffer, pH 7.4, washed 3 times and dissected into 3 to 4 pieces. AChE activity was detected by the thiocholine method. Cytochemical staining for catalytically active AChE (Karnovsky, 1964) was performed within 3 days: 15 to 20 min at 4 °C in 1.5 mM ATCh, 5 mM Na citrate, 3 mM Cu sulfate and 0.5 mM K ferricyanide in 65 mM acetate buffer, pH 6.1. After staining and rinsing, embryos were transferred to 1% osmium for 1 h, dehydrated in ethanol, embedded in Epon and sectioned. Sections of 700 Å close to the exposed surface were counterstained with uranyl acetate and Pb citrate, and examined with a Philips 300 electron microscope.

4. Administration of antisense oligonucleotides

The antisense oligodeoxynucleotide employed was phosphorothioated AS-ACHE (5'-CTGCGGGGGCCTCAT-3'), designed to complement the initiator AUG domain in AChEmRNA (Soreq et al., 1990). Intraperitoneal injection of AS-ACHE (up to 10 µl/*g*) into 3-week-old female Sabra mice was performed by dilution with phosphate buffered saline (PBS) using a Hamilton syringe. The final concentration of AS-ACHE reached 5 µg/g, following our previous experiments in cell cultures (Patinkin et al., 1990; Lapidot-Lifson et al., 1992) and studies of others (Agrawal et al., 1991).

5. In situ hybridization to bone marrow cells

[^{35}S]-labeled *in vitro* RNA transcripts (10^7 cpm/µg) were produced using the Amersham RPN 2006 kit and RNA polymerases from Boehringer/Mannheim, using plasmids linearized with *HindIII*, *XhoI* for the sense and antisense ACHE RNA probes and with *ApaI*, *SmaI* for the sense and antisense BuChEmRNA transcripts, respectively, all according to the manufacturer's instructions. Radiolabeled probes were subjected to limited alkaline hydrolysis for 20 min and resultant 200 to 400 base fragments were separated from unincorporated nucleotides by G-50 Sephadex column chromatography (Wilkinson, et al., 1987).

Bone marrow squeezed from dissected femur bones was smeared as single cell layers on microscopic slides coated with 3-aminopropyltriethoxysilane (TESPA, Sigma), to prevent loss of cells during the experimental procedure (Rentrop et al., 1986). Slides were dried at room temperature for 2 hr, fixed for 20 min at room temperature in 4% paraformaldehyde dissolved in PBS, washed once with 3x PBS and twice with 1x PBS, dehydrated through ethanol series, air-dried and stored at -20 °C for up to 2 weeks. For *in situ* hybridization, slides went through refixation, 0.2 M HCl incubation for 20 min to reduce nonspecific probe binding, proteinase K treatment, acetylation and dehydration as described (Rangini et al., 1991). Hybridization was performed in the presence of [^{35}S] RNA probes (approx. 1 x 10^7 cpm/µg, 0.5 x 10^6 cpm per slide) (Rangini et al., 1991), except that

no adenosine-5'-phosphorothioate was added. Exposure to photographic emulsion (Kodak NTB-2) was for 6 weeks. Counterstaining was made with May-Grunwald Giemsa.

The *in situ* hybridization results were analyzed using a Nikon Microphot microscope equipped with a single slide automatic stage, automatic focus and 60X plan apo-oil immersion objective and connected through an interface to a Magiscan Image Analysis microscope controller (Applied Imaging International Ltd, Dukesway, U.K.). Image analysis was carried out by the software package "GENIAS" which counts silver grains, measures cell parameters, and evaluates association of grains with cells. Data management was then performed using the "RESULTS" program, which examines the statistical significance of data obtained from "GENIAS" and subjects area and perimeter measurements to various statistical hypothesis tests.

Briefly, monochromatic images of the examined cells were captured using a red filter to improve the contrast. Since the silver grains and cells were at different focal planes, the grains were focused accurately, as their best resolution was required. Grain counts were detected automatically based on their darkness, and high-frequency noise information included in the grain image was automatically subtracted. Cell borders to be measured were manually delineated, after which grains were counted and measured separately for each cell. Background grain density was measured in parallel and subtracted from the experimental results. Collected data included cell counts and parameters (measured cell areas), number of grains per cell and per unit area and the statistical significance of variations of these parameters. Presented data are average result for separate *in vivo* treatments, with approximately 40 cells at different developmental stages analyzed/sample with each of the employed RNA probes in bone marrow preparations from four different mice/treatment.

III. RESULTS

A. Human gene architecture

1. ACHE sequence and structure

a. construction and screening of cDNA libraries

The differential screening procedure described in Methods resulted in the isolation of two similar 1.5 kb clones from neonate brain basal nuclei, Rescreening of several additional libraries (Fig. 2A) with [^{32}P]-labeled NBG8A resulted in the isolation of over 25 positive clones, all encoding a polypeptide with the expected AChE active site sequence. Subsequently, an expression library in the lambda ZapII phage vector using total RNA from adult basal nuclei was prepared and found to be enriched in AChEcDNA clones. Two clones, designated ABGACHE, included most of the coding and 3'-nontranslated sequence presented in Fig. 2A, and were essentially similar to other cDNA clones isolated from different libraries. All the isolated clones terminated about 300 nucleotides downstream from the expected initiator AUG codon. One 500 bp muscle clone, designated FEMACHE, included a complete 3'-nontranslated region ending with a polyadenylation site and a poly(A) tail. Most of the isolated clones included the regions complementary to the oligodeoxynucleotide probes CTACHE and OPSYNO, and corresponded exactly to the peptide sequences used to design them (Fig. 2B, amino acids encoded by nucleotides 1939 to 1974 and 847 to 876, respectively). In addition, the isolated cDNA clones all contained large identical overlapping sequences, suggesting that they were derived from similar mRNA transcripts.

b. search for the missing 5'-end of the ACHE coding sequence

To derive a complete AChE coding sequence, probe K-153, a 17-mer, 5'-CG GCC ATC GTA CAC GTC-3', was designed according to the nucleotide sequence at the 5'-end of the cDNA clones. K-153 is complementary to the sequence encoding the AChE-specific peptide AspValTyrAspGlyArg, and was used to screen a human genomic DNA library. The resultant genomic DNA clone, designated GNACHE, included part of the coding region for AChE in addition to intronic sequences. In particular, clone GNACHE included the absent upstream sequence encoding the N-terminus of AChE and a putative signal sequence preceded by a methionine residue. The AUG codon encoding this methionine was embedded in an appropriate consensus sequence for initiation of translation (Kozak, 1986) and was preceded by a potential splice signal at the same position (nucleotide 139, Fig. 2B) where both the human BCHE gene (Arpagaus et al., 1990) and the *Torpedo* ACHE gene (Maulet et al., 1990) appear to be spliced. Comparative analysis of clones GNACHE and ABGACHE revealed splice sites at nucleotides 1227, 1713 and 1822 and three introns (0.35, ca. 1.1 and 0.8 kb, respectively). The latter two introns were located at the same sites found in the electric fish ACHE gene (Maulet et al., 1990), reconfirming the presumed common origin of the ACHE genes shared by these two evolutionarily remote species. The 0.35 kb intron, which was found in mouse as well (Li et al., 1991) does not exist in *Torpedo* and apparently developed later in evolutionary history.

Computer analysis of the AChE coding sequence presented a hypothetical stable 300 nucleotide secondary structure of stems and loops at the 5'region of this sequence with a free energy of -117.0 kcal/mole (Devereux et al., 1984), higher than that demonstrated for the transcription attenuating region in the genome of SV_{40} (Kessler et al., 1989). This predicted folding pattern, presented in Fig. 3, could potentially prevent reverse transcriptase and/or DNA polymerase from synthesizing this sequence, apparently explaining the 5'-attenuated cDNA clones (Fig. 2A).

c. Promoter sequence and composition

Sequencing of the upstream sequence (clone GNACHE, Soreq et al., 1990; Fig. 4) revealed oligonucleotide motifs characteristic of binding sites for several known transcription factors (Faist & Meyer, 1992). These included eight MyoD motifs, characteristic of myogenic expression (CANNTG, Tapscott et al., 1988), the enhancer GCCACCTG octamer (E-box) controlling production of the heavy chain immunoglobulin gene (Ephrussi et al., 1985), and compatible with hematopoietic expression and 12 occurrences of the GGGCGG motif specific to the SP1 transcription factors which enhance productive transcription (Lemaigre et al., 1990). The cAMP response element ATF/CREB (ACGTCA (Maekawa et al., 1989)), the EGR-1 element (GCGGGGGCG, 3 sites) common in brain-specific genes subject to signal transduction pathways (Cao et al., 1990), and the AP2 element (CCCC/AGGG/CG/C, 2 sites) characteristic of genes expressed in embryonic neural crest lineages (Mitchell et al., 1991) and presumed to interact with SP1 factors (Williams & Tjian, 1991) were also found.

Elements indicating developmental control included the CGAGCG and CACTCA sequences (2 sites) that interact with the embryonically active Zeste factors, and the GAGA (AGAGAGAG) motif important for the functioning of distant enhancer elements during early *Drosophila* development (Biggin & Tjian et al., 1989). Further downstream, this sequence included TATA and CCAAT elements and the NFkB element (GGGA/GA/CTNTCC, 2 sites) characteristic of genes active in the immune and other hematopoietic lineages (Molitor et al., 1990), and implicated with the control of transition from the G0 to G1 phases in the cell cycle (Baldwin et al., 1991). Figure 4 presents the upstream sequence and these different sequence motifs.

d. Base composition and codon usage in the ACHE coding sequence

The AChE and BuChE coding sequences displayed almost mirror-image usage of nucleotides, with AChEcDNA being enriched in G,C-residues (63.8%), and BuChEcDNA in A,T residue (63.1%). Consequently, the distribution of codons in the ORFs is clearly different for the two genes. For most of the amino acids in AChE, G,C residues appear in third base positions. The opposite is true for BuChE, which is most apparent for amino acids with multiple codon choices (Table 1). For example, 45 of the 68 leucine residues in AChE are encoded by CTG, whereas in BuChE, only six of the 55 leucines are translated from this codon (Ben-Aziz et al., 1991). In addition, amino acids encoded by G,C-rich triplets (arginine and alanine but not serine and lysine) are more frequent in AChE than in BuChE. Moreover, certain codons are completely absent in the AChE but not in the BuChE gene, like ATT and ATA for isoleucine or AGA for arginine. Thus, both the nucleotide composition and the third nucleotide choices for AChEcDNA are typical of housekeeping genes (Holmquist, 1989), and its base and amino acid composition predict thermal stability and long half-life both for AChEmRNA and for its protein product.

It is interesting to note that the proteins encoded by these two sequences have almost identical amino acid compositions. In particular, the content of acidic and hydrophobic residues was precisely retained to be almost equal in the two proteins (Ben-Aziz et al., 1991). The somewhat lower content of basic amino acid residues (arginine + lysine) in AChE (53 as compared with 61 in BuChE) deviates from this rule, and results in a more acidic isoelectric point predicted for AChE (5.42 vs. 7.39 for BuChE).

e. amino acid homologies between proteins of the ChE family

Comparative analysis of the amino acid sequence inferred for the deduced hAChE sequence, hBuChE, *Torpedo* AChE and *Drosophila* ChE, *Drosophila* esterase 6 and bovine thyroglobulin revealed considerable sequence similarities (Fig. 4), higher than the percent of identically aligned residues observed at the nucleotide level for all of these sequences (Soreq et al., 1990). The human AChE inferred from this sequence has three potential sites for asparagine-linked carbohydrate chains (Fig. 2B), fewer than the four glycosylation sites in *Torpedo* AChE (Schumacher et al., 1986) and the eight sites in hBuChE (Prody et al., 1987; McTiernan et al., 1987). Its lack of sequence homology to serine proteases distinguishes this protein as a type B carboxylesterase of the cholinesterase family (Soreq & Zakut, 1993) with a C-terminal peptide that is characteristic of the soluble, asymmetric AChE forms (Taylor et al., 1987; Maulet et al., 1990; Sikorav et al., 1988). It contains seven cysteine residues as compared with eight for both *Torpedo* AChE (Schumacher et al., 1986) and hBuChE (Fig. 2, Prody et al., 1987; McTiernan et al., 1986). Three intrasubunit disulfide bonds would be predicted at Cys100-Cys127, Cys288-Cys303 and Cys440-Cys560. A fourth predicted disulfide bridge involves Cys611 which in all known asymmetric ChEs appears to be covalently attached to the parallel cysteine residue of an identical catalytic subunit (Taylor et al., 1987; Lockridge et al., 1987).

f. consensus peptide motifs

Several lines of evidence from various fields of biological research suggest that activation of cholinergic signaling pathways is directly correlated with cell division. A summary of these indications is presented in Table 2. For example, treatment of *Xenopus* oocytes with ACh and its analogue, carbamylcholine, enhances phosphoinositide turnover and releases the oocytes from their meiotic block (Oron et al., 1985). These agents also stimulate phosphoinositide turnover in primary glial cells in culture (Askhenazi et al., 1989). When transfected with particular subtypes of the muscarinic ACh receptor, the carbamylcholine-treated cultured glial cells display increased DNA synthesis (Askhenazi et al., 1989). Enhancement of phosphoinositide turnover, in turn, has been correlated with developmentally induced alterations in the phosphorylation status of substrates of the CDC2 family of protein kinases, the universal controllers of cell division (Lapidot-Lifson et al., 1989; Balduini et al., 1987; Laskey et al., 1989; Moreno & Nurse, 1990). Thus, conceivably, the changes in cell division caused by ACh administration may be associated with variations in the activity of the CDC2-related kinases.

Over the past several years, it has become apparent that the progression of the cell cycle is critically dependent on phosphorylation events mediated by CDC2-related kinases. Partial lists of the *in vitro* substrates of these kinases include both nuclear proteins (e.g., lamin, histones, RNA polymerase) and cytoplasmic proteins (e.g., pp60c-src) (Moreno & Nurse, 1990). These substrates share two common features: they all perform cell cycle-related functions, and they all contain the peptide motif Ser/Thr-Pro-X-Z (where X is a polar amino acid and Z is a basic amino acid). In the nucleus, lamin B is one of the proteins responsible for nuclear organization, nucleolins are thought to function in nucleolar organization, and histones are important for DNA organization (Moreno & Nurse, 1990). In the cytoplasm, pp60c-src is apparently involved in the synthesis of the PIP_2 phosphoinositide from phosphatidyl inositol and its monophosphate. Phosphorylation of these proteins has been shown to alter

their biochemical properties in different ways, in some cases, stimulating function, and in other cases suppressing function. Table 3 presents these examples and the relevant peptide motifs.

It is most interesting to note that both AChE and BuChE contain the Ser/Thr-Pro-X-Z motif, thus raising the possibility that these proteins too are substrates for CDC2-related kinases (Table 3). There are three such motifs in the catalytic domain of AChE (starting at residues 103, 110, and 216) and one in BuChE (starting at residue 210). Conceivably, AChE and BuChE are substrates of distinct CDC2-related kinases that, for example, are specific to particular cell types and/or cell differentiation stages. This notion is strengthened by the recent finding of CHED, a novel CDC2-like kinase, the expression of which is required for megakaryocytopoiesis in a manner similar to that of BuChE (Lapidot-Lifson et al., 1992). Additional biochemical experiments will be required to determine whether ChEs are in fact substrates of specific CDC2 kinases and, if so, how their phosphorylation state affects the biological function of ChEs and of their counterpart CDC2 kinases in normal cells and in tumor cells.

2. Human ACHE and BCHE are encoded by two distinct genes

The presence of both BCHE and ACHE coding sequences in a human cosmid library was first verified by DNA blot hybridization. For this purpose, the cosmid library was amplified and the DNA extracted from it was digested to completion with *EcoRI* and electrophoretically separated in parallel with human genomic DNA. Blot hybridization with BuChEcDNA and AChEcDNA probes confirmed that both sequences are represented in this library (not shown). Homologous recombination screening, using a 5' 190 bp fragment from BuChEcDNA cloned in puc118, resulted in the isolation of four different cosmid pCosCHEDNA clones designated C_{1-4}. Figure 5A schematically presents the recombination experiment. DNA extracted from each of the pCosCHEDNA clones was tested for its ability to hybridize with BuChEcDNA and AChEcDNA. All four clones were clearly positive with the first probe but negative with the latter, demonstrating that they all included BuChE-coding sequences but not AChE-coding ones. The blot hybridization data for this experiment are shown in Figure 5B. Enzymatic restriction, agarose gel electrophoresis and ethidium bromide staining of these pCosCHEDNA preparations revealed that the four isolated cosmid DNA fragments were all approximately 50 kb in size and displayed highly similar, although not identical, restriction patterns with four different enzymes. Blot hybridization with BuChEcDNA again demonstrated similar restriction patterns, suggesting that all four cosmid clones were derived from the same gene and encompassed overlapping DNA fragments. Figure 6 presents these DNA blots and their intricate restriction patterns.

All four cosmid clones originally had to include the 5' 190 bp sequence to recombine with the puc118 plasmids which contributed their ampicillin resistance. Moreover, they all hybridized with the 0.7 kb 3'-extension of BuChEcDNA, designated Gb5, found in cDNA libraries from nervous system tumors (Gnatt et al., 1990). This demonstrated that all four cosmids included the entire sequence encoding BuChE plus adjacent sequences. In addition, the cosmid DNAs appeared to contain several intron sequences. For example, the enzyme *HincII*, having a unique restriction site in BuChEcDNA (Prody et al., 1987; Lovrien et al., 1978), restricted the various cosmid DNAs into at least three BuChEcDNA-hybridizing fragments (Figure 6). This suggested the existence of more than one intron in these

DNA fragments, in complete agreement with observations of others (Chatonnet & Lockridge, 1989). It should be mentioned in this context that the 190 bp fragment that was used to recombine with the CHEDNA cosmids had to be actively integrated into the isolated cloned sequences. Therefore, the organization of these DNA fragments is not necessarily identical to that of the native gene; hence these blots were not used to construct detailed restriction maps for the CHE gene. Since the Gb5 3'-extended fragment was mapped to the unique 3q26-ter position by *in situ* hybridization, these findings also indicated that all of the isolated pCosCHEDNA clones were derived from a single BuChE-encoding gene, localized on the long arm of chromosome 3.

The assignment of the CHE1 gene to a unique position on chromosome 3 was further confirmed by DNA hybridization employing chromosome blots (Bios Corp.). These included DNA from different human/hamster hybrid cell lines carrying one or more human chromosomes (D'Eustachio & Ruddle, 1983). Only DNA from cell lines including human chromosome 3 contained the informative 2.4 kb *HindIII* restriction fragment hybridizing with BuChEcDNA (Soreq & Zakut, 1990a; McGuire et al., 1989). Furthermore, the pCosCHEDNA fragments were identical with those observed in parallel lanes loaded with DNA from human lymphocytes. In contrast, hamster genomic DNA or hamster/human cell hybrids carrying human chromosomes other than number 3 displayed no positive bands when hybridized with [^{32}P]-BuChEcDNA. Figure 7 presents representative examples for these hybridization results. Summary of the somatic cell hybrid mapping panel clearly demonstrated full concordance with the chromosome 3 assignment in all of the five examined cell lines which carried this chromosome (Gnatt et al., 1991). In contrast, all other chromosomes, including chromosome 16, appeared not to carry BuChEcDNA-positive sequences. Exclusion of chromosome 16 was shown by two independently derived discordant hybrids, and one hybrid cell line with chromosome 3 as the only human chromosome was clearly positive for the specific human fragment.

a. <u>location of ACHE within chromosome 7</u>

Direct PCR amplification with somatic cell hybrids and chromosome-sorted libraries was performed under species-specific conditions, so that human but not hamster DNA gave rise to four different PCR fragments informative of the ACHE gene and one for the BCHE gene. DNA blot hybridization was employed to exclude the possibility of weak or invisible fragments. ACHE-specific PCR products appeared with DNA from 2 of the 19 cell lines employed, both of which contain human chromosome 7. In contrast, no signal was observed with DNA from any of the other lines containing any human chromosome except 7 (Table 4). The validity of this chromosome assignment was examined by reconfirming our previous mapping of the BCHE gene to chromosome 3, which was performed by DNA blot hybridization using the same somatic hybrid cell panel (Gnatt et al., 1991). Ethidium bromide-stained agarose gel revealed that the 1318-bp BCHE-specific PCR product was generated from DNA from two cell lines that contain human chromosome 3. The identity of the PCR fragments was verified by hybridization using [^{32}P]-BuChEcDNAS probes.

Regional mapping of the ACHE gene on chromosome 7 was achieved by fluorescent chromosomal *in situ* hybridization using a biotinylated ACHE DNA fragment as a probe (Fig. 8). Fifteen metaphases were analyzed, all of which carried at least one fluorescent spot on 7q22 (five with one spot, seven with two spots, and three with three spots). Two of these cells were

also labeled by one spot at the 11p11 position, one with one spot on 12q13, and another with one on 12q14. These minor labelings were considered insignificant in view of the negative PCR results with somatic cell hybrids carrying chromosomes 11, 12 and 13, using four different ACHE-specific primer pairs. Additional *in situ* hybridization experiments, using a 5.5-kb genomic probe from the ACHE gene (clone GNACHE, Soreq et al., 1990), also revealed labeling on chromosome 7.

An independent assignment of the ACHE gene to chromosome 7 was obtained by direct PCR amplification using DNA from chromosome-sorted libraries. Lysed lambda phages containing fragments from sorted chromosome 7 or chromosome 3 (Deaven et al., 1986) libraries supported the appearance of the ACHE-specific PCR product from the human chromosome 7 library, but not from the chromosome 3 library. In contrast, the human BCHE-specific fragment was produced from chromosome 3 library phages, but not from chromosome 7 phages. Both of these PCR products hybridized with the relevant probes, confirming their identity as human ACHE- and BCHE-derived sequences; the hamster DNA impurity in the chromosome 7 library did not interfere with the PCR reaction because of the species-specific conditions that were employed.

b. ACHE restriction analysis

In order to initiate an RFLP study of the ACHE gene, DNA was extracted from peripheral blood of several apparently healthy, unrelated individuals and was subjected to restriction analysis by DNA blot hybridization using various probes (Fig. 9A,B). These included the ACHE expression construct, the genomic DNA clone, GNACHE and PCR fragments derived from the ACHE gene (Fig. 9A and Soreq et al., 1990; Ben Aziz-Aloya et al., 1993). Parallel hybridizations were performed with similarly digested DNA from the GNACHE clone using sequence-specific oligodeoxynucleotide probes (Fig. 9C). All of the PCR probes created subset autoradiogram patterns of those obtained with probes GNACHE and the expression construct (Fig. 9B), enabling the construction of a complete restriction map of the ACHE gene and its flanking regions for the enzymes used (Fig. 9A). No RFLPs were detected using these probes and individuals, nor were differences detected in studies of 102 additional unrelated Europeans using these and other restriction enzymes (*EcoRI* and *TaqI*). A restriction analysis of the human ACHE genomic clone GNACHE (Fig. 9C), generated using primers 1 to 10 as probes (1 to 8 are shown), yielded an identical map.

3. human genetics

To examine whether mutations in ACHE and BCHE were associated with each other, and whether the intragenic linkage reported for the ACHE and BCHE mutations in Americans is universal, we studied frequencies of these mutations in European and trans-Caucasian Georgian Israelis. To this end we employed PCR amplification followed by DNA sequencing and enzymatic restrictions, and compared the frequencies we found to corresponding reported phenotype data. Georgian Jews' Asn322 ACHE was a rather low 7.0% and was totally linked with a Pro446 mutation, in agreement with a recent report. However, in BCHE, Gly70 was a relatively high 5.8%, and the Val497 and Thr539 mutations were not found, either in Georgian or in European Jews, in contrast with reported findings in unclassified Americans. In addition, no intergenic associations were observed between the point mutations of ACHE and BCHE.

a. detection of mutations in the human ACHE and BCHE genes

In order to detect and define the distribution of ACHE and BCHE mutations and reveal characteristic haplotypes, we examined genomic DNA from 127 individuals. To this end, we used suitable primers (Table 5) to PCR amplify the amino acid 322 and 446 regions of the ACHE gene and the amino acid 70, 497 and 539 regions and nucleotide 2073 at the 3'-noncoding region of the BCHE gene (Fig. 10). The PCR fragments obtained were purified and analyzed by DNA sequencing and/or were directly subjected to restriction analysis to detect naturally occurring or RG-PCR-introduced RFLPs. Examining the ACHE codon 322 by DNA sequencing revealed genotypes homozygous for histidine (Yt^a blood group), homozygous for asparagine (Yt^b) and heterozygous genotypes (Fig. 10). All of the homozygotes for His322 or Asn322 were also homozygous for the Pro446 common codon (CCC) or the mutated codon (CCT), respectively, as was determined by DNA sequencing (data not shown). Furthermore, all heterozygotes for the His322Asn substitution were also heterozygous at codon 446, in agreement with findings in Americans (Bartels et al., 1993). The Pro561Arg mutation was found in clone GNACHE (Soreq et al., 1990), a 6.1 Kb human ACHE genomic clone; nevertheless, it was not in linkage with the Pro446 or Asn322 ACHE mutations (Karpel et al., 1993). Examining the BCHE codon 70 by *SauIIIA* RFLP analysis and DNA sequencing, and the nucleotide at position 2073 by RG-PCR-introduced *NsiI* RFLP analysis, permitted the discrimination among homozygotes of the common alleles (Asp70 and 2073dA), homozygotes of the rare alleles (Gly70 and 2073dG) and heterozygotes (Fig. 10). Examining the BCHE codons 497 and 539 by DNA sequencing and/or by *RsaI* or RG-PCR-introduced *DraI* RFLP analysis, respectively, revealed in the populations examined only the common allele, which encodes Glu497 and Ala539 (Fig. 10). In most cases haplotypes could be extracted from each known genotype.

b. discordance of phenotypically effective mutations in the ACHE and BCHE genes

Associations were sought between the His322Asn substitution in ACHE and Asp70Gly substitution in BCHE among 86 unrelated Jews of Georgian origin. DNA sequencing revealed 12 heterozygotes for the ACHE His322Asn substitution and 74 His322 homozygotes. Ten out of these same individuals were heterozygous for the BCHE Asp70Gly substitution, and the remaining 76 homozygous for Asp70. Of 86 tested, no homozygous individual was detected having the rare allele of any of the genes, only 2 had both mutations and 66 had neither. These numbers translate to allele frequencies of 7.0% for ACHE Asn322 and 5.8% for BCHE Gly70. These allele frequencies, combined with the assumption of nonassociation, predict 1.4 and 75.3 individuals, respectively, which correspond reasonably with our findings. We conclude, therefore, that these ACHE and BCHE mutations are not associated.

c. Frequent ACHE and BCHE mutations among Jewish populations

The allele frequencies of the ACHE Asn322 and BCHE Gly70 mutations may be compared with those found in phenotype surveys for other Jewish populations (Fig. 11). The ACHE Asn322 allele frequency, phenotypically the Yt^b blood group (Lockridge et al., 1992), was found to be higher than the average frequency of the Yt^b allele among Europeans, but lower than in any other Jewish population surveyed. On the other hand, the frequency of the BCHE Gly70 allele, phenotypically "atypical" BuChE (Neville et al., 1990a), was found to be higher than in every Jewish population examined except the Iranian. Taking into account that the Georgian community, like the Iranian and Iraqi communities are all descended from the ancient Babylonian Jews, the similarity in the BCHE allele frequency and the dissimilarity in the

ACHE allele frequency suggest that the ACHE and BCHE genes were subjected to different selective pressures and/or founder effects.

d. ACHE and BCHE haplotype analysis

In the ACHE gene, complete association was observed between the ACHE codons 332 and 446 among Georgians, suggesting the existence of complete linkage, yielding two possible haplotypes for them: His322/Pro446(CCC) and Asn322/Pro446(CCT). These results are in agreement with the findings of Bartels et al. (1993) regarding an American population.

Because significant linkage disequilibrium of the BCHE Asp70Gly, Glu497Val and Ala539Thr substitutions, and looser linkage to the 2073dA/dG mutations were reported for Americans (Bartels et al., 1992a,b), we wished to test the universality of this phenomenon. Therefore we extended the study and determined BCHE haplotypes of 13 Georgians heterozygous for Asp70Gly and 24 homozygous for Asp70 (Table 6). Surprisingly, all of the 37 individuals examined carried only the common codons at positions 497 and 539, coding glutamate and alanine, respectively. Together with the nt2073 variants, this yielded four different haplotypes out of the possible 16 for these four point mutations (Table 6). The other 12 haplotypes reported in the American survey (Bartels et al., 1992a,b), which involve the GluE497Val and Ala539Thr substitutions, were not found in the populations we studied. Linkage disequilibrium analysis of haplotypes containing the codon 70 and nucleotide 2073 variants (Iannuzzi et al., 1989) yielded a linkage disequilibrium constant of 0.16, indicating loose linkage, consistent with the previous report (Bartels et al., 1992b).

e. human genetics, summary

The ACHE gene, at 7q22, is not genetically linked with BCHE, mapped to 3q26, but as there is conceivably a functional interrelationship between their encoded enzymes, we searched for an association of their mutations. A screen for the more prominent ACHE and BCHE mutations (Asn322 and Gly70, respectively) revealed numbers of single and double mutants and wild-types compatible with nonassociation. This result is expected if no selection pressure exists for or against double mutants. The AChE amino acid 322 is located on the surface of the protein, well away from the active site (Sussman et al., 1991; Soreq et al., 1993) and is unlikely, when mutated, to alter functional properties of the enzyme. Indeed, no such evidence has been presented to date. Therefore, the finding of no association of this ACHE mutation with any BCHE mutation is not surprising.

We were able to confirm the recently reported (Bartels et al., 1993) total linkage between ACHE codons 322 and 446 mutations. We also found that the Pro561Arg substitution was not linked to the above mentioned ones. These findings led to the conclusion that out of eight possible haplotypes for three point mutations of the ACHE gene, four predominate: His322/Pro446(CCC)/Pro561 or Arg561 and Asn322/Pro446(CCT)/Pro561 or Arg561, of which the ones with Pro561 are most prevalent. We were surprised, however, to find an absence of the Glu497Val and Ala539Thr substitutions in BCHE among Israelis of European or trans-Caucasian Georgian origin, because these mutations were reported to be tightly linked to one another and to the Asp70Gly substitution in Americans (Bartels et al., 1992a,b). We have no explanation of this dissimilarity of findings, other than the differences in populations studied. This, in turn, suggests that for the BCHE gene in the Israeli subpopulations studied, only four haplotypes exist out of the 16 possible for four point mutations. These

are Gly70/Glu479/Ala539/2073dA or 2073dG (haplotypes II and IV, respectively, Table 6), and Asp70/Glu479/Ala539/2073dA or 2073dG (haplotypes I and III, respectively, Table 6), of which the latter two are most frequent. The Gly70 and the 2073dG mutations thus seem to have been introduced and established early in human evolution, as these exist in different ethnic groups. In contrast, the other two BCHE mutations were, so far, observed only in an unclassified group of Americans, and in linkage with the Gly70 substitution but not with the 2073dG alteration. This implies that they first appeared on a Gly70 allele and were subsequently established in European ancestors of Americans.

Our data are consistent with a Hardy-Weinberg equilibrium for Asn322 ACHE and Gly70 BCHE, indicating no major selective effect due to either of these alleles. This could be because our sample size was too small to detect slight deviations, reflecting mild selection pressures. Alternatively, or additionally, this could be due to a balance between positive and negative selection pressures: The rare Yt^b allele may be selected against in populations, especially ones characterized by large numbers of offspring, as anti-AChE antibodies may arise in mothers' sera directed against the AChE of their embryos. Individuals homozygous for one allele may carry the antibody to the protein produced by the other allele (Levene et al., 1987), these individuals being those having received transfusions of incompatible blood, and possibly homozygous mothers of heterozygous fetuses. Because AChE is an indispensable protein, expressed very early in fetal development (Soreq & Zakut, 1993), this may lead to abortion or retardation of fetal growth. In chorionic villi only BCHE, not ACHE, is expressed, suggesting that BuChE has an even earlier role in embryogenesis than that of AChE (Zakut et al., 1991). In this case, heterozygosity of "atypical" (Gly70) and common BCHE alleles may confer developmental advantage: in the presence of natural or man-made anti-ChEs, such embryos will have sufficient BuChE activity, as opposed to embryos homozygous for the common allele, whose enzyme is very susceptible to inhibition. The "atypical" homozygous embryo, having very low levels of activity, may also be at a disadvantage. The Middle Eastern diet has long been characterized by the *Solanum*, eggplant (*S. melongema*), which was first domesticated in this area, and which contains solanine-derived glycoalkaloids, potent inhibitors of normal, but not "atypical," Gly70 BuChE (Harris & Whittaker, 1962; Neville et al., 1992a). The similarity of the BCHE Gly70 allele frequency of Georgian Jews to that of Iraqi and Iranian Jews, having the same ancestry, may thus reflect a continuous selective advantage. The reduced ACHE Asn322 allele frequency among Georgians, as compared with Iraqi and Iranian Jews, all drawn from the same gene pool, may likewise be explained by a negative immunogenic selection pressure. In both cases, the different frequencies of the Georgian from the Iraqi and Iranian Jewish populations probably reflect founder effects in the ethnically isolated population of trans-Caucasian Georgian Jews.

4. Gene expression

a. transcriptional control

1. structure-function analysis of the ACHE promoter region: transcriptional potential in *Xenopus*

In search of the promoter region controlling ACHE transcription, we examined a 2.2 kb genomic DNA fragment located upstream from the initiator AUG in clone GNACHE. The ability of this 2.2 kb ACHE upstream sequence to drive transcription was studied in microinjected *Xenopus* oocytes and embryos. To this end, this sequence was ligated, either in its full form

or following enzymatic restrictions with *KpnI*, *XhoI* or *PvuII* (K, X or P forms, Fig. 12) to AChEcDNA comprised of exons 2, 3, 4 & 6 (Fig. 12; see also Soreq et al., 1990; Li et al., 1991 for gene structure), to create the HpACHE constructs. DNAs were injected into oocytes or early cleavage embryos, and transcriptional activity was determined by reverse transcription and PCR amplification (RNA-PCR) using human AChEcDNA specific primers (Fig. 12). AChEcDNA ligated to the cytomegalovirus enhancer-promoter region (CMVACHE, Velan et al., 1991b) was also injected. RNA from oocytes and embryos injected with the CMVACHE or the complete HpACHE construct, but not from those injected with any of the truncated HpACHE sequences, gave rise to the expected 275 bp PCR product (Fig. 12). Thus, the entire hydrophopbic peptide sequence, but not the truncated *KpnI*-digested construct, was sufficient to support transcription in *Xenopus*.

2. Nucleotide composition and potential methylation sites

The human ACHE gene is particularly rich in C,G residues and CpG dinucleotides (Soreq et al., 1990, Ben Aziz et al., 1991). This, in turn, implies that it is susceptible for regulation by DNA methylation (Razin & Riggs, 1980). Dissection of the ACHE gene into its various components further revealed that the C,G nucleotides and CpG dinucleotides are not distributed evenly. Thus, the promoter domain is enriched in CpG dinucleotides. This predicts clustered methylation sites and tissue-specific suppression of gene expression through interference with the binding of transcription factors at the promoter region. The abundance of CpG dinucleotides in the I1, but not the I2 intron, may further reflect the existence of functioning enhancer elements in the I1 domain, a possibility which should be pursued.

b. post-transcriptional regulation

1. Delineation of the 5'-exon boundaries through chimeric RNA-PCR reactions

Clone GNACHE was previously found to include a potential 3' splice site upstream from the initiator AUG codon (Soreq et al., 1990). Functioning 5'-splice sites were therefore searched for within the upstream sequence. Several consensus 5' splice site motifs were tested by direct PCR amplification of cDNA from human tissues. To this end, chimeric primer pairs were designed in which the twelve 5' nucleotides of each upstream primer (+) terminated at one of the various putative 5' splice sites, and the common 3' terminal 5 to 6 nucleotides corresponded to the putative 3' acceptor site at position 2227 (Fig. 4B, nucleotide 139). The downstream primer (-) was located within the coding sequence at position 2623 (Fig. 13). In this fashion, a single 5' splice site was identified at nucleotide 685 (chimeric primer no. 2), delimiting a 1.5 kb intron designated I1 within the upstream sequence. The same chimeric PCR primer was active with RNA from fetal and adult brain and from the hematopoietic cell line K562, demonstrating similar splicing of I1 in various human tissues (Fig. 13). PCR primers designed with further upstream sequences delineated a length of 74 bp for the E1 exon, starting with a consensus CAP site motif (Fig. 4B). When RNA from oocytes and embryos injected with HpACHE was subjected to amplification using the chimeric PCR primer pair 2, 10, the expected 400 bp band was also observed (Fig. 13).

2. exon-intron organization and alternative splicing in the ACHE gene

The generation of proteins with diverse properties from single genes frequently operates through alternative splicing (Maniatis, 1991). This

process involves the precise excision of intron sequences from the nuclear precursor of the relevant mRNAs (pre-mRNA). Alternative splicing is known to be cell type-, tissue- and/or developmental-specific (Smith et al., 1989) and is considered to be the principal mechanism controlling the site(s) and timing of expression and the properties of the resultant protein products from various genes (Baker, 1989). The tissue-specificity of alternative splicing depends on the availability of splicing factors. In addition, it may be affected by repressor proteins that bind to pre-mRNA recognition sequences and prevent the selection of consensus splice sites (Maniatis, 1991). In view of the polymorphism of AChE forms in different tissues and cell types, the alternative splicing pattern of the ACHE gene is therefore of special interest. This, in turn, depends on the exon-intron organization of this human gene.

The human ACHE gene spans a total of less than 7 kb (Fig. 14A) which include the promoter, six exons and four introns, all delineated by the consensus acceptor and donor sites for splicing (Fig. 12A; Table 7). The first four exons encode the major part of the AChE protein and are expressed in all of the AChEmRNA subtypes that were so far discovered. Sequencing of clone GNACHE revealed the 353 bp intron 2 (I2) between exons 2 and 3 (Fig. 14B), an additional 1.3 kb intron (I3) between E3 and E4 and a complex 829 bp domain which, in brain and muscle operates as an intron between exons 4 and 6. Similarly with the larger I1 region characterized above (Fig. 4B), both the I2 and I3 intronic sequences and the 3'-terminal domain are spliced out in the AChEmRNA form expressed in brain and muscle (Fig. 14). However, in other tissues the 3'-terminal intron displays a complex buildup. Sequence analysis demonstrated in this fragment the presence of the consensus 12 splicing motifs GA (at position 11) and GT (at position 87) and a subsequent pyrimidine stretch. This implied that nucleotides 11 to 87 in this region may constitute a smaller intron, designated I4, whereas the remaining sequence (nucleotides 88 to 839) can potentially represent an additional exon, designated E5.

The human I4 intron constitutes of an ORF continuous with that of both E4 and E5 (Fig. 14C). The ORF in E5 was found to encode a polypeptide with a potential for cleavage and subsequent linkage of a phosphoinositide moiety (Low, 1987), yet shares no homology with the *Torpedo* 3H alternative exon located at a similar position (Gibney & Taylor, 1991). The nucleotide sequence in the short ORF region from E5 was identical to that in a previous report (Li et al., 1991) except for a single nucleotide difference at position 159 (from G to C) implying a single amino acid substitution (proline instead of arginine) in the 18th amino acid residue of the E5 peptide. This difference reflects natural polymorphism (Bartels et al., 1993). The remaining 530 bp of E5 were fully sequenced and found nontranslatable (Fig. 9C).

Composition of exons in the coding domain was further examined by RNA blot hybridization and RNA-PCR. Blot hybridization revealed a broad 2.5-2.6 kb band for poly(A)+AChEmRNA, intense in basal nuclei from fetal brain but clearly apparent also in fetal hippocampus and muscle, in the decreasing order basal nuclei>>heart>hippocampus (Fig. 15A). This band predicted additional exons over E1 to E4, E6, with the total cumulative length of 2.2 kb; further experiments will be required to reveal whether additional upstream exon(s) are expressed in human brain and muscle AChEmRNAs.

In search for 3' splice options, RNA-PCR analysis was performed using primers spanning the E3, E4, E5 and E6 domains with RNA from brain, muscle and the hematopoietic cell line K562 (Fig. 10B). These experiments demonstrated a major AChEmRNA species including E3 to E4 and E6 in various brain regions, muscle and K562 cells (Fig. 10C). However, PCR primers designed to detect E5 demonstrated the presence of an AChEmRNA including this exon in K562 cells but not in any of the tissues examined. The PCR band reflecting the E5 splice alternative was considerably less intense than that representing E6, reflecting the low abundance of this mRNA in K562 cells (Fig. 10D). Interestingly, we did not observe with this primer pair the unspliced I4-E5 readthrough transcript reported in *Torpedo* electric organ (Sikorav et al., 1988) and murine bone marrow cells (Li et al., 1991). However, subsequent RNA-PCR experiments using primers internal to the I4 region revealed the readthrough transcripts in several human tumorigenic cell lines, including K562 (Karpel et al., 1993). Thus, the human AChEmRNA species encoding the common asymmetric AChE form (Soreq et al., 1990) is the major one in brain, muscle and hematopoietic cells, while the latter cells also express two minor alternative AChEmRNA species with the potential to encode two forms of phosphoinositide-anchored AChEs in addition to the major hydrophilic form of this enzyme.

3. variable translation products

The alternative splicing pattern disclosed above may potentially give rise to different AChE proteins (Fig. 16A) which divert from each other at amino acid residue 544 (Fig. 16B). The first 543 amino acids, common to all forms are encoded by exons E1 to E4. The hydrophilic form (Fig. 16B) includes a specific C-terminus which can bind to a collagen-like tail (in muscle) or a lipid-protein subunit (in brain). The peptide translated from the I4/E5 region is absent in this 583 residue long hydrophilic AChE form. The predicted phosphoinositide-linked AChEs produced from the E5 containing transcripts (Fig. 16B) should be 583 and 557 residues long, with the 40 and 14 C-terminal amino acids in the mature proteins translated from the ORF in the alternative I4+E5 or E5 domains, respectively (Fig. 17). Both E5 containing polypeptides display the necessary features (Low, 1987) for being processed for glycophospholipid attachment. These features include (a) stretches of hydrophobic residues near the C-terminus, (b) the presence of the His-Gly dipeptide (this carboxyl-terminal sequence, reviewed by Ferguson & Williams (1988) was found by Rosenberry and colleagues using carboxypeptidase digestion, in purified human erythrocyte AChE; (c) a cysteine amino-terminal to the His-Gly sequence, which would be essential for dimer formation. An interesting feature of the C-terminal peptides unique to the alternative forms of AChE is that they present no homologies to the corresponding region in BuChE (Fig. 16B), suggesting that they developed long after the two ChE genes diverged.

4. surface probability measurements

The polypeptide chains encoded by hAChEmRNAs were subjected to computerized plot structure analysis according to the Chou & Fasman prediction (1987). This analysis revealed a clear hydrophilic profile for the C-terminal peptide of the brain form, a neutral profile with a C-terminal hydrophobic nature for the E5-translated form and a yet more hydrophobic nature for the readthrough form (Fig. 17). This, in turn, predicts surface properties distinct to each of the enzyme forms (Chou & Fasman, 1987), particularly since the C-terminal domain in AChE appears to be exposed at the outer surface of this protein (Sussman et al., 1991).

The findings reached throughout this work thus demonstrate that the intensity of expression and biochemical properties of the human ACHE protein are primarily determined by both transcriptional and post-transcriptional control processes.

5. energy and stability considerations for AChEmRNAs

To examine whether certain splicing events in the ACHE gene are favored due to energy constraints, hypothetical secondary structures were separately determined for each of the exons and introns in the human ACHE gene. This was done using the FOLD program, which allows for G-C, A-T and irregular G-U pairing. The observed values of Gibbs free energy were all in the same range. Thus, minimal energy constraints could not, on their own, explain the choice of splice sites in nervous tissue vs. hemopoietic cells. This, in turn, predicts the involvement of protein factors in this process. Energy calculations were further performed for the divergent regions in the mature AChEmRNA species. In this analysis as well, there were no significant energy differences, which predicts apparently similar structural determinants affecting stability of the two mRNA species.

An interesting difference between AChE in nervous tissue and that of hemopoietic cells is that the first has to be transiently and rapidly induced according to need, whereas the latter is apparently expressed constitutively (Rakonczay & Brimijoin, 1988). Moreover, the bulk of AChEmRNA produced in the nucleated erythroid precursor should suffice to produce AChE throughout the life span of the mature anucleated and terminally differentiated erythrocyte (120 days). This, in turn, predicts that the AChEmRNA subtype encoding the erythrocyte-specific PI-linked form of the enzyme, but not brain AChEmRNA, should be especially stable. However, both mRNAs are initially designed with the same nontranslated 3'-termini, which contain a consensus motif for selective mRNA degradation (Shaw & Kamen, 1986). This AUUUA motif apparently functions as a recognition signal for an mRNA degradation pathway that is common to certain lymphokines, cytokines and protooncogenes (Mitchell et al., 1986). Interestingly, similar AUUUA signal is also included in the 3'-terminal sequence of beta-globin mRNA (Lange & Spritz, 1985), demonstrating that it does not preclude a long-term erythrocytic expression. Further experiments would hence be required to explain the mechanism(s) through which the differential stability of various AChEmRNA forms is controlled.

6. alternative splicing creates three distinct AChE forms

In addition to the AChEmRNAs expected for the two amino acid sequences that have been found in different forms of hAChE, a search of normal and transformed human tissues and cell lines indicated the presence of a third AChEmRNA in transformed cells. The three AChEmRNAs include the principal species expressed in brain and muscle and two additional transcripts containing insertions of 751 or 829 residues downstream to the E4 domain. The inserted region, which represents an intron in brain and muscle, is expressed in the tumor cell lines either as a "readthrough" form with 78 bases deleted from its 5'-end. A major band of 2.5 kb was labeled with AChEcDNA in poly(A)$^+$RNA blots from medulloblastoma cells or brain tissue, whereas a PCR-amplifed probe from the inserted domain labeled a 3.4 kb band but not the 2.5 kb band in poly(A)$^+$RNA from small cell lung carcinoma (not shown). The AChEmRNAs including the alternative insertions were only found in cell lines such as K562 or tetracarcinoma, with levels of the principal AChEmRNA species equal to or higher than in brain (1 to 10 molecules/cell), as determined by following the kinetics of mRNA-PCR amplification. In

extension of the reported expression of PI-linked AChE in hemopoietic cells, including K-562, our findings demonstrate the existence of AChEmRNAs with the potential to encode one hydrophilic and two PI-linked forms of AChE in tumor cells from both hemopoietic and non-hemopoietic origins.

c. expression in *Xenopus* oocytes

1. expression of ACHE coding sequence in *Xenopus* oocytes

In microinjected *Xenopus* oocytes, 2 ng of the *in vitro* transcribed 2.2 kb mRNA transcript of the recombined AChE coding sequence induced the biosynthesis of catalytically active AChE capable of hydrolyzing 50.4 ± 5 nmol ATCh/hr/oocyte (Table 8, average of 3 independent transcription and microinjection experiments). This represents a 10^4-fold higher activity than that obtained by the microinjection of poly(A)+ brain mRNA (Soreq et al., 1984). As expected, the recombinant enzyme appeared to hydrolyze BTCh at a rate about 50 times lower, displayed substrate inhibition above 2 mM ATCh and was sensitive to inhibition by 10^{-5} M of the selective AChE inhibitor 1,5-bis (4-allyldimethyl-ammoniumphenyl)-pentan-3-one dibromide (BW284C51) but not the selective OP BuChE inhibitor iso-OMPA at the same concentration (Table 8). In sucrose gradient centrifugation (Dreyfus et al., 1988) of products from two independent experiments, it yielded a major peak centered at 4.5 ± 0.1 S. Altogether, these experiments demonstrated that the combined sequence encodes for authentic, monomeric human AChE.

2. *Xenopus* expressed AChE is biochemically indistinguishable from native hAChE

Microinjected into mature *Xenopus laevis* oocytes, 5 ng *in vitro* transcribed AChEmRNA directed the production of catalytically active AChE displaying substrate and inhibitor interactions characteristic of the native human enzyme (Figure 18A,B). The apparent Km calculated for rhAChE against ATCh was 0.3 mM, essentially identical to that displayed by rhAChE expressed in cell lines (Velan et al., 1991a) and native human erythrocyte AChE (Gnagey et al., 1987). In sucrose density centrifugation rhAChE sedimented primarily as monomers and dimers, although a discernible peak apparently representing globular tetrameric AChE was also observed (Figure 18C). When plasmid DNA carrying AChEcDNA downstream from the cytomegalovirus promoter-enhancer element (CMVACHE, Velan et al., 1991a) was microinjected into oocytes, active AChE in yields 10- to 20-fold higher than that observed following RNA injections was obtained (Figure 18D), demonstrating efficient transcription from this promoter in *Xenopus*.

d. expression in transiently transgenic embryos

1. transcription in *Xenopus*: comparison of promoters

The ability of the 2.2 kb ACHE upstream sequence to drive transcription was examined in microinjected *Xenopus* oocytes and embryos. This sequence was ligated, either in its full form or following enzymatic restrictions with *KpnI*, *XhoI* or *PvuII* (K, X or P forms, Fig. 12) to AChEcDNA comprised of exons 2, 3, 4 & 6 (Fig. 2; see also Soreq et al., 1990 and Li et al., 1991 for gene structure) to create the hydrophobic AChE (hpAChE) constructs. DNAs were injected into oocytes or early cleavage embryos, and transcriptional activity was determined by reverse transcription and PCR amplification (RNA-PCR) using hAChEcDNA specific primers (Fig. 2). AChEcDNA ligated to the cytomegalovirus enhancer-promoter region (CMVACHE, Velan et al., 1991 a,b) was also injected. RNA from oocytes and embryos injected with the CMVACHE or the complete hpACHE construct, but not from those injected with any of the truncated hpACHE sequences, gave rise to the expected 275 bp PCR product (Fig. 2). Thus, the entire hydrophobic

sequence, but not the TATA and CAAT boxes included in the truncated *KpnI*-digested construct, was sufficient to support transcription in *Xenopus*.

2. transient expression of CMVACHE in *Xenopus* embryos

Microinjected into cleaving *Xenopus* embryos, CMVACHE directed the biosynthesis of rhAChE at levels similar to those observed in DNA-injected oocytes, yet the gross morphology and development of CMVACHE-injected embryos appeared completely normal (Fig. 19). Moreover, gross motor function of microinjected embryos, as evaluated by twitching and hatching on day 2, reflexive swimming on day 3, and free swimming on later days, was unimpaired compared to normal, uninjected controls. Microinjected tadpoles survived up to 4 weeks, showing no overt developmental handicaps. Following overnight incubation, at which time embryos had reached the late gastrula stage, endogenous AChE levels were negligible and rhAChE activity represented a 50- to 100-fold excess over normal (Figure 20A). From day 2 after fertilization, detectable endogenous AChE activities increased steadily. Using the irreversible AChE inhibitor ecothiophate (Neville et al., 1992) to distinguish between endogenous frog AChE and rhAChE (Figure 20A, inset), we observed the persistence of receding levels of rhAChE for at least 4 days after fertilization. For the first 3 days, rHAChE accounted for >50% of the total measured AChE activity in microinjected embryos and resulted in a state of general overexpression compared to uninjected controls. By day 6 after fertilization, no heterologous enzyme was detected in homogenates. At all time points examined, the level of frog AChE in CMVACHE-injected tadpoles appeared to be less than that observed in uninjected embryos, suggesting that feedback regulation may be involved in modulating AChE biosynthesis in these transiently transgenic embryos.

In immunoblot analysis following denaturing gel electrophoresis, rhAChE was observed to comigrate with native human brain AChE, yielding a clearly visible doublet band at around 68 kDa (Figure 20B). rhAChE was selectively recognized by a pool of monoclonal antibodies raised against denatured human brain AChE, and no cross-immunoreactivity with embryonic *Xenopus* AChE was observed (Figure 20B). The doublet band observed may reflect differences in glycosylation (Kronman et al., 1992a). Sequential extractions with low-salt, detergent, and high-salt buffers revealed that approximately 35% of rhAChE synthesized in transiently transgenic embryos was associated with membranes, requiring detergent for solubilization (Table 9). Whereas up to 33% of the endogenous enzyme in day 3 uninjected tadpoles appeared in the high-salt extractable fraction, salt-soluble rhAChE remained primarily in the low-salt fraction at all days examined (Table 9). Enzyme-antigen immunoassay (EAIA) utilizing a species-specific monoclonal antibody (mAb 101-1) was employed to differentiate between human and frog enzyme in the fractions.

3. expression of the ACHE promoter-reporter construct in developing *Xenopus* embryos

Whole-cell extracts prepared from *Xenopus* embryos injected with HpACHE DNA displayed a small but significant ($P > 0.01$, Student's t-test) increase in AChE activity over native endogenous levels. In contrast, microinjected CMVACHE induced 20-fold greater levels of heterologous enzyme (Table 10). Up to 50% of the total AChE produced in CMVACHE-injected embryos was extractable in a low-salt buffer, suggesting that a significant proportion of the heterologous enzyme may be secreted under conditions of high

overexpression. The overexpressed enzyme was identified as the human protein as it was efficiently inhibited by 3 X 10^{-7} M of the OP inhibitor ecothiophate, which at this concentration does not inhibit amphibian AChE (Seidman et al., 1993). Moreover, monoclonal antibodies specific to mammalian AChEs reacted with this enzyme but not with the frog enzyme, both in immunoblots and in a multiwell binding assay (Seidman et al., 1993).

5. Post-transcriptional processes

a. rhAChE remains monomeric in *Xenopus* embryos

To examine the possibility that heterologous hAChE undergoes homomeric assembly or interacts with either catalytic or noncatalytic subunits of *Xenopus* AChE to produce hybrid oligomers, sucrose density centrifugation and EAIA were performed. At all time points examined, we observed rhAChE exclusively as nonassembled monomers sedimenting at approximately 3.2 S, despite the concomitant accumulation of various multimeric forms of the endogenous frog enzyme (Figure 21). These observations were confirmed using selective inhibition with ecothiophate. When oligomeric AChE purified from CMVACHE-transfected cell cultures (Velan et al., 1991b) or from human brain (Liao et al., 1992) was preincubated with extracts of day 3 uninjected embryos and similarly analyzed, monomers, dimers, and tetramers were detected, and the distribution of oligomeric forms observed was identical to that of control samples. Thus, mAb 101-1 detects all the globular configurations of rhAChE, and proteolytic activity does not appear to degrade stable oligomeric AChE in embryo extracts. Endogenous *Xenopus* AChE appeared primarily as a dimer on day 2 after fertilization with globular tetrameric and asymmetric tailed forms appearing and increasing from day 3 onward (Figure 21, insets). Superimposition of the gradient gels from control and CMVACHE-injected embryos demonstrated that the normal developmental progression of *Xenopus* AChE oligomeric assembly was conserved in CMVACHE-injected embryos despite the high excess of rhAChE monomers (Figure 21).

b. synaptic targeting of human AChE

In search of muscle-expressed heterologous human enzyme, we combined electron microscopy with the sensitive thiocholine technique for cytochemical activity staining (Koelle & Friedenwald, 1949). For this purpose, developing myotomes from 2-day-old embryos were first examined (Fig. 22A). Neuromuscular junctions and the adjacent nerve and muscle structures in all of the examined embryos appeared morphologically normal (Fig. 22B,a-c). Synaptic staining for AChE in both HpAChE-injected (Fig. 22B,b) and CMVACHE-injected embryos (Fig. 22B,c) resulted in significantly more conspicuous depositions of the electron dense reaction product at the synapse than that observed in controls (Fig. 22B,a). While in NMJs of noninjected embryos the average area covered by reaction product was in the range of 20 $nm^2/\mu m$ contact length, staining efficiency in HpACHE-injected embryos reached values of 195 $nm^2/\mu m$ and CMVACHE injections yielded labeling of up to 220 $nm^2/\mu m$. Uncharacteristic accumulations of reaction product were further observed in association with myofibrils of embryos injected with either the HpACHE or CMVACHE constructs (Fig. 22B, e-f).

Both the overall incidence and intensity of staining in sections prepared from embryos injected with HpACHE were enhanced compared to controls, but less than those observed in CMVACHE-injected embryos. Sections prepared from uninjected embryos displayed minimal staining around the myofibrils, and when present, staining was sparse and considerably less intense (Fig. 22B, d). No morphogenic or behavioral barriers to normal hatching, muscle

twitching or development were observed in microinjected embryos, and we have reared such embryos for up to 4 weeks, demonstrating that overexpression of heterologous AChE in microinjected *Xenopus* embryos provides a viable model for developing NMJs.

c. subcellular disposition of rhACHE in myotomes of CMVACHE-injected embryos

Increases in AChE activity are directly correlated with the ultrastructural and functional maturation of muscle during early embryonic development in *Xenopus* (Kullberg et al., 1977). We therefore undertook an ultrastructural analysis, at the electron microscope level, of myotomes from 2- and 3-day-old embryos microinjected with CMVACHE as compared to normal uninjected controls. Longitudinal and transverse sections from rostral trunk somites revealed clearly discernible myofibers PF day 2 in both injected and uninjected embryos (Figs. 23 and 24). By PF day 3, both groups displayed significant increases in their numbers of myofibrilar elements and in maturation of the sarcoplasmic reticulum (Fig. 24). To examine the subcellular localization of nascent AChE in transgenic and control embryos we employed cytochemical activity staining (Karnovsky, 1964). In both the experimental and control groups, crystalline deposits of electron dense reaction product were observed primarily in association with myofibrils, among the myofilaments and within the sarcoplasmic reticulum (Figs. 23 and 24). Various organelles, including the nuclear membrane, free and bound polyribosomes, Golgi apparatus, and sometimes mitochondria, were also observed to be stained (Figs. 23 and 24 and data not shown).

At PF day 2, staining in CMVACHE-injected embryos was conspicuously more pronounced than that observed in uninjected controls, in both the quantity and the intensity of reaction product (Fig. 23). However, variability was observed between tissue blocks, probably reflecting mosaic expression of the injected DNA and/or variability in the efficiency of expression among embryos (S. Seidman, unpublished data; see also Vize et al., 1991). In longitudinal sections from CMVACHE-injected embryos, staining appeared to be concentrated at the I band of myofibers, particularly around the triad marking the intersection of the sarcoplasmic reticulum and transverse tubule systems. In contrast, the sparse staining observed in control sections appeared randomly distributed. By PF day 3, the general staining intensity in both groups had significantly increased, while observable differences between the groups were less dramatic. Cross-sections revealed especially prominent staining within the sarcoplasmic reticulum (Figure 24A, B). Strong staining was now observed at both the A and I bands, and for the first time, within the transverse tubules (Figure 24C,D). Overall, day 2 CMVACHE-injected myotomes resembled day 3 uninjected control myotomes in staining incidence and intensity (Figures 23A,C and 24B,D). Taken together, these data indicate that the subcellular compartmentalization of transiently overexpressed rhAChE in developing *Xenopus* myotomes paralleled that of native embryonic *Xenopus* AChE. In this way, CMVACHE-microinjection appeared to advance the normal accumulation of AChE in embryonic myotomes by up to one day.

d. ultrastructural consequences of overexpressed AChE in *Xenopus* NMJs

We demonstrated up to 10-fold overexpression of catalytically active AChE in neuromuscular junctions (NMJs) of CMVACHE-injected embryos 2 days after fertilization (Ben Aziz-Aloya et al., 1993). To examine the persistence of this state and its implications for synaptic ultrastructure, we studied both cytochemically stained and closely appositioned unstained NMJs from 3-

day-old injected and control embryos (Fig. 25 and Table 11). In the injected group, 72% of the postsynaptic membrane length (SL/PSL, Table 11) was stained, on average, for active AChE. In contrast, only 22% of the postsynaptic length was stained in controls. Moreover, the total area covered by reaction product was approximately 4-fold greater in NMJs from CMVACHE-injected embryos than in those from controls (SA, Table 11). In addition, the staining observed in NMJs from injected embryos was considerably more intense than that displayed by control NMJs, forming large black accumulations of reaction product as opposed to the lighter, more diffuse staining observed in controls (Figure 25A-B,D-E).

Ultrastructural features of NMJs from injected and uninjected embryos were best discerned in unstained synapses. NMJs from control embryos generally appeared smooth and relatively undeveloped, with up to two secondary folds of the postsynaptic membrane, and a single nerve-muscle contact (Figure 25C). In contrast, NMJs from CMVACHE-injected embryos displayed an average of three secondary folds and one-three discrete contacts between pre- and postsynaptic membranes (Figure 25F). Furthermore, the average postsynaptic membrane length in NMJs from CMVACHE-injected embryos was 30% larger and considerably less variable than that measured in control embryos (SL, Table 11), yet, the distance across the synaptic cleft was both larger and more variable in injected embryos than in controls (129±72 μm vs. 94±23 μm; n=14). NMJs overexpressing rhAChE thus appeared more developed in their structural buildup than controls.

6. Tumorigenic expression

a. aberrations in tumor CHE genes and their protein products

Experiments performed over the last four decades have provided compelling evidence that genes are aberrantly expressed in many types of human tumors. The aberrant expression of these genes can be manifested at the DNA, mRNA, or protein level. Both the ACHE and the BCHE genes are amplified *in vivo* in leukemias (Lapidot-Lifson et al., 1989) and ovarian carcinomas (Zakut et al., 1990); the BCHE gene is mutated in neuroblastoma, glioblastoma, and other tumors of nervous system origin (Gnatt et al., 1990); and both AChE and BuChE mRNAs are overexpressed in ovarian carcinoma (Zakut et al., 1990), meningioma (Soreq et al., 1984), and glioblastoma (Gnatt et al., 1990). Interestingly, BuChEmRNA transcripts of abnormal length at their 3' end have also been detected in glioblastomas (Gnatt et al., 1990), suggesting that there may be abnormal modulation of mRNA processing in these tumors.

Some tumors express CHE genes that are altered in their protein coding regions. For example, point mutations Asp70Gly and Ser425Pro have been detected in neuroblastoma BuChEmRNA (Gnatt et al., 1990). Other tumors produce abnormally processed and/or assembled BuChE proteins. As evidenced by sucrose gradient sedimentation experiments, the BuChE protein in meningiomas appears to exist primarily in monomeric and dimeric form (Razon et al., 1984; Soreq et al., 1984) rather than in its usual tetrameric structure (Rakonczay & Brimijoin, 1988). Finally, biochemical studies have provided evidence of altered levels and altered sensitivity of tumor ChEs to selective inhibitors in extracts of human brain tumors (Razon et al., 1984) and in the serum of carcinoma patients (Zakut et al., 1988).

b. tumor-associated chromosome abnormalities affecting the ACHE and BCHE genes

The shared propensity of the ACHE and BCHE genes to undergo amplification is unlikely to be due to sequence similarities, since the two genes display drastically different base compositions (Soreq & Zakut, 1990a) and do not cross-hybridize (Lapidot-Lifson et al., 1989). Thus, the alteration of these genes in neoplastic cells could either be related to the biological function(s) of their protein products or could simply be an incidental event, resulting from the chromosome location of the genes. To help distinguish between these possibilities, we have examined the frequency of chromosome abnormalities in tumors at or near the map positions of the ACHE and BCHE genes.

Errors in chromosome propagation are common in tumors and are considered to be one of the major classes of genetic alterations underlying the malignant phenotype (Tycko & Sklar, 1990). Holliday has hypothesized that initial changes in gene dosage, brought about by chromosome nondisjunction or rearrangement, trigger a general loss of accuracy in chromosome segregation in tumor cells at mitosis (Holliday, 1989). Gene amplification is thought to be an early event in tumorigenesis (Schimke, 1990) and one that plays a central role in chromosome breakage (Windle et al., 1991). In some human cancers, gene amplification may be a useful marker for predicting clinical outcome (Schwab & Amler, 1990; Bishop, 1991).

ACHE is amplified in leukemias (Lapidot-Lifson et al., 1989), ovarian carcinomas (Zakut et al., 1990), and platelet disorders (Zakut et al., 1992). The long arm of chromosome 7 tends to break in cancerous cells (Mitelman, 1988). It is interesting to note that the AT-rich region of BCHE, which presents almost a mirror image of the properties of ACHE, is likewise subject to frequent amplification and resides on the 3q26-ter chromosomal fragment, which is found broken in thrombopoietic disorders (Pedersen, 1990).

c. amplification of CHE genes in a premalignant condition

If CHE gene amplification and/or mutagenesis is indeed a causal factor in tumorigenesis, one would expect to observe this phenomenon in premalignant conditions. Polycythemia vera is a premalignant blood cell disorder characterized by sphenomegaly and increased production of erythrocytes, granulocytes and platelets. The disease has a gradual onset and runs a chronic but usually slowly progressive course; affected individuals show an increased incidence of leukemia (Landaw, 1986). Risk mounts to 1 to 2% in phlebotomy-treated patients, in contrast to 10 to 15% in patients treated by the drug chlorambucil or by irradiation (Bloomfield & Brunning, 1976). This suggests that mutagenic agents may be secondary inducers which, when added to the predisposing state in polycythemia vera patients, lead to tumorigenesis. When acute myelocytic leukemia develops secondarily to polycythemia vera, the patients are resistant to therapy and their prognosis is poor (Bloomfield & Brunning, 1976).

We have examined a sample of peripheral blood cell DNA from an untreated polycythemia vera patient for evidence of gene amplification. Considerable amplification of both the ACHE and the BCHE genes (15-fold) and three oncogenes (RAF1, MYC, and FES/FPS)(5- to 20-fold) was observed in this patient. The amplification in this patient was not attributable to the presence of malignant cells, to chemotherapy, or to multidrug resistance (Slamon et al. 1984; Biedler et al., 1988). Careful follow-up of this and

other polycythemia vera patients is warranted in order to determine whether these gene amplification events play a role in leukemic transformation.

d. amplification of CHE genes in a nonmalignant condition

Because ACHE and BCHE co-amplify with several oncogenes in leukemic patients with platelet deficiencies, we wished to find out whether amplification of these genes also occurs in noncancerous platelet disorders, and if so, whether oncogenes would amplify in such cases as well. The autoimmune disease systemic lupus erythematosus (SLE) presents an appropriate model system for this issue, since patients with SLE may suffer from thrombocytopenia resistant to most treatments. We find a 40- to 80-fold amplification of genomic sequences from ACHE and BCHE, as well as the C-raf, V-sis and C-fes/pfs oncogenes in peripheral blood cells from an SLE patient with severe thrombocytopenia (Fig. 2A, Zakut et al., 1992). *PvuII* restriction analysis and DNA blot hybridization of the amplified ACHE and BCHE sequences demonstrate apparent aberrations in both genes (Fig. 2B, Zakut et al., 1992), suggesting that malfunctioning of modified, partially amplified CHE genes may be involved in the etiology of SLE.

7. Hematopoietic effects of *in vivo* antisense inhibition of ACHE gene expression

Cell culture experiments revealed that μM concentrations of AS-ACHE, but not the matching "sense" oligonucleotide interfered in erythropoiesis (Soreq et al., in preparation). To study the *in vivo* hematopoietic expression of the ACHE gene, groups of four different mice were injected once with 5 μg/g of AS-ACHE. Untreated mice served as controls. Twelve days following the injection, AChEmRNA levels in the bone marrow and lymph nodes of control and injected mice were evaluated. To this end, we employed reverse transcription coupled with kinetic follow-up of PCR amplification products (RNA-PCR) to detect and quantify broad range differences in mRNA levels. For calibration, we subjected measured amounts of shorter *in vitro* transcribed ACHEmRNA to the same procedure. Signals appeared earlier when higher amounts of AChEmRNA were present, and as low as 10^5 molecules of AChE per 100 ng RNA yielded signals starting at cycle 33. Gel electrophoresis and blot hybridization of the resultant mouse PCR products revealed the appearance of ACHEcDNA fragments already at cycle 26 in RNA preparations from both bone marrow and lymph nodes of control mice, suggesting a concentration of $\geq 10^7$ molecules/100 ng RNA for AChEmRNA in both these samples. In contrast, there were no observable signals in either sample within AS-ACHE-treated mice up to cycle 41, which implied drastic reductions of at least 1000-fold in AChEmRNA levels in both lymph nodes and bone marrow at this time. Parallel analyses of actin mRNA levels revealed more limited yet most conspicuous 10- and 100-fold reductions in the lymph nodes and bone marrow respectively, demonstrating secondary effect of the AS-ACHE treatment on actin mRNA (Fig. 26).

Differential cell counts of the major bone marrow cell types showed drastic changes in cell composition at 12 days after injection as compared with controls, with dramatic reduction in lymphocytes and erythroid cells and compensating increases in myelocytes, granulocytes and neutrophils. By day 20 after treatment, the lymphocyte and erythroid fractions both repopulated to above normal levels while granulocyte and neutrophil fractions were reduced below normal levels, demonstrating the transient nature of the hematopoietic alterations observed at day 12. Peripheral automated blood profiles of the animals at day 20 after treatment further displayed 75% lymphocytes, 18% neutrophils, 5% monocytes and 2% eosinophils, a normal

composition, characteristic of healthy animals, for both treated and control mice. Thus both bone marrow and blood cell composition indicated major restoration from the AS-ACHE treatment by 20 days after injection.

Megakaryocytes constitute a minor fraction of the bone marrow (ca. 0.5%) and display an exceptionally long half-life. Therefore, differential MK compositions were only determined at day 20 after injection, when the entire MK population was renewed. Significant 3-fold increase in the fraction of pro-MK out of total MK was observed in AS-ACHE treated mice as compared with controls (5% in chi-square test). A corresponding decrease occurred in AS-ACHE-treated mice in the larger fraction of intermedial MK (from 85.3 to 75.2%), whereas mature MK increased by ca. twofold. This, in turn, implicates ACHE as a potential modulator of specific steps in the pathway of megakaryocytopoiesis (Table 12).

At day 12 AS-ACHE after treatment, ACHEmRNA levels in the bone marrow were too low to be detected by RNA-PCR. To examine ChEmRNA levels in the novel developing MK at 20 days after treatment, we employed the high resolution *in situ* hybridization technique. In view of our previous observations of interference with MK development in culture by AS-BCHE (Patinkin et al., 1990; Lapidot-Lifson, et al., 1992), we also followed BuChEmRNA levels in this experiment. To this end, bone marrow smears from AS-ACHE-injected and control mice were hybridized with each of the [^{35}S]-ChEcRNA probes.

Hybridization was slightly lower in intensity in bone marrow smears prepared from AS-ACHE-treated mice, as compared with mice injected with PBS. In mature MK from AS-ACHE-treated mice, silver grain counts (average for at least 40 cells/sample in four mice with each probe) were ca. 40% and 70% of PBS-treated controls for AChEmRNA and BuChEmRNA, respectively. Bidirectional variance analysis (Hoel, 1976) revealed for these values a significance level of 5%. The difference between AChEmRNA levels in AS-ACHE-treated and control mice hence was reduced from >1000-fold at day 12 to ca. twofold at day 20. Silver grain counts were also lower to the same extent on non-MK cells from AS-ACHE-treated animals as compared with controls. RNA-PCR analysis also revealed actin mRNA levels at the same order of magnitude in AS-ACHE-treated and control mice. The suppressed levels of AChEmRNA within intermedial and mature MK reflected the specificity of the AS-ACHE treatment, as evident from the more limited reductions in BCHEmRNA in these cells (Fig. 27). Thus, recurrence of apparently normal hematopoietic profiles in the treated mice by day 20 was accompanied by restoration of close to normal levels of ACHE and actin mRNAs.

8. Structure/function relations in the enzymes

a. recombinant BuChE variants

It is generally believed that the active site of ChEs comprises a catalytic (esteratic) site, an acyl binding site, and a cation-binding site, all of which contribute to enzyme function and inhibition. We have sought to identify some of the specific amino acid residues that comprise these sites. The binding of ligands (substrates or inhibitors) is a measure of the integrity of the binding sites. Pharmacological studies have shown different dissociation coefficients for the substrates and inhibitors that interact with the ChEs and their naturally occurring variants. While AChE interacts only with ACh, "usual" (wild-type) BuChE also hydrolyzes this, BuCh and SuccCh. This already implies differences in the active site, as do the differing binding constants of OP inhibitors to AChE and BuChE. The

common prophylaxis and therapy against OP poisoning involves the use of cationic oximes such as 2-PAM, assumed to bind to the cation-binding site and to position its nucleophilic oxime moiety toward the phosphoryl-serine bond of the OP-inhibited enzyme (discussed in Neville et al., 1990b). Comparison of the interactions of recombinant ChEs with these different ligands, substrates and inhibitors, was therefore initiated, using the oocyte expression system. We prepared recombinant enzymes representing natural and new mutations. (The natural mutations, although described in the literature, were not available to us on a routine basis, so we have prepared the recombinant enzyme as requrired.)

Over 20 CHEDNA constructs encoding various subtypes of hAChE and hBuChE were expressed in microinjected oocytes. Measurements of catalytic activities revealed that several of the examined amino acid substitutions introduced into these ChE forms caused considerable decreases in substrate hydrolysis rates by the oocyte-produced recombinant enzymes, as will be summarized in the following.

b. substrate hydrolytic activities of native and recombinant oocyte-produced enzymes

Recombination and site-directed engineering of four naturally occurring allelic BuChEcDNA clones (I-IV) was employed to create ten distinct BuChEcDNA constructs (Nos. 2-11) carrying different combinations of single point mutations, all of which result in amino acid substitutions. Fig. 28A presents these clones in a schematic manner, and Fig. 28B,C present the experimental design of the site-directed mutagenesis employed to modify Glu441 and Glu443. At a substrate concentration of 10 mM, all mutations examined reduced the ability of these oocyte-produced enzymes to hydrolyze BTCh (with the exception of Gly70/His114).

To examine whether the dramatic loss in catalytic activities which occurred in the inactive Gly1441/Gln443 BuChE reflected changes in protein quantity or altered catalytic properties, an immunoblot analysis was performed on detergent extracts of oocytes. The intensity of the relevant immunoreactive protein band produced from the mutated constructs appeared in this semiquantitative test to be indistinguishable from that obtained with the wild-type BuChE (not shown). This implied that the site-directed Gly441/Gln443 mutation impairs BuChE activity without substantially affecting its rate of synthesis or its stability in the oocytes.

c. nontolerated mutations

The nontolerated BuChE mutants, which have very low or undetectable levels of enzymatic activity, were expressed as proteins at levels comparable to those of recombinant wild-type BuChE, as determined by competitive binding to anti-BuChE (data not shown). Not surprisingly, we found the active site Ser198 to be essential for BuChE activity. Its substitution by threonine, glutamine, histidine or aspartate resulted in the complete absence of activity, even after doubling the time of oocyte incubation. Even the substitution of cysteine was very deleterious, having only approximately 1% of the activity measured for the unmodified enzyme in control injections of unmodified BuChEmRNA. Mutation of Met437 to aspartate (Gnatt et al., 1994) also resulted in near abolition of detectable activity, presumably because the aspartate residue is introduced close to the active site histidine residue, and disturbs the carefully constructed arrangement of the catalytic triad.

One of the charged residues located in the active site region, Glu441, seems to be hydrogen-bonded to Glu197 by one or two water molecules (Schrag et al., 1991). These water molecules may have an important function in the catalytic process. Indeed, Glu441Gly/Glu443Gln (Neville et al., 1992) severely lowers enzyme activity. Alternatively, or additionally, the lowered activity in the double mutant Gly441Gly/Glu443Gln, might be the result of alterations in the structure of the substrate binding sites.

d. Km modifications

The Km values toward BTCh were determined for the catalytically active BuChE mutants, i.e., with modified Leu286, Phe329 or Tyr440. Impairment of enzyme activity was more limited than with Ser198 or Met437 substitutions. Modifications of Phe329 into cysteine, aspartate, leucine or glutamine were all well tolerated, and the Km values of all these mutants did not differ from the value measured for wild-type BuChE by more than threefold (Fig. 29A). In contrast, all of the examined modifications of Leu286 demonstrated up to 10-fold changes in K_m, increasing in the sequence Asp<Arg<Gln<Lys (Fig. 29B).

e. inhibition rate measurements

Pseudo-first-order rate constants were determined for the inactivation of BuChE and two mutants by DFP (Fig. 30) and were compared with the IC_{50} values (Table 13). The fact that over a wide range, IC_{50} values closely track the rate constants -- their ratio remains roughly the same -- indicates that IC_{50} values reflect rate of inactivation. However, there is also a striking parallel between Km values for the Leu286 mutants and the IC_{50} values (Table 13), which suggests that IC_{50} values are determined by affinity for the enzymes. Taken together, these observations indicate that both reactivity and affinity are reflected in the IC_{50} values.

f. inhibition of variant hBuChEs by anticholinesterases

The inhibitory efficacy of nine different anti-ChE drugs was examined with recombinant forms of several of the natural occurring hBuChE variants. The single substitution in BuChE, Asp70Gly, was found in these experiments to render the enzyme insensitive to inhibition by SuccCh or *Solanum* alkaloids (see below) and resistant to 2-PAM reactivation following DFP inhibition (Neville et al., 1990b). Table 14 details the natural mutations in BuChE and the variations in IC_{50} values of these various anti-ChE compounds. It is obvious from this table that several of these mutations altered multi-drug responses in the modified BuChE proteins.

g. Pro425 enhances "atypical" properties of Gly70 BuChE

The "atypical" BuChE phenotype is clinically characterized by the resistance of the variant enzyme to SuccCh and dibucaine (Whittaker, 1986). Using the separate Gly70 and Pro425 mutations in distinct transcription constructs, the contribution of each mutation toward this defective phenotype was assessed. For this purpose, IC_{50} values with dibucaine or SuccCh were determined for each of the recombinant muteins as compared with the wild-type enzyme of normal human serum. The single Gly70 mutation was found in these measurements to increase the IC_{50} with SuccCh by more than an order of magnitude, in agreement with the finding of this mutation in patients with records of post-anesthetic apnea (McGuire et al., 1989). However, a much higher and apparently absolute resistance to SuccCh was noted for the double mutant Gly70/Pro425 (IC_{50} > 1000 mM), demonstrating a synergistic contribution of the Pro425 substitution toward a yet more extreme "atypical" phenotype. Moreover, the IC_{50} for dibucaine was

increased only twofold in the Gly70 mutein as compared with the normal enzyme. In contrast, the double Gly70/Pro425 mutant became completely resistant to dibucaine as well. The combination of Gly70 and Pro425 substitutions thus makes hBuChE fully resistant to solanidine (see below), SuccCh and dibucaine inhibition, in addition to preventing its reactivation by oximes following OP poisoning.

h. substrate specificity altered in recombinant BuChE variants

To determine whether reduced catalytic activities observed for the various BuChE variants reflected changes in the microenvironment of their active sites, their affinities to various substrate analogs were examined (Fig. 31A,B). The choline esters studied included BTCh, benzoylcholine (BzCh), ACh, SuccCh and propionylcholine (PrCh), all of which interact with BuChE through its presumed anionic (cation-binding) site. Normal Michaelis constants, Km, with BTCh and dissociation constants, Ki, for BzCh were observed for all mutants, varying slightly within a twofold range. Fig. 31A displays the Km and Ki values obtained for the various mutants. Tyr561 BuChE exhibited similarly normal binding to SuccCh, with a Ki of 1.7 mM. However, all the other mutants displayed markedly higher (>15-fold) Ki values for SuccCh, indicative of major reductions in the enzyme's affinity for this choline ester. The triple mutant Gly70/His114/Tyr561 displayed the highest affinity, whereas the double mutants Gly70/Tyr561 and Gly70/His114 exhibited less weakened binding of SuccCh. However, the addition of Pro425 to Gly70/His114 resulted in complete resistance to SucCh binding, with no inhibition being apparent, even at 200 mM SuccCh, which is similar to previous observations with the double Gly70/Pro425 BuChE variant (Neville et al., 1990a).

All Gly70-containing mutants displayed approximately 4- to 5-fold reductions in binding of ACh as compared with the wild-type and Tyr561 enzymes, which showed profiles similar to those observed with SuccCh. In contrast, PrCh binding was unchanged in the Tyr561 and Gly70/Tyr561 mutants. This conspicuous effect is shown in Fig. 31B. Addition of the His114 substitution to Gly70, with or without Tyr561, resulted in 4-fold reductions in PrCh binding, and addition of Pro425 to Gly70/His114 BuChE further decreased binding.

i. resistance of Gly70 BuChE muteins to solanidine

Stable mutations in metabolically important proteins are occasionally advantageous to organisms in which they occur, explaining the evolutionary acceptance of the mutation and survival of the organism (Whittaker, 1986). To reveal whether any of the tested variants belong to this category, we examined their sensitivity to inhibition by naturally occurring *Solanum* alkaloids (both aglycones and glycoalkaloid) and the cocaine derivative, dibucaine. Solanidine, a steroidal alkaloid, is found in components of common diets (the *Solanaceae* include the potato, the tomato and the eggplant), and its consumption causes acute poisoning (Whittaker, 1986). On the other hand, it does not inhibit AChE (Roddick, 1989). At the non-physiological concentration of 100 μM, solanidine reduced to 65% the normal serum enzyme activity and to 75% the activity of its oocyte-produced recombinant form. Similarly effective inhibition (78%) was observed with the recombinant Pro425 variant. In contrast, the two recombinant BuChE muteins possessing the Gly70 substitution remained fully active in the presence of 100 μM solanidine (86 and 98% remaining activities, respectively), demonstrating that the Asp70Gly substitution is sufficient to render BuChE resistant to toxic concentrations of this common dietary alkaloid.

A similar inhibitory trend was observed for the steroidal glycoalkaloid alpha-solanine, which potently inhibits the usual recombinant and Tyr561 BuChEs with IC_{50}s of 5.2 and 3.5 µM. The alpha-solanine inhibition curves are presented in Fig. 32B. However, Gly70-containing BuChE mutants interacted with this drug, but displayed a much higher IC_{50} value of 170 µM (Fig. 32B). In contrast, the third *Solanum* compound examined, alpha-chaconine, was found to be a potent inhibitor of all Gly70-containing muteins with IC_{50} values 4 to 8 times lower than their corresponding values obtained with alpha-solanine. Fig. 32C shows the distinct effects of alpha-chaconine on the mutant ChEs.

Dose-response curves revealed normal binding of dibucaine to Tyr561 BuChE (IC_{50} 30 µM). Gly70 mutants carrying either His114 or His114/Pro425 displayed marked resistance to dibucaine. In contrast, the Gly70/His114/Tyr561 triple point mutant showed a decreased and an interestingly biphasic dibucaine binding profile: at 0.1 mM dibucaine, this mutant was significantly inhibited, but at 1 mM dibucaine, its inhibition was not further modified. Fig. 32A presents these changes in dibucaine interactions for the different mutants.

In order to compare the effects of the site-directed mutations Gly441 and Gln443 on dibucaine with those on SuccCh binding, enzymes were incubated with two concentrations of dibucaine (0.1 mM, 1 mM) and SuccCh (10 mM, 50 mM), and their remaining BTCh-hydrolyzing activities were determined. While the ability of Gly441/Gln443 BuChE to bind SuccCh was virtually unaffected, its ability to bind dibucaine was markedly reduced.

j. <u>Gly70 BuChEs resist oxime reactivation</u>

Oxime reactivation is employed in research and therapy to reverse the inhibition of ChEs by toxic OP compounds (Edery & Schatzberg-Porath, 1958). Estimations are that up to 1 million accidental poisoning cases occur per year worldwide, due to agricultural uses of OP insecticides leading to inhibition of AChE and BuChE (reviewed in Soreq & Zakut, 1990a). To examine whether the BuChE in individuals who carry the Gly70 and/or Pro425 mutations would potentially respond to oxime therapy, recombinant BuChE muteins were first subjected to complete inhibition by 0.5 µM of the OP compound DFP, and then were incubated with 10 mM of the commonly used oxime, 2-PAM. When administered alone, 2-PAM caused a limited reduction in the activities of all four recombinant BuChEs. Following complete DFP inhibition, 2-PAM restored 65% and 55% of normal serum BuChE as well as of the oocyte produced normal Asp70/Ser425 counterpart. The Asp70/Pro425 enzyme was also reactivated, although to a somewhat lower level of 45%. In contrast, both of the recombinant muteins carrying the Gly70 mutation completely failed to be reactivated by 2-PAM. Furthermore, 20 mM of the nonspecific nucleophile, hydroxylamine, effectively reversed DFP intoxication in all of the recombinant BuChE muteins, demonstrating that the resistance of these muteins to 2-PAM reactivation was not due to accelerated "aging" of the Gly70 variant of BuChE (Silver, 1974). In view of the generally accepted notion that the cationic 2-PAM interacts with an anionic amino acid residue (Quinn, 1987), this finding further demonstrates the involvement of Asp70 in such electrostatic interactions.

k. <u>disrupted interaction of Gly70 BuChE variants with OP and carbamate inhibitors is ameliorated by additional substitutions</u>

Interactions of all BuChE enzymes with the BuChE-specific OP compound iso-OMPA, the nonspecific AChE/BuChE OP drug ecothiophate and the BuChE-

specific carbamate prodrug bambuterol were markedly reduced by the presence of the single Gly70 mutation, whereas the single Tyr561 and Pro425 mutations totally failed to influence binding of these compounds. However, inclusion of other mutations in conjunction with the Gly70 mutation restored binding to various extents (Neville et al., 1992).

The expression system we employed provided useful comparisons to natural ChEs, since both substrate specificity and selective inhibition of oocyte-expressed AChE and BuChE were nearly identical to those of the native enzymes. Functional alterations were displayed by many of the recombinantly produced BuChEs. Together with structural analysis, these findings enable a dissection of functional regions in the studied proteins. Mutant BuChEs were thus classified into four principal subgroups, according to effects on enzyme function, as detailed in the following.

1. <u>disturbance of ligand entrance into the active site gorge</u>
A natural variant of serum BuChE, Asp70Gly, the "atypical" enzyme (Soreq & Zakut, 1990a; Lockridge & La Du, 1978), displayed varied affinity to numerous ligands (Neville et al., 1992; Neville et al., 1990a,b). IC_{50} values obtained from inhibition by SuccCh, dibucaine, bambuterol, physostigmine, ecothiophate and iso-OMPA were increased by at least 10-fold over values measured for the wild-type enzyme (Neville et al., 1992; Neville et al., 1990a,b). Although no change in Km toward BTCh was observed, the affinity to ACh was clearly reduced. Previous studies of individuals with the "atypical" enzyme have, in fact, displayed lowered affinity to dibucaine (Whittaker, 1986). However, biochemical studies alone could not attribute the differences in ligand affinity to specific amino acid residues or define their position in the protein. Thus, both disturbed ligand interactions and disturbed ligand penetration to the active site can display lowered affinity. To comprehend what determines the ChE affinity constants toward specific ligands, it is therefore crucial to assess the regions in ChEs that are involved in binding and penetration of ligands.

In essence, binding affinity consists of ligand penetration in addition to its binding to the various subsites in the active site center. Thus, not only the hydrophobic binding sites but the rim of the gorge, residues around the rim, and the gorge lining may contribute to the affinity constant. The altered affinity displayed by Asp70Gly (which changes the acidic aspartate to a neutral glycine residue) to some basic ligands, such as ACh and SuccCh, suggests that the charge plays a role in drawing these ligands into the gorge. This is supported by the unaltered affinity to this variant of choline esters that contain bulky hydrophobic chains, such as BzCh (Neville et al., 1992). Thus, the Asp70 residue may constitute part of the previously predicted peripheral site. This raises the possibility that the peripheral binding site inferred from biochemical studies may exist, in addition to the hydrophobic choline binding site, as a composite of multiple residues to which these hydrophobic ligands bind. The rim area which contains additional hydrophobic residues, hence might contain yet other sites involved in attracting hydrophobic ligands. These could function before the ligands are pulled into the gorge by Asp70, and prior to their "sliding down" the hydrophobic lining until they reach the active site.

m. <u>interrelationship between substrate and inhibitor interactions</u>
Changes in inhibitor sensitivities of mutants of Leu286, Phe329 and Tyr440 were routinely screened by determination of IC_{50} values. We employed three

OP inhibitors with different properties: DFP, a potent ChE inhibitor with relatively small volume, iso-OMPA, a relatively bulky OP agent selective for BuChE, and ecothiophate, an OP with structure analogous to BTCh (Fig. 29B). Table 13B presents their IC_{50} values as determined for each of the analyzed BuChE mutants, and as compared with the changes observed in K_m for these mutants. As noted, IC_{50} values increased for various Leu286 mutants in the same order as the K_m values i.e. Asp<Gln<Lys, yet in certain mutants, IC_{50} variations were far more pronounced than those observed for K_m values. The Leu286 mutants, Leu286Lys and Leu286Asp, in particular showed little change in K_m, but decreased sensitivity to both ecothiophate and iso-OMPA. Sensitivity to the smaller OP agent DFP was less affected.

OP sensitivity was either decreased or enhanced for Phe329 mutants. Thus, substitution of Phe329 by the polar cysteine or glutamine residues, which did not cause any significant change in Km, resulted in a 10-fold decrease in the IC_{50} of the BuChE-specific OP, iso-OMPA, demonstrating distinct requirements for inhibitor and substrate interactions at the acyl binding pocket. In contrast, with the Phe329Gln and Phe329Leu mutants, decreases in the IC_{50}s of the smaller OP, DFP, were only approximately 3-fold, while the IC_{50} values of the substrate analog OP, ecothiophate, were increased 10-fold. Decreased sensitivity to ecothiophate was also observed for Phe329Leu and Phe329Asp, indicating that many kinds of substitutions of Phe329 -- acidic, basic, polar and nonpolar -- were effective in reducing sensitivity. However, for iso-OMPA and DFP, substitution with aspartate somewhat reduced sensitivity, but other substitutions -- cysteine, leucine and glutamine -- all increased sensitivity. Tyr440Asp showed an unmodified K_m, and nearly uniformly decreased sensitivity to all three OPs. Thus, inhibitor and substrate interactions are affected by charge, polarity and volume in a structure-dependent manner for each inhibitor and modified residue.

n. an AChE/BuChE chimera

Toward learning which residues determine ChE specificity, we replaced residues 58 through 133 of rhBuChE with the corresponding residues of rhAChE, those that form the outer rim and surface of the active site gorge, and the choline-binding site. The resulting chimera had properties intermediate between its two parents: it retained the specificity and Km value toward BTCh of BuChE, including its sensitivity to SuccCh and physostigmine, but acquired the AChE-like sensitivity to ecothiophate and iso-OMPA, and had characteristics intermediate between the two parents toward the inhibitors bambuterol, dibucaine and BW284C51 (Figs. 33, 34, Table 15). We analyzed these findings in light of the 3-dimensional model that had been constructed by placing the hBuChE sequence into the *Torpedo* AChE structure. The data suggest that the residues that affect the attraction of ligands to the active site are Tyr72, Asp74, Tyr124 and Trp286, and in BuChE, residues Asn68, Gln199 and Ala277, in addition to the conserved Asp70. Moreover, the chimera seemed to have lost substrate activation, characteristic of BuChE. Therefore, the peripheral anionic site, historically identified by such activation or inhibition studies, has apparently been altered.

DISCUSSION

A. The AChE coding sequence, structural and biological properties

Amino acid sequence homologies to other CHEs, the ATCh hydrolyzing activity of the recombinant enzyme and its inhibition by ACHE-specific but not by BCHE-specific inhibitors clearly identified our composite nucleotide sequence as a DNA encoding human AChE. This made *Homo sapiens* the first species in which ACHE and BCHE sequences could be compared. The overall sequence conservation between these two proteins implies some common physiological role(s) and is compatible with the cross-homologies displayed by polyclonal antibodies directed against recombinant, nonglycosylated BuChE peptides (Dreyfus et al., 1988). In contrast, the considerable differences between these primary amino acid sequences and their dissimilar glycosylation levels may explain their previously reported lack of cross-immunoreactivity with monoclonal antibodies (Rakonczay & Brimjoin, 1988, Liao et al., 1992).

ACHE DNA presents a G,C-rich pattern of codon usage, characteristic of housekeeping genes with tendencies to replicate and be transcribed early in the cell cycle (Holmquist et al., 1988), yet it is not a usual housekeeping gene as it is mostly expressed in terminally differentiated cells (i.e., nerve, muscle and hematopoietic lineages committed for differentiation). In contrast, BCHE DNA is A,T-rich (Prody et al., 1987, McTiernan et al., 1986), as expected from a tissue-specific gene with transiently high levels of activity following cell division (Layer et al., 1988). Consequently, there is essentially no cross-hybridization between the AChE and the BuChE cDNAs (Lapidot-Lifson et al., 1989). The BCHE gene, too, is not a typical tissue specific gene. It is expressed in similar yet not identical cell types to those expressing ACHE, and its major site of expression is in hepatocytes, which do not express AChE (Prody et al., 1987, Soreq et al., 1990b). Thus, although these two genes apparently diverged long ago in evolutionary history, selection pressures apparently kept their encoded polypeptides from extreme evolutionary drift. Being a G,C-rich gene, ACHE, in contrast to BCHE, displays abundance of Arg and Ala residues (not Ser, Lys). This should increase the thermostability of the AChE protein and may serve as a selection advantage for warm-blooded animals (Bernardi, 1989). Consequently, the folding energies for ACHE polypeptides have apparently adapted according to the living temperatures of their corresponding organisms of origin. Indeed, it was found difficult to express Torpedo AChE in mammalian cell culture unless temperature was lowered (Krejci et al., 1991a). The G,C-rich composition of the ACHE gene further implies differences in transcription control. Thus, the G,C-rich attenuator sequence in ACHE DNA may serve to control the transcriptional activity of this gene in analogy to the attenuating function of structures with similarly high free energy which have been observed in viral sequences (Kessler et al., 1989). The origin and mechanisms responsible for the surprising phenomenon of cholinesterase gene amplifications in germ (Beeri et al., 1992) and tumor tissues (Zakut et al., 1990) may also be related with this particular gene structure.

Apart from its conspicuous homology with members of the hydrolase family, the primary sequence of human AChE resembles that of noncatalytically active proteins such as thyroglobulin (Krejci et al., 1991a) and *Drosophila* neurotactin (De la Escalera et al., 1990). While the homology with thyroglobulin was taken as merely reflecting evolutionary divergence of common peptide domains (Taylor et al., 1991), the homology with neurotactin

is far more intriguing as it may shed new light on noncatalytic activities in which AChE is involved. Neurotactin is an integral membrane protein of the *Drosophila* nervous system, expressed early in the embryonic development of differentiating neurons (De la Escalera et al., 1990). It confers heterophilic adhesive properties to cells that express it (Barthalay et al., 1990). The existence of the LRE (Leucine-Arginine-Glutamate) motif, important for adhesion of neurons to the extracellular protein S-laminin (Hunter et al., 1991), has been implicated with the mechanism for adhesion of neurotactin. This motif is present only in human AChE protein and resides on the protein surface (position 395). Methods of genetic engineering and cell biology (i.e., transfection following site directed mutagenesis in the LRE motif) should be used in order to reveal whether the LRE motif participates in cell adhesion properties conferred by ChEs.

B. The AChE promoter region and its cross-species activity

Nucleotide sequencing of a 596 bp fragment upstream from the initiation site for transcription in the AChE gene revealed numerous consensus motifs, characteristic of binding sites for various transcription factors. This region thus contains consensus recognition sites for ubiquitous and tissue-specific transcription factors characteristic of genes expressed in muscle and nervous tissue, in hematopoietic cells, and during embryonic development. This complement of potential regulatory elements is in good agreement with the multiplicity of human tissues and developmental stages where the AChE protein has been observed (Silver, 1974; Soreq & Zakut, 1990a). Furthermore, binding sites for early/immediate gene products (i.e., Egr1) may explain AChE expression in tumor tissues, and may relate to the tumorigenic amplification of this gene (Zakut et al., 1990; Soreq & Zakut., 1993). The CREB and Egr1 elements predict a developmentally regulated response of the AChE gene to cAMP-inducing stimuli and signal transduction pathways, respectively, in nervous system cell lineages. The existence of an NFkB element within the first intron could further imply that expression of the AChE gene in lymphocytes is subject to cell cycle-related control, limited to the G0-G1 transition phase (Baldwin et al., 1991). The presence of a GAGA element suggests control by additional distant enhancer sequences (Biggin and Tjian, 1989).

The long-standing contentions that the spatiotemporal regulation of AChE indicates a role for this enzyme in the morphogenesis of various organs and tissues (Drews, 1975; Layer, 1991) is supported by the presence of AP_2 elements (Mitchell et al., 1991) in the AChE promoter and corroborated by our recent findings that AChE overexpression induces structural changes in developing *Xenopus* NMJ (Seidman et al., 1993). The human AChE promoter also displays similarities with the promoters for testicular proenkephalin (Kilpatrick et al., 1990), rat cytochrome C (Virbasius & Scarpulla, 1988), human porphobilinogen (Chretien et al., 1988) and the mouse AChE gene (Li et al., 1993a) in its independence from canonical CAAT and TATA boxes and its inclusion of C,G-rich regions and SP1 binding sites. This may account for our previous observations of AChE expression in developing human oocytes (Malinger et al., 1989) and sperm (unpublished). In particular, the possible role of the SP1 recognition sequence, as well as those of other promoter features, in germ cell transcription of the AChE gene merits further investigation. It will be necessary to delete and/or to mutate those putative binding sites in order to fully understand their role/s.

Conjugated to an AChE-encoding reporter sequence, the human AChE promoter directed transcription of AChEmRNA in microinjected *Xenopus* oocytes and

early embryos. Microinjected *Xenopus* oocytes (reviewed by Soreq & Seidman, 1992) and embryos (Etkin et al., 1984) have been shown to transcribe a variety of heterologous promoters. However, stage or tissue-specific regulation of exogenous DNAs has been difficult to achieve (discussed by Krieg & Melton, 1984). To our knowledge, the present study may represent the first successful attempt to express a human promoter in *Xenopus* embryos. We cannot yet conclude to what extent the accumulation of ACHE in myotomes of 2-day-old microinjected embryos reflects the involvement of developmentally regulated or tissue-specific factors. However, we observed a steady, developmentally regulated increase in endogenous ACHE levels correlated with nervous system development and the acquisition of motor function in the embryos, at about this time (Seidman et al., 1993, in agreement with others (Gindi & Knowland, 1979). It is therefore tempting to speculate that the deposition of catalytically active ACHE in muscle reflects the specialized nature of these cells, and may coincide with the developmentally regulated expression of other muscle-specific proteins (Hopwood et al., 1992). The low levels of detectable ACHE in homogenates of HpAChE-injected embryos suggests that the spatiotemporal expression of catalytically active enzyme from this plasmid in the embryo may be restricted. Since the differential cytochemical staining patterns observed between HpAChE- and CMVACHE-injected embryos do not appear to account for the 20-fold difference in biochemical activities, it is possible that the CMVACHE construct is less limited in its tissue specificity than the HpAChE construct, and that a significant proportion of the heterologous enzyme produced from the CMVACHE construct is secreted under conditions of high overexpression.

The high levels of ACHE hydrolyzing activity that have been found in embryos and oocytes injected with the CMV promoter-enhancer construct can be explained in light of the transcription factor binding sites included in this sequence. This calls for a comparative analysis of these two eukaryotic promoters. The CMV promoter-enhancer region, in contrast to the human ACHE promoter, contains functional TATA and CAAT boxes, active in the initiation of transcription. Five SP1 elements can enhance the levels of transcription from the CMV promoter. In addition, this region contains four binding sites to NFkB, known as a transcription regulator in the hematopoietic system and the Zeste factor, controlling embryonic transcription in *Drosophila*. Altogether, the factors found in the CMV may be responsible for its strong transcription activity, as compared with the lower efficiency HpACHE sequence. In addition, it is possible that the 2.2 kb upstream region of the ACHE gene, or particularly intron I in this gene, contains one or several repressor elements responsible for its low level of expression. Molecular studies using intron I deleted constructs will be useful to verify this issue.

It is interesting to note that there is no MyoD element in the CMV promoter-enhancer region (as compared with 6 sites in the human ACHE promoter), an element important for expression in muscle and which exists in promoters of other NMJ genes, such as the nicotinic cholinergic receptors (Heinemann et al., 1987). Three putative binding sites for MyoD have been found in the enhancer region of the mouse gene encoding the beta-subunit of the nicotinic acetylcholine receptor, one of the major components of vertebrate NMJ, (Prody & Merlie, 1991). Moreover, all of the genes encoding acetylcholine receptor subunits in all species examined so far have putative binding sites for a multitude of additional myogenic factors (discussed in Prody & Merlie, 1991). However, transgenic mice

constructed with different genes driven by the CMV promoter show transcriptional activity in myotomes and adult skeletal muscle, despite the fact that the CMV promoter lacks MyoD elements (Kothany et al., 1991). In our study the CMV promoter was active in embryonic myotomes and muscle, perhaps suggesting that its activity there is due to some other factor(s) (e.g., ?este, SP1) which drive expression in embryonic tissues. Alternatively, it is possible that we observed expression products of residual AChEmRNA molecules transcribed from the CMVACHE construct at an earlier phase in embryonic *Xenopus* development.

The high steady-state levels of AChEmRNA found by hybridization in brain basal nuclei as compared with hippocampus most likely reflect intensive transcription of the ACHE gene in brain areas enriched with cholinergic cell bodies. These observations are in line with recent in *situ* hybridization studies, where high levels of AChEmRNA and catalytically active AChE were observed in human striatum, included in the basal nuclei. Moreover, cholinoceptive hippocampal neurons were shown in this latter work to express considerably lower levels of AChEmRNA as compared with cholinergic neurons such as those in the basal nuclei. In muscle, the relatively low levels of AChEmRNA may be attributed to the limitation of transcription to subsynaptic muscle nuclei (Rotundo et al., 1992). However, other factors such as differential stability of muscle AChEmRNA should also be considered (Taylor, 1991). Also, adult brain and muscle may differ in their AChEmRNA levels from the fetal tissues studied in the course of this work.

It has been shown that ectopic expression/overexpression of developmentally important genes can lead to gross morphogenic aberrations. Several examples can be given to this phenomenon: ectopic expression of the proto-oncogene Int-1 results in duplication of the embryonic axis in *Xenopus* (McMahon & Moon, 1989). In another example, changes in cell fate in *Xenopus* embryos result from ectopic expression of a homeobox gene (Niehrs & De Robertis, 1991). In contrast, ectopic overexpression of human AChE in early *Xenopus* embryos imposed no overt barriers to apparent normal development. This finding is striking considering the dramatic 10-fold increase in AChE at NMJs of injected embryos and in view of the high rate of hydrolysis and the important physiological function attributed to this enzyme (Soreq & Zakut, 1990a, 1993; Soreq et al., 1992). Refined electron microscopy revealed no apparent differences in the integrity of myofibrils, yet demonstrated that overexpressed human AChE alters the properties of NMJs in transgenic *Xenopus* embryos (Seidman et al., 1993). The short time course of these experiments should also provide a convenient framework in which to assess the physiological import of natural and site-directed mutants of recombinant human ChE's (Neville et al., 1992; Soreq et al., 1992). Moreover, our present observations foreshadow the use of *Xenopus* embryos for coinjection experiments approaching the transactivation of various promoter elements and/or other elements in the vicinity of the ACHE gene by tissue-specific mRNAs (see, for example, Benvenisty et al., 1989). Furthermore, coinjection with DNA encoding other important synaptic proteins may lend insight into the complex interactions between these molecules at their site of function. Transiently transgenic *Xenopus* embryos thus provide a convenient, versatile system for integrative studies of the multileveled regulation of synapse formation and functioning.

The deposition of overexpressed enzyme in developing NMJs indicates tissue-specific trafficking of recombinant AChE to the correct

extracellular compartment surrounding somitic muscle cells. Indeed, these experiments add the targeting of AChE to NMJs to the list of evolutionarily conserved properties characteristic of this enzyme. Together with the spatially restricted expression shown for AChE (Rotundo & Gomez, 1990) and the nicotinic acetylcholine receptor (Changeux, 1991) in cultured muscle cells, these results may indicate the existence of a dedicated transport mechanism for localizing postsynaptic membrane proteins.

The human ACHE promoter is particularly rich in C,G residues and CpG dinucleotides. This, in turn, implies that it is susceptible for regulation by DNA methylation (Razin & Riggs, 1980). Dissection of the ACHE gene into its various components further revealed that the C,G nucleotides and CpG dinucleotides are not distributed evenly. Thus, the promoter domain is most enriched in clustered CpG dinucleotides, predicting suppression of tissue-specific gene expression through methylation sites interference with the binding of transcription factors at the promoter region. The abundance of CpG dinucleotides in the I1, but not the I2 intron, may further reflect the existence of functioning enhancer elements in the I1 domain, a possibility which should be pursued.

C. Alternative splicing in the human ACHE gene as a mechanism to create AChE polymorphism

Combined analyses of genomic DNA and RNA from human brain, muscle and myeloid K562 cells delineated a 1.5 Kb intron (I1) and a short 74 bp exon (E1) in the 5' upstream region of the human ACHE gene. The ACHE gene further appears subject to a similar, dominant splicing of two more introns (I2, I3) in all of the above analyzed tissues. The resultant major mRNA, representing exons E1, E2, E3, E4, and E6, encodes a globular hydrophilic ACHE. This is the catalytic subunit which may remain soluble (Doctor et al., 1991), interact with the collagen-like subunit characteristic of asymmetric ACHE at the neuromuscular junction (Krejci et al., 1991a), or associate with a lipid-containing stuctural subunit in brain (Inestrosa et al., 1987; Roberts et al., 1991). Moreover, brain tissues express relatively high levels of AChEmRNA, much more than muscle tissue as shown by RNA blot hybridization. In addition, cDNA libraries constucted from the brain tissue were found to be relatively rich in AChEcDNA as compared with a muscle library.

The variable intensity of AChEmRNA expression may further reflect yet uncharacterized contribution of additional promoter sequences and/or alternative splicing pattern(s) at the 5'-domain. In mouse, there is recent evidence for three alternatively spliced mRNA species which differ in their 5'-untranslated region (Li et al., 1993b). The first contains a 60-70 bp long exon 1 detected in muscle, brain and erythrocytes (as in the human hydrophilic AChEmRNA). The second contains a longer exon 1, with at least 229 bp upstream to the brain exon 1 sequence, and is primarily detected in brain. In the third, a minor species appearing in mRNA tested from muscle, brain and erythrocytes, splicing of exon 1 with 2 occurs 860 bp upstream from the major exon 2 acceptor site (i.e., 860 bp from intron 1 are, in this product, included in exon 2). It is possible that the apparently larger size of AChEmRNA from basal nuclei as compared with the cumulative length of exons 1 through 6 reflects similar phenomena in human tissues. A 200 bp larger exon 1 could tentatively explain the excessive length of mRNA, 0.4 longer than the cumulative length of E1-4+E6. However,

the relatively low levels of AChEmRNA in human brain hampered with our efforts to detect a yet larger species of AChEmRNA (the third type) or to examine this issue by 5'-extension.

Concerning the 3' region of AChEmRNA, we observed in RNA-PCR analyses that the fourth intron (I4) which follows the fourth exon, is variable in size. Within human brain and muscle, I4 is 829 bp long and its splicing connects the E4 and the E6 exons. Alternatively, in the tumor cell line K562, the 3'-terminal 751 residues from I4-E5 or the entire 829 residues, including I4, are expressed and directly continued by the E6 exon. This leads to the production of the I4-E5 or the E5-containing AChEmRNAs. The two predicted alternative enzymes produced from these mRNAs share their C-terminal peptide, which provides a potential link to membranes through phosphoinositide (PI) moieties (Roberts et al., 1991).

The I4 intron as well as the other introns conform with the 5' and 3' consensus splice sites and the poly-pyrimidine stretch rule (see also Li et al., 1991). Apart from these requirements, there are also non-sequence-specific requirements for minimal distances between the conserved elements. These are fulfilled in all introns, including I4, which is a very small intron (78 nucleotides). In mammalian introns, the minimal distance between the branch point and 5' splice site is about 50 and 18 nucleotides for the separation of the branch point from the 3' splicing site (58 and 20 nucleotides, respectively, in I4) (reviewed by Smith et al., 1989). These minimal separation requirements are likely to reflect the steric constrains for binding of splicing factors to the pre-mRNA substrate (Chabot & Steitz, 1987).

The abundance of E6 mRNA in K562 cells, similar to various vertebrate erythrocytes in their apparently exclusive production of PI-linked AChE (Roberts et al., 1991), remains puzzling. The minor mRNA (including E5) detected in these cells and in murine bone marrow (Li et al., 1991) potentially encodes a PI-linked AChE. However, blot hybridization of the PCR product derived from the alternative E5 containing transcript revealed a weak signal in K562 cells compared to that reflecting E6. Together these data indicate a substantial excess of E6 over E5 AChEmRNA in K562 cells, leaving the fate of E6 mRNA and its putative protein product in erythropoietic lineages unresolved. Peptide-specific antibodies will reveal if the predominant E4,E6 containing AChEmRNA species in K562 cells is translated into an active hydrophilic protein.

An interesting difference between AChE in nervous tissue and that of hematopoietic cells is that the first has to be transiently and rapidly induced according to need, whereas the latter is apparently expressed constitutively (Rakonczay & Brimijoin, 1988). Moreover, the bulk of AChEmRNA produced in the nucleated erythroid precursor should suffice to produce AChE throughout the life span of the mature anucleated and terminally differentiated erythrocyte (120 days). This, in turn, predicts that the AChEmRNA subtype encoding the erythrocyte-specific PI-linked form of the enzyme, but not brain AChEmRNA, should be especially stable. However, both mRNAs are initially designed with the same nontranslated 3'-termini, which contain a consensus motif for selective mRNA degradation (Shaw & Kamen, 1986). This AUUUA motif apparently functions as a recognition signal for an mRNA degradation pathway that is common to certain lymphokines, cytokines and protooncogenes. Interestingly, a similar AUUUA signal is also included in the 3'-terminal sequence of ß-

globin mRNA (Lange and Spritz, 1985), demonstrating that it does not preclude a long-term erythrocytic expression. Moreover, differential stability was shown for muscle AChEmRNA in cell cultures (Fuentes & Taylor, 1993), suggesting that it depends on elements other than sequence alone. Further experiments hence would be required to explain the mechanism(s) through which the differential stability of various AChERNA forms is controlled.

D. Potential differences between the 3 variable protein products of the ACHE gene

The above described pattern of alternative splicing predicts differences in the mature protein product. Thus, the 583 amino acids (aa) long AChE in brain is composed of four peptides contributed by exons 2,3,4 and 6 as transcribed in the major AChEmRNA. RNA-PCR analyses predict that in the K562 hematopoietic cells in humans, two additional different ACHE subunits should be produced. Thus, the hydrophobic, hematopoietic ACHE should divert from the major sequence at position 544, which corresponds to the site where alternative splicing connects the I4-E5 or E5 domains to the nascent AChEmRNA and modifies the inferred translation product. Both of the alternative AChE peptides interestingly contain a free cystein residue, which implies that both may be linked through a disulfide bond to another subunit, to create the AChE dimers characteristic of erythrocyte AChE (Gennari et al., 1987). The predicted hydrophobic ACHE should be 557 aa long, with its 14 C-terminal aa translated from the open reading frame in the alternative E5 exon. The readthrough form should be 583 aa long with its 40 C-terminal aa translated from I4-E5 (Karpel et al., 1993). Yet 29 more residues, also translated from the E5 exon, constitute a hydrophobic cleavable peptide characteristic of precursors to PI-linked proteins (Low, 1987; Ferguson, 1988) and present in both the hydrophobic and the readthrough forms. Such peptides are known to be proteolysed off the precursor polypeptide soon after its translation, which provides the energy required for linkage of the PI anchor. The trypanosoma VSG coat protein (Boothroyd et al., 1985) and the nervous system Thy-1 protein (Seki et al., 1985) are known examples for such processes. Interestingly, the human gene differs in this region from the mouse gene, which encodes only one PI-anchored protein as the I4 domain in mouse is nontranslatable (Li et al., 1991).

The cleavable C-terminal peptide encoded by the E5 domain in the ACHE gene bears no homology to other GPI-anchored peptides, whether AChE-related or others. However, comparing different GPI-anchored proteins revealed no homology among them either and suggested that the signal is of a general nature. To this end, Moran & Caras (1991) showed that in order to produce GPI-anchored proteins, the sequence should contain a hydrophobic tail and a site for cleavage that includes two small amino acids (Histidine and Glycine in E5) located 10-12 aa downstream from the cleavage site. The above requirements are both fulfilled in E5. Moreover, Synthetic signals which fulfill these requirements were shown to direct human growth hormone, a screted protein, to the plasma membrane via a GPI-anchor (Moran & Caras, 1991). In *Torpedo*, it has been shown that the C-terminal peptide of the GPI form of ACHE is sufficient to determine the addition of a GPI anchor (Duval et al., 1992). Thus co-expression of the ACHE catalytic subunits with a chimeric subunit in which the N-terminal domain of the collagenic subunit (QN) was linked to the C-terminal peptide of the GPI form of *Torpedo*, produced GPI anchored tetramers. The authors concluded that the QN domain is sufficient to bind catalytic AChE tetramers. It therefore

seems likely that the human E5-originated cleavable peptide would be similarly effective in this goal.

The polypeptide chains encoded by human AChE were subjected to computerized plot structure analysis according to the Chou-Fasman prediction (1987). This analysis provides best-guess predictions regarding folding patterns within the analyzed proteins as well as evaluations on the probability of particular peptide domains to be located at the surface of the fully folded enzymes. The outcome of this analysis is in line with the crystallography data depicting a globular structure with a central well where catalysis takes place and with an external position for the C-terminal peptide on the surface of the catalytic subunit (Sussman et al., 1991).

AChE forms with apparently modified biochemical properties were found associated with various tumor types (Zakut et al., 1988, reviewed by Soreq et al., 1991, 1992) and the demented brain of Alzheimer's disease patients (Navaratnam et al., 1991); one wonders whether alternative splicing could contribute to these modifications. Also, AChE is expressed in a variety of hematopoietic lineages, and particular cell types within the bone marrow may differ in their choice of splicing options for AChEmRNA. This may be physiologically important, since C-terminally mutated variants of human BuChE display distinct differences in their inhibitor interactions as compared with the normal enzyme (Neville et al., 1992). It is therefore possible that the alternatively terminated hematopoietic AChE forms may also demonstrate inhibitor interactions distinguishable from those of the brain enzyme. In addition, splicing of AChEmRNA in early embryogenesis calls for further investigation. Thus, the regulation of AChE biosynthesis presents an intricate model for the complex modulation of tissue-specific gene expression and involves multiple stages of the biosynthetic pathway. Having the necessary molecular tools and expression systems, integrated studies of these different levels of control in various tissues and stages of development may now be instigated.

Several experimental approaches may be useful for verification of the above predictions. Structure-function relationship studies using *in vivo* as well as cell culture model systems based on site-directed mutagenesis will map the major domains involved in the various aspects of ChE activities. Comparison with x-ray crystallography studies which delineated the three-dimensional structure of the active enzymes (Sussman et al., 1991, Harel et al., 1992) can verify the significance of such studies at the submicroscopic level. The detailed molecular mechanisms leading to the polymorphic properties of ChEs in various tissues can thus be searched for in different expression systems. Eventually, the combination of multiple scientific approaches and model systems will hopefully reveal the biological function(s) of ChEs in specific cell types and developmental stages.

In summary, the pleiotropic, developmentally modulated expression and molecular polymorphism of AChE in humans may be attributed to transcriptional, posttranscriptional and posttranslational control mechanisms. These, in turn, depend on the functioning of multiple nuclear transcription and splicing factors and on the association of the different C-terminal peptides in the catalytic subunits with variable structural elements. Understanding of the molecular mechanisms involved in this intricate expression pattern now provides the necessary tools to investigate the implication of AChE in mechanisms of cholinergic function and dysfunction.

E. AChE is implicated in neuromuscular junction development

In both oocytes and embryos, rhAChE retained the biochemical and immunochemical characteristics of the native human enzyme and was clearly distinguished from endogenous *Xenopus* AChE. Although no direct interactions between rhAChE and endogenous *Xenopus* AChE catalytic or structural subunits were observed, calculations of *Xenopus* AChE levels in microinjected embryos indicated that some feedback regulation may be operative in repressing endogenous AChE biosynthesis under conditions of overexpression.

Ectopic gene expression/overexpression often results in gross morphogenic aberrations (Harvey & Melton, 1988; McMahon & Moon, 1989; Sokol et al., 1991), yet we found that *Xenopus* embryos can tolerate large excesses of catalytically active heterologous AChE without suffering gross morphological or developmental abnormalities. This observation is especially interesting in light of evidence implicating AChE with the early embryonic development of noncholinergic tissues (Drews, 1975) and with developmental processes such as gastrulation and cell migration (Drews, 1975; Fitzpatrick-McElligot & Stent, 1981), nerve outgrowth and differentiation (Layer, 1991), and proliferation and differentiation of hematopoietic cells (Lapidot-Lifson et al., 1989,1992; Patinkin et al., 1990). As neither the overall rate of development nor the general morphology of CMVACHE-injected embryos was altered by 50- to 100-fold excesses of the active enzyme at the gastrula stage, our findings do not support a role for rhAChE in modulating cell growth, proliferation, or movement in very early *Xenopus* embryogenesis. However, since these biological activities may be unassociated with acetylcholine hydrolysis, they may demonstrate species specificity and remain undetected in our system. Nonetheless, the teratogenic effects of several OP poisons on skeleton formation (Meneely & Wyttenbach, 1989) and somitogenesis (Hanneman, 1992) have been correlated to their anti-ChE activities (see also Zakut et al., 1991) and suggest the use of AChE-transgenic *Xenopus* tadpoles to examine the mechanisms underlying these effects.

Despite their lack of MyoD elements, some constructs carrying the pan-active CMV promoter (Schmidt et al., 1990) were shown to be expressed in myotomes of transgenic mouse embryos (Kothary et al., 1991). Therefore, the characteristic subcellular segregation of overexpressed rhAChE in muscle may reflect either tissue-specific biosynthesis or posttranslational processing of nascent enzyme present in myotomal progenitor cells at the onset of myogenesis. The high levels of rhAChE present in gastrula stage embryos may argue for the latter possibility. In that case, the cytochemical data indicate the existence of an intrinsic, evolutionarily conserved property directing the subcellular trafficking of AChE in muscle, and thus explain the accumulation of rhAChE in NMJs of ACHEDNA-injected embryos. Furthermore, these results may imply that cotranslational processes are not required for the correct compartmentalization of AChE in muscle cells. In a similar vein, purified recombinant synapsin was shown to be incorporated into synaptic nerve terminals of cultured myotomes following microinjection into fertilized *Xenopus* eggs (Lu et al., 1992). The conspicuous intracellular accumulation of active AChE in developing myotomes of both control and experimental embryos reflects the retention of an enzyme presumably destined, by its possession of a signal peptide, for transport to the cell membrane. Our observations therefore indicate that some fraction of nascent AChE may be produced on smooth polyribosomes in muscle and remain within an intracellular cytoplasmic pool.

The general state of myotomal overexpression induced by microinjection of CMVACHE persists at least 3 days. However, the area covered by reaction product in cytochemically stained NMJs derived from day 3, CMVACHE-injected embryos was only 4- to 5-fold over that observed in controls. This figure represents a 2-fold lower excess than that measured in day 2 NMJs (Ben Aziz-Aloya et al., 1993) yet is slightly greater than the ratio of recombinant human to frog AChE as determined in homogenates at day 3 (Seidman et al., 1993). The apparent reduction in the level of synaptic overexpression from PF day 2 to day 3 may reflect the overall decline in total rhAChE activity observed during this period. However, since this calculation does not consider the higher-density staining observed in NMJs from CMVACHE-injected embryos, it represents an underestimate of the actual synaptic AChE content. Therefore, our data indicate enhanced stability of rhAChE at the NMJ compared to the total pool, a conclusion consistent with the observation that extracellular matrix-associated AChE persists *in situ* long after denervation of adult frog skeletal muscle (Anglister & McMahan, 1985).

Mammalian cells cotransfected with cDNAs encoding catalytic and noncatalytic AChE subunits (Krejci et al., 1991b) produce multimeric globular and asymmetric AChE, indicating that spatial coexistence may normally be the only requirement for multimeric assembly. Human cell lines transfected with various CMVACHE constructs similarly express and secrete homooligomers (Velan et al., 1991a; Kronman et al., 1992b). rhAChE displayed oligomeric assembly in microinjected *Xenopus* oocytes, but not in developing embryos where only monomeric rhAChE was detected. Nonetheless, rhAChE was found to accumulate in its natural subcellular compartments and was correctly transported to the NMJ of transiently transfected tadpoles. These findings are puzzling in light of the demonstration that secretion appears linked to oligomerization in transfected human 293 cells (Velan et al., 1991b; Kerem et al., 1993). Furthermore, the lack of demonstrable oligomeric assembly leaves the mode of association of rhAChE with the extracellular surface unexplained. It is thus possible that a tissue-specific posttranslational modification of rhAChE may be effected in developing myotomes, permitting secretion and extracellular deposition of nascent monomeric rhAChE.

In humans, ultrastructural and physiological alterations of the neuromuscular junction have been associated with congenital AChE and AChE deficiencies (Wokke et al., 1989; Jennekens et al., 1992) and may be associated with changes in the balance between these two molecules at the synapse. In one of these syndromes, patients presented, in addition to AChE/AChR deficits, NMJs displaying decreased miniature end plate potentials, reduced postsynaptic membrane lengths, and severely impaired postsynaptic secondary folding (Smit et al., 1988) - opposite features to those observed in our NMJs overexpressing AChE. It is unclear whether the reduced expression of synaptic AChE and/or AChR represents a cause or an effect of the ultrastructural aberrations observed in these patients. Our current observations suggest that disturbed regulation of the ACHE gene may indeed carry ultrastructural consequences for synaptic development. It will be interesting now to assess the impact of AChE overexpression on the expression and organization of AChR and other key synaptic proteins in these transiently transgenic tadpoles.

F. Chromosomal mapping of the ACHE gene suggests correlation with tumorigenic chromosomal breaks

Mapping of the human ACHE gene to a defined chromosomal location was

performed in three steps. The first phase of this study consisted of direct PCR amplification of human ACHE-specific DNA fragments from somatic cell hybrid DNAs and chromosome-sorted libraries. Reexamination by this technique of the chromosomal location of the BCHE gene, which we previously mapped to chromosome 3q26-ter (Gnatt et al., 1990), demonstrated the reliability and sensitivity of direct PCR amplification as compared with blot hybridizations of somatic cell hybrid DNAs. To circumvent technical difficulties resulting from the high G,C content in the ACHE gene (Soreq et al., 1990), a particularly high annealing temperature (72°C) was employed in the PCR procedure. This prevented the formation of nonspecific PCR fragments, which at 65°C also occurred with hamster DNA, but displayed no hybridization with the human ACHE DNA probe. Using the ACHE-specific primers, DNA from two different cell lines and one chromosome-sorted library supported PCR amplification of the ACHE fragment, as tested by blot hybridization. The common element to these sources was that they all contained DNA from human chromosome 7. In contrast, 17 cell lines and one chromosome-sorted library devoid of chromosome 7 gave negative signals. Regional mapping of the ACHE gene within chromosome no. 7 was thereafter achieved by fluorescent *in situ* hybridization with biotinylated-ACHEDNA. Double fluorescent spots were observed at the 7q22 location. Moreover, the two cell lines were positive for chromosome 7 also carried the cystic fibrosis transmembrane regulator gene, known to reside on chromosome 7q31.1. Altogether, this reinforced the assignment of the ACHE gene to chromosome 7q22.

Our findings imply that a single chromosomal site harbors ACHE coding sequences in the human genome, corroborating previous genetic predictions (Coates & Simpson, 1972). In addition, the data presented in this report confirm and extend our previous observations that the ACHE and BCHE genes, which encode two closely related ChE proteins, are not genetically linked to each other in the human genome (Gnatt et al., 1991). The similar yet not identical exon-intron organization in these two human genes (Soreq & Zakut, 1990a; Taylor, 1991) implies that they arose during evolution by gene duplication. This is evident from the presence of both ACHE and BCHE in early species such as *Torpedo marmorata* (Toutant et al., 1985), although in insects, a single gene encodes one ChE protein with mixed ACHE/BCHE properties (see Hall & Malcolm, 1991 for a recent example). All mammals studied so far have distinct ACHE and BCHE genes, with each of the homologous amino acid sequences within these ChEs being highly conserved (Soreq & Zakut, 1990b). This suggests that the two ChEs are both physiologically required in mammalian species and that the gene duplication event which led to their appearance might have occurred before the evolution of mammals (Taylor, 1991). The different composition of nucleotide sequences in the BCHE gene as compared with the ACHE gene (Soreq et al., 1990) further indicates that these two genes are evolutionarily relatively distant from each other, and the mapping results presented in this paper that the ACHE and BCHE genes are located on separate chromosomes strengthen this assumption.

The ACHE gene amplifies in leukemias (Lapidot-Lifson et al., 1989), ovarian carcinomas (Zakut et al., 1990) and platelet disorders (Zakut et al.,1992). The long arm of chromosome 7 tends to break in cancerous cells (Mitelman, 1988). Further studies will be required to search for putative correlation(s) between these events and the ACHE gene. It is interesting to note that the A,T-rich BCHE gene, which presents almost a mirror image to the properties of the ACHE gene, is likewise subject to frequent

amplifications and resides in the 3q26-ter chromosomal fragment, breakable in thrombopoietic disorders (Pedersen, 1990), a phenomenon which awaits explanation.

G. Tumorigenic expression of alternative AChEmRNA transcripts

The findings presented in this report reflect a surprising complexity of alternative splicing patterns of AChEmRNA transcripts in tumor cell lines from heterogeneous tissue origins. Furthermore, these variable AChEmRNA species may encode 3 different AChE polypeptides, with potentially distinct properties, one of which is unique to humans.

That the alternative transcripts found in tumor cells are the molecular origin(s) for PI-linked AChE is indicated from reports that K-562 cells (Toutant et al., 1990) are similar to various vertebrate erythrocytes (Roberts et al., 1991) in their production of PI-linked AChE. It should be noted that in both the mouse and rat ACHE genes, the I4 domain includes a termination codon (Li et al., 1991; Legay et al., 1993b). The inferred "readthrough" enzyme in human may hence be distinguished from the ones in rodent both in its length (583 residues) and in its capacity for PI-linkage. Yet, expression of AChEmRNA does not necessarily imply production of its protein, as is indicated from the presence of AChEmRNA (our results) and the absence of AChE activity in 293 cells (Velan et al., 1991a). Elicitation of antibodies specific to the alternative peptides will therefore be required to reveal whether the inferred AChE forms are expressed in human tumor cells and find out if they may serve as tumor-specific markers. Peptide-specific antibodies also will reveal if the predominant E4,E6 containing AChEmRNA species in K562 cells is translated into an active hydrophilic protein.

Different choices of splicing options for AChEmRNA may be physiologically important; thus, C-terminally mutated variants of the closely related human enzyme BChE display distinct differences in their inhibitor interactions as compared with the normal enzyme (Neville et al., 1992). This, in turn, suggests that altered C-terminus may modify the biochemical properties of ChEs. AChE forms with apparently modified biochemical properties were indeed found associated with various tumor types (Zakut et al, 1988; reviewed in Soreq et al., 1991) and in the demented brain of Alzheimer's disease patients (Navaratnam et al., 1991); one wonders whether alternative splicing could contribute to these modifications and to the distinct properties of embryonic AChE (Soreq & Zakut, 1990b).

The question of whether ChEs play a developmental role in tumorigenesis has been put forth by many (reviewed in Soreq et al., 1992), and may be reevaluated in view of our present findings. Cholinesterase gene amplifications (Soreq & Zakut, 1990b) have been correlated with a variety of tumors including those of the nervous (Gnatt et al., 1990), reproductive (Zakut et al., 1990) and hemopoietic systems (Lapidot-Lifson et al., 1989). However, the tumor-amplified ACHE gene tended to be incomplete (Zakut et al., 1992) and therefore unlikely to drive effective transcription. Hence, it is not surprising that AChEmRNA levels in the tumor cells were higher, yet within the same range as in normal developing tissues. The presence of an E-box motif in the recently cloned ACHE promoter (Ben Aziz-Aloya et al., 1993) suggests an alternative route for a more limited tumorigenic induction of ACHE, by the enhancement of transcription through c-Myc (Blackwell et al., 1991). Intensive transcription may thus explain the presently described alternative splicing patterns. This can occur by

default, perhaps due to the tumorigenic lack of sufficient amounts of the specific protein factor(s) controlling the common splicing pattern of AChEmRNA in brain. That transcription is particularly intensive in the tumor cell lines is evident from the high levels of ACHE, BCHE and CHED transcripts in them.

Interestingly, our findings demonstrate three alternative pathways for ACHE transcripts in tumor cell lines, yet not in primary tumor tissues. This may reflect mechanism(s) related with the mode of cell growth and which distinguish cultured cells from the *in vivo* situation. It should be noted in this respect that the ACHE promoter includes an Egr-1 motif, predicting serum induction (Ben Aziz-Aloya et al., 1993). Absence of angiogenic limitations under culture conditions can therefore up-regulate AChEmRNA transcription. Further studies should be performed to find out if this contributes to the alternative splicing and to reveal whether the predicted PI-linked AChE forms induce tumorigenic processes. The growth-regulatory role reported for AChE in murine erythroleukemic Friend cells (Paoletti et al., 1992) and observed recently by *in vivo* antisense inhibition of ACHE gene expression (Lev-Lehman et al., 1993) is in line with this latter prediction. In conclusion, the pattern of AChE biosynthesis at multiple stages of the biosynthetic pathway presents an intricate model for the complex modulation of tumor-specific gene expression. Having the necessary molecular tools and expression systems, integrated studies of these different levels of control in various tissues and stages of development may now be instigated.

H. Antisense approach to the hematopoietic role of AChE

To pursue the potential hematopoietic role of AChE and its cell lineage specificity, we employed *in vivo* antisense inhibition of ACHE gene expression. When injected intraperitoneally, AS-ACHE was found to exert transient effects on both the levels of its target AChEmRNA and on the composition of lymphocytes, megakaryocytes (MKs), myeloid and erythroid cells within the bone marrow. This attributes a hematopoietic role to AChE, the production of which was prevented by this treatment. The hematopoietic system is an appropriate target for such AS-oligo paradigms because of its extreme sensitivity to external stimuli and due to the high turnover of cells, differentiating from proliferating stem cells (Handin, 1991). Both stem and committed and/or differentiated cells could serve as targets for the AS-ACHE effects, which should principally be limited to the life span of the affected cells. Indeed, the AS-ACHE oligo induced drastic, hematopoietic changes at 12 days, yet hematopoietic balance was apparently restored at 20 days after treatment, when most of the bone marrow cells in the treated mice could be assumed to have developed after the single-dose treatment.

Quantitative RNA-PCR, differential cell counts and *in situ* hybridization were employed to demonstrate the selective degradation and restoration of AChEmRNA and its correlation with hematopoiesis under AS-ACHE treatment *in vivo*. The RNA-PCR analysis demonstrated an apparently total abolishment of AChEmRNA at 12 days after treatment, when lymphocyte and erythroid fractions were drastically reduced in the bone marrow of treated mice. This implicates AChE in the development of both lymphocytes and erythrocytes, two cell lineages expressing this enzyme (see Soreq & Zakut, 1993 for a recent review). Because of their small numbers and longevity, it was difficult to evaluate differences in the MKs fraction at day 12. However, the secondary decrease in actin mRNA in the bone marrow, where MKs

are replete with this mRNA species (Rentrop et al., 1986), was taken as an indication for decrease in MK as well. Since MK and erythroid cells are considered to share a common progenitor (Martin et al., 1990; Romeo et al., 1990), our findings further suggest that these progenitors are sensitive to the AS-AChE effects.

The mechanism through which AChE controls proliferation and/or differentiation of hematopoietic cells is still unknown. In principle, it could either involve cholinergic signaling or relate to the putative cell-adhesion properties of AChE, which resembles *Drosophila* neurotactin in its primary sequence and includes the LRE element for binding laminin (Soreq & Zakut, 1993). Lymph nodes were selected as an additional tissue for the RNA-PCR experiments because lymph node epithelium expresses AChE (Karnovsky & Roots, 1964) and is subject to continuous replacement, similarly to bone marrow cells. The drastic decrease in lymph node AChEmRNA levels 12 days after treatment demonstrated efficient tissue distribution of the administrated AS-AChE oligo and the more limited secondary decrease in lymph node actin mRNA could either reflect general toxicity of this treatment or implicate AChE in epithelial development as well.

The *in situ* hybridization approach provided cell type and developmental correlations for the AS-AChE effects, with particular reference to the megakaryocytopoietic process. Both AChE- and BuChEmRNAs were found to be efficiently expressed in MK, more than in other hematopoietic cell types. In the case of actin mRNA, also shown to be efficiently expressed in MK (Courtney et al., 1991), the megakaryocytopoietic increase was taken as an indication for actin involvement in MK development and functioning (there). In contrast, fibronectin mRNA, presumably required solely for MK development, was shown to decrease during megakaryocytopoiesis (Courtney et al., 1991). Our findings therefore suggest that both ACHE and BCHE may be needed for MK development and that ACHE, more than BCHE, may further be involved in MK maturation and functioning. This, in turn, foreshadows the use of *in situ* hybridization with CHEcRNA probes for analyzing the molecular mechanisms leading to defects in MK development.

Within mature MK, the variations in labeling intensities with [^{35}S]-AChEcRNA probably reflect a transcription rate which exceeds the rate of nucleolytic degradation for AChEmRNA, leading to its accumulation. This is compatible with the long life span of several days for mature MK (Handin, 1991), and the half-life of approximately 10 hr for mammalian AChEmRNA (Soreq et al., 1984). That mature MK continue to produce AChEmRNA throughout their life span further implicates ACHE in MK functioning and/or platelet production and indicates that AS-ACHE treatment may modify these properties *in vivo*.

Subclassification of MK sizes at 12 days after AS-ACHE treatment would not be informative due to the longevity of MK, part of which would still represent cells from the pretreatment period. The concomitant increase in both pro- and mature MK at 20 days after treatment may reflect enhancement in both development and maturation of these cells, at the time when AChEmRNA levels were almost completely restored. This apparent induction of promegakaryocytopoiesis could be a feedback response to earlier reduction in MK development, reflected in the drastic suppression of actin and AChEmRNA levels in the bone marrow at 12 days. This corroborates previous observations of platelet increases following ACHE inhibition at the protein level (Burstein et al., 1980; Burstein & Harker, 1983), and

attributes the defective platelet production in patients with various blood cell disorders to the amplification and mutability observed in their ACHE genes (Lapidot-Lifson et al., 1989; Zakut et al., 1992). The increased risk for farmers exposed to ACHE-inhibitory insecticides to develop leukemias (Brown et al., 1990) is also in line with these observations. Parallel experiments in erythropoietic cell cultures may directly reveal whether AS-ACHE affects stem cell proliferation, distinguish between its effects and those of AS-BCHE (Patinkin et al., 1990; Lapidot-Lifson et al., 1992), and determine the mechanism(s) by which AS-CHEs exert their effects on distinct hematopoietic cell lineages.

I. Structure-function relationship studies in hChEs

Structure-function relationship studies were performed on a set of natural ChE variants and site-directed mutants, the aim being to delineate important domains contributing to the biochemical properties of these enzymes and determining their sensitivity to different anti-ChE drugs.

Previous biochemical studies have indicated that the binding center in ChEs contains several functionally important subsites (Quinn, 1987). Our studies with the recombinant natural variants of human BCHEs imply that intramolecular structural relationships exist between C- and N-terminal domains in ChEs and contribute to binding of substrates and inhibitors to these subsites. Composite interactions between the three cysteine loops in ChEs are indicated from the binding site properties of the natural BuChE variants, and anionic as well as hydrophobic interactions apparently participate in binding of substrates and inhibitors, with varying interplays for different ligands. This, in turn, creates a selection advantage for several double BuChE mutants over the single Gly70 variant, in that these double mutants possess high catalytic activities combined with resistance to various natural inhibitors.

Use of the site-directed BuChE mutants demonstrated that more than a single electronegative domain contributes to binding different substrates and inhibitors, and that certain domains are principal for binding specific inhibitors.

1. Resistance to charged ligands in *in ovo* produced hBuChE

The findings presented in this report directly demonstrate the involvement of Asp70 in electrostatic interactions of hBuChE, through the use of the *Xenopus* (Arpagaus et al., 1990) oocyte expression system (Soreq & Seidman, 1992). In addition, these observations indicate that other regions in the catalytic subunit may contribute significantly to part of the characteristic "atypical" properties of the enzyme in individuals carrying the Gly70 substitution, with certain physiologically important consequences.

BuChE is generally assumed to act as a scavenger, removing compounds that are toxic to ACh-binding proteins from the circulation (Whittaker, 1986). Biochemical, genetic and molecular biological approaches have gradually revealed that the BCHE gene appears in several differently mutagenized allelic variants (La Du, 1989; Gnatt et al., 1991; Zakut et al., 1991; Whittaker, 1986). Therefore, naturally occurring toxic compounds that normally interact with ChEs have been sought whose binding to mutated BuChEs is reduced. Assuming that BuChE activity is essential for certain vital processes, either directly or as a replacement for inhibited AChE, such mutations may provide the individuals carrying them with a selection

advantage. This would explain both the abundance of BuChE alleles and their characteristic frequencies in different populations, which may be subject to toxic compounds (Whittaker, 1986).

The steroidal alkaloid solanidine apparently interacts selectively with mammalian BuChE (Harris & Whittaker, 1962) but not AChE (Roddick, 1989) and inhibits its catalytic activity. This aglycone, as well as its parent glycoalkaloid compound, solanine, are naturally present in all members of the *Solanum* plant family, including *Solanum tuberosa* (potatoes), and are likely to be present in extremely high and toxic concentrations in blighted potatoes. In addition to these recorded acute toxicities, solasodine was also found to be teratogenic in mammals (Keeler, et al., 1976). Therefore, the reduced ability of "atypical" BuChE to bind the *Solanum* poisons can clearly have a survival advantage, particularly in heterozygotes to this mutation where scavenging and catalytic activities may be retained under intoxication. Our findings indicate that the single substitution of Asp70Gly by itself is sufficient to provide individuals with such advantage by modification of BuChE subsite(s).

The apparently crucial role of Asp70 within BuChE in binding charged ligands was further probed by reactivation experiments with the oxime 2-PAM, previously shown to reverse OP intoxication of the esteratic site serine in ChEs (Edery & Schatzberg-Porath, 1958) by an action specifically mediated by electrostatic binding (Barnett & Rosenbery, 1977). Replacement of Asp70 by glycine completely prevented this reactivation, regardless of the additional substitution Ser425Pro. Asp70 is, therefore, an essential and sufficient requirement to the interaction of solanidine and 2-PAM with the charged subsite in hBuChE.

Molecular genetics approach has demonstrated that the N-terminal Gly70 mutation is frequently linked with additional substitutions, altering single amino acid residues in the C-terminal part of the BuChE molecule (Arapagus et al., 1990). The Ser425Pro mutation which co-appeared with Gly70 in glioblastoma and neuroblastoma tumors (Gnatt et al., 1990) demonstrates yet another case of such linkage. According to our line of thought, the combination of two amino acid substitutions should provide the enzyme with yet higher resistance, at least toward some charged ligands, to create the selection advantage leading to the observed genetic linkage. The apparent synergistic resistance of the double Gly70/Pro425 mutant to inhibition by SuccCh and dibucaine demonstrates that this may be true.

Full log dose-response inhibition curves with dibucaine, and, more important, SuccCh, to calculate IC50 values provided a complete characterization of the differences caused by each of the mutations alone and by both of them together. Such inhibition studies were performed for two different reasons. First, phenotyping "atypical" individuals on the basis of dibucaine numbers (Kalow & Genest, 1957) required the use of different and specific assay conditions. Second, it allowed us to overcome anomalies in which BuChE may be observed as "normal" from its apparent interaction with dibucaine, yet behaves in a completely contrasting manner with SuccCh and fails to bind the muscle relaxant. Such surprising patterns of inhibition have been observed following the phenotyping of a number of different human serum BuChE samples from individuals displaying clinical SuccCh sensitivity (Agarwal et al., 1976). The double Gly70/Pro425 mutant appeared in our experiments to be far more resistant to both dibucaine and SuccCh than the single Gly70 mutant, whereas the Pro425

substitution alone was ineffective with both ligands. It is possible that such differences have so far been overlooked by the standard clinical protocol, employing single point reference numbers as indications for dibucaine or SuccCh resistance (see McGuire et al., 1989 for an example). Further experiments will be required to determine the abundance of the double Gly70/Pro425 substitution and whether other C-terminal modifications linked to the Gly70 substitution are similarly effective with anionic site ligands. Also, other naturally occurring inhibitors should be pursued (see, for example, Abramson et al., 1989) which may explain the biological background to these mutations.

To resume the above predicted evolutionary selection pressure, BuChE should have a developmentally essential role either in germ cells or early in embryogenesis. The intensive expression of the BuChE gene in developing human tissues (Drews, 1975) and oocytes (Malinger et al., 1989; Soreq et al., 1987a) and the transiently elevated levels of BuChE in embryonic human brain (Zakut et al., 1985) are indications that BuChE might have a developmental role. The observation that a synthetic phosphorothioate "antisense" oligonucleotide spanning the initiator AUG sequence in hBuChEmRNA inhibits bone marrow cell development in culture (Patinkin et al., 1990) directly proves an essential role for BuChE in hematopoiesis, whereas the apparently heritable germline amplification of the BCHE gene in two generations from a family of farmers exposed to the agricultural anti-ChE insecticide Parathion (Prody et al., 1989), points toward a function in germ cells. Altogether, it therefore appears that BuChE activity is indeed developmentally essential, which creates evolutionary pressure for genetic modifications in the BCHE gene under conditions where its protein product is blocked by inhibition.

The general nature of these considerations is clearly indicated by the large number of identically aligned amino acid residues in the peptide regions harboring Asp70 and Ser425 throughout the entire family of ChEs (Soreq & Prody, 1989). In particular, the highly conserved Glutamate-Isoleucine-Glutamate (EIE) domain upstream from Ser425 should be noted. This electronegative domain may be of crucial importance in the presumed binding of certain charged non-sulfur-containing choline substrates by Gly70-containing BuChE muteins (Neville et al., 1990a,b). The importance of such domains in ChEs which serve to bind positively charged choline substrates should be further examined either by pursuing additional and yet unknown variants in the CHE genes from humans or other species, or by employing site-directed mutagenesis in conjunction with the efficient *Xenopus* oocyte microinjection assay to examine substitutions in predefined peptide domains.

2. <u>Oocyte expression of site-directed and natural variants of BuChE</u>

A major aim in this study was to investigate intramolecular interactions in ChEs by analyzing the effects of naturally occurring and site-directed mutations within hBuChE. The tolerance of the BCHE gene to phenotypically apparent mutations altering various amino acid residues throughout the BuChE polypeptide, an important asset in these experiments, may reflect certain evolutionary advantages exerted by these variably combined mutations. Thus, both resistance to solanine- or quinoline-derived natural poisons (Whittaker, 1986) and the restoration, demonstrated herein of hydrolytic activities in inhibitor-resistant double and triple mutants could enable BCHE expression at levels sufficient for survival under exposure to such poisons. Similarly, the high mutability rate in the human

albumin gene, with recurrent variants that have arisen independently in diverse populations (Brennan et al, 1990), was recently correlated with variable affinities to drugs (Kragh-Hansen et al., 1990). Thus, the evolution of drug-resistant mutants may be common to various plasma proteins.

The Asp70Gly substitution reduced the hydrolytic activity of BuChE in an apparently dominant manner, unaffected by the additional Pro425 or Tyr561 mutations, which by themselves exerted only limited effects on substrate hydrolysis. However, the presence of His114 in conjunction with Gly70 totally restored the hydrolytic activity of Gly70 BuChE. This observation clearly demonstrates an interactive and opposing effect between these two mutations. The complete restorative effect of His114 on Gly70 BuChE substrate hydrolysis may be related to the structural alpha-helix-forming ability of this aromatic residue in a potentially alpha-helix-forming sequence in analogy with His18 in barnase (Sali et al, 1988), or in a manner parallel to the stabilizing effects of additional alanine residues within an alpha-helix of T4 lysozyme (Zhang et al., 1991). The failure to affect BTCh hydrolysis of the presumed alpha-helical breaking ability of a Pro mutation (Piela et al., 1987) which resides only 16 amino acid residues upstream from the electronegative Glu441, Ile442, Glu443 sequence suggests that the dramatic depressant effects of the site-directed Gly441/Gln443 mutations on BTCh hydrolysis do not reflect steric changes but an effect related to loss in charge. It is likely that the presence of Gly441/Gln443 drastically modifies the crucial electronegative environment at this region which harbors the basic and highly conserved His438 residue implicated in the ChE catalytic triad (Gibney et al., 1990), thus lessening the hydrolytic capability of the triad mechanism. In addition, the possibility that the negatively charged Glu441 and Glu443 residues are directly involved in the catalytic process *per se* cannot be excluded, since parallel domains in lipases (Sussman et al., 1992) are known to attract water molecules.

All BuChE variants interacted normally with BzCh and PrCh (the latter in His114-deficient Gly70-containing BuChE mutants), in accord with previous findings (Neville et al., 1990a). Thus Asp70, which exerts a crucial role in binding of SuccCh and reactivation by 2-aldoxime methiodide (2-PAM) of DFP-intoxicated BuChEs (Neville et al., 1990a), is not required for BzCh and PrCh binding. If binding of quaternary-charged choline esters is mediated via charge interactions (Rosenberry, 1975; Quinn, 1987), electronegative domains other than those harboring the highly conserved Asp70 would be implicated in such electrostatic interactions in agreement with the notion of multiple negative charges at the ChE active site (Nolte et al., 1980). Alternatively, these observations require assessment of the importance of charged anionic site interactions in ChEs, as opposed to a hydrophobic binding site. Indeed, the observations of effective binding of both uncharged ACh analogues/inhibitors (Hasan et al., 1980,1981; Cohen et al., 1982) and hydrophobic compounds (Naveh et al., 1981) to AChE have indicated the likely location of hydrophobic domains contiguous with its active center (Quinn, 1987). The influence of such hydrophobic interactions in BuChE may explain the minimal, 10-fold increase in BzCh binding to all BuChE enzymes in comparison with other choline esters. Furthermore, the selective labeling of the cationic, irreversible alkylating agent N,N-dimethyl-2-phenyl-aziridinium (DPA) tTrp84 in *Torpedo* AChE (Weise et al., 1990) also indicates the likely role of aromatic residues in constituting the ChE binding domain, supporting previous

biophysical (Shinitzky et al., 1973; Berman et al., 1985) and biochemical (Majumdar & Balasubramanian, 1984; Page & Wilson, 1985) studies. In addition, x-ray crystallography data for human lipase, also functioning by a catalytic triad, reveals tryptophan and tyrosine residues in close apposition to the nucleophilic active center serine (Brady et al., 1990; Winkler et al., 1990). Hence, hydrophobic domains may be important contributors to the catalytic center in ChEs, with long-range electrostatic interactions playing an important role in binding specific positively charged substrates, as, for example in subtilisin (Russel et al., 1987; Russel & Fersht, 1987). This latter assumption was proven correct by recent high-resolution x-ray crystallography studies (Sussman et al., 1991).

The marked changes in binding of SuccCh and ACh to Gly70 BuChE variants suggest that negative-charge interactions play a major role in binding these esters. However, these binding reactions also depend upon the overall tertiary structure of the polypeptide chain, as indicated by the modulatory effects of additional His114, Pro425 and Tyr561 mutations on the Gly70-induced disruption of SuccCh binding. Thus, the Gly70 mutation affects a region that closely interacts with the His114 region and, more important, with the C-terminal domains harboring Pro425 and Tyr561. This, in turn, strengthens previous suggestions (Neville et al., 1990b; Prody et al., 1989) that the genetic linkage between Gly70 and various C-terminal mutations in BuChE provides an evolutionary advantage related to drug resistance. In contrast to SuccCh, dibucaine interactions appear to be principally dependent upon a charged C-terminal domain in BCHE. That the C-terminal region interacts with the N-terminal domain in creating active-site volume is implied from the disrupted dibucaine binding in the double Gly70/Pro425 variant and the triple Gly70/His114/Pro425 variant.

The steroidal alkaloid solanidine and its parent glycoalkaloids (Harris & Whittaker, 1962; Roddick, 1989) were employed to further investigate structural restrictions on charge interactions in ChEs. While usual BuChE effectively interacted with the triose-containing glycoalkaloids alpha-solanine and alpha-chaconine, as well as with their active BuChE-inhibiting moiety solanidine, Gly70 BuChE variants all failed to interact with solanidine, yet bound to some extent with alpha-solanine and effectively to the rhamnose-enriched alpha-chaconine. Since no major change in charge is involved, these graded inhibition patterns suggest that Asp70 asserts a primary binding capability, yet the hydrophobic and structural elements of the sugar moieties stabilize this binding. Furthermore, it is likely that the presence of sugar residues repositions electrostatic components required for active-site binding of these alkaloids. Altogether, these observations as well as the substrate binding data raise the intriguing possibility that the relative flexibility of ligand recognition by BCHE reflects a restricted set of configurations involving interactions between peptides in various domains throughout the molecule, as well as an interplay between electrostatic and hydrophobic interactions.

Mutation-related alterations in IC_{50} values for carbamate and OP inhibitors provided further insights into the active center domain in ChEs. Gly70 appeared to interrupt binding of the BuChE-specific OP iso-OMPA and the carbamate prodrug bambuterol, as its substitution for Asp70 dramatically increased the apparent IC_{50} values for these two inhibitors. However, binding to both iso-OMPA and bambuterol was far tighter with all other

Gly70 variants, suggesting that this interaction also involves other domains in the protein. That Asp70 is particularly important for binding BuChE-specific inhibitors is implied from the relatively limited differences asserted by Gly70 on binding the nonspecific ChE inhibitors ecothiophate and physostigmine. However, in these cases as well, interference with binding was restored by additional mutations. This, in turn, could reflect the exposure of, and interaction with, alternative residues which could be either hydrophobic or negatively charged. Exchange of the Asp70 domain in BuChE by its parallel counterpart loop from AChE should be useful for testing these options.

The BuChE polypeptide in man includes three loops (A,B and C) governed by cysteine-cysteine bonds. Taking into consideration the synergistic interactions between loop A constituents (i.e., Asp70) and loop C constituents (such as Pro425), and in view of the apparently important structural role of the Glu441-Glu443 region, we distinguish between the C1 (Cys400 to Met437) and C2 (His438 to Cys520) peptide sequences. Assuming a stem structure for the peptide domain which starts with the key His438 residue and ends with Glu443, a two-dimensional structure emerges which complies with these distinctions. This model represents a modification of previous two-dimensional ChE models (MacPhee-Quigley et al., 1986; Lockridge, 1984) in that it displays intricate interweaving of BuChE-specific and ChE-common peptides throughout the molecule, demonstrates the positions of the studied mutations and other available ones in BuChE, and exposes new candidate residues for key functions in the catalytic hydrolysis of choline esters. Hence, the highly conserved amino acid sequence 318-341, adjacent in this structure to Ser200 and His438, contributes to the charged Glu327 residue involved in the catalytic triad (Sussman et al., 1991). In addition, multiple hydrophobic residues (His77; Trp82, 414, 430, 469 and Tyr147, 258) emerge in close proximities to loop foldings, which could reflect their participation in forming part of the active site groove as in human lipase (Brady et al., 1990; Winkler et al., 1990). Further insights into the secondary and tertiary structures of ChEs will arise from combined interpretations of high-resolution x-ray diffraction patterns with expression data of site-directed and chimeric BuChE/AChE constructs from various species and further natural variants of BuChE and possibly AChE.

3. <u>hBuChE as a potential decoy for OP poisons</u>

The goal is the development of a molecular decoy, an agent that will react with OP agents and remove or inactivate them before irreparable harm can be done to AChE. Our approach has been to begin with a natural human protein, BuChE, and to make variants of it by improving its useful features. Reasons for choosing to base our work on BuChE are:

a. It already serves this function.
b. As a serum enzyme, it is well-placed to protect the CNS as well as vital organs by intercepting OP agents before they can reach their target at synapses and NMJs.
c. Very different natural levels of this enzyme are tolerated in man. The enzyme is present in serum in rather large quantities and is very active; thus the actual levels of the enzyme are not critical to health.
d. As a natural protein, BuChE is nonimmunogenic. We expect, further, that as changes to be introduced into it will be inside the active site gorge, and not on the surface, the variants, too, will be non-immunogenic.

The basic techniques of site-directed mutagenesis are well-established, but in order to develop an effective decoy, several conditions must be met:

a. The BCHE gene must be isolated, cloned and sequenced.
b. The three-dimensional model of the protein must be known so that residues can be intelligently selected for testing for essentiality for catalysis, contribution to substrate and inhibitior binding, and just as important, for nonessentiality.
c. There must be appropriate expression and assay systems available. Expression must be at a sufficient level for the sensitivity of the assay system.

The gene has been isolated, cloned and sequenced. A model derived from the x-ray crystallography model of *Torpedo* AChE is available, and we have expended considerable effort in developing the *Xenopus* oocyte for expression, and the 96-well microtiter assay system, especially coupled with immunosorption of the enzyme to the wells, as an assay system.

Criteria for the decoy must be developed so that success may be evaluated:

a. Compared to natural BuChE, the successful decoy will bind a wide range of OP agents more tightly and will react faster with them to form the phosphoryl-variant enzyme.
b. Ideally, the phosphoryl-enzyme will be reactivatable with 2-pyridinyloxime methiodide (2-PAM) or other reactivator in order, by recycling, to increase its effectiveness as a decoy.
c. It will be nonimmunogenic and will not be cleared from the circulatory system unusually fast.

V. CONCLUSION

The search for a readily available defense against the recently attempted threat of chemical weapons impresses us with its urgency. The vulnerability of vital nervous functions, via ChE inhibition, is clearly apparent. The population-specific distribution of even more OP-vulnerable individuals, which we have described, emphsizes the geopolitical implications of the problem. Several approaches to this problem have grown out of our exploitation of recent developments in molecular biology.

First, our cloning of the human ACHE gene, followed by scaled-up production of recombinant hAChE in suitable hosts, offers the potential for a prophylactic treatment of ChE inhibition, based on the introduction into an affected individual of quantities of a ChE as biological scavenger. A more elegant approach might be to construct biologically compatible ChE mutants with an increased OP affinity, as compared to the native enzyme, or with a capacity to hydrolyze OPs. Our initial site-directed mutagenesis studies have provided the groundwork for a second round of studies that now can be more precisely directed at areas of interest in the ChE molecule.

Second, given an understanding of the mechanisms involved in regulating ChE biosynthesis *in vivo*, one might be able to devise triggers for the controlled stimulation of AChE synthesis either in crisis situations or as a precaution in a threatening environment. Our studies on alternative splicing and tissue targeting of the several forms of AChE also offer the possibility of another level of control over the placement of prophylactic quantities of AChE within the body of an OP-vulnerable individual.

A thorough understanding of the mechanisms involved in ligand binding may subsequently offer a third advancement in this principle: introduction of a synthetic peptide capable of scavenging circulating ChE inhibitors. The advantages of a small peptide are, of course, increased concentrations of the active agent, economic considerations, and perhaps delivery of the substance and a minimization of antigenic stimulation.

In light of the accumulating evidence for the multileveled regulation of AChE production in various tissues, it is now possible for the first time to study its control in sufficient detail to understand its responses to lethal and sublethal OP poisoning. In terms of the implications for human ecology, both the prevalent use of agricultural OP insecticides and the threat of long-term environmental damage might be associated with "fallout" from the overuse of OP poisons. Therefore, these aspects of AChE regulation, its properties and its role(s) now need more attention than ever.

VI. FIGURES AND TABLES

Figure 1. **Human ACHE polymorphism: Quarternary structure of the major oligomeric forms**

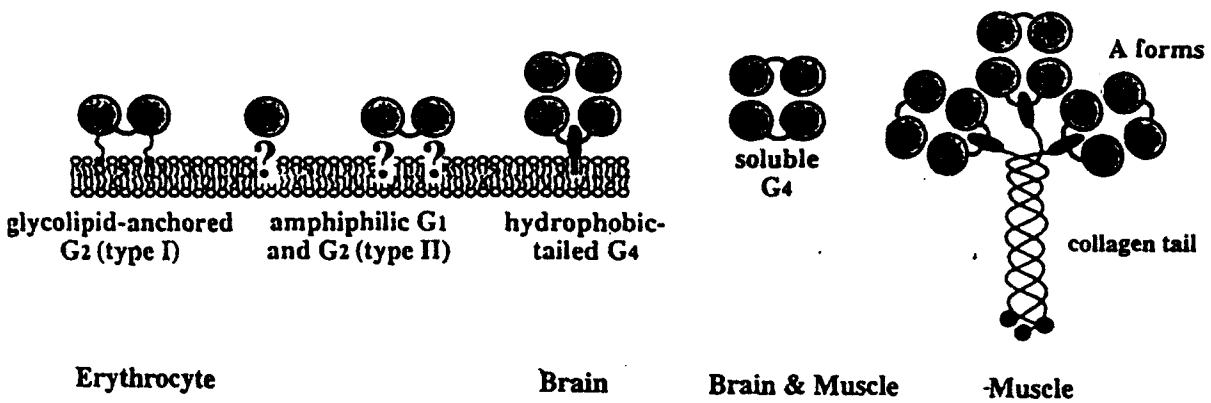

Quarternary structure of the major oligomeric forms of ChE's in vertebrates. The globular (G) forms as well as the asymmetric (A) form are included: Glycolipid-anchored dimers, in erythrocytes, soluble G4 expressed in brain and muscle and the hydrophobic tailed G4 (brain form) contains 20kd subunit. In the asymmetric, hydrophilic form A12, three catalytic tetramers are disulfide-bonded to a collagenic triple helical tail (Drawing after Massoulie et al., 1993).

Figure 2: Construction and characterization of the ACHE coding sequence

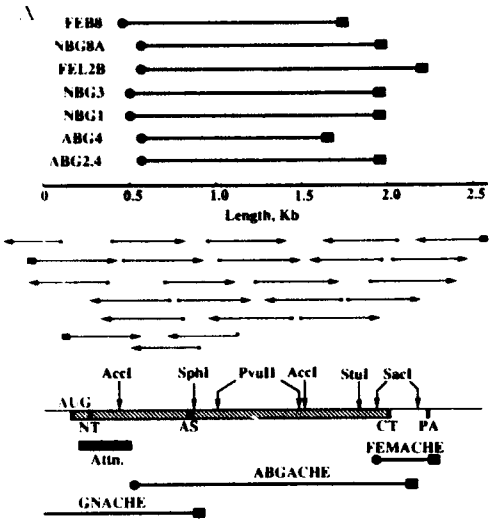

A. ACHEcDNA clones attenuated at the 5' region, and the construction of a complete ACHE coding sequence.
Top: Several selected representative cDNA clones isolated by screening cDNA libraries from different human tissue origins and/or stages of development with labeled ACHEcDNA (Lapidot-Lifson et al., 1989) are schemmatically presented. Libraries screened included: FEB - Fetal Brain, NBG - Neonatal Basal Ganglia, FEL - Fetal Liver, ABG - Adult Basal Ganglia (see Methods). The isolated clones (FEB8; NBG1, 3. and 8A; FEL2B; ABG4, and 2.4) display variable 3'-termini and all are truncated within a narrow attenuating region (Attn.) at the 5' end of the coding sequence.

B

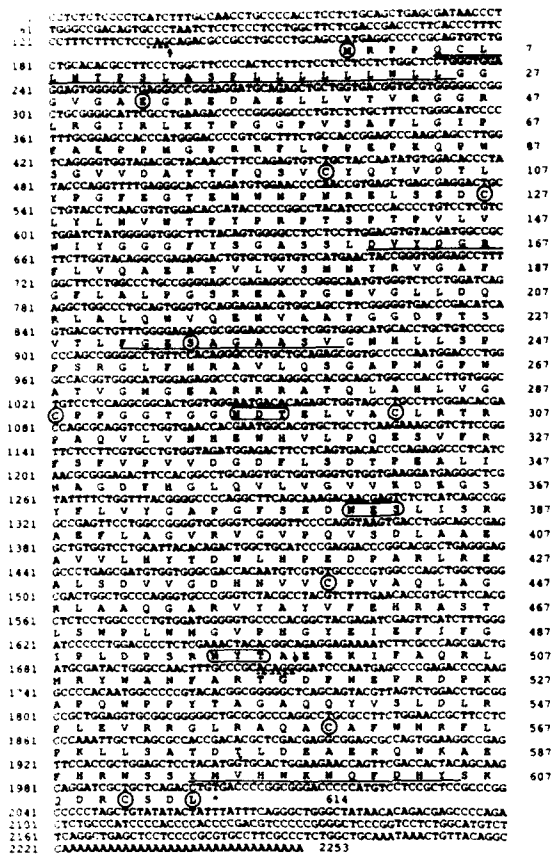

B. Primary structure of the nucleotide sequence and its inferred AChE product. The 2.2-Kb composite nunleotide sequence of clones ABGACHE, FEMACHE and GNACHE and its encoded amino acid sequence are presented. Nucleotides are numbered (left-hand side) 5'-to-3'. The single letter codes for the predicted amino acids are shown below the corresponding codons starting with the first AUG. Amino acids in the predicted polypeptide product are numbered (right-hand side) starting with the initiator methionine expected by analogy with ACHEcDNA from Torpedo (Schumacher et al., 1986; Maulet et al., 1990) and BCHEcDNA from man (Prody et al., 1987; McTeirnan et al., 1987). Underlined are putative signal sequence (amino acid residues 5-25) and the region encoding the esteratic site sequence (amino acid residues 231-240). The latter was found to match exactly the parallel peptide present in human serum BCHE. Also underlined is the C-terminal, selective 12 amino acid sequence which matched with a single nucleotide mismatch (notched) the ACHE-specific probe CTACHE (see Methods) and which was expected and found to be completely different from the parallel peptide in BCHE; and the 7 amino acid residues ecncoded by the K-153 primer (residues 161-167). Three putative sites for potential N-linked glycosylation, predicted by the sequence Asn-Xaa-Thr/Ser, in which Xaa represents any amino acid except proline, are ovally encircled. Cys residues are also circled, as are the first methionine residue, the esteratic site serine and the first and last amino acid residues in the mature protein based on analogies with other ACHEs. Dashed underlines and arrows note putative splice signals identified in the coding sequence (nucleotides No. 139, upstream from the intiator AUG codon, and 1227, 1713 and 1882 in the coding region).

Figure 3: Hypthetical secondary structure of ACHE mRNA and/or DNA

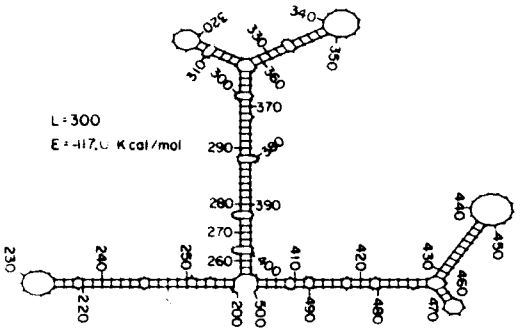

Stable RNA/DNA structures in the ACHE coding sequence were searched for using the FOLD program (Devereux et al., 1984) of the University of Wisconsin Sequence Analysis software package (UWGCG), which allows for G-C, A-T and the irregular G-U pairing. The segment presented (nucleotides 200-500 in the composite sequence initiating with residue 200 in Fig. 2) is the most stable structure for this sequence and was found to have free energy of -117.0 kcal/mole.

Figure 4: The ACHE upstream region; sequence and consensus motifs

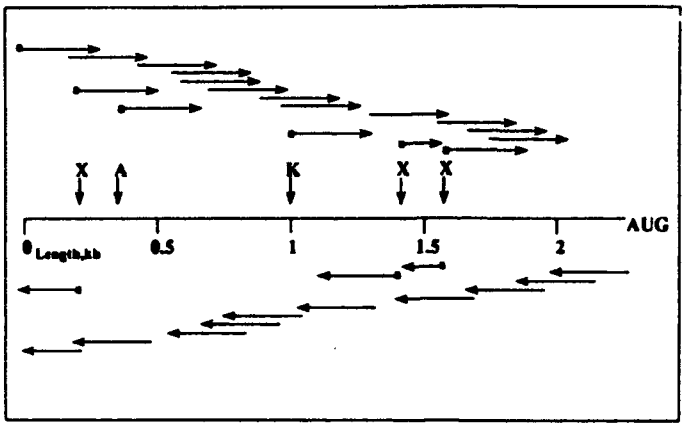

Sequencing strategy of the ACHE upstream region DNA sequencing was performed by the dideoxy chain-termination technique using the commercial universal or reverse-universal primer (Stratagene) (indicated by black box at the beginning of the arrow) or with unique 17-mer primers determined by sequencing (indicated by arrow). An AccI (A) fragment including most of the 5' region was subcloned into phage M13 and was used for single strand sequencing. Fragments digested with XhoI (X) and KpnI (K) were subcloned into the pGEM plasmid and used for double stranded sequencing.

Figure 5: Recombinant screening and isolation of CHE cosmid clones

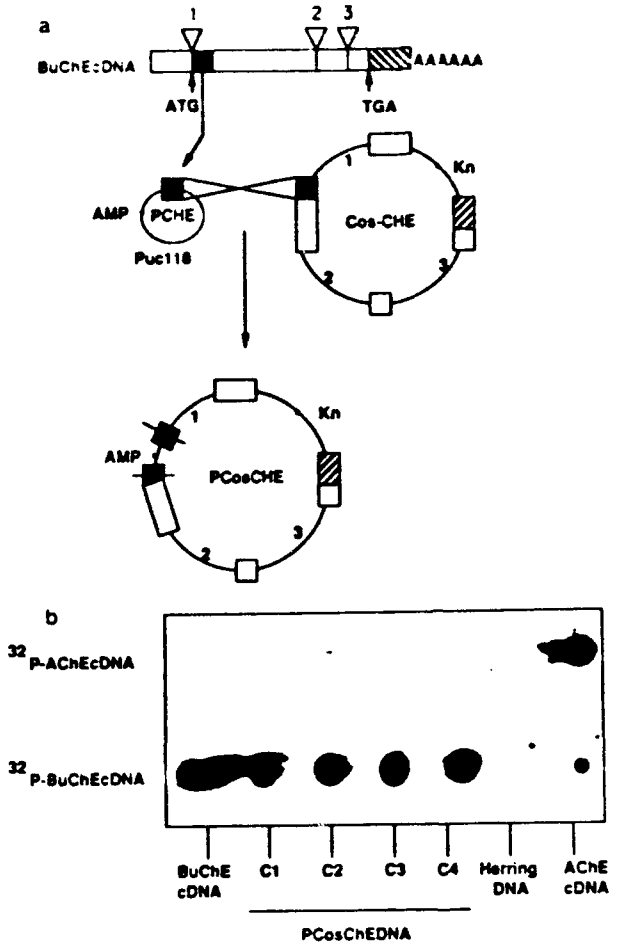

A: A 190 bp fragment form the 5'-domain of BCHEcDNA (74), was inserted into the Ampcillin (Amp) resistant vector puc 118 (PCHE) and transfected into the rec E. coli strain BHB3169, which permits natural recombination. PCHE-carrying bacteria were in turn infected by the genomic kanamycin resistant cosmid phage library and recombination between PCHE and CHE cosmid clones (CosCHE) took place. Dual antibiontic resistant recombinant clones (PCosCHE) were purified for analysis. B: One microgram of DNA from four such clones (PcosCHEDNA clones C1-C4) and 60 ng of either BCHE or ACHEcDNA were blotted onto nitrocellulose filters with herring DNA used as a negative control. Probes employed were labeled with [^{32}p] as detailed under Methods. Note that all cosmid clone DNAs hybridized with BCHEcDNA but not with ACHEcDNA.

Figure 5b: 5'-upstream sequence.

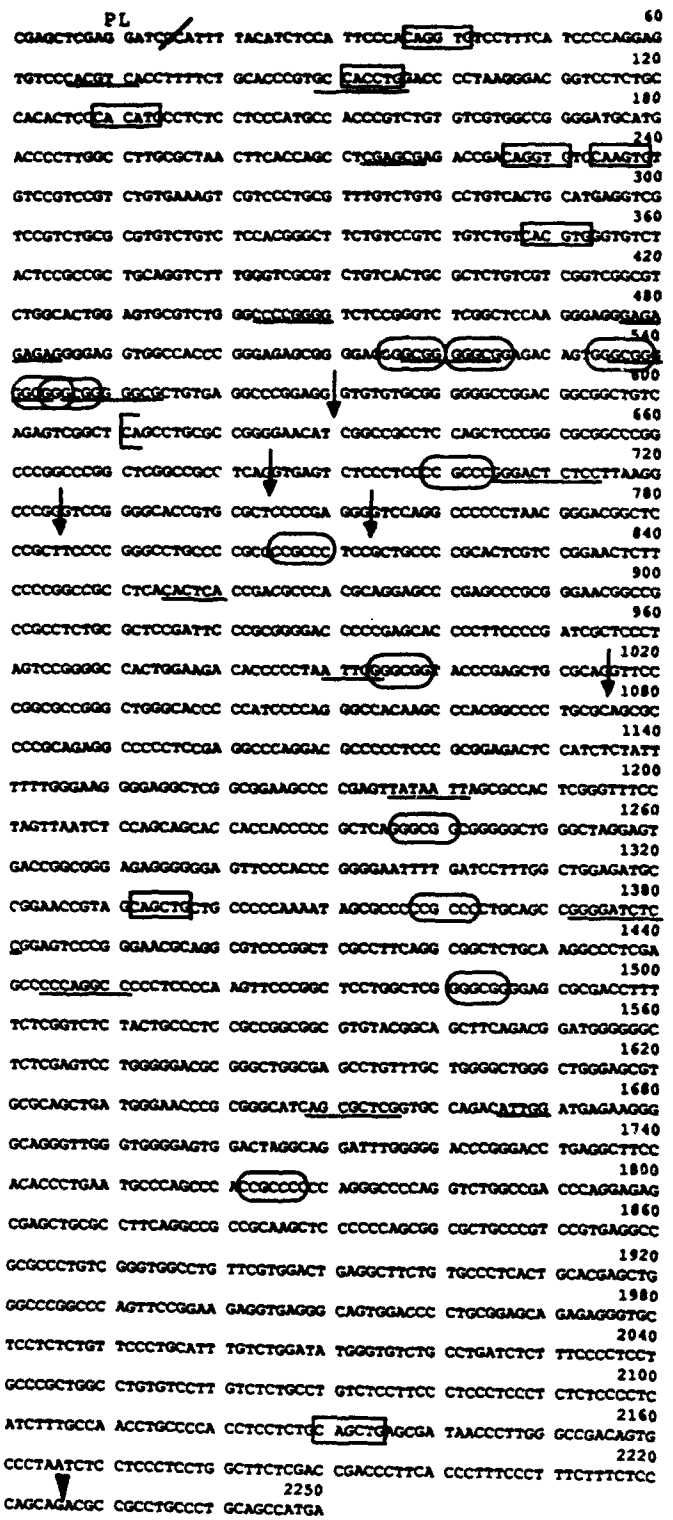

Data analysis (N-sites program, University of Wisconsin) revealed potential binding sites for several transcription factors, including MyoD (nucleotides 57, 91, 129, 226, 234, 348, 1332 & 2130, boxed), Sp1 (515, 521, 534, 540, 544, 699, 805, 994, 1246, 1358, 1481 & 1762, circled), and additional sites (underlined): ATF/CREB (67), E-box (89), Zeste (213 and 855), AP2 (443 and 1444), GAGA (477), EGR-1 (517, 536, 546), NFkB (705, 1372), CCAAT box (990 and 1666) and the TATA box (1176). Arrowns indicate potential sites for splicing at the 5' acceptor site (G/GT). The consensus splicing smotif (CAG/A) required at the 3'-boundaries of introns is noted by an arrowhead. One of several putative CAP sites is noted by a [sign. Pl/ -polylinker, including a SacI site. According to our results the sequence domains between nucleotides 16-610, 611 -684 and 685-2226 represent the promoter region, exon I and intron I, respectively. Thus, the 3'-end of the 5'-upstream sequence starts at nucleotide no. 2088, equivalent to the 5' region of the sequence presented in Fig. 2B.

Figure 6 Blot hybridization of human cosmid CHEDNAs.

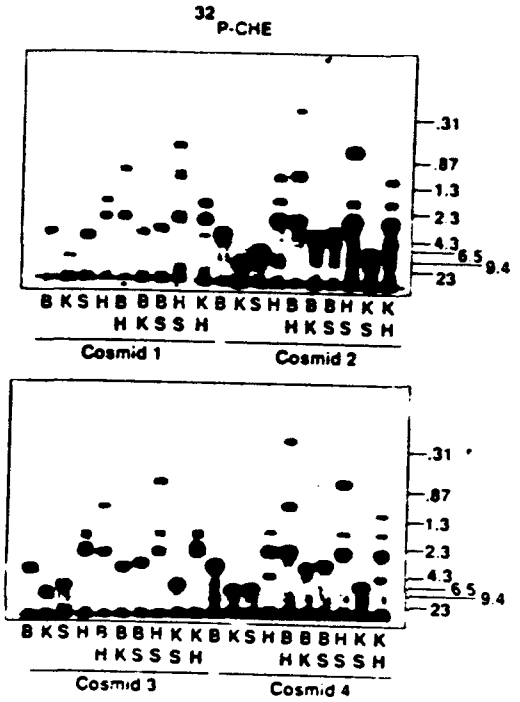

)NA from cosmid clones was digested to completion by one or more of the restriction enzymes SacI (S), HincII (H), BamHI (B) and KpnI (K) and electrophoresed in a 0.8% TBE agarose gel (TBE = Tris-borate 0.089 M, boric acid 0.089 M and 0.002 M EDTA). [^{32}p]-BCHEcDNA probe was employed in hybridization. Size markers were Lambda HindIII and PhiX HaeIII digested fragments, the migration positions of some are illustrated. Highly similar restriction patterns can be obeserved in all of the cosmid DNA preparations in bcth single and double enzymatic restrictions. Note that KH double restrictions reveal a closer restriction pattern between Cosmids 1 and 3 as opposed to 2 and 4.

Figure 7: **Human/hamster chromosomal blot hybridization**

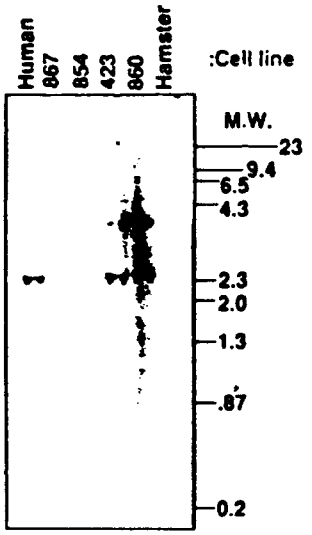

DNA from human/hamster somatic cell hybrids containing one or more human chromosomes on a background of hamster chromosomes was enzymatically restricted with HindIII. Blots were prepared by Bios. Corp. and hybridization performed with ^{32}p-BCHEcDNA. For chromosomal contents see Table I.A 2.3 kb HindIII fragment characteristic of the human CHE gene appeared only in lanes loaded with DNA from cell hybrids containing human chromosome no. 3 (423, 860) or with total human DNA, but not in lanes loaded with hamster DNA or with DNA from hybrid cell lines that do not carry the human chromosome no. 3 (967, 854).

Figure 8: Refinement of ACHE gene mapping to 7q22 by fluorescent in situ hybridization with biotinylated ACHE cDNA

In situ hybridization was performed in metaphase cells obtained from lymphocyte cultures of normal donors. The probe employed was a 2.2-kb-long recombinant ACHE DNA (Soreq et al., 1990) nick-translated by biotinyl dUTP (BioRad Labs) according to Boehringer-Mannheim protocols and as previously described (Viegas-Pequignot et al., 1989). Detection was by indirect immunofluorescence. The first antibody was an anti-biotin and the second a fluorescein conjugate. Chromosomes were counter-stained by propidium iodide. Arrows indicate fluorescent spots located on 7q22 over the R-band chromosomes.

Figure 9: Restriction analysis of the human ACHE gene

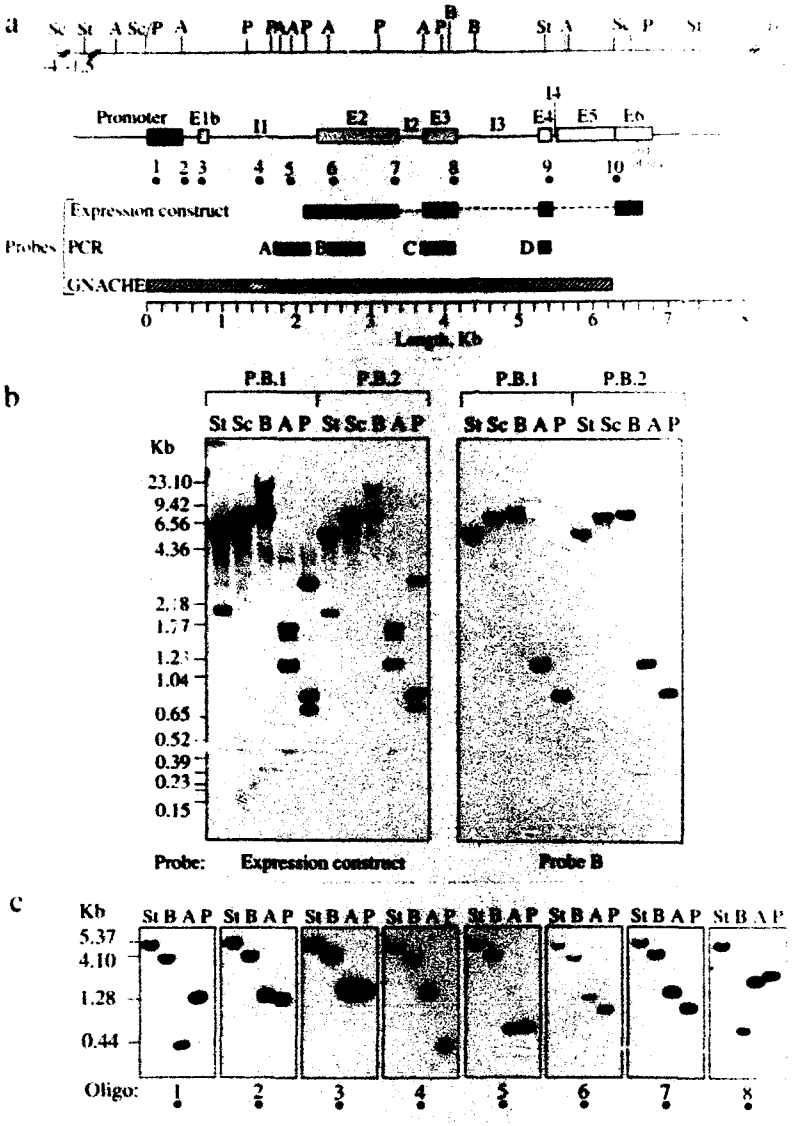

a. A schematic diagram of the ACHE gene. Exons (E) and introns (I) are presented along with restriction endonuclease recognition sites: Sc = *SacI*; P = *PvuII*; St = *StuI*; B = *BamHI*; A = *ApaI*. The restriction map was generated using various DNA probes: GNACHE (Soreq et al., 1990) is a 6.1 Kb *SacI* genomic fragment. A, B, C and D are PCR fragments specific for unique exons or introns of the ACHE gene: A, 1653 to 2159 in Ben Aziz-Aloya et al. (1993); B, 340 to 790, C, 1241 to 1695 and D, 1712 to 1869 in Soreq et al. (1990), and the expression construct is a probe that encodes the predominant, asymmetric form of human AChE (Soreq et al., 1990). Oligodeoxynucleotide probes 1 to 10 (noted by dots) were designed to detect selected sequences along the ACHE gene (Soreq et al., 1990; Ben Aziz-Aloya et al., 1993). Except for the breaks shown in the restriction map, length in Kb is shown on the scale below.
b. Southern blot analysis of human genomic DNA. The above-mentioned probes were used for DNA blot hybridization with genomic DNA obtained from peripheral blood (P.B.) of two unrelated apparently healthy individuals. Two such hybridizations, using the expression construct probe and probe B, are shown. These hybridizations enabled the construction of the restriction map (a, above). Indications of size in Kb, shown on the left, were those of standard Markers II and IV (Boehringer/Mannheim).
c. Southern blot analysis of human ACHE genomic clone. The 6.1 Kb *SacI* fragment of clone GNACHE, derived from a third individual, was digested with the indicated restriction endonucleases, electrophoresed and blotted for hybridization analysis with the 10 [^{32}P]-end-labeled oligodeoxynucleotide probes (1 to 8 are shown). The restriction map obtained from this analysis was compatible with the one obtained in b (above), suggesting one copy per haploid genome for the human ACHE gene. Sizes of fragments, shown as an example for oligodeoxynucleotide probe 1, are calculated by interpolation from standard markers (as in b, above).

Figure 11: Allele frequencies of CHE mutation in Jewish populations

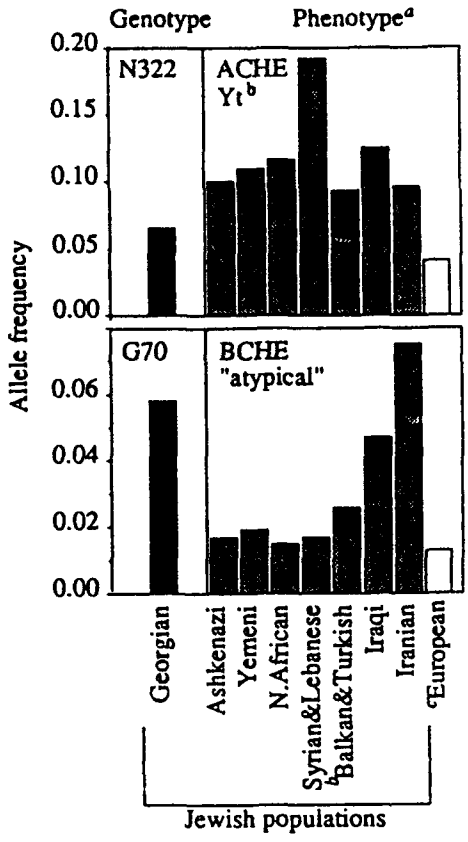

The genomic frequencies of the ACHE N322 allele, determined for 92 Georgians by DNA sequencing (upper left), and of BCHE G70 allele, determined for 86 of them by RFLP analysis (lower left), are compared with the appropriate published phenotype data. The genotype data indicate apparent conformity to the ACHE mutation, 80 were homozygous for H322 and 12 were heterozygous, the allele frequency predicting 80.4 and 11.2, respectively and 0.4 homozygous for G70. [a]The Yt^b allele frequency had been determined for 773 Israeli Jews from various Middle Eastern countries of origin, 438 Ashkenazi Israeli Jews (Levene, et al., 1987) and 1,399 Europeans, chiefly British and Swiss (Giles et al., 1967); the "atypical" BCHE allele frequency, for 3,658 Middle Eastern Israeli Jews, 4,196 Ashkenazi Israelis (Szeinberg et al., 1972) and 35,770 Europeans (Whittaker, 1986).
[b]In the study of "atypical" BuChE, Turkish-Jewish and Balkan-Jewish population data had been pooled. [c]These results are a compilation of 34 different surveys reporting a range of "atypical" allele frequencies of 0.000 to 0.078, but which, in sum, do not representatively sample the entire European and Finnish Sami and Greenland Inuit are an additional 5%). Also, there can be wide variations among regions of a single country, e.g., frequencies in Spain range from 0.004 to 0.073.

Figure 12: Transcription of HpACHE in Xenopus

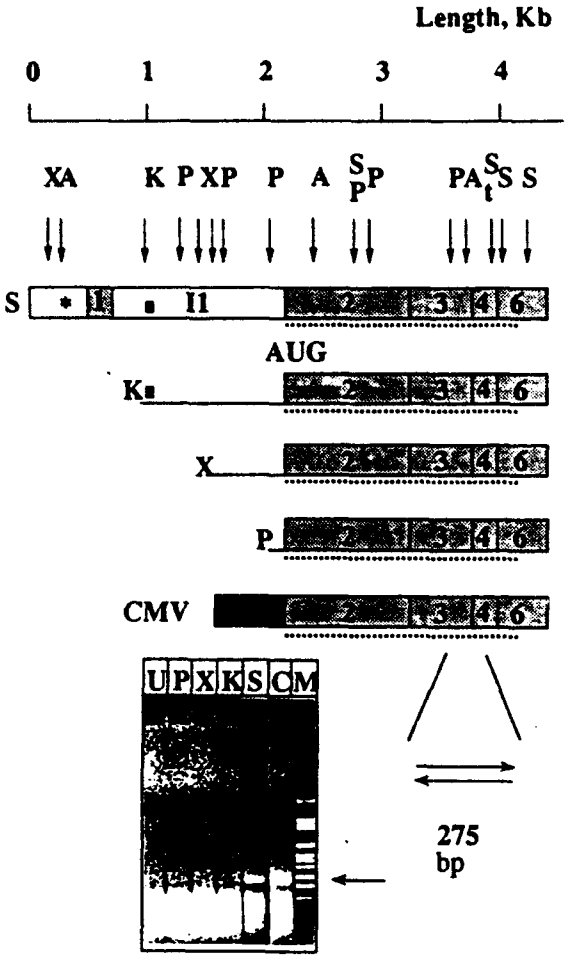

Injected HpACHE DNAs included the 2.2 Kb ACHE upstream sequence or its deletion constructs linked to the ACHE coding sequence. Characteristic restriction sites (S-SacI, X-XhoI, A-AccI, St-StuI) included in the ACHE coding exons (no. 2,3,4 & 6, shaded boxes) and in the region upstream of the initiator AUG codon within clone GNACHE (Soreq et al., 1990) were predicted according to sequence data and confirmed by blot hybridization of genomic DNA with PCR-amplified or subcloned probes from this sequence. Relative positions are noted on the length scale in kilobase (kb), where the first sequenced nucleotide equals 0. A fifth construct, carrying the ACHE coding sequence downstream of the CMV IE gene enhancer-promoter sequence (black), was as previously described (Velan et al., 1991b). Putative TATA box and cluster of transcription factor binding sites were found by sequencing and are marked by a black box and a star, respectively.

Open reading frames in exons are noted by dotted underlines. Positions of the first exon (1) and intron (I1) were determined by RNA-PCR experiments (Fig.6). inset: RNA was extracted from Xenopus oocytes 2 days after injection (50 ng/oocyte) with the noted linearized constructs. Residual injected DNA was eliminated by DNase I treatment (20 min at 37°C, 2 U/sample (Promega, Madison, WI) in 40 mM Tris-HCl, 10mM NaCl, 6mM $MgCl_2$ in the presence of 20 U/sample RNasin (Boehringer, Mannheim, Germany). DNaseI was heat-inactivated (90°C, 8 min) and RNA-PCR amplification was performed using the primer pair 11,12 (Methods). U-uninjected, C-CMVACHE, M-DNA size marker VI (Boehringer). bp-base pairs. PCR products are indicated by arrows.

Figure 13: RNA-PCR analysis of exon-intron boundaries

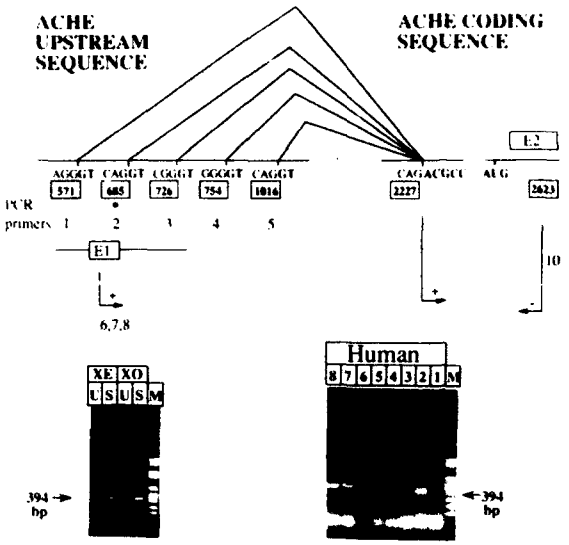

Potential 5' splice sites (consensus G/GT) were found in the ACHE upstream region at position 573, 687, 728, 756 & 1017 in the sequence drawn in Fig. 6, and detailed in Fig. 7B. A potential 3' splice site was known to be located at position 2227 (Fig. 2B, nucleotide no. 139), 21 nucleotides upstream from the first AUG (Soreq et al., 1990; Li et al., 1991). Chimeric downstream oriented (+) PCR primers were computer designed (Rychlik and Rhoads, 1989) to function only if their entrire consecutive sequence would be present, i.e., werever splicing occurred. These included 15-21 nucleotides upstream from each potential 5' splice site and an additional 5-6 nucleotides from exon 2 (ACGCCG, nucleotides nos. 2227-2232) and were tested with a single upstream (-) primer (No. 10, Methods). Asterisk indicated the experimentally confirmed active 5' splice site. *Insets: Right-* Total RNA was extracted from adult human (70 years old) brain basal nuclei. Primers no. 6-8 (Methods and scheme) resulted in PCR products with increasing lengths (lanes 2, 6-8). An additional primer at position 590 remained inactive (not shown), delineating a length of 74 bp for E1. M-molecular weight marker (Boehringer Mannheim). Left - RNA extracted from Xenopus oocytes (XO) and 2-day-old embryos (XE) injected with the HpACHE (S)-construct (Fig.5) was used for RNA-PCR experiments using primers, 2,10. U - uninjected.

A. **Gene structure and restriction sites**

The human ACHE gene includes a promoter (P), six exons, designated in this scheme E1-E6 (shaded boxes) and four introns (I1-I4, empty boxes). Relative positions are noted on the length scale in kilobase (kb) where the first sequenced nucleotide equals -0-. Characteristic restriction sites (S-SacI, X-XhoI, A-AccI, K-KpnI, P-PvuI, SP-SphI, St-StuI) included in the ACHE coding exons (E2, E3, E4 & E6) and in the region upstream of the initiator AUG codon within clone GNACHE were predicted according to sequence data and confirmed by DNA blot hybridization using genomic DNA and differential PCR-amplified or subcloned probes from this sequence. Length of introns was determined by PCR amplification of genomic DNA and cDNA sequences using primers flanking each intron, and was confirmed by DNA sequencing (except for I3, which was only partially sequenced). The I4-E5 domain is boxed.

B. **Nucleotide sequence of intron no. 2**

2 and 3. This intron is unique to mammals and does not exist in the Torpedo ACHE gene. Intron-exon boundaries (5' and 3') are marked by arrows.

C. **Nucleotide sequence of the I4-E5 domain and open reading frame**

DNA sequence is presented for the I4-E5 domain. Nucleotides are numbered at the right hand side. Analysis of this region revealed a continuous ORF connecting the E4-I4-E5 region. The predicted polypeptide diverts from the common ACHE sequence at amino acid residue 544 and is numbered accordingly on the lefthand side. The I4 peptide (white letters on black background) and the cleavable C-terminal peptide (shaded) are presented. E4 and E6 splice sites are marked by arrows.

Figure 14: ACHE gene structure and DNA sequencing of intron domains

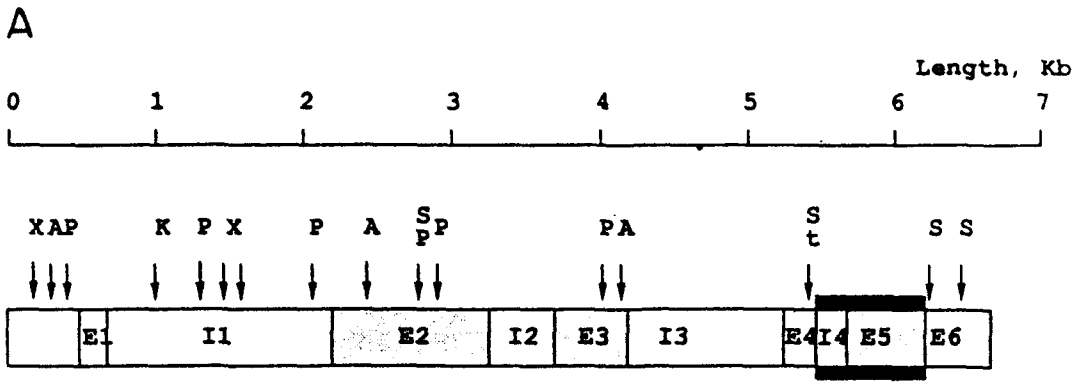

B

E2 I2

```
AGGTAACTAGTGGCTAGCTGGCGTGAAGCTGGCTCCTCTGGGTCCCAACGGTCCCTCCCC  60
TCCCTGCAGGGACCCAGGCATGAGGGCTTCTCCAGGCCCATTCCCAGAAGTCCCAGAAGT 120
CCTCCCTGAGGGCTCAGCATCCCAGGGTGGTCAGCAGGGCAGACAGGAAAGCCACCATGG 180
GTCTCATTTTCTCTTTCTCTGCATCCCTCCCCTGATCTCGTCCTCTCTCTGTCCATGGTT 240
CCGGGTCTGTAACTGTTCATCTCTCTGGCTCTTTGTCTGTCCTATCTGTTTCTGTCTACT 300
TGTCTGTCTGTGCCTGTCGCTCCATCCCACCCCCCTCCCCCTCACCCCCAGGT- 353
```

E3

C

I4+E5

E4

```
    AGCGCCACCGGTATGCAGGGGCCAGCGGGCAGCGCTGGGAGGAGGGGAGTGGGAGCCCGC  60
541 S  A  T  G  M  Q  G  P  A  G  S  A  G  R  R  G  V  G  A  R
    CAGTGTAACCCCTCTCTTCTCCCCCTAGCCTCGGAGGCTCCCAGCACCTGCCCAGGCTTC 120
561 Q  C  N  P  S  L  L  P  L  A  S  E  A  P  S  T  C  P  G  F
    ACCCATGGGGAGGCTGCTCCGAGGCCCGGCCTCCCCCTGCCCCTCCTCCTCCTCCACCAG 180
581 T  H  G  E  A  A  P  R  P  G  L  P  L  P  L  L  L  L  H  C
    CTTCTCCTCCTCTTCCTCTCCCACCTCCGGCGGCTGTGAACACGGCCTCTTCCCCTACGG 240
601 L  L  L  L  F  L  S  H  L  R  R  L
    CCTACAGGGGCCCCTCCTCTAATGAGTGGTAGGACCTGTGGGGAAGGGCCCCACTCAGGG 300
    ATCTCAGACCTAGTGCTCCCTTCCTCCTCAAACCGAGAGACTCACACTGGACAGGGCAGG 360
    AGGAGGGGCCGTGCCTCCCACCCTTCTCAGGGACCCCCACGCCTTTGTTGTTTGAATGGA 420
    AATGGAAAAGCCAGTATTCTTTTATAAAATTATCTTTTGGAACCTGAGCCTGACATTGGG 480
    GGAAGTGGAGGCCCGGAAACGGGGTAGCACCCCCATTGGGGCTATAACGGTCAACCATTT 540
    CTGTCTCTTCTTTTTCCCCCAACCTCCCCCTCCTGTCCCCTCTGTTCCCGTCTTCCGGTC 600
    ATTCTTTTCTCCTCCTCTCTCCTTCCTGCTGTCCTTCTCGGCCCCGCCTCTGCCCTCATC 660
    CTCCCTCTCGTCTTTCGCACATTCTCCTGATCCTCTTGCCACCGTCCCACGTGGTCGCCT 720
    GCATTTCTCCGTGCGTCCTCCCTGCACTCATACCCCCCCTTCAACCCGCCCAAATGTCCG 780
    ATCCCCGACCTTCCTCGTGCCGTCCTCCCCTCCCGCCTCGCTGGGCGCCCTGGCCGCAGA 840
    CACGCTC
    D T  L
```

E6

PRODUCTS

- ■ I4
- □ E5-mature protein
- □ E5-cleaved c'-terminus

Figure 15: Alternative ACHEmRNA transcripts in fetal and adult human tissues and in hematopoietic cells

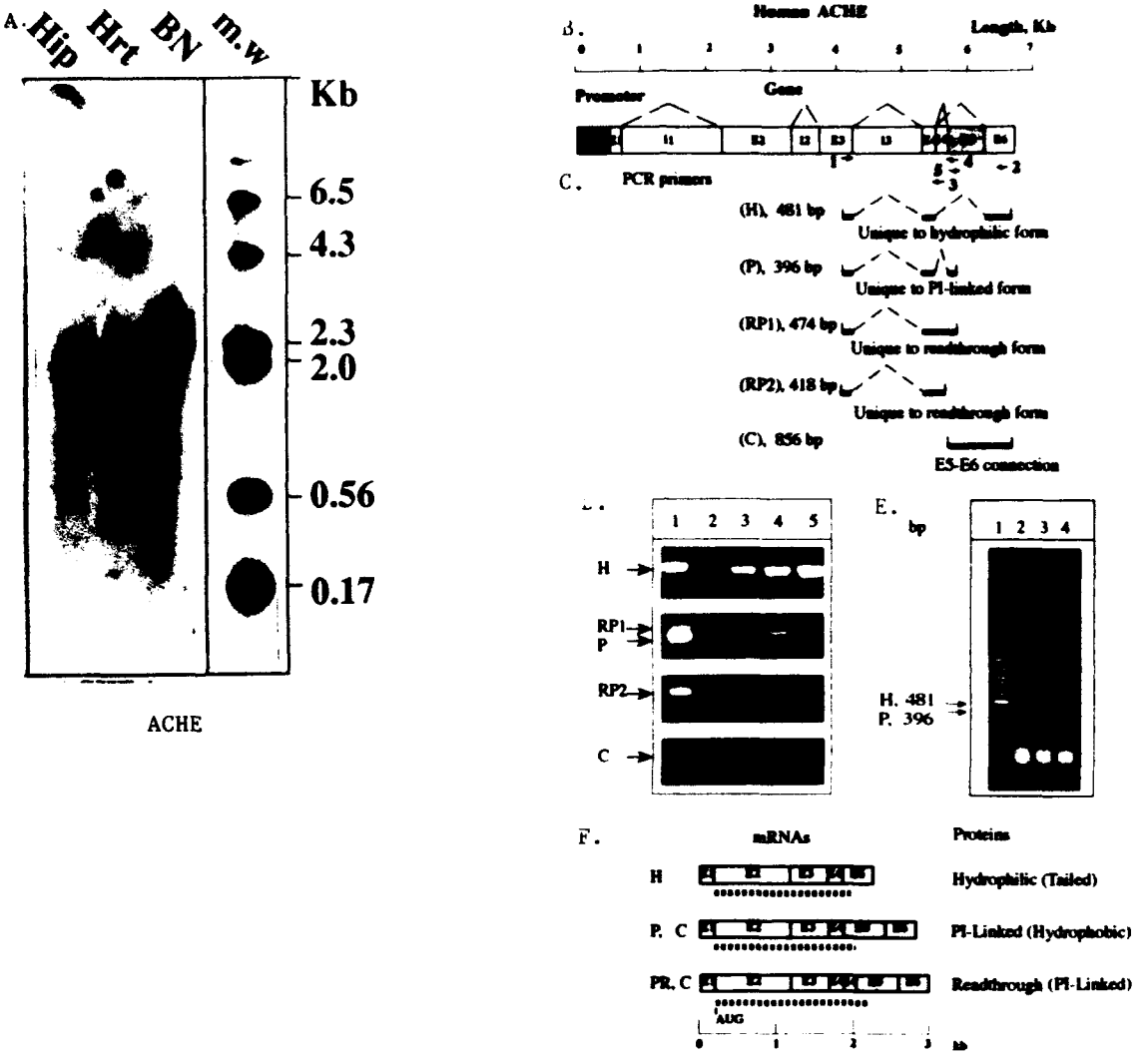

. **RNA blot hybridization detects ACHEmRNA in human fetal brain and heart.**
Poly A+ RNA (10 ug/lane) was prepared from fetal (18 weeks gestation) brain basal uclei (BN), Hippocamp... (Hip) and heart (Hrt) by extraction with guanidinium hiocyanate followed by two rounds of Oligo (dT)-cullulose chromatography. lectrophoresis and ...otting wee as previously described (Prody et al., 1987). ybridization was ...ch a [^{32}P]-labeled ACHEcDNA probe covering the complete 2.2 kb ong sequence encoding asymmetric ACHE (Soreq et al., 1990), produced by enzymatic igestion from plasmid DNA, electroeluted from gel and column purified. Washing was or 1 hr in 1 x SSPE (0.15 M CaCl, 0.01 M NaH_2PO_4, 1 mM EDTA) at 65°C. lectrophoretic migration of 28s and 18s ribosomal RNA was used to determine the and's size (28s = 5sb, 18s = 2kb).

. **Splicing patterns.**
Splicing in the ACHE gene (scheme) is displayed by dashed trangles. Splicing of 1, I2 and I3 generates, in all tissues examined, the core domain of the coding equence from exons E2-E4. Alternative splicing occurs in the I4,E5 region and ncludes three options: E4-E6, E4-E5,E6, and E4,I4,E5,E6.

. **PCR primer pairs and the selective RT-PCR products.**
The primer pair 1,2 could potentially create several alternative products, but ractically it amplified only ACHEmRNA sequences including the E3,E4 and E6 regions, haracteristic of the hydrophilic (H) form, with the potential for tailing. This was robably due to unfavorable competition with the realtively more abundant major CHEmRNA species. The primer pair 1,4 detected expression of the putative mRNA ubtypes including the E5 exon which encodes PI-linked AChE (P) or the I4/E5 'readthrough" form of ACHEmRNA encoding a longer PI-linked AChE (RP1). The primer pair ,3 was unique to the readthrough (RP2) form, and the primer pair 2,5 amplified all CHEcDNAs where the E5 exon in the AHCE gene is continued by E6 (C).

). **RT-PCR analysis of tumor cell lines.**
Cell lines were NT2/D1 teratocarcinoma, H9T lymphoma, 293 embryonal kidney cells, CI-N-592 small cell lung carcinoma, and TE671 medulloblastoma. RT-PCR experiments ere performed with 100 ng samples of total RNA and the noted primer pairs. Arrows ndicate PCR products reflecting the various ACHEmRNA transcripts designated as in C.

E. **Coexpression of common and alternative ACHEmRNAs in K-562 erythroleukemia cells.**
Total RNA from K-562 cells was subjected to RT-PCR amplification using the primer pairs 1,4 (lane 2,4) or 1,2 (lane 3). The lane 4 reaction was performed without reverse transcriptase, to exclude presence of genomic DNA contaminations. Molecular weight marker were electrophoresed in parallel (lane 1). Arrows indicate PCR products and their sizes.

F. **Predicted ACHEmRNAs and proteins.**
The three alternative ACHEmRNA transcrips and their putative protein products are schematically displayed. Open reading frames initiated by the AUG codon are marked by a dotted underline, all according to the bottom scale in kb. The resultant protein products would either be hydrophilic (H) and capable of being tailed by noncatalytic subunits or hydrophobic and amenable to linkage of phosphoinositide moieties (P or PR). In both latter cases, direct connection between E5 and E6 is predicted.

Figure 16 Alternative splicing in the ACHE gene creates 3 mRNAs with potentially distinct protein products

A

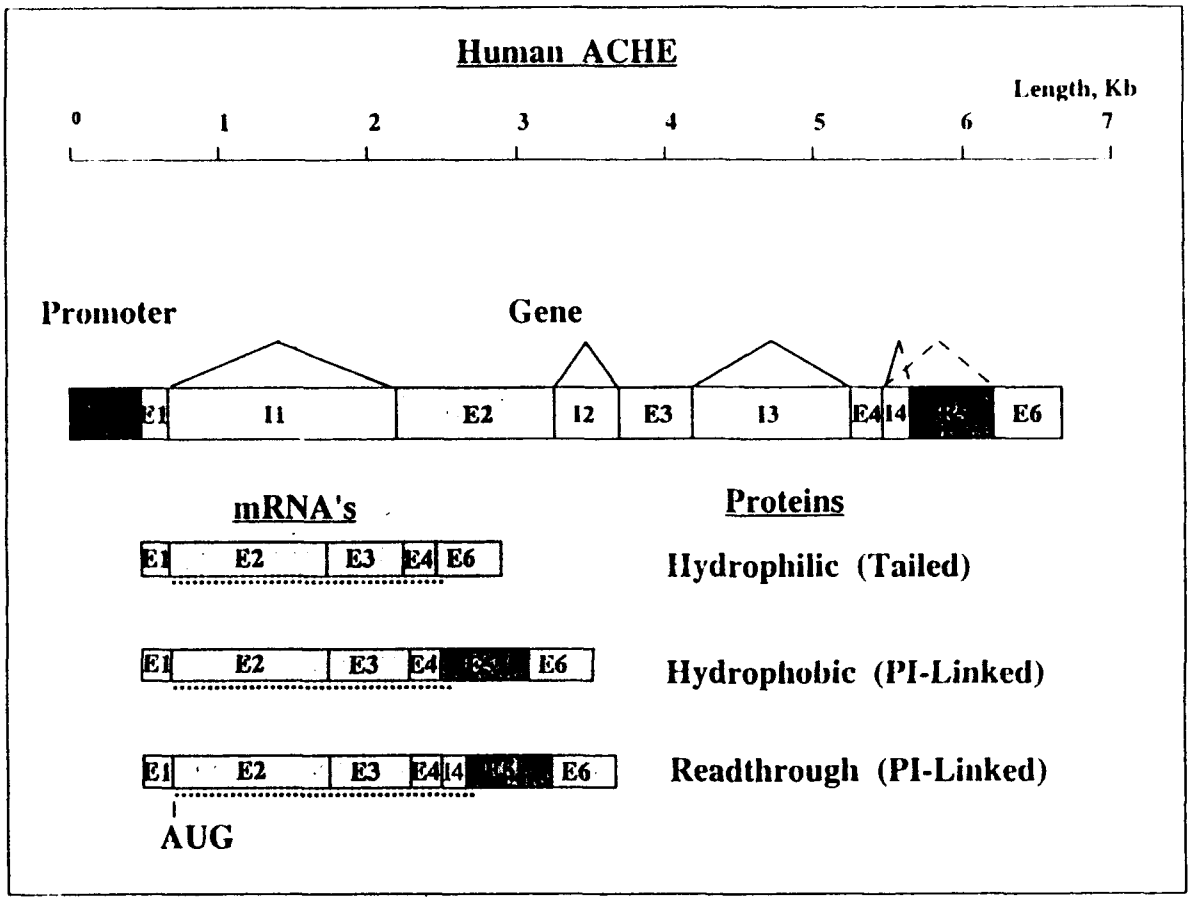

A. Three splicing products from the ACHE gene

Promoter region and exon-intron organization of the 7kb long ACHE gene. Triangles above the introns represent the obligatory splicing boundaries. Dashed triangles represent optional splicing leading to alternative transcripts. Three different mRNAs can be spliced out from this gene: that leading to the hydrophilic tailed form (Fig. 3), that producing the hydrophobic PI-linked form including the product of E5, or the mRNA translated into the readthrough PI-linked form including the product of I4-E5.

B Hydrophilic

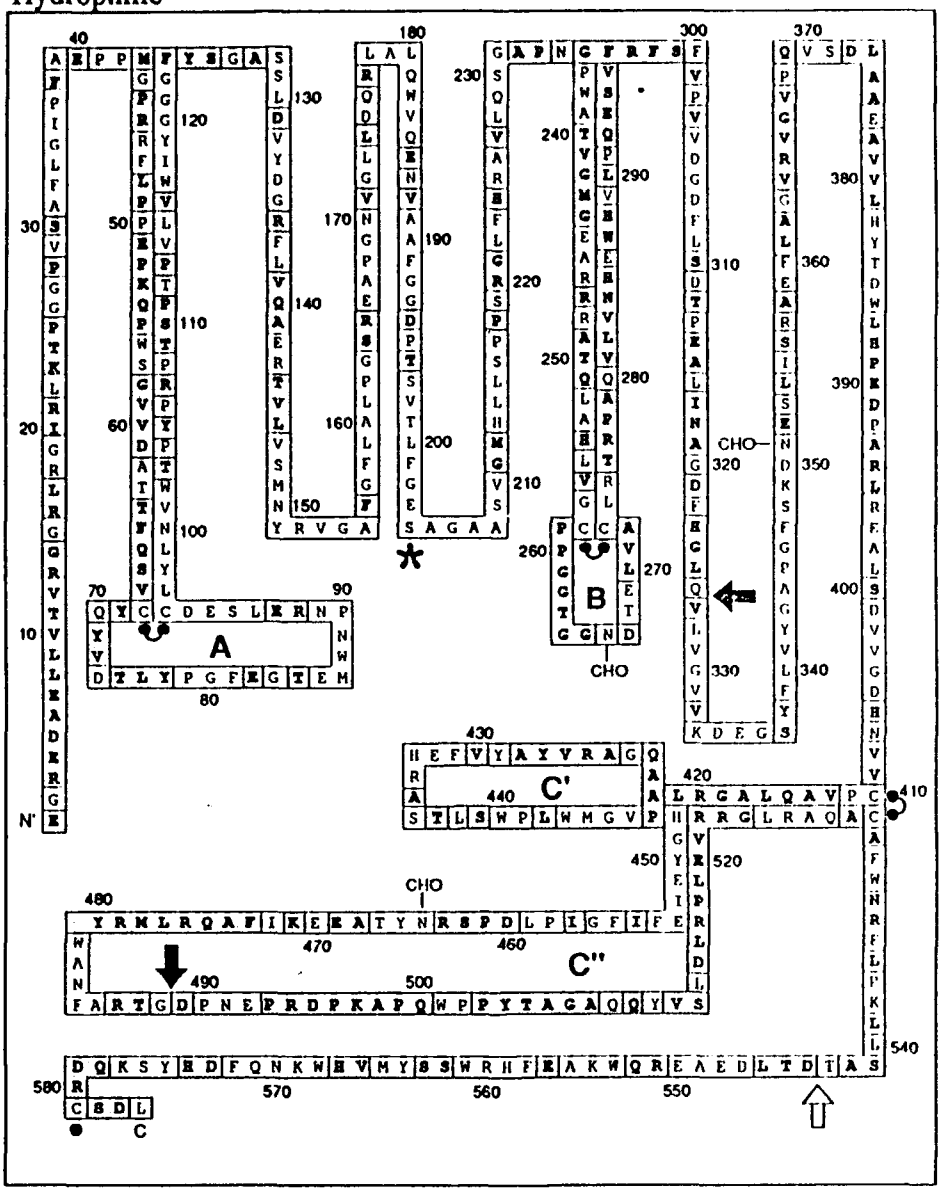

PI - linked C - terminus

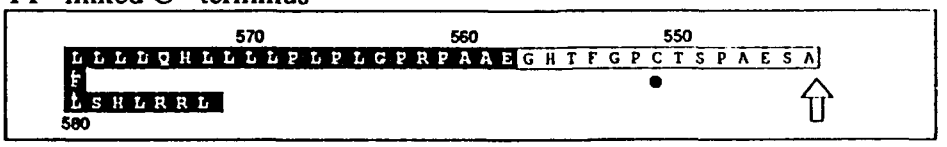

Complete Readthrough domain

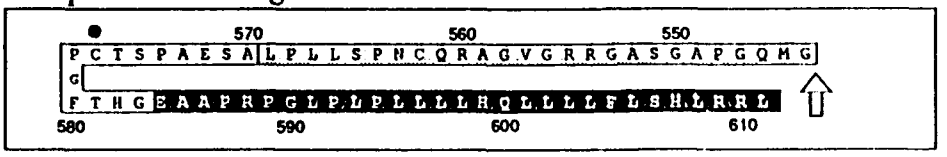

B. **Alternative C-terminal peptide sequences in the 3 different forms of human ACHE.**

The primary sequence (see Fig. 2B) follows a parallel model for human BCHE (Neville et al., 1992). Amino acid residues, in the single letter code, are nubered starting with the N-terminus. White regions denote areas identically aligned with the corresponding residues in BCHE, while regions unique to ACHE are shaded. Disulfide bonds are dotted and intercoccected. The active site serine residue is starred, and potential glycosylation sites are marked (-CHO). The cystine loops A,B,C' and C" are marked. The C-terminal half cystine residue linking catalytic subunits, is dotted and marked by a black circle. Common splice sites are marked by filled arrows and the alternative splice site by an empty arrow. The putative C-terminal peptide of the alternative hydrophobic, PI-linked from of hematopoietic ACHE is shown below, starting with residue 544, where alternative splicing modifies the peptide sequence. The putative PI-linked read-through form is shown in the lowest box, also starting with residue 544. The I4 region is shaded. The hydrophobic C-terminal peptide, to be released from this domain by proteolytic cleavage which enables PI linkage, is shown in black for both the alternative forms.

Figure 17: Hydrophobicity profiles of the alternative C-termini in AChE subtypes

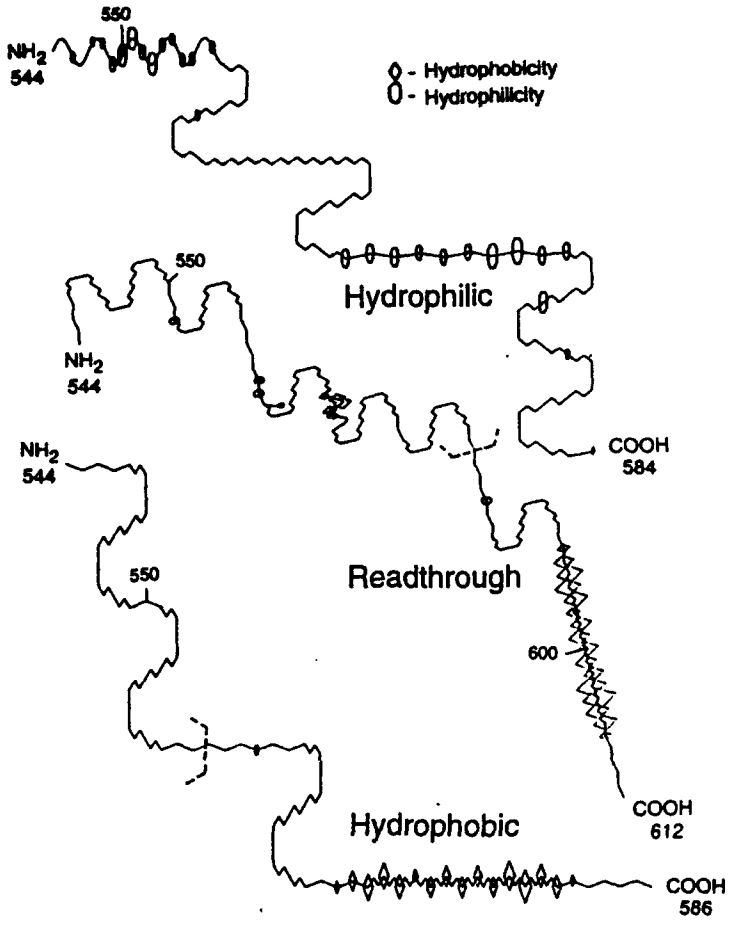

Each of the C-termina. peptides was subjected to plot structure analysis by the Chou and Fasman prediction (1987). This analysis provides best-guess predictions regarding folding patterns within the analyzed proteins as well as evaluations on the probability of particular peptide domains to be located at the surface of the fully folded enzymes. Peptide domains with high hydrophilicity are circled and those with high hydrophobicity marked by black diamonds. Predicted turns are displayed by 180-degree turns, helices are shown by sine waves, ß sheets as sharp saw-tooth waves and coils as dull saw-tooth waves. The cleavage site of the hydrophobic C-terminal peptide is marked by a dashed line.

Figure 18: Biochemical characterization of recombinant human AChE produced in Xenopus oocytes.

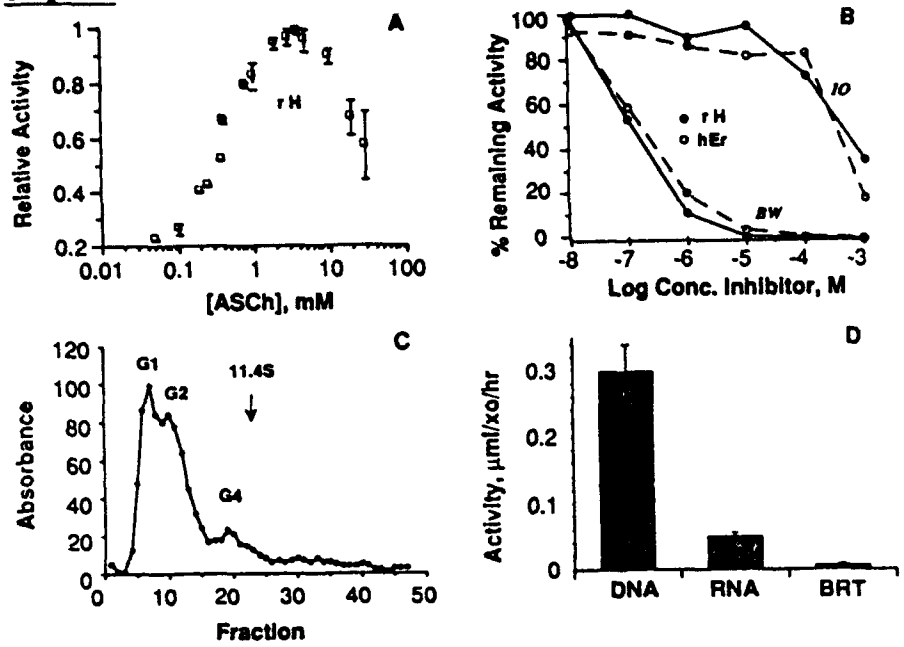

A. **Inhibition by excess substrate.** Mature Xenopus oocytes were injected with 5 ng of in vitro transcribed AChEmRNA (soreq et al., 1990) and incubate overnight at 17°C. Homogenates corresponding to 1/3 oocyte were assayed for AChE activity in the presence of various concentrations of acetylthiocholine substrate (average of 3 experiments +/- SEM).

B. **Sensitivity to selective inhibitors.** Oocyte homogenates were preincubated for 30 min in assay buffer contining the AChE-specific, reversible inhibitor 1,5 bis (4-allyldimethylammoniumphenyl)-pentan-3-one dibromide (BW284C51, BW) or the butyrylcholinesterase-specific inhibitor tetraisopyopylpyrophosphoramide (iso-OMPA, IO) at the indicated concentrations and assayed for remaining activity following addition of 3mM ASCh. (average of duplicate assays from 2 independent microinjection experiments). AChE extracted from human erythrocytes (hEr) served as control.

C. **Oligomeric assembly.** Homogenates from ACHEmRNA-injected oocytes were subjected to sucrose density centrifugation as described in Methods (average of 3 experiments). Note that in addition to the free monomer (3.2S, G1), the oocyte appears to generate dimers (5.6S, G2) and to a lesser extent eteramers (10.2S, G4) of human AChE. Endogenous oocyte AChE activity is undetectable under these conditions. Arrow marks position of bovine liver catalase (11.4S).

D. **Expression of ACHE DNA in Xenopus.** Oocytes were injected with 5 mg synthetic ACHEmRNA or ACHEcDNA under control of the cytomegalovirus promoter-unhancer element (CMXACHE; Velan et al., 1991a) and incubated for 1 (RNA) to 3 (DNA) days. Oocytes served as control. Activity is expressed as moles substrate hydrolyzed per hour per oocyte +/- SEM for 3 independent microinjection experiments.

Figure 19: **Transiently transgenic Xenopus embryos as an in vivo expression system for AChE**

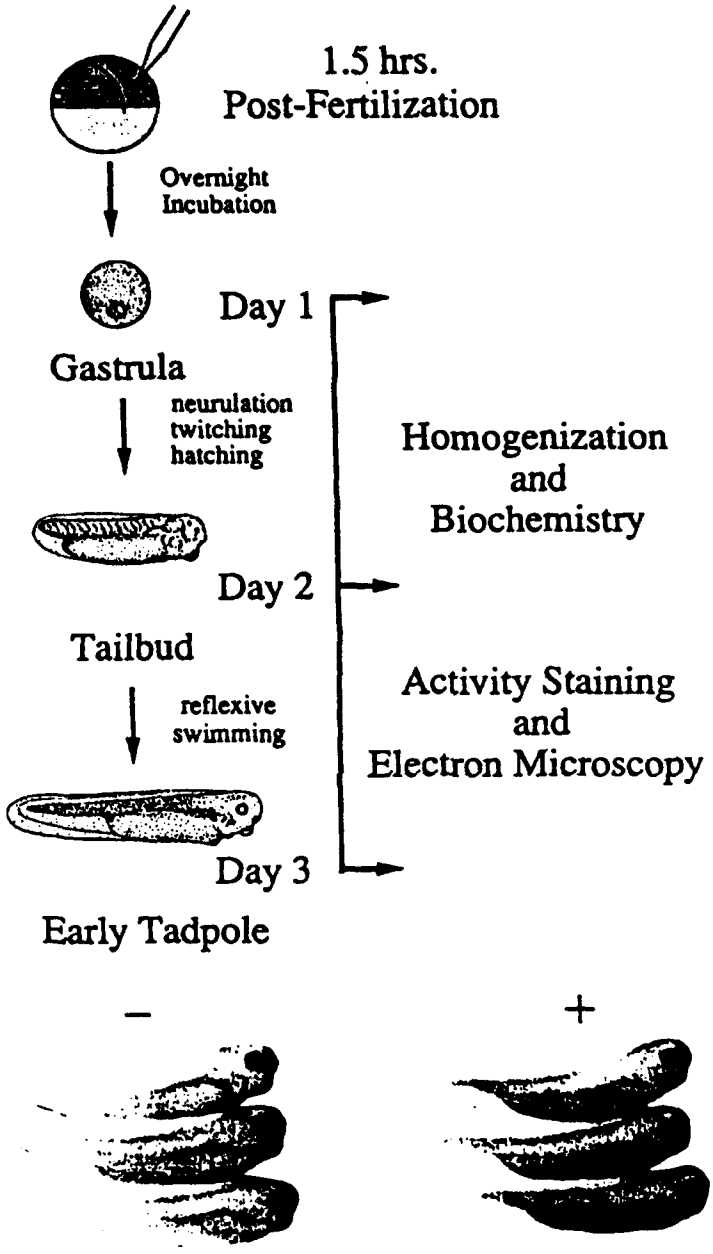

A schematic representation of a microinjection experiment depicting the principal developmental stages and analytical approaches used in this work is shown together with photographs displaying the normal gross development of unstained microinjected embryos (+) compared with control uninjected embryos (-) 3 days after fertilization. In vitro fertilized eggs of Xenopus laevis were injected with 1 ng of CMVACHE and cultured for 1-4 days. Sketches after Duchar (1966).

Figure 20: Developmental profile of rhAChE overexpression in Xenopus embryos

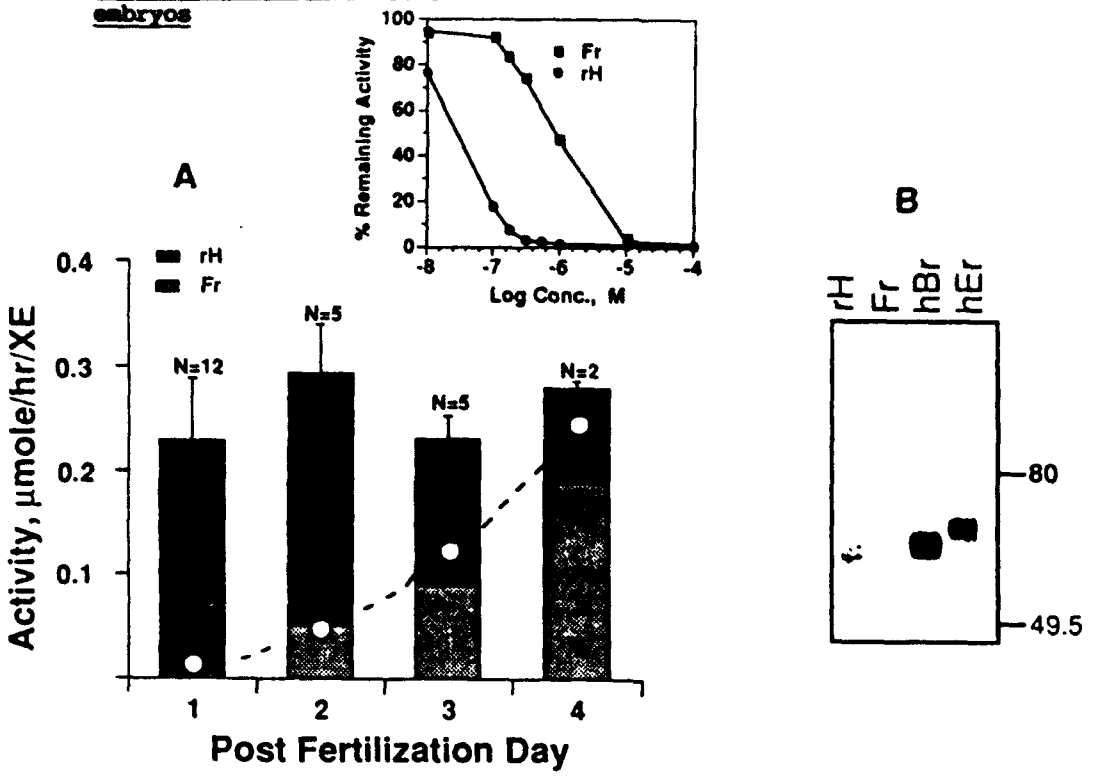

A. Overexpression of rhAChE in developing embryos. High salt/detergent extracts of CMVACHE-injected and uninjected embryos were prepared and assayed for AChE activity in the presence and absence of the selective inhibitor ecothiophate (3.3 X 10-7 M, inset). Endogenous AChE activity was calculated according to an algorithm assuming 90% inhibition of rhAChE and 20% inhibition of frog AChE at this concentration of inhibitor. Bar graph represents the total AChE activity measured per microinjected embryo at various time points following microinjection and the calculated activities attributable to rhAChE (dark shading) and endogenous frog AChE (light shading). The total AChE activity measured in uninjected control embryos at the same time points is indicated by white circles. Data represent average of 4-6 embryos for the indicated number (N) of independent microinjection experiments +/- SEM. INSET: Selective inhibition of recombinant human AChE by ecothiophate. Homogenates representing endogenous frog (Fr) or recombinant human (rh) AChE were assayed for activity following 40 min preincubation with the indicated concentrations of ecothiophate. Average of 3 experiments.

B. Immunochemical discrimination between rhAChE and embryonic Xenopus AChE. Affinity purified AChE form CMVACHE-injected Xenopus embryos (rh), control uninjected embryos (Fr), human brain (hBr) and erythrocytes (hEr) was subjected to deaturing gel electrophoresis and protein blot analysis as described in Methods. Each lane represents approx. 20 ng protein, except rh which contained only 6 ng. Note the complete absence of immunoreactivity with embryonic Xenopus AChE although silver staining of a parallel gel demonstrated detectable protein at the corresponding position (not shown). The faint upper bands (140-160 Kd) in the lanes displaying native human AChEs represent dimeric forms resulting from incomplete reduction of the intersubunit disulfide bonds (See Liao et al., 1992). Prestained molecular weight markers indicated on the right were from BioRad, USA.

Figure 21: rhAChE in microinjected Xenopus embryos remains monomeric

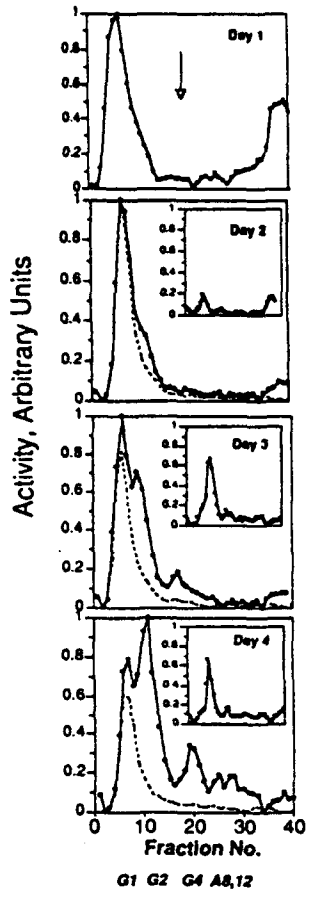

High salt/detergent extracts representing 2 embryos were subjected to sucrose density centrifugation as described in Methods. Figure represents total AChE (solid line) and immunoreactive rhAChE (dotted line) from CMVACHE-injected embryos 1 to 4 days after fertilization. rhAChE appeared exclusively as a peak representing monomeric AChE (approx. 3.2S) at all time points. Arrow marks position of bovine liver catalase (11.4S). INSETS: AChE molecular forms in control uninjected embryos scaled to the total activity levels observed in DNA-injected embryos (see Figure 2). Peak analysis demonstrated that the distribution of oligomeric forms was identical to that observed in CMVACHE-injected embryos. Note that monomeric AChE is essentially undetectable in control embryos. G1, G2 and G4 indicate the expected positions of the globular monomer, dimer and tetramer in the gradient; A8 and 12 - positions of "tailed" asymmetric forms. Fraction 0 represents the top of the gradient.

Figure 22. AChE expression in developing Xenopus embryos

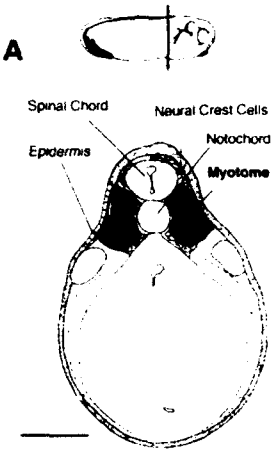

A. Schematic presentation of sectioned embryos. Thin sections (700 Angstroms) were prepared from the anterior trunk region of 2-day-old embryos. Cross sections at this level reveal the close proximity of the muscle-forming myotomes and the principal components of the developing central cervous system. At this stage embryos displayed clearly differentiated muscle cells and the sporadic twitching which accompanies hatching. Following cytochemical staining for catalytically active ACHE, electron microscopy was employed to detect high desity accumulations of thiocholine reaction product in myotome areas (shaded). (Diagrams after Hausen and Riebesell (1991)). Scale bar=200 μm.

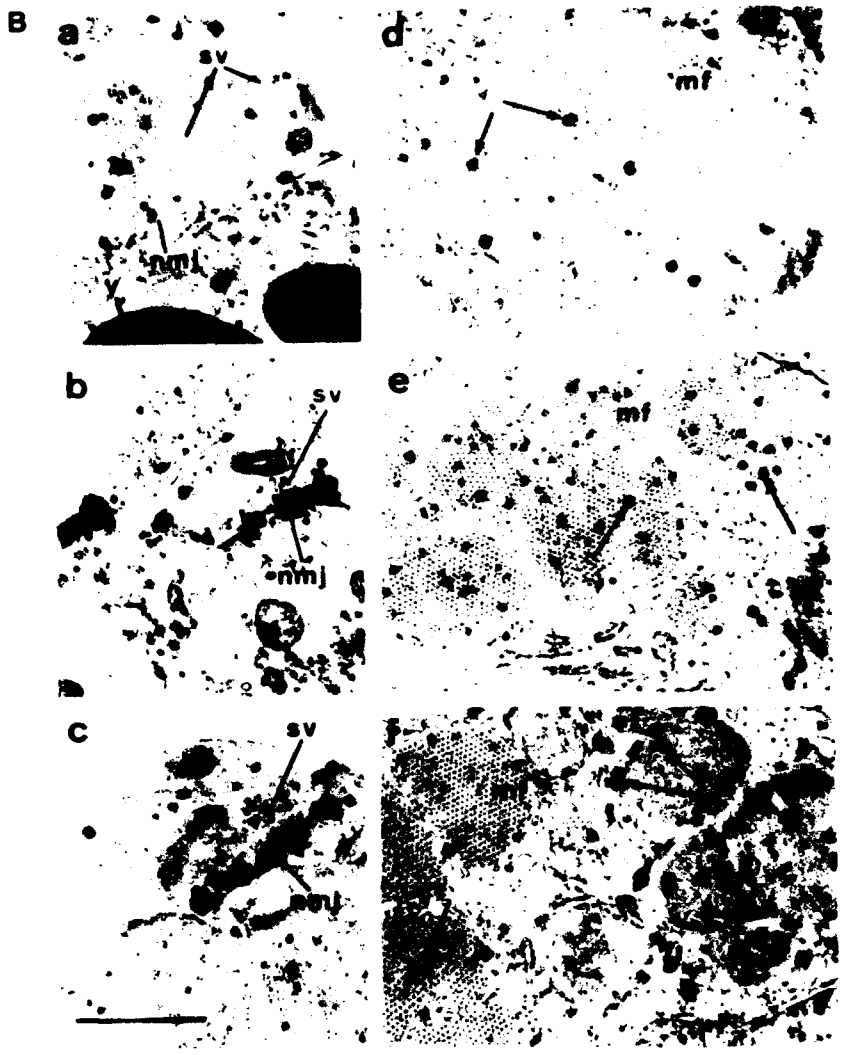

B. **Accumulation of ACHE in myotomes of transgenic Xenopus embryos.**

Two-cell cleaving embryos of Xenopus laevis microinjected with 1 ng plasmid DNA were cultured for 2 days. Shortly after hatching (stage 26 (Hausen and RIebesell, 1991)) embryos were fixed and stained for catalytically active ACHE by the hiocholine hydrolysis method (Koelle and Freidenwald, 1949; Karnovsky and Roots, 1964). Deposits of electron-dense reaction product appear as dark rectangular crystals which vary in size and intensity (arrows). Control sections incubated in reaction buffer lacking substrate displayed no reaction product. a-c: Neuromuscular junctions (nmjs) demonstrating uncharacteristic synaptic accumulation of ACHE following microinjection of HpACHE (b) and CMVACHE (c) DNAs. a-uninjected; b-HpACHE; c-CMVACHE. d-f: Sections through somitic muscle cells from control uninjected (d), HpACHE (e), or CMVACHE (f) injected embryos illustrating overexpression of ACHE around and between the myofibrils (mf) of both DNA-injected groups. Arrows denote crystals of reaction product. sv-synaptic vesicles; y-yolk platelets. (Bar=1 μm).

Figure 23: Disposition of rhAChE in myotomes from 2-day-old microinjected Xenopus embryos

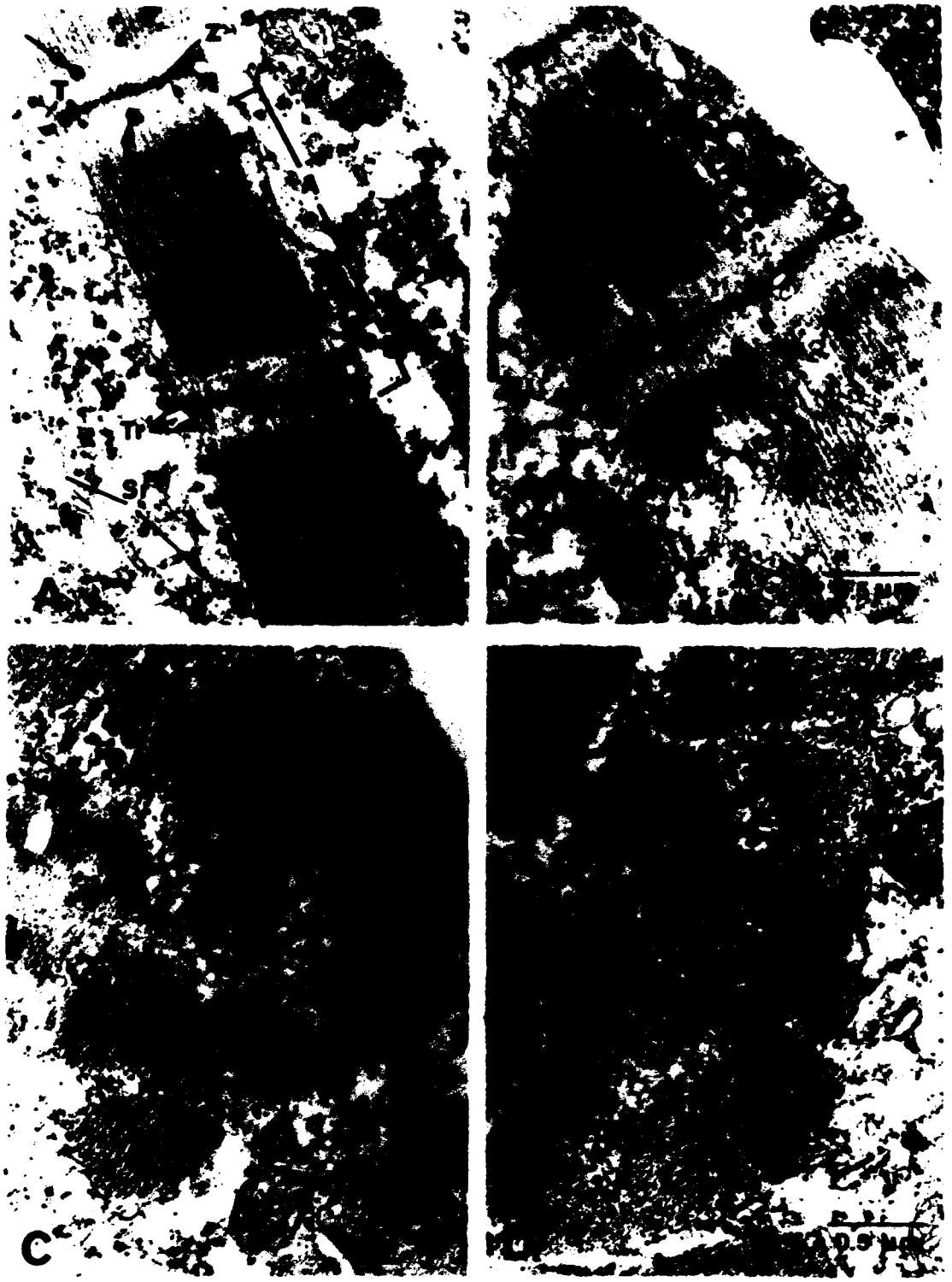

Fertilized Xenopus eggs were microinjected with 1 ng CMVACHE, incubated for 2 days at 17°C, fixed, stained and prepared for electron microscopy as described in Methods. Uninjected embryos from the same fertilization served as controls and were similarly treated. Arrows mark accumulations of reaction product indicating sites of catalytically active AChE.

A. Uninjected control myotome in longitudinal section following activity staining for AChE.

B. Myotome section from CMVACHE-injected embryo.

C. Uninjected control myotome in transverse section.

D. Transverse section from CMVACHE-injected embryo. Note the increased intensity of staining in sections from injected embryos vs. uninjected controls within the same subcellular compartments, especially with the sarcoplasmic reticulum (SR). A-A band; I-I band; Z-Z disc; Tr - triad; SR - sarcoplasmic reticulum; T-T tubules; G - glycogen particles; Size bar represents 0.5 μm.

Figure 24: Overexpression of AChE in myotomes of CMVACHE-injected embryos persists to day 3

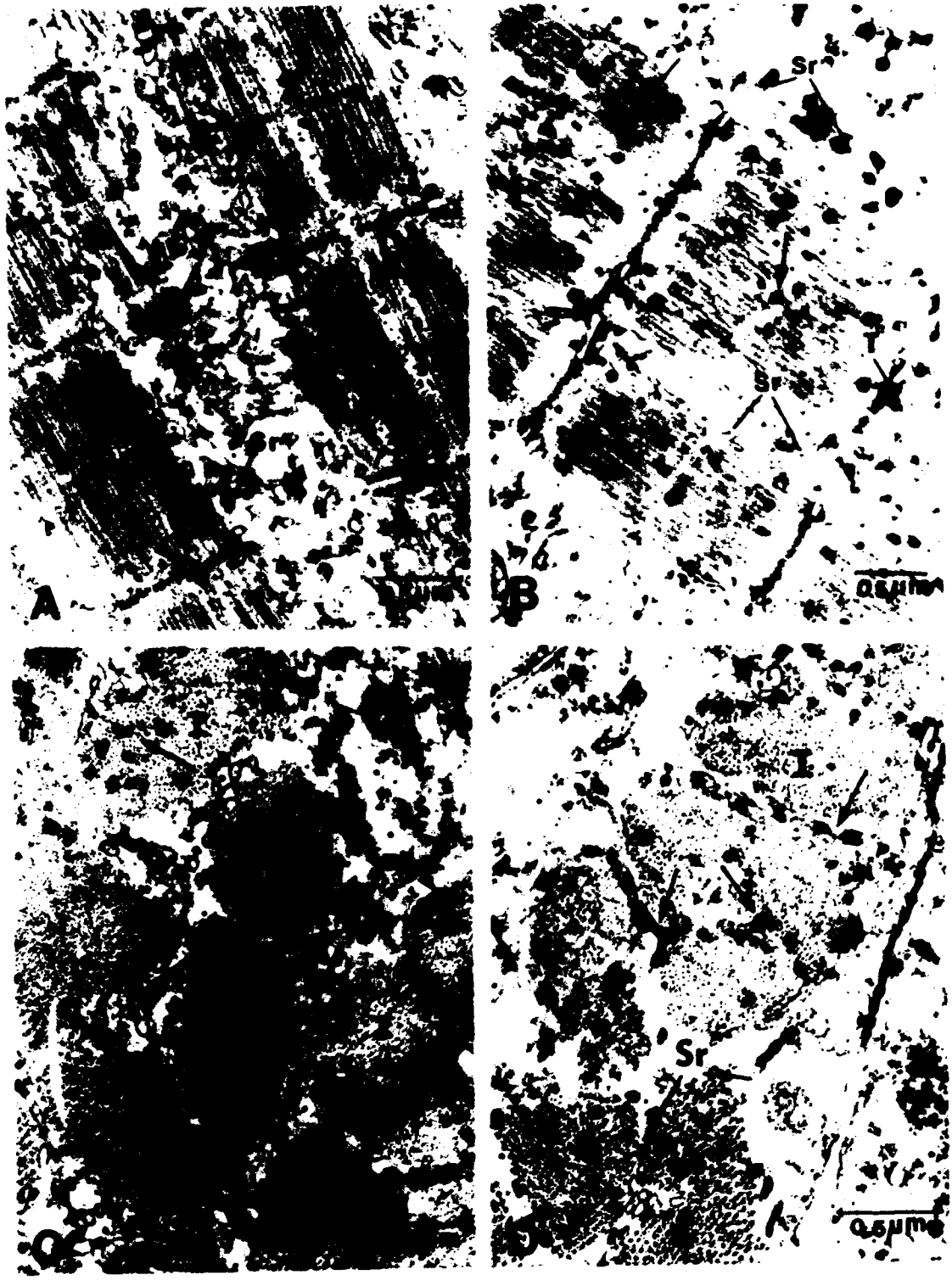

Analyses were as in Figure 23 except that embryos were analyzed after 3 days incubation. Note the developmental increases in myotomal AChE in both control uninjected (A,C) and CMVACHE-injected sections (B,D) especially within the SR and T-tubules. Size bar represents 0.5 μm.

Figure 25: Structural features in neuromuscular junctions of 3-day-old CMVACHE-injected Xenopus embryos overexpressing AChE

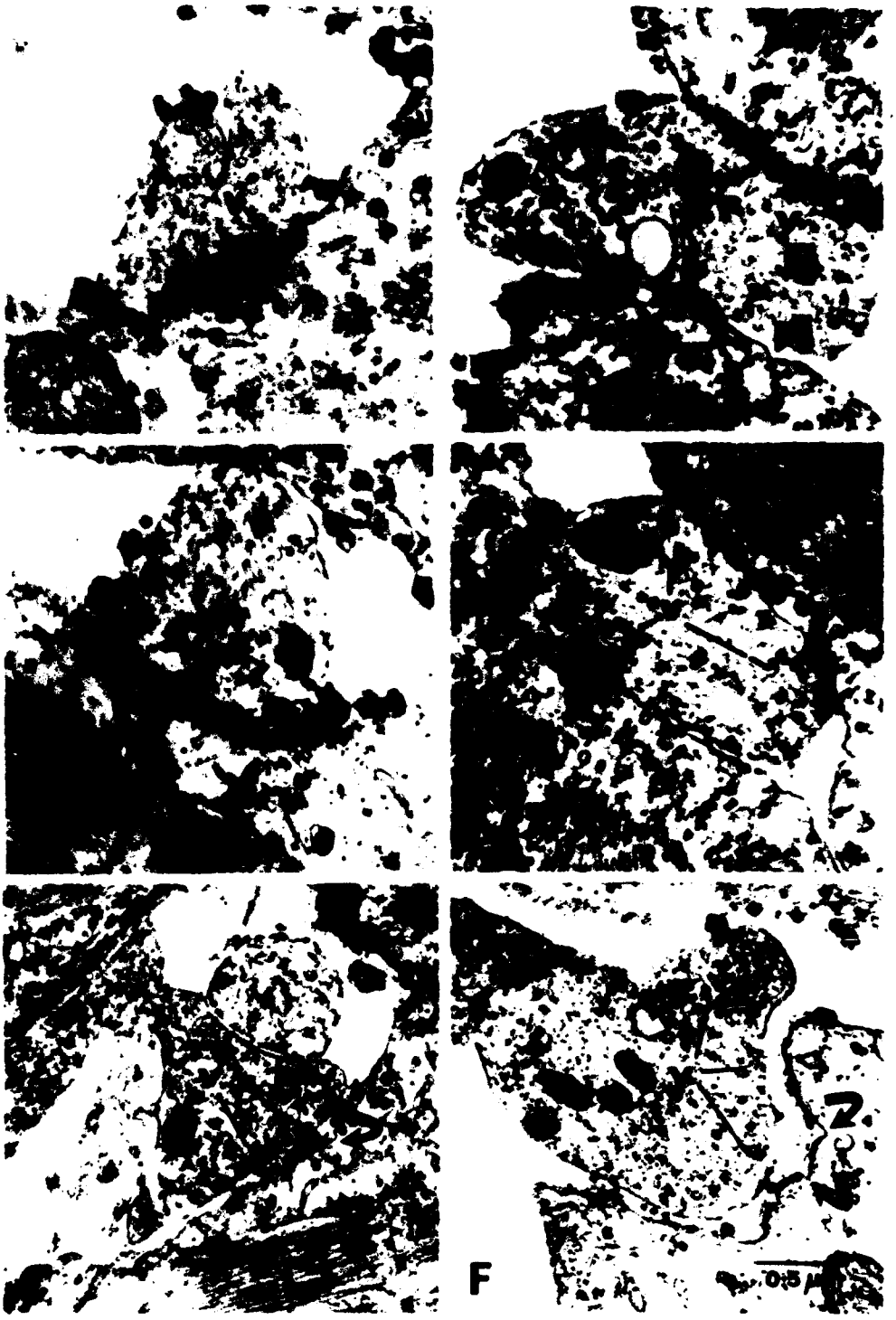

Fertilized Xenopus eggs were cultured for 3 days, fixed, stained for AChE catalytic activity and examined by transmission electron microscopy. Two cytochemically stained synapses are presented from uninjected control (A-B) and CMVACHE-injected (D-E) embryos. Note the particularly high density staining in areas directly opposite nerve terminal zones enriched in neurotransmitter vesicles (V). C,F illustrate representative unstained NMJs from a control and a CMVACHE-injected embryo, respectively. The synapse presented in B represents the highest degree of staining observed in a control section. mf - myofibril; v - pre-synaptic neurotransmitter vesicles; Arrows - post-synaptic folds.

Figure 26: **ACHEmRNA levels are selectively reduced at 12 days after treatment**

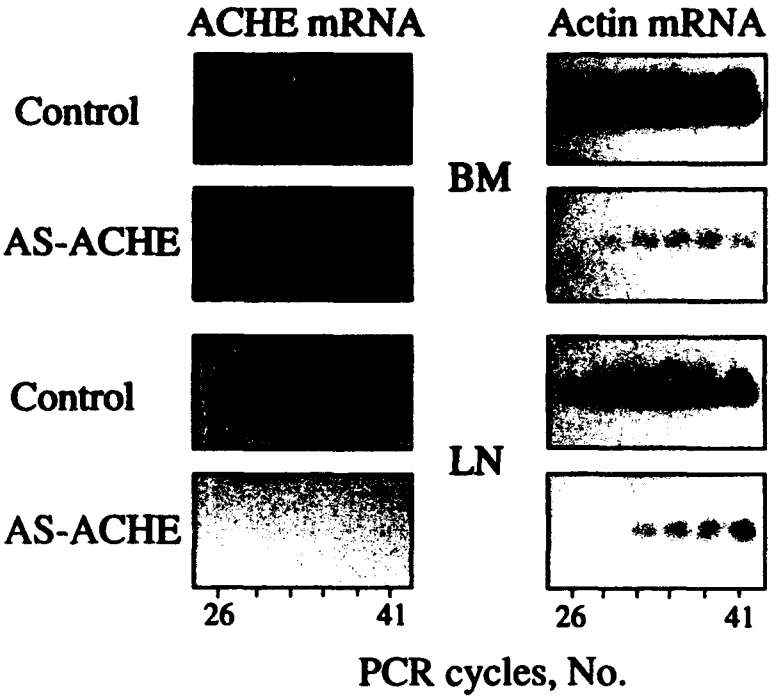

RNA samples (100ng) extracted from dissected lymph nodes (LN) or extruded femoral bone marrow (BM) of treated (AS-ACHE) and untreated (Control) animals were subjected to reverse transcription, PCR amplification and DNA blot hybridization as described under Methods. Primers employed were specific to ACHEcDNA (left) or mouse actin cDNA (right). Cycle nos. at which samples were withdrawn are noted.

Figure 27: Restoration of CHEmRNA levels in MK 20 days after treatment

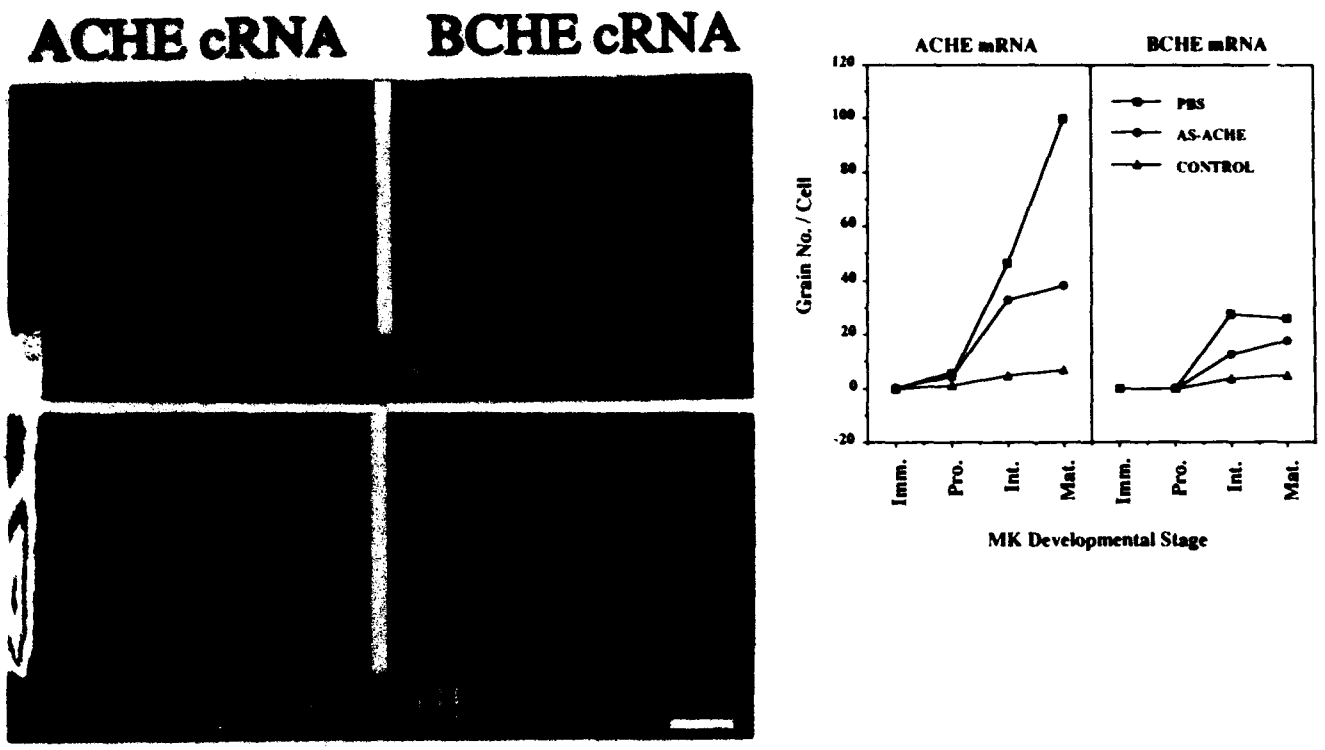

A. **Selective labeling in mice administered in vivo with AS-ACHE.**

Bone marrow smears were prepared from adult female mice treated once with AS-ACHE or with PBS as detailed under Methods, 20 days after treatment. The presented photographs display representative mature MK from a single mouse out of 4 in each group, hybridized with antisense [^{35}S]-ACHEcRNA or BCHEcRNA as compared with ACHEcRNA in all mice, and the reduction in hibridization intensity with both probes in the treated as compared with the PBS-injected mice.

B. **Modulation of CHEmRNA levels in MK from PBS- and AS-ACHE-injected mice.**

CHEmRNA levels in immature, pro-intermedial and mature MK were determined in average no. of silver grains per cell as detailed in text for >40 cells per sample in 4 different mice treated with PBS or AS-ACHE. "Sense" ACHEmRNA and BCHEmRNA probes served as controls for the hybridization. Note the differential changes in ACHE and BCHEmRNA levels through MK development in control and treated mice.

Figure 28: Construction of native and site-directed BCHE mutants

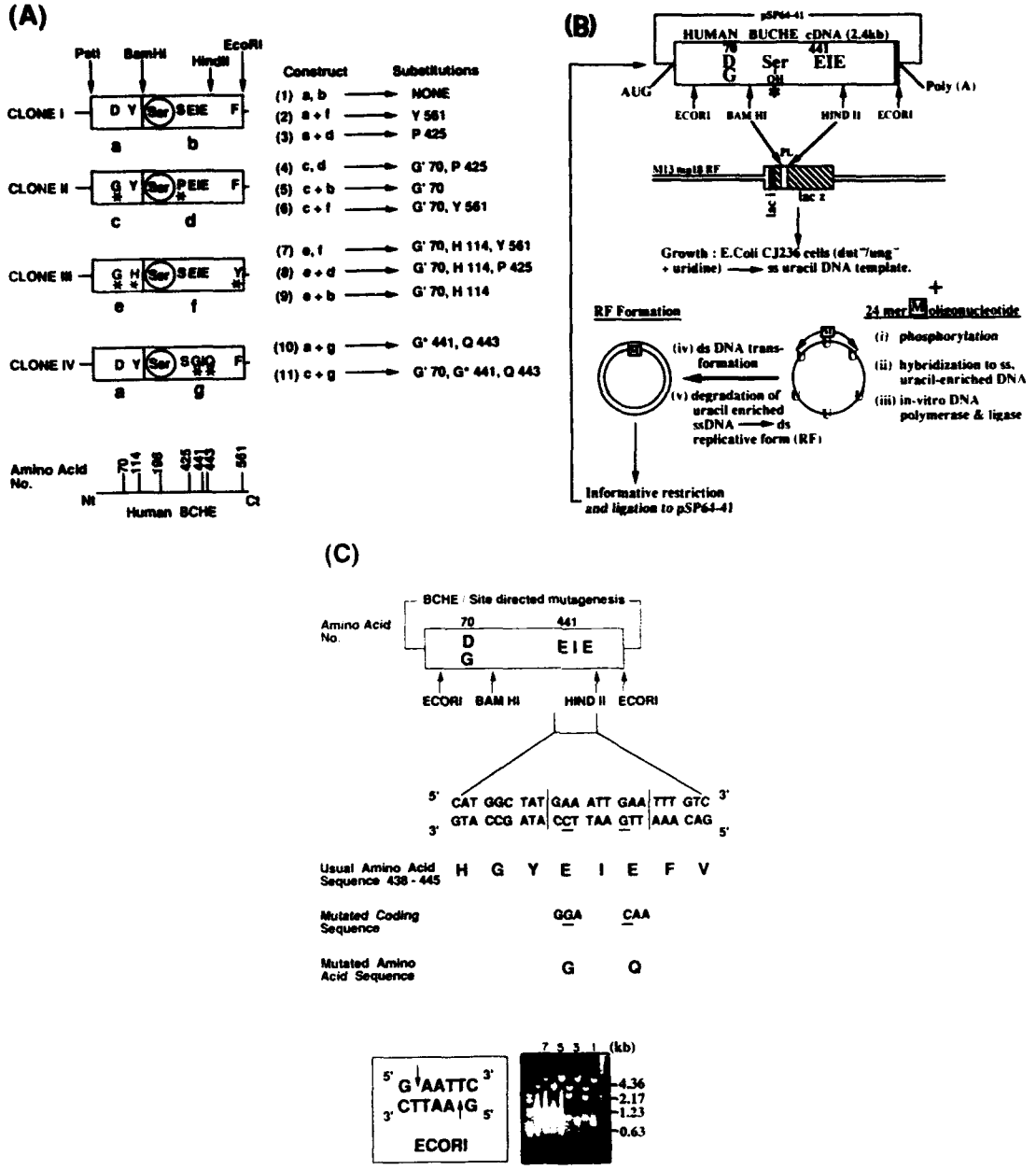

A. **Positions of mutations examined and the respective amino acid substitutions.** BCHEcDNA Clones I, II and III representing the normal BCHE, the unusual BCHE species present in human neuroblastomas and glioblastomas and a novel lambda gt10 ·BCHEcDNA clone, respectively, were used to engineer constructs 1-9 by enzymatic restriction with PStI and BamHI and religation of the resultant a-g frgments in the noted combinations. Amino acid substitutions in each of these BCHE variants are marked in the single letter code. Site-directed mutagenesis of the gly441-gln443 domain into the normal BCHE coding region created Clone IV, from which constructs 10 and 11 were generated in a similar manner, containing the gly441,gln443 domain with or without the gly70 mutation. Respective positions of each of these substitutions along the BCHE polypeptide chain are noted below.

B. **Substitution of the glu441-glu443 domain by site-directed mutagenesis.** DNA from the usual BCHE Clone I was restricted with BamH1/HindII and the resultant 800 bp fragment containing the glu441-glu443 (EIE) domain was subcloned into identically restricted souble-stranded M13mp18RF vector (Boehringer, Mannheim). Single-stranded uracil-enriched DNA including this fragment was obtained (see materials and methods) and double-mutated M 24-mer oligonucleotide, containing 2 mismatches at the EIE region was hybridized to the extracted phage single-stranded DNA. Second strand DNA synthesis was subsequently catalyzed by DNA polymerase and ligase in the presence of dNTPs. Following transformation into competent E. coli MV1190 cells, selective degradation of the uracil-enriched strand occurred and the resultant DNA containing the corresponding 2 mismatches, was restricted pSP64-41 plasmid containing the human BCHEcDNA.

C. **Mutagenesis of glu441-glu443 to gly441-443 introduces an informative EcoR1 site in BCHEcDNA.** Nucleotides nos. 1471-1497 in BCHEcDNA (upper sequence) encode the amino acid residues no. 438-446 in the mature BCHE protein, including the electronegative domain of interest (top peptide sequence). By utilizing the minus strand 24-mer M oligonucleotide (lower nucleotide sequence) which contains 2 mismatches directed at the EIE domain 5'-TTGAATTCC-3', a mutated peptide is encoded by the complementary mutant strand 5'-GGAATTCAA-3' (noted below) which encodes gly441-isoleu442-gln443 (GIQ). This sequence introduces a third and novel EcoRI site in BCHEcDNA which has been used to isolate GIQ encoding mutants. Samples 1, 3, 5 and 7, extracted from constructs 1, 5, 10 and 11, respectively, were each subjected to enzymatic restriction with BamHI/HindII. Parallel restrictions with EcoRI are shown in lanes 2, 4, 6 and 8. Note that the BCHE insert of the mutated plasmids 5 and 7 realized 2 fragments with EcoRI, of sizes 1.2 kb and 1.0 kb, as compared with a single 2.2 kb insert fragment for samples 1 and 3.

Figure 29: Mutagenesis and characterization of active site residues in BuChE

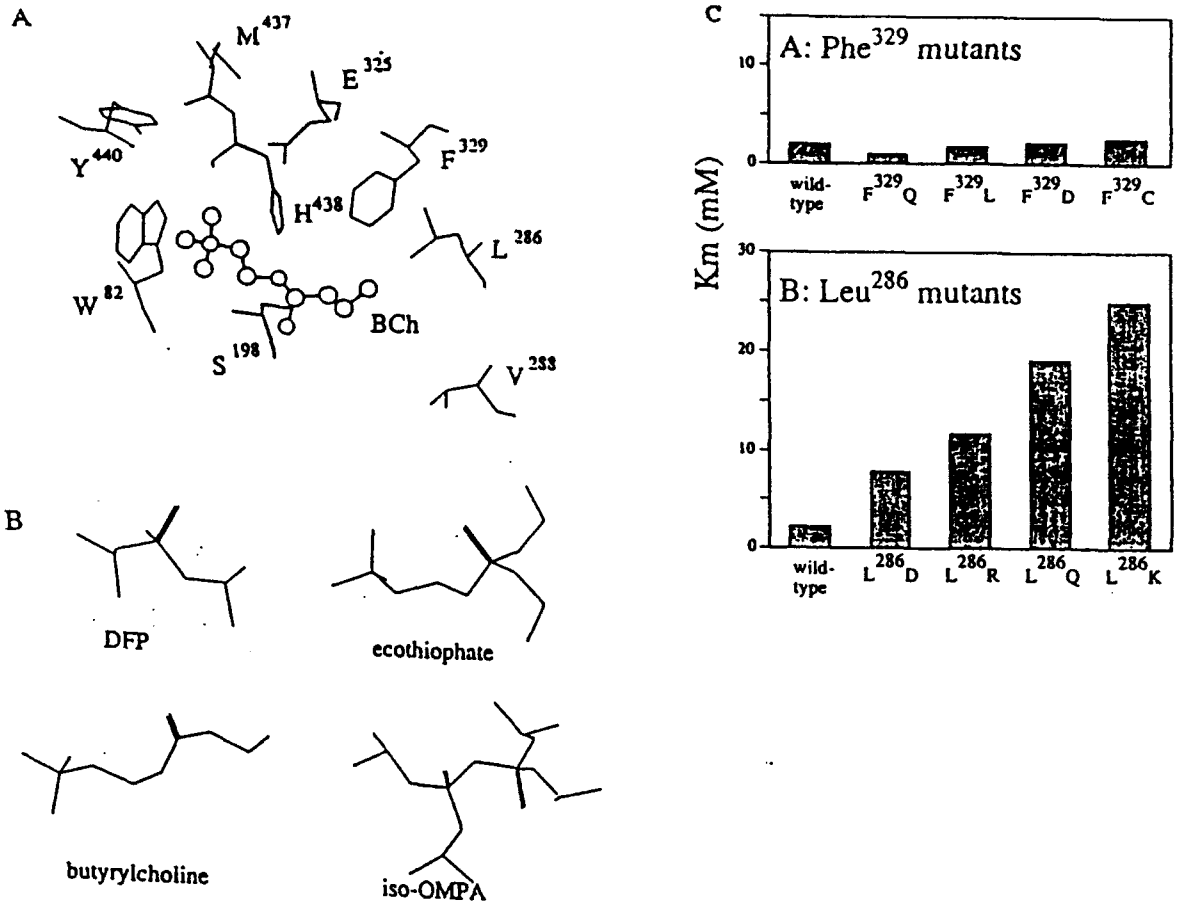

A. **Close view of the active site of BuChE with butyrylcholine (BCh).** The substrate is shown in reaction with Ser^{198}, as its carbonyl carbon passes through a tetrahedral transition state (Harel et al., 1992), and the catalytic triad residues are in heavier outline. Note the acyl-binding region surrounding the right side of the substrate (shown as a ball-and-stick model), and the choline-binding region surrounding its left side.

B. **Three OP inhibitors and the substrate used in this study.**

C. **K_m values for wild-type BuChE and mutations.** Top, Phe^{329}; Bottom, Leu^{286}. Standards deviations were 0.1, 4.0, 3.4, 2.6 and 15.0 mM for wild-type BuChE and $L^{286}D$, $L^{286}R$, $L^{286}Q$, $F^{329}L$, $F^{329}D$ and $F^{329}C$, respectively, for 3 independent transcription and microinjection experiments.

Figure 30: Inhibition of wild-type and two mutant BuChEs by DFP

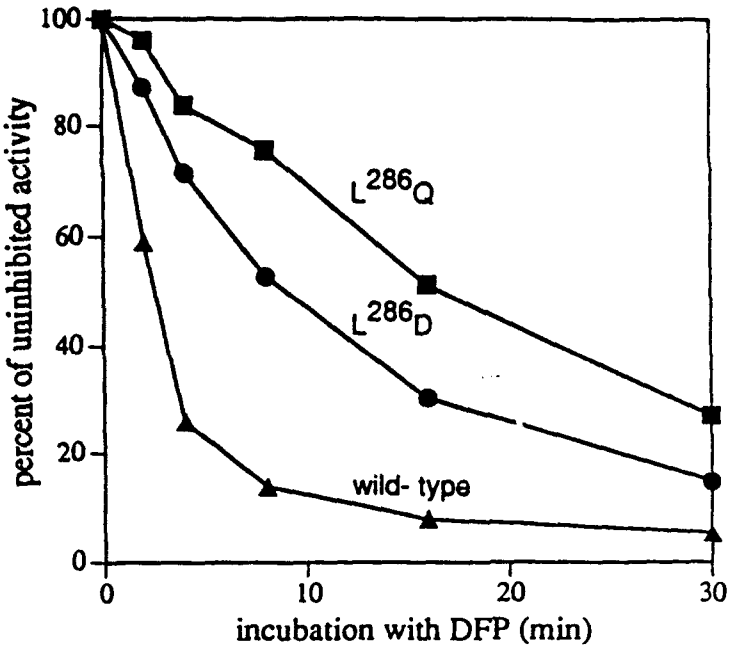

Percent remaining activity of enzyme immobilized through monoclonal antibody onto microtiter plate wells is shown as a function of time of exposure to 5 X 10^{-5} M DFP, 21 °C, pH 7.4. ▲, wild-type enzyme; ■, $L^{286}Q$; ●, $L^{286}D$.

Figure 31: **Alterations in binding affinities of recombinant BuChE variants to choline esters**

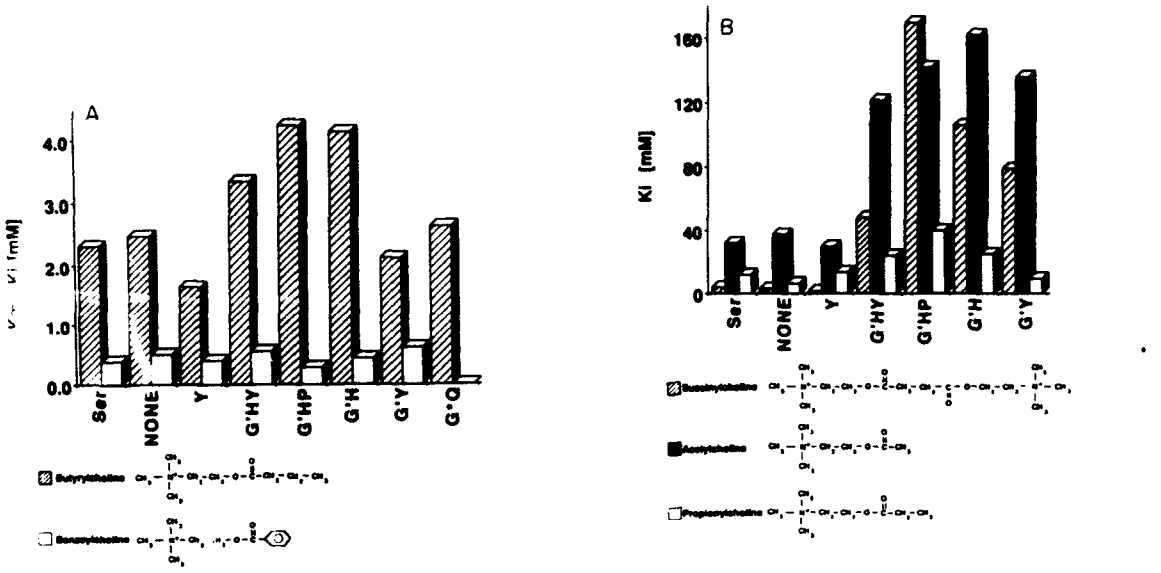

(A) Limited influence on binding to BTCh and BenzCh substrates. Binding of BTCh and BenzCh to recombinant BCHE mutants was measured as described in Materials and Methods and is presented in apparent Km and Ki values (columns). Variations in BTCh Km's ranged between 1.64 mM for the single tyr561 containing mutant and 4.25 mM for the triple gly70, his114, pro425 variant. Also, the site-directed gly441, gln443 BCHE mutant displayed apparently normal binding (Km = 2.64 mM) towards BTCh and that binding affinities of all BCHE variants towards BenzCh were approximately 10-fold higher than affinities to BTCh. Note that BenzCh binding to gly441, gln443 was not evaluated in this study.

(B) Decreased affinity to various substrate analogs induced by gly70 and modulated by other mutations. Ki determinations (mM) for three choline esters (SucCh, PropCh, ACh) were derived from the equation Ki=IC50/1+S/Km and are presented in columns. Note that the triple BCHE mutant gly70,his114,pro425 and, to a lower extent, other gly70 variants presented Ki values increased as much as 100-fold for SucCh, 6.5-fold for PropCh and 5-fold for ACh as compared with the usual recombinant enzyme. The corresponding structures are displayed for each of these choline esters.

Figure 32: **Presence of gly70 within BuChE variants decreases inhibition by cocaine and solanine-derived alkaloids**

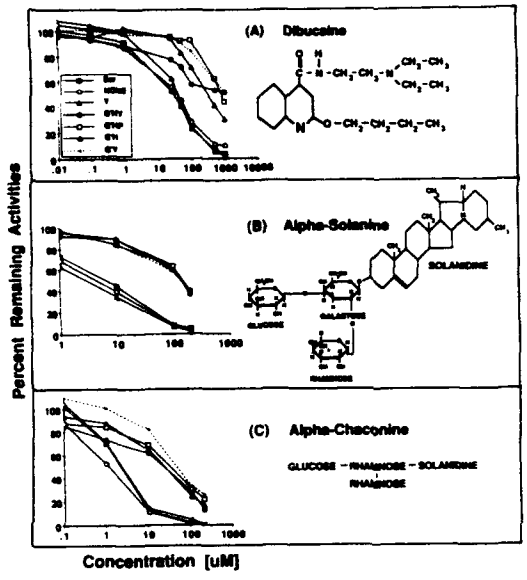

Recombinant BCHEs were incubated with the various inhibitors whose structures are displayed at the noted concentrations and their respective % remaining activies calculated by assays of the hydrolytic activities of 10 mM BTCh.
(A) Dibucaine binding
(B) Alpha-Solanine binding and
(C) Alpha-Chaconine binding. Note that the potent inhibitory properties of alpha-chacoine are also apparent toward all *gly70 containing BCHE muteins*, although with lower affinities that the usual recombinant BCHE enzyme.

Figure 33: Conservation of substrate specificity and loss of substrate activation in the AChE-BuChE chimera

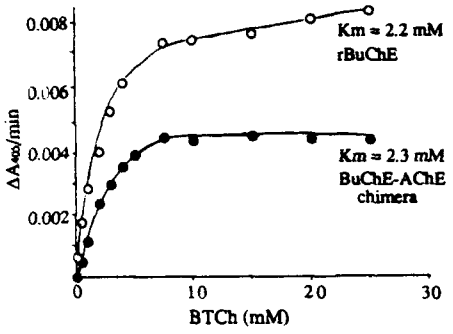

(a)

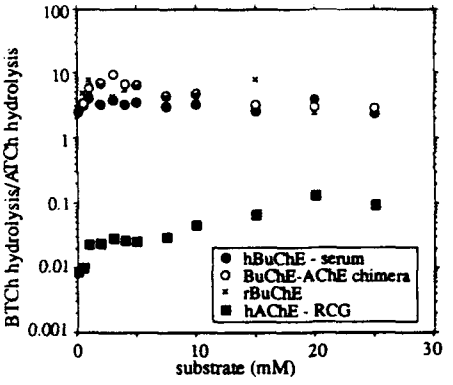

(b)

(a) Apparent Km values. In vitro transcription, Xenopus oocye microinjection, homogenization and enzymatic activity (Neville et al., 1990b, 1992). For Km determinations, hydrolytic activities of the recombinant enzymes were measured using BTCh as substrate in the concentration range of 0.1 mM to 25 mM. Kinetic values were obtained using Enzfitter (version 1.03, Elsevier Biosolft). Serum BuChE and RCG AChE activities served as controls, all as detailed previously (Neville et al., 1990b, 1992). Representative determinations of Km are shown for rBuChE (2.2(±0.17)mM) and for the chimera (2.3(±0.44)mM). Note activation at high substrate concentrations for rBuChE but not for the chimera.

(b) Substrate preference. Rates of hydrolytic activity with BTCh were divided by those with ATCh at identical concentrations, over the range of 0.1 to 25 mM. Resultant BTch/ATCh hydrolytic ratios are shown for rBuChE and chimera, as well as for human serum BuChE and RCG AChE (average of 7 experiments for the chimera and the other proteins).

Figure 34: Inhibition profiles of AChE-BuChE chimera

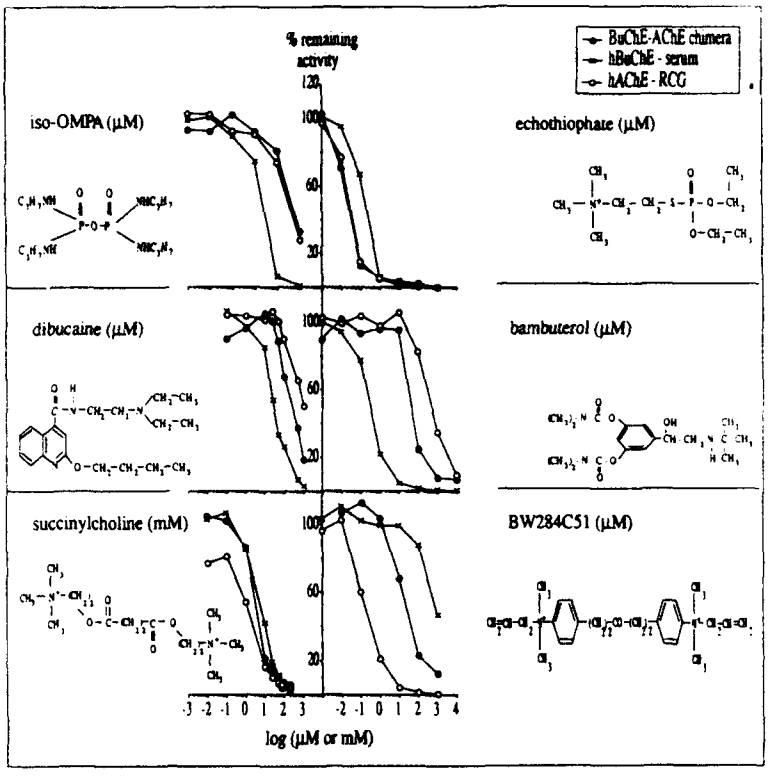

Inhibition profiles for the noted 6 compounds were determined for the chimera, serum BuChE and RCG AChE as detailed previously (Neville et al., 1990b, 1992) at 5 mM BTCh. Each curve is an average of 3 to 8 different experiments from at least 2 separate transcriptions and microinjections, with S.D.≤30%. Iso-OMPA, dibucaine, physostigmine, succinylcholine and BW284C51 were all obtained from Sigma Chemical Co. (St. Louis, MO), ecothiophate iodide from Ayerst Laboratories (Montreal, PQ) and bambuterol from AC Draco (Lund). Percent remaining activity, compared with activity without inhibitor (not shown), was determined for inhibitor concentrations over a range of 5 orders of magnitude.

Table 1: Distribution of amino acid residues and A,T and G,C rich codons in the open reading frame of human ACHE and BCHE coding regions.

Amino acid residues (A/B)		Triple base Choices, %			
		ACHE		BCHE	
		A,T	G,C	A,T	G,C
Ala	(55/34)	2.3	6.7	3.8	1.9
Arg	(43/24)	1.9	5.1	3.1	0.8
Asn	(17/40)	0.8	2.0	4.3	2.3
Asp	(29/24)	3.4	1.3	2.8	1.2
Cys	(08/10)	0.3	1.0	0.8	0.8
Gln	(24/20)	0.5	3.4	1.8	1.5
Glu	(34/37)	0.5	5.0	4.3	1.8
Gly	(58/47)	3.0	6.5	5.8	2.0
His	(15/10)	0.3	2.1	1.5	0.2
Ile	(09/31)	0.2	1.3	4.2	1.0
Leu	(69/55)	0.7	8.6	4.5	4.7
Lys	(10/37)	0.5	1.1	4.5	1.7
Met	(09/13)	-	1.5	-	2.2
Phe	(29/42)	1.5	3.3	5.0	2.0
Pro	(51/30)	2.9	5.4	4.2	0.8
Ser	(36/39)	1.8	4.1	4.4	2.1
Thr	(26/37)	1.6	2.6	4.7	1.5
Trp	(17/19)	-	2.8	-	3.2
Tyr	(21/20)	0.5	2.9	2.3	1.0
Val	(54/33)	1.3	7.5	3.0	2.5

The distribution of different amino acid residues (total numbers are shown in parentheses) and of triple base choices (in %, G,C vs. A,T in the third position of codons) in the open reading frame (ORF) for human ACHE (A) and BCHE (B) coding regions. The sequences analyzed begin, in each case, with the presumptive initiator AUG codon and end with the first "nonsense" codon in the cDNA encoding BCHE (Prody et al., 1987) or ACHE (Fig. 2B).

Table 2: Possible links between cholinergic signaling and cell division control

Signaling inducer	System	Response
Acetylcholine	cholinoceptive CNS cells in vitro	enhanced PI metabolism
Acetylcholine	glioma cell line	increased DNA synthesis
Carbamylcholine or physostigmine	bone marrow cells in vitro and in vivo	induced platelet production
Agents that enhance PI metabolism	developing brain	altered phosphorylation patterns; altered levels of cdc2-related kinases; increased cell division
Antisense-mediated block of *BCHE* gene expression	bone marrow cells in vitro	hemopoiesis diverted; increased production of myeloid cells

Abbreviations: (CNS) Central nervous system; (PI) phosphoinositide; (BCHE) butyrylcholinesterase.

Table 3: The S/T-P-X-Z peptide motif in known and potential substrates of cdc2-related kinases, including cholinesterases

The S/T-P-X-Z Peptide Motif in Known and Potential Substrates of cdc-2-Related Kinases

Known substrates	Cell cycle related function	Sequence
lamin B	nuclear organization	S-P-T-R
histone H1	nucleosomal organization	S-P-X-K
		T-P-X-K
N038, nucleolin	nucleolar arrangement	T-P-X-K
RNA polymerase	transcriptional initiation	S-P-T-S-P-S-Y
$pp60^{c\text{-}src}$	cytoskeletal reorganization	T-P-N-K
		T-P-S-R
		S-P-Q-R
Potential substrates	**Cell cycle related function**	**Sequence**
acetylcholinesterase	cholinergic signaling?	T-P-Y-P-R
		S-P-T-P
		S-P-P-S-R
butyrylcholinesterase	cholinergic signaling?	S-P-G-S
	Consensus motif	S/T-P-X-Z

The sequences of ACHE and BCHE, from which the peptide sequences are derived, can be found for ACHE in Fig. 2B and for BCHE in Prody et al., 1987.

Table 4: **Mapping of the ACHE and BCHE genes to chromosomes 7 and 3 by using a human/hamster somatic cell hybrid panel**

	Appearance of human CHE1 gene in human–hamster cell hybrids																								
Cell line	CHE1 gene	1	2	3	4	5	6	7	8	9	10	11	12	13	14	15	16	17	18	19	20	21	22	X	Y
867	–	+	–	–	–	+	–	–	–	–	–	–	–	–	+	–	–	–	+	+	–	–	–	–	–
854	–	–	+	–	–	+	–	–	–	–	–	–	–	–	–	–	–	–	–	–	–	–	–	–	–
423	+	–	–	+	–	–	–	–	–	–	–	–	–	–	–	–	–	–	–	–	–	–	–	–	–
860	+	–	–	+	–	+	+	–	–	–	+	10%[b]	–	–	–	–	–	–	–	+	–	+	–	–	–
803	–	–	–	–	+	+	–	–	+	–	–	–	–	–	–	–	–	–	–	–	–	–	+	+	–
909	–	–	–	–	–	D[c]	+	–	+	–	–	–	–	–	+	–	–	–	–	–	–	–	–	+	–
151	–	–	–	–	–	–	–	+	–	–	–	–	+	–	–	–	–	–	–	–	–	–	–	–	–
811	–	–	–	–	–	–	–	–	+	–	–	–	–	–	–	–	–	+	–	–	–	–	–	–	–
967	–	–	–	–	–	+	–	–	+	–	–	–	–	–	–	–	+	–	–	–	–	–	–	–	–
734	–	–	–	–	–	+	–	–	–	+	–	–	–	–	–	–	–	–	+	–	–	–	–	–	–
968	–	–	–	–	–	+	–	–	–	+	–	–	–	+	–	–	–	–	–	–	+	–	–	+	–
683	–	–	–	–	–	+	–	–	–	–	–	+	+	–	+	–	–	–	–	+	–	+	+	–	–
507	+	–	–	+	–	+	–	–	–	–	–	+	–	–	+	–	–	–	–	–	+	–	+	–	+
750	–	–	–	–	–	D	–	–	–	–	–	–	–	+	+	+	–	–	–	+	–	–	–	–	–
1099	–	–	–	–	–	D	–	–	–	–	–	–	–	+	–	–	–	–	–	+	–	+	+	–	–
324	–	–	–	–	–	–	–	–	–	–	–	–	–	–	–	–	–	–	+	–	–	–	–	–	–
940	–	–	–	–	–	+	–	–	–	–	–	–	–	–	–	–	–	–	–	–	+	–	–	–	–
937	–	+	–	–	–	+	–	–	–	–	–	–	–	–	+	+	–	+	–	–	–	+	–	–	–
861	+	–	–	+	–	+	–	–	–	–	75%	–	–	–	–	–	–	–	–	–	–	–	–	–	–
1079	+	–	–	+	–	+	–	+	+	–	+	–	–	–	–	–	+	–	–	–	–	–	–	–	–
1006	–	–	–	–	+	+	–	+	–	+	–	–	–	+	–	–	–	–	–	+	–	+	–	–	–
756	–	–	–	–	–	D	+	–	–	–	–	–	+	+	+	–	–	–	–	+	+	+	–	–	+
904	–	–	–	–	–	D	+	–	–	–	–	–	+	–	–	–	+	–	–	–	–	+	–	–	+
909	–	–	–	–	–	D	+	–	+	–	–	–	–	–	+	–	–	–	–	–	–	–	–	+	–
862	–	–	–	–	–	+	–	–	–	+	–	–	–	–	–	–	–	–	–	–	–	–	–	–	–
1049	–	–	–	–	–	+	–	–	–	–	–	+	–	–	–	–	–	–	–	–	–	–	–	–	–
212	–	–	–	–	–	D	–	–	–	–	–	–	–	–	–	–	–	–	–	–	–	–	–	–	–
% Discordance		26	22	0	26	74	30	22	33	33	7	15	33	37	41	26	22	26	30	30	26	37	26	30	22

27 different hybrid cell lines containing one or more human chromosomes were examined in each consecutive lane. Chromosomes present in each hybrid cell line are denoted by + signs. The percents of hybrids that are discordant with the human BCHEcDNA sequence is given for each chromosome. Notice that only DNA from hybrid cell lines containing Chromosome No. 3 were found to positively hybridize with BCHEcDNA.

Table 5: PCR primers and conditions employed to detect point mutations in the hCHE genes

	name	position	PCR*	sequence (5'-3')	use
	A C H E				
1	H322N (+)	E2 (1010)	403 bp 65°C	TTGTGGGCTGTCCTCCAGGCGG	amplification and sequencing of the a.a.322 (Yt) region
2	H322N (-)	5'end of I2 (186)		AAAATGAGACCCATGGTGGCTTTCCTGTCT	
3	H322N seq (-)	5' end of I2 (78)		CATGCCTGGGTCCCTGCA	
4	P446 (+)	3' end of I2 (83)	662 bp 60°C	CTCTTTGTCTGTCCATCTGTTTCTGTC	amplification and sequencing of the a.a.446 region
5	P446 (-)	5' end of I3 (93)		CCCGTCCTTTCTGTCTCCGTGTG	
6	P446 seq (+)	E3 (1365)		TGACCTGGCAGCCGAGG	
	B C H E				
7	D70G (+)	E2 (271)	186 bp 55°C	CTTGGTAGACTTCGATTCAAAAAGCCACAGTCT	amplification and sequencing of the a.a.70 region ("atypical"variant)
8	D70G (-)	E2 (457)		GAATCCATACATTTAGATATAAACAGTCTTCACTG	
9	D70G seq (-)	E2 (287)		TCAAAAAGCCACAGTCT	
10	E497V (+)	3' end of I2 (88)	336 bp 55°C	GCTCTGTGAACAGTGTTAGAAAACAATATTCTTTTTAATC	amplification and sequencing of the a.a.497 region (J variant)
11	E497V (-)	5' end of I3 (82)		CCGTGCCTTGGAGAGTATACTTCATCCCTTTTTTACATAACCC	
12	E497Vseq (+)	3' end of I2 (36)		CAATTTTACTATAATGTCTC	
13	A539T DraI (+)	I3 E4 junction (I3-25 to E4-1773)	323 bp 50°C	ATACAACTTATTCCATATTTTACAGGAAATATTGtTtAA	amplification and sequencing of the a.a.539 (K variant) and analysis of nt2073
14	nt2073 NsiI (-)	E4 (2111)		TAACTGTAGAACTTTATATTGTGAAATTTAATTAtgCA	
15	A539T seq (-)	E4 (1881)		GAGACCCACACAACTTTC	

Primer names are derived from the amino acid substitution region that is amplified or sequenced (seq) by them. (+) and (-) refer to the sense and anti-sense directions, respectively. Numbers in parentheses refer to the position of the 5'-end nucleotide of each primer. Primers in exons (E) are numbered according to Soreq et al. (1990) for ACHE and Prody et al. (1987) for BCHE. Primers in introns (I) are designated according to the number of bases from the nearest intron/exon junction. For RG-PCR-introduced RFLP analyses, primers 13 and 14 contain deliberately mis-matched bases (underlined lower case letters) to create a restriction endonuclease recognition sequence for DraI and/or NsiI when amplifying BCHE alleles containing T539 but not A539, and/or dA but not dG at nt2073, respectively. *The size of the PCR fragment generated by using the two upper primers in each box and the annealing temperature used for amplification are indicated.

Table 6: Haplotypes of CHE genes in Jewish populations

	codons			nt.	
haplotype	70	497	539	2073	chromosomes
I	D	E	A	dA	35
II	G	E	A	dG	5
III	D	E	A	dG	21
IV	G	E	A	dA	3
indeterminate	D/G	E	A	dA/dG	10

Thirteen unrelated Georgians heterozygous for the BCHE D70G substitution, and 24 homozygous for D70 were analyzed for three other nucleotide alterations in the BCHE gene, two of which cause amino acid substitutions (E497V and A539T), the third being a nucleotide alteration at the 3' non-coding region, 2073dA or 2073dG. (+) and (-) represent the common and rare forms, respectively. These are sorted into four haplotypes. The observed genotypes were: haplotype I/I, 11 individuals; I/III, 10; I/IV, 3; II/III, 5; III/III, 3. For 10 chromosomes (5 individuals), noted as "indeterminate", we could not assign haplotypes because of double heterozygosity (codon 70 and nt2073).

Table 7: Intron-exon boundaries in the ACHE gene

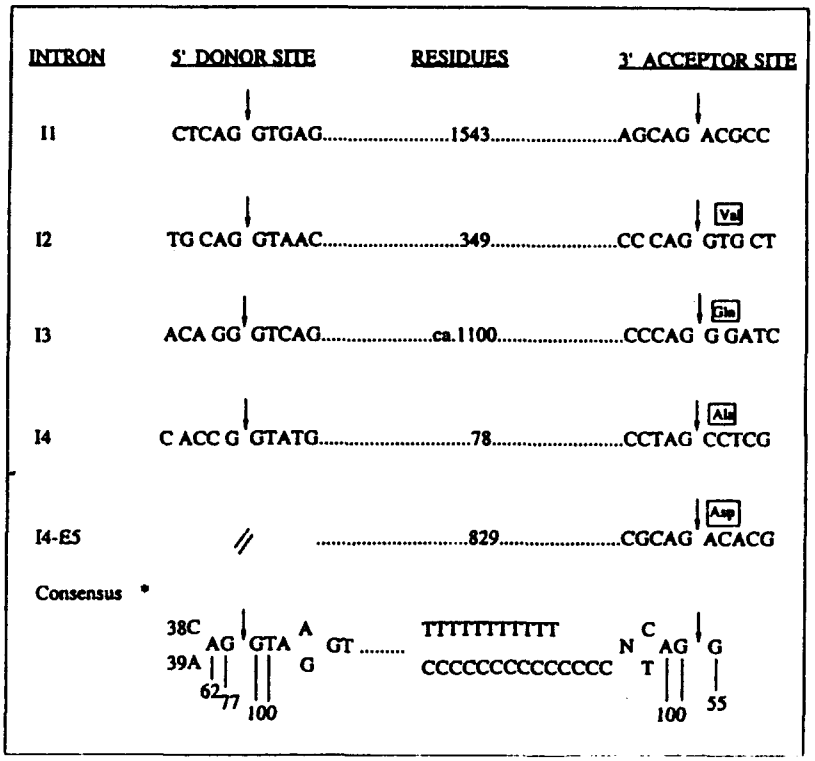

Donor (5') and acceptor (3') sites for each of the introns in the ACHE gene (I2-I4 in the coding sequence and upstream intron, I-1), were determined by DNA sequencing of ACHE genomic DNA and ACHEcDNA sequences (see Figure 10A for schematic representation of ACHE gene). Insertion positions within the ACHE gene are numbered below. Amino acids, wherever encoded at acceptor positions, are noted in boxes above (except for I-1, which is an untranslated sequence). Consensus sequence data for intron-exon boundaries (Krainer and Maniatis, 1988). The numbers denote the frequency of occurrence of each consensus base at specific positions (in %).

Table 8: Recombinant human ACHE production in microinjected Xenopus oocytes

Oocytes injected with:	ACHEmRNA	Barth Medium
Acetylthiocholine hydrolysis rate, mOD 405/min	11.9 ± 1.9	1.1 ± 0.2
Substrate degraded, nmol/hr/oocyte	50.4 ± 5.0	5.2 ± 0.9
% remaining activity		
+ BW284C51	4.6 ± 0.35	48.7 ± 10.6
+ iso-OMPA	94.8 ± 1.4	88.3 ± 5.9

Recombinant ACHEmRNA from 3 separate in vitro transcription reactions (Ben Aziz and Soreq, 1990) was injected into 30 oocytes per experiment (2 ng mRNA per oocyte). Parallel groups of oocytes were injected with Barth's medium and served as controls. Following incubation, oocyte homogenates from 3 separate microinjection experiments were used for analyzes of total ACHE-mediated hydrolysis of acetylthiocholine essentially as detailed previously (Soreq et al., 1989; Dreyfus et al., 1988). Acetylthiocholine concentration was 1 mM. In order to ascertain sensitivity to inhibitors, either BW284C51 or iso-OMPA was added to the reaction mixtures 40 min prior to the addition of substrate in a final concentration of 10 μM. Hydrolytic activities and percent inhibition values for the recombinant ACHE enzyme are shown in comparison with the endogenous ACHE activities in control oocytes. Spontaneous substrate hydrolysis (up to 0.6 mOD/min) was subtracted. Data shown represent mean values ± standard evaluation of the mean (SEM). Note residual endogenous, BW284C51-insensitive, non-specific hydrolytic activity accounting for approximately 2.5 nmol/hr per oocyte in all samples.

Table 9: Subcellular fractionation of rhAChE in CMVACHE-injected Xenopus embryos

FRACTION	rH			Fr
	DAY 1	DAY 2	DAY 3	DAY 3
LSS	57 ± 2	60 ± 4	53 ± 3	36 ± 5
DS	37 ± 2	34 ± 4	36 ± 3	31 ± 4
HSS	6 ± 2	5 ± 1	10 ± 1	33 ± 7

Fertilized Xenopus eggs were microinjected with 1 ng CMVACHE-DNA, cultured for 1-3 days and subjected to homogenization and subcellular fractionation. rhAChE in each fraction (rH) was detected by Enzyme Antigen Immunoassay (Liao et al., 1992) using a specific mAb (101-1) raised against human brain AChE. Endogenous AChE activity in uninjected tadpoles (Fr) was determined by the standard colorimetric assay. Percent enzyme activity in each fraction (average ± SEM) is shown for 3 to 5 groups of 3 embryos from a single minroinjection experiment. LSS - Low salt soluble; DS - Detergent soluble; HSS - High salt soluble.

Table 10: Biochemical assessment of AChE production in injected embryos

	Thiocholine release (mOD/min)						Net added activity (nmls/hr/HE)
GROUP	1	2	3	Avg	SEM	N	Avg
HpACHE	3.25	3.26	3.49	3.33	0.08	6	13.4
CMVACHE	19.54	11.35	---	15.48	4.11	4	228.1
Uninjected	2.85	2.24	---	2.55	0.31	4	---

Acetylthiocholine hydrolyzing activity was determined in homogenates prepared from 2-3 groups of 2 embryos each from a single microinjection experiment with the specified ACHE encoding DNA (see Methods for details). Raw data for individual groups are expressed as A_{405} (mOD/min) and net induced activity and standard deviation are presented in nanomoles substrate hydrolyzed/embryo/hr.

Spontaneous substrate hydrolysis of 0.3 mOD/min has been subtracted, values in parentheses refer to total number of embryos tested in the entire experiment.

Table 11: Modified neuromuscular junctions in 3-day old Xenopus embryos over-expressing rhAChE

EXP.	Post-Synaptic Length, (PSL), μm	Stained Length, (SL), μm	SL/PSL, ratio	Stained Area, (SA), μm^2
Uninj.	2.57	0.79	0.004	0.156
	3.95	0.79	0.200	0.126
	1.54	0.80	0.060	0.080
	2.35	0.73	0.310	0.082
	1.17	0.44	0.085	0.063
	1.60	0.29	0.180	0.056
	1.02	0.29	0.280	0.040
	0.88	0.58	0.650	0.075
Av.±SD	1.88 ± 0.93	0.58 ± 0.22	0.22 ± 0.19	0.084 ± 0.038
+CMVACHE	1.76	1.17	0.660	0.284
	2.50	2.05	0.820	0.331
	2.64	1.91	0.720	0.285
	2.50	2.40	0.960	0.476
	3.50	2.03	0.580	0.396
	1.85	1.66	0.900	0.333
	3.10	1.85	0.600	0.535
	3.23	1.76	0.540	0.289
Av.±SD	2.64 ± 0.58	1.85 ± 0.33	0.72 ± 0.15	0.37 ± 0.09
P value	P<0.01	P<0.002	P<0.002	P<0.002

Eight representative synapses from CMVACHE-injected or control uninjected embryos were assessed for post-synaptic membrane length in μm (PSL), the sum total length covered by reaction product in μm (SL), the fraction of nerve-muscle contact distance displaying reaction product (SL/PSL), and the total stained area in μm^2 (SA). Average values (Av.) ± Standard Deviation (SD) are presented. Measurements were performed on EM photographs using a hand-held mapping device.

Table 12: Hematopoietic effects of AS-ACHE

A) In vivo modulation of bone marrow cell composition by AS-ACHE

Treatment	Days Post-Treatment	Lymphocytes + stem cells	Myelocytes	Granulocytes + Neutrophils	Erythroid cells
None	0 (N=4)	19.0	20.0	32.0	29.0
AS-ACHE	12 (N=4)	4.5	34.5	47.0	13.0
AS-ACHE	20 (N=4)	25.0	22.5	17.0	35.5

B) MK subclassification at 20 days after injection

Treatment	Pro-MK	Int. MK	Mat. MK
PBS (N=2)	0.8	85.3	13.9
AS-ACHE (N=4)	2.1	75.2	22.7

A. Three week old Sabra mice were injected intraperitoneally with 5µg/g weight AS-ACHE. Untreated bone marrow served for control. At the noted day after treatment, bone marrow smears were prepared as detailed under Methods and differentially distinguished into lymphocytes and stem cells, myelocytes, granulocytes and neutrophils and erythroid cells. At least 1000 cells were counted in each case and results are given in percentages. Note the dramatic change in cell composition 12 days after treatment and its apparent reversal by day 20.

B. Percent fractions of specific MK subtypes were determined 20 days after treatment. Note the significant increase in both promegakaryocytes and mature MK fractions in AS-ACHE, but not in PBS-injected controls.

Table 13A. Substrate and inhibitor interactions with hBuChE

enzyme	relative K_m[a]	IC_{50}[b](μM)		
		ecothiophate	iso-OMPA	DFP
Wild-type[c]	1.0	0.27	22	0.02
$L^{286}K$	11	>1000	100	N.D.
$L^{286}Q$	9	5.5	140	0.25
$L^{286}R$	5	N.D.	N.D.	N.D.
$L^{286}D$	4	2.5	55	0.17
$F^{329}Q$	0.4	3.7	2	0.006
$F^{329}L$	0.8	2.5	4.8	0.004
$F^{329}C$	1.2	3.1	3	0.006
$F^{329}D$	1.0	2	30	0.03
$Y^{440}D$	2.1	0.68	85	0.07

[a]Ratios of K_m values toward butyrylthiocholine (wild-type = 2.2 mM). Determinations were made on material from 3 or more different in vitro transcription and microinjection experiments with standard deviations noted in Fig. 31.

[b]IC_{50} values are an average of 3 or more determinations of material from 2 or more microinjections, obtained by assay of activity after incubation with the inhibitor for 30 min, 22°C, pH 7.4. N.D., not determined; certain Leu^{286} mutants showed low activities, which made difficult precise determination of IC_{50} values.

[c]Oocyte activity following an injection of unmodified BuChEmRNA was used. This activity has K_m and IC_{50} values identical to those of human serum BuChE.

Table 13B: Comparison of IC_{50} with kinetic data

enzyme	$1/IC_{50}$ (μM)[a]	$k(min^{-1})$[b]	$(1/IC_{50})/k$
Wild-type	50	0.338[a]	148
L^{286}_{D}	6	0.066	90
L^{286}_{Q}	4	0.022	90

Inactivations of the wild-type and two mutant enzymes were performed with 5×10^{-8} M DFP, pH 7.4 at 20°C. Assay of remaining activity was performed in 20 mM BTCh.

[a] IC_{50} data appear also in Table 13A.

[b] Pseudo-first order rate constants were calculated from the data of Fig.30 by linear regression analysis of plots of the logarithms of remaining activity vs. time of exposure to DFP.

[c] Commercial human BuChE was used for this determination.

Table 14: Mutations resulting in significant IC_{50} variations

	Drug/ substitution	none	Tyr561	Gly70 His114 Tyr561	Gly70 Tyr561	Gly70 His114	Gly70 His114 Pro425	Gly70 Pro425	Gly70
1	Succinylcholine	2.5	2.5	25	30	30	30	>1000	60
2	Alpha Solanine	5.2	3.5	170	170	170	170	170	170
3	Solanidine	55	55	>200	>200	>200	>200	>200	>200
4	Alpha Chaconine	2	3	35	35	35	35	35	35
5	Dibucaine	30	30	100	1000	500	1000	1000	50
6	Bambuterol	0.5	0.5	0.5	5	5	5	10	100
7	Ecothiophate	0.2	0.2	1	1	1	5	10	5
8	iso-OMPA	2	8	1	2	0.5	1	10	>1000
9	Physostigmine	0.7	0.7	2	5	5	2	0.7	10

Naturally occurring point mutations, each leading to a particular amino acid substitution, were introduced in several combinations into BuChEcDNA constructs and their corresponding enzyme products analyzed for their sensitivity to inhibition by the above listed anti-ChE drugs and poisons. Binding affinity to the noted drug is presented (Gnatt et al., 1992, 1993).

Table 15: IC_{50} values (μM) with several inhibitors for the BuChE-AChE chimera

	ecothiophate	BW284C51	iso-OMPA	succinylcholine	dibucaine	physostigmine	bambuterol
hBuChE serum	0.19	820	24	6500	28	0.29	0.31
rBuChE	0.21	>1000	18	--	45	0.57	0.36
BuChE-AChE chimera	0.023	26	450	3700	260	0.25	43
hAChE RCG	0.028	0.18	330	1400	990	0.025	480

The concentrations of inhibitor that resulted in 50% of the control rates of activity were determined from the inhibition curves.

Inhibtion profiles for the noted 6 compounds were determined for the chimera, serum BuChE and RCG AChE as detailed previously (Neville et al., 1990b, 1992) at 5 mM BTCH.

VII. BIBLIOGRAPHY

Abramson, SN, Radic Z, Manker D, Faulkner DJ, Taylor P (1989) Oncidal: A naturally occurring irreversible inhibitor of acetylcholinesterase with a novel mechanism of action, Mol. Pharmacol. 36, 349-354.

Agarwal DP, Stivastava LM, Goedde HW (1976) A note on suxamethonium sensitivity and serum cholinesterase variants, Hum. Genet. 32, 85-88.

Agrawal S, Temsamani J, Tang JY (1991) Pharmacokinetics, biodistribution, and stability of oligodeoxynucleotide phosphorothioates in mice, Proc. Natl. Acad. Sci. USA 88, 7595-7599.

Alles GA, Hawes RC (1940) Cholinesterases in the blood of man, J. Biol. Chem. 133, 375-390.

Anglister L, McMahan UJ (1985) Basal lamina directs acetylcholinesterase accumulation at synaptic sites in regenerating muscle, J. Cell. Biol. 101, 735-743.

Arias S, Rolo M, Gonzalez N (1985) Gene dosage effect present in trisomy 3q25.2qter for serum-cholinesterase (CHE1) and absent for transferrin (TF) and ceruloplasmin (CP), Cytogenet. Cell Genet. 40, 571.

Arpagaus M, Kott, M, Vatsis KP, Bartels KP, La Du BN, Lockridge O (1990) Structure of the gene for human butyrylcholinesterase. Evidence for a single copy, Biochemistry 29, 124-131.

Ashkenazi A, Ramachandran J, Capon DJ (1989) Acetylcholine analogue stimulates DNA synthesis in brain-derived cells via specific muscarinic receptor subtypes, Nature 340, 146-150.

Baker BS (1989) Sex in flies: The splice of life, Nature 340, 521-524.

Baker RT, Board PG (1989) Unequal crossover generates variation in ubiquitin coding unit number at the human UbC polyubiquitin locus, Am. J. Hum. Genet. 44, 534-542.

Balduini W, Murphy SD, Costa LG (1987) Developmental changes in muscarinic receptor-stimulated phosphoinositide metabolism in rat brain, J. Pharmacol. Exp. Ther. 241, 421-427.

Baldwin AS Jr., Azizkhan JC, Jensen DE, Beg AA, Coodly LR (1991) Induction of NF-kappa B DNA-binding activity during the G0-to-G1 transition in mouse fibroblasts, Mol. Cell. Biol. 11, 4943-4951.

Barnett P, Rosenberry TL (1977) Catalysis by Acetylcholinesterase: acceleration of the hydrolysis of neutral acetic acid esters by certain aromatic cations, J. Biol. Chem. 252, 7200-7206.

Bartels CF, James K, La Du BN (1992a) DNA mutations associated with the human butyrylcholinesterase J-variant, Am. J. Hum. Genet. 50, 1104-1114

Bartels CF, Jensen FS, Lockridge O, van der Spek AFL, Rubinstein HM, Lubrano T, La Du BN (1992b) DNA mutation associated with the human butyrylcholinesterase K-variant and its linkage to the atypical variant mutation and other polymorphic sites, Am. J. Hum. Genet. 50, 1086-1103

Bartels CF, Zelinski T, Lockridge O (1993) Mutation at codon 322 in the human acetylcholinesterase (ACHE) gene accounts for YT blood group polymorphism, Am. J. Hum. Genet. 52, 928-936.

Barthalay Y, Hipeau-Jacquotte R, de la Escalera S, Jimenez F, Piovant M (1990) Drosophila neurotactin mediates heterophilic cell adhesion, EMBO J. 9, 3603-3609.

Bartus RT, Dean RL III, Beer B, Lippa AS (1982) The cholinergic hypothesis of geriatric memory dysfunction, Science 217, 408-417.

Beeri R, Gnatt A, Lapidot-Lifson Y, Ginzberg D, Shani M, Zakut H, Soreq H (1992) Testicular gene amplification and impaired BCHE transcription induced in transgenic mice by the human BCHE coding sequence; in Multidiciplinary Approaches to Cholinesterase Functions, Shafferman A, Velan B, eds., Plenum Press, New York, pp. 91-94.

Ben Aziz R, Soreq H (1990) Improving poor in vitro transcription from G,C-rich genes, Nucl. Acids Res. 18, 3418.

Ben Aziz R, Gnatt A, Prody C, Lev-Lehman E, Neville L, Seidman S, Ginzberg D, Soreq H, Lapidot-Lifson Y, Zakut H (1991) Differential codon usage and distinct surface probabilities in human acetylcholinesterase and butyrylcholinesterase; in Cholinesterases: Structure, Function, Mechanism, Genetics, and Cell Biology, Massoulie J, Bacou F, Barnard E, Chattonet A, Doctor BP, Quinn DM, eds., ACS Books, Washington, pp. 172-178.

Ben Aziz-Aloya R, Seidman S, Timberg R, Sternfeld M, Zakut H, Soreq H (1993) Expression of a human acetylcholinesterase promoter-reporter construct in developing neuromuscular junctions of *Xenopus* embryos. Proc. Natl. Acad. Sci. USA 90, 2471-2475.

Benvenisty N, Shoshani T, Farkash Y, Soreq H, Reshef L (1989) Trans-activation of phosphoenolpyruvate carboxykinase (GTP) gene expression by micro-coinjection of rat liver mRNA in *Xenopus* laevis oocytes, Mol. Cell. Biol. 9, 5244-5247.

Berman HA, Olshefski DF, Gilbert M, Decker MM (1985) Fluorescent phosphonate labels for serine hydrolases: kinetic and spectroscopic properties of (7-nitrobenz-2-oxa-1,3-diazole)aminoalkyl methylphosphofluoridates and their conjugates with acetylcholinesterase molecular forms, J. Biol. Chem. 260, 3462-3468.

Bernardi G (1989) Compositional genome, mapping: The isochore organization of the human genome, Ann. Rev. Genet. 23, 637-661.

Biedler JL, Chang TD, Scotto KW, Melera PW, Spengler BA (1988) Chromosomal organization of amplified genes in multidrug-resistant Chinese hamster cells, Cancer Res. 48, 3179-3187.

Bielinska A, Shivdasani RA, Zhang LQ Nabel GJ (1990) Regulation of gene expression with double-stranded phosphorothioate oligonucleotides, Science 250, 997-1000.

Biggin MD, Tjian R (1989) Transcription factors and the control of Drosophila development, Trends Genet. 5, 377-383.

Bishop JM (1991) Molecular themes in oncogenesis, Cell 64, 235-248.

Blackwell TK, Kretzner L, Blackwood EM, Eisenman RN, Weintraub H (1990) Sequence-specific DNA binding by the c-Myc protein, Science 250 1149-1151.

Bloomfield CD, Brunning RD (1976) Acute leukemia as a terminal event in nonleukemic hematopoietic disorders, Semin. Oncol. 3, 297-317.

Boiziau C, Kurfurst R, Cazenave C, Roig V, Thoung NT, Toulme JJ (1991) Inhibition of translation initiation by antisense oligonucleotides via an RNase-H independent mechanism, Nucl. Acids Res. 19, 1113-1119.

Boothroyd JC (1985) Antigenic variation in African trypanosomes, Ann. Rev. Microbiol. 39, 475-502.

Brady L, Brzozowski AM, Derewenda ZS, Dodson E, Dodson G, Tolley S, Turkenberg JP, Christiansen L, Huge-Jensen B, Norskov L, Thim L, Menge U (1990) A serine protease forms the catalytic center of a triacylglycerol lipase, Nature 343, 767-770.

Brennan SO, Arai K, Madison J, Laurell CB, Galliano M, Watkins S, Peach P, Myles T, George P, Putnam FW (1990) Hypermutability of CpG nucleotides in the propeptide-encoding sequence of the human albumin gene, Proc. Natl. Acad. Sci. 87, 3909-3913.

Brock DJH, Bader P (1983) The use of commercial antisera in resolving the cholinesterase bands of human amniotic fluids, Clin. Chim. Acta 127, 419-422.

Brodbeck U, Liao J (1992) Subunit assembly and glycosylation of mammalian brain acetylcholinesterases; in Multidisciplinary Approaches to Cholinesterase Functions, Shafferman A, Velan B, eds., Plenum Press, New York, pp 33-38.

Brown LM, Blair A, Gibson R, Everett GD, Cantor KP, Schuman LM, Burmeister LF, Van Lier SF, Dick F (1990) Pesticide exposures and other agricultural risk factors for leukemia among men in Iowa and Minnesota, Cancer Res. 50, 6585-6591.

Burstein SA, Harker LA. (1983) Control of platelet production. Clinics Haematol. 12, 3-22.

Burstein SA, Adamson JW, Harker LA (1980) Megakaryocytopoiesis in culture: modulation by cholinergic mechanisms, J. Cell. Physiol. 103, 201-208.

Burstein SA, Boyd CN, Dale GL (1985) Quantitation of megakaryocytopoiesis in liquid culture by enzymatic determination of acetylcholinesterase, J. Cell. Physiol. 122, 159-165.

Calabretta B, Sims RB, Valtieri M, Caracciolo D, Szczylik C, Venturelli D, Ratajczak M, Beran M, Gewirtz AM (1991) Normal and leukemic hematopoietic cells manifest differential sensitivity to inhibitory effects of c-myb antisense oligodeoxynucleotides: an in vitro study relevant to bone marrow purging, Proc. Natl. Acad. Sci. USA 88, 2351-2355.

Cao XM, Koski RA, Gashler A, McKiernan M, Morris CF, Gaffney R, Hay RV, Sukhatme VP (1990) Identification and characterization of the Egr-1 gene product, a DNA-binding zinc finger protein induced by differentiation and growth signals, Mol. Cell. Biol. 10, 1931-1939.

Chabot B, Steitz JA (1987) Recognition of mutant and cryptic 5' splice sites by the U1 small nuclear ribonucleoprotein in vitro, Mol. Cell. Biol. 7, 698-707.

Changeux JP (1991) Compartmentalized transcription of acetylcholine receptor genes during motor endplate epigenesis, New Biologist 3, 413-429.

Chatonnet A, Lockridge O (1989) Comparison of butyrylcholinesterase and acetylcholinesterase, Biochem. J. 260, 625-634.

Chiang MY, Chan H, Zounes MA, Freier SM, Lima WF, Bennett CF (1991) Antisense oligonucleotides inhibit intercellular adhesion molecule 1 expression by two distinct mechanisms, J. Biol. Chem. 266, 18162-18171.

Chou PY, Fasman GD (1978) Empirical predictions of protein conformation, Ann. Rev. Biochem. 47, 251-276.

Chretien S, Dubart A, Beaupain D, Raich N, Grandchamp B, Rosa J, Goossens M, Romeo PH (1988) Alternative transcription and splicing of the human porphobilinogen deaminase gene result either in tissue-specific or in housekeeping expression, Proc. Natl. Acad. Sci. USA 85, 6-10.

Coates PM, Simpson NE (1972) Genetic variation in human erythrocyte acetylcholinesterase, Science 175, 1466-1467.

Cohen SG, Lieberman DL, Hasan FB, Cohen JB (1982) 1-Bromopinacolone, an active site-directed covalent inhibitor for acetylcholinesterase, J. Biol. Chem. 257, 14087-14092.

Courtney MA, Stoler MH, Marder VJ, Haidaris PJ (1991) Developmental expression of mRNAs encoding platelet proteins in rat megakaryocytes, Blood 77, 560-568.

D'Eustachio P, Ruddle FH (1983) Somatic cell genetics and gene families, Science 220, 919-924.

de la Escalera S, Bockamp EO, Moya F, Piovant M, Jimenez F (1990) Characterization and gene cloning of neurotactin, a Drosophila transmembrane protein related to cholinesterases, EMBO J. 9, 3593-3601.

Deavan LL, Vandilla MA, Bartholdi MF, Carrano AV, Cram LS, Fuscoe JC, Gray JW, Hildebrand CE, Moyzis RK,Perlman J (1986) Construction of human chromosome-specific DNA libraries from flow-sorted chromosomes, Cold Spring Harb. Symp. Quant. Biol. 51, 159-167.

Deuchar EM (1966) Biochemical Aspects of Amphibian Development, Methuen, London.

Devereux J, Haeberli P, Smithies O (1984) A comprehensive set of sequence analysis programs for the VAX, Nucl. Acids. Res. 12, 387-395.

Doctor BP, Chapman TC, Christner CE, Deal CD, De La Hoz DM, Gentry MK, Ogert RA, Bush RS, Smyth KK, Wolfe AD (1991) Complete amino acid sequence of fetal bovine serum acetylcholinesterase and its comparison in various regions with other cholinesterases, FEBS Lett. 266, 123-127.

Drews U (1975) Cholinesterase in embryonic development, Prog. Histochem. Cytochem. 7, 1-52.

Dreyfus P, Zevin-Sonkin D, Seidman S, Prody C, Zisling R, Zakut H, Soreq H (1988) Cross homologies and structural differences between human cholinesterases revealed by antibodies against cDNA-produced human butyrylcholinesterase peptides. J. Neurochem. 51, 1858-1867.

Dreyfus PA, Pincon-Raymond M, Zakut H, Seidman S, Soreq H (1991) Search for the molecular origins of butyrylcholinesterase polymorphism by cDNA screening, deletion mutagenesis and *Xenopus* oocytes co-injections; in Cholinesterases: Structure Function, Mechanism, Genetics and Cell Biology, Massoulie J, Bacou F, Barnard E, Chatonnet A, Doctor BP, Quinn DM, eds., ACS Books, Washington, pp. 162-167.

Duval N, Massoulie J, Bon S (1992) H and T subunits of acetylcholinesterase from Torpedo, expressed in COS cells, generate all types of globular forms, J. Cell Biol. 118, 641-653.

Eckstein F. (1985) Nucleoside phosphorothioates, Ann. Rev. Biochem. 54, 367-402.

Edery H, Schatzberg-Porath G (1958) Pyridine-2-aldoxime methiodide and diacetyl-monoxime against organophosphorous poisoning, Science 128, 1137-1138.

Ehrlich G, Viegas-Pequignot E, Ginzberg D, Sindel L, Soreq H, Zakut H (1992) Mapping the human acetylcholinesterase gene to chromosome 7q22 by fluorescent *in situ* hybridization coupled with selective PCR amplification from a somatic hybrid cell panel and chromosome-sorted DNA libraries, Genomics 13, 1192-1197.

Eiberg H, Nielsen LS, Klausen J, Dahlen M, Kristensen M, Bisgaard ML, Moller N. Mohr J (1989) Linkage between serum cholinesterase 2, (CHE2) and gamma-crystallin gene cluster (CRYG): assignment to chromosome 2, Clin. Genet. 35, 313-321.

Ellman GL, Courtney KD, Andres V Jr, Featherstone RM (1961) A new and rapid colorimetric determination of acetylcholinesterase activity, Biochem. Pharmacol. 7, 88-95.

Ephrussi A, Church GM, Tonegawa S, Gilbert W (1985) B lineage-specific interactions of an immunoglobulin enhancer with cellular factors in vivo, Science 227, 134-140.

Etkin LD, Pearman B, Roberts M, Bektesh SL (1984) Replication, integration and expression of exogenous DNA injected into fertilized eggs of *Xenopus* laevis, Differentiation 26, 194-202.

Faisst S, Meyer S (1992) Compilation of vertebrate-encoded transcription factors, Nucl. Acids Res. 20, 3-26.

Ferguson MAJ, Williams AF (1988) Cell-surface anchoring of proteins via glycosyl-phosphatidylinositol structures, Ann. Rev. Biochem. 57, 285-320.

Fitzpatrick-McElligot S, Stent GS (1981) Appearance and localization of acetylcholinesterase in embryo of the leech Helodbella triserialis, J. Neurosci. 1, 901-907.

Fuentes ME, Taylor P (1993) Control of acetylcholinesterase gene expression during myogenesis, Neuron 10, 679-687.

Gennari K, Brodbeck U (1985) Molecular forms of acetylcholinesterase from human caudate nucleus: comparison of salt-soluble and detergent-soluble tetrameric enzyme species, J. Neurochem. 44, 697-704.

Gennari K, Brunner J, Brodbeck U (1987) Tetrameric detergent-soluble acetylcholinesterase from human caudate nucleus: subunit composition and number of active sites, J. Neurochem. 49, 12-18.

Ghosh MK, Cohen JS (1992) Oligodeoxynucleotides as antisense inhibitors of gene expression, Prog. Nucl. Acids Res. Mol. Biol., 42, 79-126.

Gibney G, Taylor P (1990) Biosynthesis of Torpedo acetylcholinesterase in mammalian cells. Functional expression and mutagenesis of the glycophospholipid-anchored form, J. Biol. Chem. 265, 12576-12583.

Gibney G, Camp S, Dionne M, MacPhee-Quigley K, Taylor P (1990) Mutagenesis of essential functional residues in acetylcholinesterase, Proc. Natl. Acad. Sci. 87, 7546-7550.

Giles CM, Metaxas-Buhler M, Romanski Y, Metaxas MN, Studies on the Yt blood group system, Vox Sang. 13, 171-180, 1967.

Gindi T, Knowland J (1979) The activity of cholinesterases during the development of *Xenopus* laevis, J. Embryol. Exp. Morph. 51, 209-215.

Gnagey AL, Forte M, Rosenberry TL (1987) Isolation and characterization of acetylcholinesterase from Drosophila, J. Biol. Chem. 262, 13290-13298.

Gnatt A (1990) PhD Thesis, Structure Function Relationships in Human Cholinesterase Genes and their Protein Products, Hebrew University of Jerusalem, Israel.

Gnatt A, Soreq H (1987) Molecular cloning of human cholinesterase genes: Potential applications in neurotoxicology; in Model Systems in Neurotoxicology: Alternative Approaches to Animal Testing, Shahar A, Goldberg AM, eds., Alan R. Liss, New York. pp 111-119.

Gnatt A, Prody CA, Zamir R, Lieman-Hurwitz J, Zakut H, Soreq H (1990) Expression of alternatively terminated unusual human butyrylcholinesterase messenger RNA transcripts, mapping to chromosome 3q26-ter, in nervous system tumors, Cancer Res. 50, 1983-1987.

Gnatt A, Ginzberg D, Lieman-Hurwitz J, Zakut H, Soreq H (1991) Human acetylcholinesterase and butyrylcholinesterase are encoded by two distinct genes, Cell. Mol. Neurobiol. 11, 91-104.

Gnatt A, Loewenstein Y, Yaron A, Schwarz M, Soreq H. (1994) Site-directed mutagenesis of active site residues reveals plasticity of human butyrylcholinesterase in substrate and inhibitor interactions, J. Neurochem. 62, (in press).

Hall LMC, Malcolm CA (1991) The acetylcholinesterase gene of Anoepheles stephensi, Cell. Molec. Neurobiol. 11, 131-141.

Handin RI (1991) in Harrison's Principles of Internal Medicine, 12th Ed., Wilson JD, Braunwald E, Isselbacher KJ, Petersdorph RG, Martin JB, Fauci AS, Root RK, eds., McGraw-Hill, New York, pp 348-353.

Hanneman EH (1992) Diisopropylfluorophosphate inhibits acetylcholinesterase activity and disrupts somitogenesis in the zebrafish, J. Exp. Zool. 263, 41-53.

Harel M, Sussman JL, Krejci E, Bon S, Chanal P, Massoulie J, Silman I (1992) Conversion of acetylcholinesterase to butyrylcholinesterase: modeling and mutagenesis, Proc. Natl. Acad. Sci. USA 89, 10827-10831.

Harris H, Whittaker M (1962) Differential inhibition of the serum cholinesterase phenotypes by solanine and solanidine, Ann. Hum. Genet., Lond. 26, 73-76.

Harvey RP, Melton DA (1988) Microinjection of synthetic Xhox-1A homeobox mRNA disrupts somite formation in developing *Xenopus* embryos, Cell 53, 687-697.

Hasan FB, Cohen SG, Cohen JB (1980) Hydrolysis by acetylcholinesterases: apparent molal volumes and trimethyl and methyl subsites, J. Biol. Chem. 255, 3898-3904.

Hasan FB, Elkind JL, Cohen SG, Cohen JB (1981) Cationic and uncharged substrates and reversable inhibitors in hydrolysis by acetylcholinesterase (EC 3.1.1.7), J. Biol. Chem. 256, 7781-7785.

Hausen P, Riebensell M (1991) The Early Development of Xenopus Laevis: an Atlas of the Histology, Springer-Verlag, Berlin.

Heikkila R, Schwab G, Wickstrom E, Loke SL, Pluznik DH, Watt R, Neckers LM (1987) A c-myc antisense oligodeoxynucleotide inhibits entry into S phase but not progress from G_0 to G_1, Nature 328, 445-449.

Heinemann S, Asouline G, Ballivet M, Boulter J, Connolly J, Deneris E, Evans K, Evans S, Forrest J, Gardner P, Goldman D, Kochhar A, Luyten W, Mason P, Treco D, Patrick J (1987) Molecular biology of the neural and muscle nicotinic acetylcholine receptors; in Molecular Neurobiology; Recombinant DNA Approaches, Heinemann S, Patrick J eds., Plenum Press, New York, pp.45-96.

Higuchi R (1990) Recombinant PCR; in PCR Protocols: A Guide to Methods and Applications, Innis MA, Gelfand DH, Sninsky JJ, White TJ, eds., Academic Press, San Diego, pp. 177-183.

Hodgkin WE, Giblett ER, Levine H, Bauer W, Motulsky AG (1965) Complete pseudocholinesterase deficiency: genetic and immunologic characterization, J. Clin. Invest. 44, 486-497.

Hoel PG (1976) Elementary Statistics, 4th edition, Wiley, New York.

Hoke GD, Draper K, Freier SM, Gonzalez C, Driver VB, Zounes MC, Ecker DJ (1991) Effects of phosphorothioate capping on antisense oligonucleotide stability, hybridization and antiviral efficacy versus herpes simplex virus infection, Nucl. Acids Res. 19, 5743-5748.

Holliday R (1989) Chromosome error propagation and cancer, Trends Genet. 5, 42-45.

Holmquist GP (1989) Evolution of chromosome bands: molecular ecology of noncoding DNA, J. Mol. Evol. 28, 469-486.

Holmquist G (1988) DNA sequences in G-bands and R-bands; in Chromosomes and Chromatin, Vol. II, Adolph KW, ed., CRC Press, Boca Raton, pp. 75-121.

Hopwood ND, Pluck A, Gurdon JB, Dilworth SM (1992) Expression of XMyoD protein in early *Xenopus* laevis embryos, Development 114, 31-38.

Hunter DD, Cashman N, Morris-Valero R, Bulock JW, Adams SP, Sanes JR (1991) An LRE (leucine-arginine-glutamate)-dependent mechanism for adhesion of neurons to S-laminin, J. Neurosci. 11, 3960-3971.

Iannuzzi MC, Dean M, Drumm ML, Hidaka N, Cole JL, Perry A, Stewart C, Gerrard B, Collins FS (1989) Isolation of additional polymorphic clones from the cystic fibrosis region, using chromosome jumping from D7S8, Am. J. Hum. Genet. 44, 695-703

Inestrosa NC, Roberts WL, Marshall TL, Rosenberry TL (1987) Acetylcholinesterase from bovine caudate nucleus is attached to membranes by a novel subunit distinct from those of acetylcholinesterases in other tissues, J. Biol. Chem. 262, 4441- 4444.

Jennekens FGI, Hesselmans LFGM, Veldman H, Jansen ENH, Spaans F, Molenaar PC (1992) Deficiency of acetlycholine receptors in a case of end-plate acetylcholinesterase deficiency: a histochemical investigation, Muscle Nerve 15, 63-72.

Kalow W, Genest K (1957) A method for the detection of atypical forms of human serum cholinesterase. Determination of dibucaine numbers, Can. J. Biochem. Physiol. 35, 339-346.

Karlog O, Hopfnerp-Peterson, HEH (1963) The influence of oximes on the acetylthiocholine hydrolysis rate, Biochem. Pharmacol. 12, 590-591.

Karnovsky MJ (1964) The localization of cholinesterase activity in rat cardiac muscle by electron microscopy, J. Cell Biol. 23, 217-232.

Karnovsky MJ, Roots L (1964) A "direct coloring" thiocholine method for cholinesterases, J. Histochem. Cytochem. 12, 219-221.

Karpel R, Ben Aziz-Aloya R, Sternfeld M, Ehrlich G, Ginzberg D, Tarroni P, Clementi F, Zakut H, Soreq H (1994) Expression of three alternative acetylcholinesterase messenger RNAs in human tumor cell lines of different tissue origins, Exp. Cell Res. 210 (in press).

Keeler RF, Brown D, Douglas DR, Stallknecht GF, Young S (1976) Teratogenicity of the solanum alkaloid solasodine and of "Kennebec" potato sprouts in hamsters, Bull. Environ. Contamtam. Toxicol. 15, 522-524.

Kerem A, Kronman C, Bar-Nun S, Shafferman A, Velan B (1993) Interrelations between assembly and secretion of recombinant human acetylcholinesterase, J. Biol. Chem. 268, 180-184.

Kessler M, Ben-Asher E, Aloni Y (1989) Elements modulating the block of transcription elongation at the adenovirus 2 attenuation site, J. Biol. Chem. 264, 9785-9790.

Kilpatrick DL, Zinn SA, Fitzgerald M, Higuchi H, Sabol SL, Meyerhardt J (1990) Transcription of the rat and mouse proenkephalin genes is initiated at distinct sites in spermatogenic and somatic cells, Mol. Cell. Biol. 10, 3717-3726.

Koelle GB, Freidenwald JS (1949) A histochemical method for localizing cholinesterase activity, Proc. Soc. Exp. Biol. Med. 70, 617-622.

Kole R, Shukla RR, Akhtar S (1991) Pre-messenger-RNA splicing as a target for antisense oligonucleotides, Adv. Drug Deliv. Rev. 6, 271-286.

Kothary R, Barton SC, Franz T, Norris ML, Hettle S, Surani MA (1991) Unusual cell specific expression of a major human cytomegalovirus immediate early gene promoter-lacZ hybrid gene in tansgenic mouse embryos, Mech. Dev. 35, 25-31.

Koury MJ (1992) Programmed cell death (apoptosis) in hematopoiesis, Exp. Hematol. 20, 391-394.

Koury MJ, Bondurant MC (1990) Erythropoietin retards DNA breakdown and prevents programmed death in erythroid progenitor cells, Science 248, 378-381.

Kozak M (1986) Bifunctional messenger RNAs in eukaryotes, Cell 47, 481-483.

Kragh-Hansen U, Brennan SO, Galliano M, Sugita O (1990) Binding of warfarin, salicylate and diazepam to genetic variants of human serum albumin with known mutations, Mol. Pharmacol. 37, 238-242.

Krainer AR, Maniatis T (1988) RNA splicing; in Transcription and Splicing, Hames BD, Glover DM, eds., IRL Press, Oxford, pp. 132-206.

Krejci E, Coussen F, Duval N, Chatel J-M, Legay C, Puype M, Vandekerckhove J, Cartaud J, Bon S, Massoulie J (1991a) Primary structure of a collagenic tail peptide of Torpedo acetylcholinesterase: co-expression with catalytic subunit induces the production of collagen-tailed forms in transfected cells, EMBO J. 10, 1285-1293.

Krejci E, Duval N, Chatonnet A, Vincens P, Massoulie J (1991b) Cholinesterase-like domains in enzymes and structural proteins: Functional and evolutionary relationships and identification of a catalytically essential aspartic acid, Proc. Natl. Acad. Sci. USA 88, 6647-6651.

Krieg PA, Melton DA (1984) Functional messenger RNAs are produced by SP6 in vitro transcription of cloned cDNAs, Nucl. Acids Res. 12, 7057-7070.

Kronman C, Velan B, Gozes Y, Leitner M, Flashner Y, Lazar A, Marcus D, Sery T, Papier A, Grosfeld H, Cohen S, Shafferman A (1992) Production and secretion of high levels of recombinant human acetylcholinesterase in cultured cell lines: microheterogeneity of the catalytic subunit, Gene 121, 295-304.

Kullberg RW, Lentz TL, Cohen MW (1977) Development of the myotomal neuromuscular junction in *Xenopus* laevis: an electrophysiological and fine-structural study, Dev. Biol. 60, 101-129.

Kunkel TA, Roberts JD, Zakour RA (1987) Rapid and efficient site-specific mutagenesis without phenotypic selection, Methods Enzymol. 154, 367-382.

La Du BN (1989) Identification of human serum cholinesterase variants using the polymerase chain reaction amplification technique, Trends Pharmacol. Sci. 10, 309-313.

Landaw SA (1986) Acute leukemia in polycythemia vera, Semin. Hematol. 23, 156-165.

Lang KM, Spritz RA (1985) Cloning specific complete polyadenylated 3'-terminal cDNA segments, Gene 33, 191-196.

Lapidot-Lifson Y, Prody CA, Ginzberg D, Meytes D, Zakut H, Soreq H (1989) Coamplification of human acetylcholinesterase and butyrylcholinesterase genes in blood cells: Correlation with various leukemias and abnormal megakaryocytopoiesis, Proc. Natl. Acad. Sci. USA 86, 4715-4719.

Lapidot-Lifson Y, Patinkin D, Prody CA, Ehrlich G, Seidman S, Ben-Aziz R, Benseler F, Eckstein F, Zakut H, Soreq H. (1992) Cloning and antisense oligodeoxynucleotide inhibition of a human homolog of cdc2 required in hematopoiesis, Proc. Natl. Acad. Sci. USA 89, 579-583.

Laskey RA, Fairman MP, Blow JJ (1989) S phase of the cell cycle, Science 246, 609-614.

Layer PG (1991) Cholinesterases during development of the avian nervous system, Cell. Mol. Neurobiol. 11, 7-33.

Layer PG, Sporns O (1987) Spatiotemporal relationship of embryonic cholinesterases with cell proliferation in chicken brain and eye, Proc. Natl. Acad. Sci. 84, 284-288.

Layer PG, Alber R, Rathjen FG (1988) Sequential activation of butyrylcholinesterase in rostral half somites and acetylcholinesterase in motoneurons and myotomes preceding growth of motor axons, Development 102, 387-396.

Legay C, Bon S, Massoulie J (1993a) Expression of a cDNA encoding the glycolipid-anchored form of rat acetylcholinesterase, FEBS Lett. 315, 163-166.

Legay C, Bon S, Vernier P, Coussen F, Massoulie J (1993b). Cloning and expression of a rat acetylcholinesterase subunit: generation of multiple molecular forms and complementarity with a Torpedo collagenic subunit, Neurochem, 60, 337-346.

Lemaigre FP, Lafontaine DA, Courtois SJ, Durviaux SM, Rousseau GG (1990) Sp1 can displace GHF-1 from its distal binding site and stimulate transcription from the growth hormone gene promoter, Mol. Cell. Biol. 10, 1811-1814.

Lev-Lehman E, Ginzberg D, Hornreich G, Ehrlich G, Meshorer A, Eckstein F, Soreq H, Zakut H (1993) Antisense inhibition of acetylcholinesterase gene expression causes transient hematopoietic alteration *in vivo*, Gene Therapy 1,1-11.

Levene C, Steinberg AG, Friedlander Y, Brautbar C, Cohen T (1984) Genetic polymorphisms among Bukharan and Georgian Jews in Israel Am. J. Med. Genet. 19, 623-641

Levene C, Bar-Shany S, Manny N, Moulds JJ, Cohen T (1987) The Yt blood groups in Israeli Jews, Arabs, and Druse, Transfusion 27, 471-474

Li Y, Camp S, Rachinsky TL, Getman D, Taylor P (1991) Gene structure of mammalian acetylcholinesterase. Alternative exons dictate tissue-specific expression, J. Biol. Chem. 266, 23083-23090.

Li Y, Camp S, Rachinsky TL, Bongiorno C, Taylor P (1993a) Promotor elements and transcriptional control of the mouse acetylcholinesterase gene, J. Biol. Chem. 268, 3563-3572.

Li Y, Camp S, Taylor P (1993b) Tissue-specific expression and alternative mRNA processing of the mammalian acetylcholinesterase gene, J. Biol. Chem. 268, 5790-5797.

Liao J, Heider H, Sun MC, Brodbeck U (1992) Different glycosylation in acetylcholinesterases from mammalian brain and erythrocytes, J. Neurochem. 58, 1230-1238.

Libermann TA, Razon N, Bartal AD, Yarden Y, Schlessinger J, Soreq H (1984) Expression of epidermal growth factor receptors in human brain tumors, Cancer Res. 44, 753-760.

Lockridge O (1984) Amino acid composition and sequence of human serum cholinesterase: a progress report; in Cholinesterases Fundamental and Applied Aspects, Brzin M, Barnard EA, Sket D, eds., Walter de Gruyter, Berlin, pp. 5-11.

Lockridge O, La Du BN (1978) Comparison of atypical and usual human serum cholinesterase: purification, number of active sites, substrate affinity, and turnover number, J. Biol. Chem. 253, 361-366.

Lockridge O, Bartels CF, Vaughan TA, Wong CK, Norton SE, Johnson LL (1987) Complete amino acid sequence of human serum cholinesterase, J. Biol. Chem. 262, 549-557.

Lockridge O, Bartels CF, Zelinski T, Jbilo O, Kris M (1992) Genetic variant of human acetylcholinesterase, in Multidisciplinary Approaches to Cholinesterase Functions, Shafferman A, Velan B, eds., Plenum Press, New York, pp. 53-59.

Loke SL, Stein CA, Zhang XH, Mori K, Nakanishi M, Subasinghe C, Cohen JS, Neckers LM (1989) Characterization of oligonucleotide transport into living cells, Proc. Natl. Acad. Sci. USA 86, 3474-3478.

Lovrien EW, Magenis RE, Rivas ML, Lamvik N, Rowe S, Wood J, Hemmerling J (1978) Serum cholinesterase (E_2) linkage analysis: possible evidence for localization to chromosome 16, Cytogenet. Cell Genet. 22, 324-326.

Low MG (1987) Biochemistry of the glycosyl-phosphatidylinositol membrane protein anchors, Biochem. J. 244, 1-13.

Lu B, Greengard P, Poo M (1992) Exogenous synapsin I promotes functional maturation of developing neuromuscular synapses, Neuron 8, 521-529.

MacPhee-Quigley K, Vedvick TS, Taylor P, Taylor SS (1986) Profile of the disulfide bonds in acetylcholinesterase, J. Biol. Chem. 261, 13565-13570.

Maekawa T, Sakura H, Kanei-Ishii C, Sudo T, Yoshimura T, Fujisawa J, Yoshida M, Ishii S (1989) Leucine zipper structure of the protein CRE-BP1 binding to the cyclic AMP response element in brain, EMBO J. 8, 2023-2028.

Majumdar R, Balasubramanian AS (1984) Chemical modification of acetyl cholinesterase from eel and basal ganglia: effect on the acetylcholinesterases and arylamidase activities, Biochemistry, 23, 4088-4093.

Malinger G, Zakut H, Soreq H (1989) Cholinoceptive properties of human primordial, preantral, and antral oocytes: *in situ* hybridization and biochemical evidence for expression of cholinesterase genes, J. Mol. Neurosci. 1, 77-84.

Maniatis T (1991) Mechanisms of alternative pre-mRNA splicing, Science 251, 33-34.

Martin DIK, Zon LI, Mutter G, Orkin SH (1990) Expression of an erythroid transcription factor in megakaryocytic and mast cell lineages, Nature 344, 444-447.

Massoulie J, Toutant JP (1988) Cholinesterases, Structure and types of Interaction; in The Cholinergic Synapse, Whittaker VP, ed. (Handbook of Experimental Pharmacology Vol. 86), Springer-Verlag, Berlin, pp. 167-224.

Massoulie J, Pezzementi L, Bon S, Krejci E, Vallette FM (1993) Molecular and cellular biology of cholinesterases, Prog. Neurobiol. 41, 31-91.

Matsukura M, Shinozuka K, Zon G, Mitsuya H, Reitz M, Cohen JS, Broder S (1987) Phosphorothioate analogs of oligodeoxynucleotides: inhibitors of replication and cytopathic effects of human immunodeficiency virus, Proc. Natl. Acad. Sci. USA 84, 7706-7710.

Maulet Y, Camp S, Gibney G, Rachinsky TL, Ekstrom TJ, Taylor P (1990) A single gene encodes glycolipid-anchored and asymmetric acetylcholinesterase forms: alternative coding exons contain inverted repeat sequences, Neuron 4, 289-301.

Mazur EM (1987) Megakaryocytopoiesis and platelet production: a review, Exp. Hematol. 15, 340-350.

McGuire MC, Nogueira CP, Bartels CF, Lightstone H, Hajra A, Van der Spek AFL, Lockridge O, La Du BN (1989) Identification of the structural mutation responsible for the dibucaine-resistant (atypical) variant form of human serum cholinesterase, Proc. Natl. Acad. Sci. USA 86, 953-957.

McMahon AP, Moon RT (1989) Ectopic expression of the proto-oncogene int-1 in *Xenopus* embryos leads to duplication of the embryonic axis, Cell 58, 1075-1084.

McTiernan C, Adkins S, Chatonnet A, Vaughan TA, Bartels CF, Kott M, Rosenberry TL, La Du BN, Lockridge O (1986) Brain cDNA clone for human cholinesterase, Proc. Natl. Acad. Sci. USA 84, 6682-6686.

Meneely GA, Wyttenbach CR (1989) Effects of the organophosphate insecticides diazinon and parathion on bobwhite quail embryos: skeletal defects and acetylcholinesterase activity, J. Exp. Zool. 252, 60-70.

Metcalf D (1992) Hemopoietic regulators, Trends Biochem. Sci. 17, 286-289.

Mitchell PJ, Timmons PM, Hebert JM, Rigby PW, Tjian R (1991) Transcription factor AP-2 is expressed in neural crest cell lineages during mouse embryogenesis, Gene Dev. 5, 105-119.

Mitchell, RL, Henning-Chubb C, Huberman E, Verma IM (1986) c-fos expresson is neither sufficient nor obligatory for differentiation of monomyelocytes to macrophages, Cell 45, 497-504.

Mitelman F (1988) Cataloge of Chromosone Abberations in Cancer, 3rd Ed., Alan R. Liss, New York.

Molitor JA, Walker WH, Doerre S, Ballard DW, Greene WC (1990) NF-kappa B: a family of inducible and differentialy expressed enhancer-binding proteins in human T cells, Proc. Natl. Acad. Sci. USA 87, 10028-10032.

Moran P, Caras IW (1991) Fusion of sequence elements from non-anchored proteins to generate a fully functional signal for glycophosphatidylinositol membrane anchor attachment, J. Cell Biol. 115, 1595-1600.

Moreno S, Nurse P (1990) Substrates for p34cdc2: in vivo veritas? Cell 61, 549-551.

Navaratnam DS, Priddle JD, McDonald B, Esiri MM, Robinson JR, Smith AD (1991) Anomalous molecular form of acetylcholinesterase in cerebrospinal fluid in histologically diagnosed Alzheimer's disease, Lancet 337, 447-450.

Naveh M, Bernstein Z, Segal D, Shalitin Y (1981) New substrates of acetylcholinesterases, FEBS Letts. 134, 53-56.

Neville LF, Gnatt A, Loewenstein Y, Soreq H (1990a) Aspartate-70 to glycine substitution confers resistance to naturally occurring and synthetic anionic-site ligands on in-ovo produced human butyrylcholinesterase, J. Neurosci. Res. 27, 452-460.

Neville LF, Gnatt A, Padan R, Seidman S, Soreq H (1990b) Anionic site interactions in human butyrylcholinesterase disrupted by two single point mutations, J. Biol. Chem. 265, 20735-20738.

Neville LF, Gnatt A, Loewenstein Y, Seidman S, Ehrlich G, Soreq H (1992) Intramolecular relationships in cholinesterases revealed by oocyte expression of site-directed and natural variants of human BCHE, EMBO J. 11, 1641-1649.

Niehrs C, De Robertis EM (1991) Ectopic expression of a homeobox gene changes cell fate in *Xenopus* embryos in a position-specific manner, EMBO J. 10, 3621-3629.

Nolte H-J, Rosenberry TL, Neumann E (1980) Effective changes in acetylcholinesterase active sites determined from the ionic strength dependence of association rate constants with cationic ligands, Biochemistry 19, 3705-3711.

Olsson OAT, Svensson LA (1984) New lipophilic terbutaline ester prodrugs with long effect duration. Pharm. Res. 1, 19-23.

Oron Y, Dascal N, Nadler E, Lupu M (1985) Inositol 1,4,5-trisphosphate mimics muscarinic response in *Xenopus* oocytes, Nature 313, 141-143.

Page JD, Wilson IB (1985) Acetylcholinesterase: inhibition by tetranitromethane and arsenite: binding of arsenite by tyrosine residues, J. Biol. Chem. 260, 1475-1478.

Paoletti F, Mocali A, Vannucchi AM (1992) Acetylcholinesterase in murine erythroleukemia (Friend) cells : evidence for megakaryocyte-like expression and potential growth-regulatory role of enzyme activity, Blood 79, 2873-2879.

Patinkin D, Seidman S, Eckstein F, Benseler F, Zakut H, Soreq (1990) H. Manipulations of cholinesterase gene expression modulate murine megakaryocytopoiesis in vitro, Mol. Cell. Biol. 10, 6046-6050.

Pedersen B (1990) Thrombopoiesis and structural rearrangements of the long arm of chromosome 3. Review and analysis of data on 64 published patients, Leukem. Lymph. 2, 93-102.

Piela L, Nemethy G, Scheraga HA (1987) Proline-induced constraints in α-helices, Biopolymers 26, 1587-1600.

Pintado T, Ferro MT, Roman CS, Mayayo M, Larana JG (1985) Clinical correlations of the 3q21q26 cytogenetic anomaly. A leukemic or myelodysplastic syndrome with preserved or increased platelet production and lack of response to cytotoxic drug therapy, Cancer 55, 535-541.

Poustka A, Rackwitz H-R, Frischauf A-M, Hohn B, Lehrach H (1984) Selective isolation of cosmid clones by homologous recombination in Escherichia coli, Proc. Natl. Acad. Sci. 81, 4129-4133.

Prody CA, Merlie JP (1991) A developmental and tissue-specific enhancer in the mouse skeletal muscle acetylcholine receptor alfa-subunit gene regulated by myogenic factors, J. Biol. Chem. 266, 22588-22596.

Prody C, Zevin-Sonkin D, Gnatt A, Koch R, Zisling R, Goldberg O, Soreq H (1986) Use of synthetic oligodeoxynucleotide probes for the isolation of a human cholinesterase cDNA clone, J. Neurosci. Res. 16, 25-35.

Prody CA, Zevin-Sonkin D, Gnatt A, Goldberg O, Soreq H (1987) Isolation and characterization of full length clones coding for human cholinesterase from fetal human tissues, Proc. Natl. Acad Sci. USA 84, 3555-3559.

Prody CA, Dreyfus PA, Zamir R, Zakut H, Soreq H (1989) De novo amplification within a "silent" human cholinesterase gene in a family subjected to prolonged exposure to organophosphorous insecticides, Proc. Natl. Acad. Sci. USA 86, 690-694.

Quinn DM (1987) Acetylcholinesterase: enzyme structure, reaction dynamics, and virtual transition states, Chem. Rev. 87, 955-979.

Rakonczay Z, Brimijoin S (1988) Biochemistry and pathophysiology of the molecular forms of cholinesterases; in Subcellular Biochemistry, Vol. 12, Harris JR, ed., Plenum Press, New York, pp. 335-377.

Rama Sastry BV, Sadavongvivad C (1979) Cholinergic systems in non-nervous tissues, Pharmacol. Rev. 30, 65-132.

Rangini Z, Ben-Yehuda A, Shapira E, Gruenbaum Y, Fainsod A, (1991) CHox E, a chicken homeogene of the H2.0 type exhibits dorsal-ventral restriction in proliferating region of the spinal cord, Mech. Dev. 35, 13-24.

Ratajczak MZ, Kant JA, Luger SM, Hijiya N, Zhang J, Zon G, Gewirtz AM (1992) In vivo treatment of human leukemia in a scid mouse model with c-myb antisense oligodeoxynucleotides, Proc. Natl. Acad. Sci. USA 89, 11823-11827.

Razin A, Riggs AD (1980) DNA methylation and gene function, Science 210, 604-610.

Razon N, Soreq H, Roth E, Bartal A, Silman I (1984) Characterization of activities and forms of cholinesterases in human primary brain tumors, Exp. Neurol. 84, 681-695.

Reed JC, Stein C, Subasinghe C, Haldar S, Croce CM, Yum S, Cohen J (1990) Antisense-mediated inhibition of BCL2 protooncogene expression and leukemic cell growth and survival: comparisons of phosphodiester and phosphorothioate oligodeoxynucleotides, Cancer Res. 50, 6565-6570.

Rentrop M, Knapp B, Winter H, Schweizer J (1986) Aminoalkylsilane-treated glass slides as support for in situ hybridization of keratin cDNAs to frozen tissue sections under varying fixation and pretreatment conditions, Histochem. J. 18, 271-276.

Roberts WL, Doctor BP, Foster JD, Rosenberry TL (1991) Bovine brain acetylcholinesterase primary sequence involved in intersubunit disulfide linkages, J. Biol. Chem. 266, 7481-7487.

Roddick JG (1989) The acetylcholinesterase-inhibitory activity of steroidal glycoalkaloids and their aglycones, Phytochem. 28, 2631-2634.

Romeo PH, Prandini MH, Joulin V, Mignotte V, Prenant M, Vainchenker W, Marguerie G, Uzan G (1990) Megakaryocytic and erythrocytic lineages share specific transcription factors, Nature 344, 447-449.

Rosenberry TL (1975) Acetylcholinesterase, Adv. Enzymol. 43, 103-218.

Rotundo RL (1984) Purification and properties of the membrane-bound form of acetylcholinesterase from chicken brain: evidence for two distinct polypeptide chains, J. Biol. Chem. 259, 13186-13194.

Rotundo RL, Gomez AM (1990) Nucleus-specific translation and assembly of acetylcholinesterase in multinucleated muscle cells, J. Cell Biol. 110, 715-719.

Rotundo RL, Jasmin BJ, Lee RK, Rossi SG (1992) Compartmentalization of acetylcholinesterase mRNA and protein expression in skeletal muscle in vitro and in vivo: implications for regulation at the neuromuscular junction; in: Multidisciplinary Approaches to Cholinesterase Functions, Shafferman A, Velan B, eds., Plenum Press, New York, pp. 217-222.

Ruiz i Altaba A, Melton DA (1989) Involvement of the *Xenopus* homeobox gene Xhox3 in pattern formation along the anterior-posterior axis, Cell 57, 317-326.

Russell AJ, Fersht AR (1987) Rational modification of enzyme catalysis by engineering surface charge, Nature, 328, 496-500.

Russell AJ, Thomas PG, Fersht AR (1987) Electrostatic effects on modification of charged groups in the active site cleft of subtilisin by protein engineering, J. Mol. Biol. 193, 803-813.

Rychlik W, Rhoads RE (1989) A computer program for choosing optimal oligonucleotides for filter hybridization, sequencing and in vitro amplification of DNA, Nucl. Acids Res. 17, 8543-8551.

Sali D, Bycroft M, Fersht AR (1988) Stabilization of protein structure by interaction of alpha-helix dipole with a charged side chain, Nature, 335, 740-743.

Sambrook J, Fritsch EF, Maniatis T (1989) Molecular cloning: A Laboratory Manual, 2nd ed. Cold Spring Harbor Laboratory Press, Cold Spring Harbor.

Schimke RT (1990) The search for early genetic events in tumorigenesis: an amplification paradigm, Cancer Cells 2, 149-151.

Schmidt EV, Christoph G, Zeller R, Leder P (1990) The cytomegalovirus enhancer: a pan-active control element in transgenic mice, Mol. Cell. Biol. 10, 4406-4411.

Schrag JD, Li, YG, Wu S, Cygler M (1991) Ser-His-Glu triad forms the catalytic site of the lipase from Geotrichum candidum, Nature, 351, 761-764.

Schumacher M, Camp S, Maulet Y, Newton M, MacPhee-Quigley K, Taylor SS, Freidmann T, Taylor P (1986) Primary structure of Torpedo californica acetylcholinesterase deduced from its cDNA sequence, Nature 319, 407-409.

Schwab M, Amler LC (1990) Amplification of cellular oncogenes: a predictor of clinical outcome in human cancer, Genes Chromosom. Cancer 1, 181-193.

Seidman S, Ben Aziz-Aloya R, Timberg R, Loewenstein Y, Velan B, Shafferman A, Liao J, Norgaard-Pedersen B, Brodbeck U, Soreq H (1994) Overexpressed monomeric human acetylcholinesterase induces subtle ultrastructural modifications in developing neuromuscular junctions of *Xenopus* laevis embryos, J. Neurochem., 62 (in press).

Seki T, Spurr N, Obata F, Goyert S, Goodfellow P, Silver J (1985) The human Thy-1 gene: structure and chromosomal location, Proc. Natl. Acad. Sci. USA 82, 6657-6661.

Shaw JP, Kent K, Bird J, Fishback J, Froehler B (1991) Modified deoxyoligonucleotides stable to exonuclease degradation in serum, Nucl. Acids Res. 19, 747-750.

Shaw G, Kamen R (1986) A conserved AU sequence from the 3' untranslated region of GM-CSF mRNA mediates selective mRNA degradation, Cell 46, 659-667.

Shinitzky M, Dudai Y, Silman I (1973) Spectral evidence for the presence of tryptophan in the binding site of acetylcholinesterase, FEBS Letts. 30, 125-128.

Sikorav JL, Duval N, Anselmet A, Bon S, Krejci E, Legay C, Osterlund M, Reimund B, Massoulie J (1988) Complex alternative splicing of acetylcholinesterase transcripts in Torpedo electric organ; primary structure of the precursor of the glycolipid-anchored dimeric form, EMBO J. 7, 2983-2993.

Silman I, Futerman AH (1987) Modes of attachment of acetylcholinesterase to the surface membrane, Eur. J. Biochem. 170, 11-22.

Silver A (1974) The Biology of Cholinesterases, North Holland, Amsterdam.

Slamon DJ, deKernion JB, Verma IM, Cline MJ (1984) Expression of cellular oncogenes in human malignancies, Science 224, 256-262.

Smit LME, Hageman G, Veldman H, Molenaar PC, Oen BS, Jennekens FGI (1988) A myasthenic syndrome with congenital paucity of secondary clefts: CPSC syndrome, Muscle Nerve 11, 337-348.

Smith CWJ, Patton JG, Nadal-Ginard B (1989) Alternative splicing in the control of gene expression, Ann. Rev. Genet. 23, 527-77.

Sokol S, Christian JL, Moon RT, Melton DA (1991) Injected Wnt RNA induces a complete body axis in *Xenopus* embryos, Cell 67, 741-752.

Soreq H, Gnatt A (1987) Molecular biological search for human genes encoding cholinesterases, Molec. Neurobiol. 1, 47-80.

Soreq H, Prody CA (1989) Sequence similarities between human acetylcholinesterase and related proteins: putative implications for therapy of anticholinesterase intoxication. In: Computer-Assisted Modeling of Receptor-Ligand Interactions: Theoretical Aspects and Applications to Drug Design, Golombeck A, Rein R, eds., Alan R Liss, New York, pp. 347-359.

Soreq H, Seidman S (1992) *Xenopus* oocyte microinjection: From gene to protein, Methods Enzymol. 207, 225-265.

Soreq H, Zakut H (1990a) Cholinesterase Genes: Multilevelled Regulation, Karger, Basel.

Soreq H, Zakut H (1990b) Amplification of butyrylcholinesterase and acetylcholinesterase genes in normal and tumor tissues: putative relationship to organophosphorous poisoning, Pharm. Res. 7, 1-7.

Soreq H, Zakut H. (1993) Human Cholinesterases and Anticholinesterases, Academic Press, San Diego.

Soreq H, Zevin-Sonkin D, Razon N (1984) Expression of cholinesterase gene(s) in human brain tissue: translational evidence for multiple mRNA species, EMBO J. 3, 1371-1375.

Soreq H, Malinger G, Zakut H (1987a) Expression of cholinesterase genes in human oocytes revealed by in-situ hybridization, Hum. Reprod. 2, 689-693.

Soreq H, Zamir R, Zevin-Sonkin D, Zakut H (1987b) Human cholinesterase genes localized by hybridization to chromosomes 3 and 16, Hum. Genet. 77, 325-328.

Soreq H, Seidman S, Dreyfus PA, Zevin-Sonkin D, Zakut H (1989) Expression and tissue-specific assembly of human butyrylcholine esterase in microinjected *Xenopus* laevis oocytes, J. Biol. Chem. 264, 10608-10613.

Soreq H, Ben-Aziz R, Prody CA, Seidman S, Gnatt A, Neville L, Lieman-Hurwitz J, Lev-Lehman E, Ginsberg D, Lapidot-Lifson Y, Zakut H (1990) Molecular cloning and construction of the coding region for human acetylcholinesterase reveals a G+C-rich attenuating structure, Proc. Natl. Acad. Sci. USA, 87, 9688-9692.

Soreq H, Lapidot-Lifson Y, Zakut H (1991a) A role for cholinesterase in tumorigenesis? Cancer Cells 3, 511-516.

Soreq H, Neville L, Gnatt A, Ben-Aziz R, Lapidot-Lifson Y, Ehrlich G, Seidman S, Lev-Lehman E, Beeri R, Ginzberg D, Zakut H (1991b) Structure-function relationships, in vivo mutageneity and gene amplification in human cholinesterases, targets for organophosphorous poisons; in Biotechnology: Binding Research and Applications, Kamely D, Chakrabarty AM, Kornguth SE, eds., Kluwer Academic Publishers, Boston.

Soreq H, Gnatt A, Loewenstein Y, Neville LF (1992) Excavations into the active-site gorge of cholinesterases, Trends Biochem. Sci. 17, 353-358.

Soreq H, Ehrlich G, Schwarz M, Loewenstein Y, Zakut H (1994) Mutations and impaired expression in the human ACHE and BCHE genes: neurological implications; in Neurological Implications of Human Genetics, Felous M, ed., Karger, Basel (in press)

Sparkes RS, Field LL, Sparkes MC, Crist M, Spence MA, James K, Garry PJ (1984) Genetic linkage studies of transferrin, pseudocholinesterase, and chromosome 1 loci, Hum. Hered. 34, 96-100.

Spitzer F, Eckstein F (1988) Inhibition of deoxyribonucleases by phosphorothioate groups in oligodeoxyribonucleotides, Nucl. Acids Res. 111691-11704.

Spralding A (1987) Gene amplification in Dipteran chromosomes; in Results and Problems in Cell Differentiation, Vol. 14 Structure and Function of Eukaryotic Chromosomes, Hennig W, Sheer U, eds., Springer-Verlag, Berlin, pp. 199-212.

Spring FA, Gardner B, Anstee DJ (1992) Evidence that the antigens of the Yt blood group system are located on human erythrocyte acetylcholinesterase, Blood 80, 2136-2141.

Sussman JL, Harel M, Silman I (1992) Three-dimensional structure of acetylcholinesterase; in Multidisciplinary Approaches to Cholinesterase Functions, Shafferman A, Velan B, eds., Plenum Press, New York, pp. 95-107.

Sussman JL, Harel M, Frolow F, Oefner C, Goldman A, Toker L, Silman I (1991) Atomic structure of acetylcholinesterase from *Torpedo californica*: A prototypic acetylcholine-binding protein, Science 253, 872-879.

Szczylik C, Skorski T, Nicolaides NC, Manzella L, Malaguarnera L, Vanturelli D, Gewirtz AM, Calabretta B (1991) Selective inhibition of leukemia cell proliferation by BCR-ABL antisense oligodeoxynucleotides, Science 253, 562-565.

Szeinberg A, Pipano S, Assa M, Medalie JH, Neufeld HN (1972) High frequency of atypical pseudocholinesterase gene among Iraqi and Iranian Jews, Clin. Genet. 3, 123-127.

Tapscott SJ, Davis RL, Thayer MJ, Cheng PF, Weintraub H, Lassar AB (1988) MyoD1 a nuclear phosphoprotein requiring a Myc homology region to convert fibroblasts to myoblasts, Science 242, 405-411.

Taylor P (1990a) Cholinergic agonists; in The Pharmacological Basis of Therapeutics, Gilman AG, Goodman LS, Rall TW, Nies AS, Taylor P, eds., Pergamon Press, New York pp. 122-149.

Taylor P (1990b) Cholinergic antagonists; in The Pharmacological Basis of Therapeutics, Gilman AG, Rall TW, Nies AS and Palmer T, eds., 8th ed., Pergamon Press, New York, pp. 131-149.

Taylor P (1991) The cholinesterases, J. Biol. Chem. 266:4025-4028

Taylor P, Schumacher M, MacPhee-Quigley K, Friedmann T, Taylor S (1987) The structure of acetylcholinesterase: relationship to its function and cellular disposition, Trends Neurol. Sci. 10, 93-95.

Toutant JP, Massoulie J, Bon S (1985) Polymorphism of pseudocholinesterase in Torpedo marmorata tissues: comparative study of the catalytic and molecular properties of this enzyme with acetylcholinesterase, J. Neurochem. 44, 580-92.

Toutant JP, Richards MK, Krall JA, Rosenberry TL (1990) Molecular forms of acetylcholinesterase in two sublines of human erythroleukemia K562 cells. Sensitivity or resistance to phosphatidylinositol-specific phospholipase C and biosynthesis, Eur. Biochem. 187, 31-38.

Tycko B, Sklar J (1990) Chromosomal translocations in lymphoid neoplasia: a reappraisal of the recombinase model, Cancer Cells 2, 1-8.

Valentino RJ, Lockridge O, Eckerson HW, La Du BN (1981) Prediction of drug sensitivity in individuals with atypical serum cholinesterase based on in vitro biochemical studies, Biochem. Pharmacol. 30, 1643-1649.

Velan B, Grosfeld H, Kronman C, Leitner, M, Gozes Y, Lazar A, Flashner Y, Marcus D, Cohen S, Shafferman A (1991a) The effect of elimination of intersubunit disulfide bonds on the activity, assembly, and secretion of recombinant human acetylcholinesterase, J. Biol. Chem. 266, 23977-23984.

Velan B, Kronman C, Grosfeld H, Leitner M, Gozes Y, Flashner Y, Sery T, Cohen S, Ben-Aziz R, Seidman S, Shafferman A, Soreq H (1991b) Recombinant human acetylcholinesterase is secreted from transiently transfected 293 cells as a soluble globular enzyme, Cell. Mol. Neurobiol. 11, 143-156.

Velan B, Kronman C, Leitner M, Grosfeld H, Flashner Y, Marcus D, Lazar A, Kerem A, Bar-Nun S, Cohen S, Shafferman A (1992) Molecular organization of recombinant human acetylcholinesterase; in Multidisciplinary Approaches to Cholinesterase Function, Shafferman A, Velan B, eds., Plenum Press, New York, pp. 39-47.

Viegas-Pequignot, E, Dutrillaux B, Magdelenat H, Coppey-Moisan M (1989) Mapping of single-copy DNA sequences on human chromosomes by in situ hybridization with biotinylated probes: enhancement of detection sensitivity by intensified-fluorescence digital-imaging microscopy, Proc. Natl. Acad. Sci. USA 86, 582-86.

Virbasius JV, Scarpulla RC (1988) Structure and expression of rodent genes encoding the testis-specific cytochrome, J. Biol. Chem. 263, 6791-6796.

Vize PD, Melton DA, Hemmati-Brivanlou A, Harland RM (1991) Assays for gene function in developing *Xenopus* embryos, Methods Cell Biol. 36, 367-387.

Weise C, Kreienkamp HJ, Raba R, Pedak A, Aaviksaar A, Hucho F (1990) Anionic subsites of the acetylcholinesterase from *Torpedo california*: affinity labelling with the cationic reagent N,N-dimethyl-2-phenyl-aziridinium, EMBO J., 9, 3885-3888.

Whittaker M. (1986) Cholinesterase, Karger, Basel.

Wickstrom EL, Bacon TA, Gonzalez A, Freeman DL, Lyman GH, Wickstrom E (1988) Human promyelocytic leukemia HL-60 cell proliferation and c-myc protein expression are inhibited by an antisense pentadecadeoxynucleotide targeted against c-myc mRNA, Proc. Natl. Acad. Sci. USA 85, 1028-1032.

Wilkinson DG, Bailes JA, McMahon AP (1987) Expression of the proto-oncogene int-1 is restricted to specific neural cells in the developing mouse embryo, Cell 50, 79-88.

Williams KR, Spicer EK, LoPresti MB, Guggenheimer RA, Chase JW (1983) Limited proteolysis studies on Escherichia coli single-stranded DNA binding protein, J. Biol. Chem. 258, 3346-3355.

Williams T, Tjian R (1991) Analysis of the DNA binding and activation properties of the human transription factor AP-2, Gene Develop. 5, 670-682.

Windle B, Draper BW, Yin YX, O'Gorman S, Wahl GM (1991) A central role for chromosome breakage in gene amplification, deletion formation, and amplicon integration, Genes Develop. 5, 160-174.

Winkler FK, D'Arcy A, Hunziker W (1990) Structure of human pancreatic lipase, Nature 343, 771-774.

Wokke JHJ, Jennekens FGI, Molenaar PC, Van den Oord CJM, Oen BS, Busch HFM (1989) Congenital paucity of secondary synaptic clefts (CPSC) syndrome in 2 adult sibs, Neurology 38, 648-654.

Woolf TM, Jennings CGB, Rebagliati M, Melton DA (1990) The stability, toxicity and effectiveness of unmodified and phosphorothioate antisense oligodeoxynucleotides in *Xenopus* oocytes and embryos, Nucl. Acids Res. 18, 1763-1769.

Zakut H, Matzkel A, Schejter E, Avni A, Soreq H (1985) Polymorphism of acetylcholinesterase in discrete regions of the developing human fetal brain, J. Neurochem. 45, 382-389.

Zakut H, Even L, Birkenfeld S, Malinger G, Zisling R, Soreq H (1988) Modified properties of serum cholinesterases in primary carcinomas, Cancer 61, 727-737.

Zakut H, Zamir R, Sindel L, Soreq H (1989) Gene mapping on chorionic villi chromosomes by hybridization in situ: localization of cholinesterase cDNA binding sites to chromosomes 3q21, 3q26-ter and 16q21, Hum. Reprod. 4, 941-946.

Zakut H, Ehrlich G, Ayalon A, Prody CA, Malinger G, Seidman S, Ginzberg D, Kehlenbach R, Soreq H (1990) Acetylcholinesterase and butyrylcholinesterase genes coamplify in primary ovarian carcinomas, J. Clin. Invest. 86, 900-908.

Zakut H, Leiman-Hurwitz J, Zamir R, Sindell L, Ginzberg D, Soreq H (1991) Chorionic villus cDNA library displays expression of butyrylcholinesterase: putative genetic disposition for ecological danger, Prenat. Diagn. 11:597-607

Zakut H, Lapidot-Lifson Y, Beeri R, Ballin A, Soreq H (1992) In vivo gene amplification in non-cancerous cells: cholinesterase genes and oncogens amplify in thrombocytopenia associated with lupus erythematosus, Mut. Res. 276, 275-284.

Zelinski T, White L, Coghlan G, Philips S (1991) Assignment of the Yt blood group locus to chromosome 7q, Genomics 11:165-167

Zhang XJ, Baase WA, Matthews BW (1991) Toward a simplification of the protein binding problem: a stabilizing polyalanine alpha-helix engineered T4 lysozyme, Biochemistry 30, 2012-2017

VIII. PERSONNEL RECEIVING PAY FROM GRANT SUPPORT

Rachel Beeri, M.Sc.
Revital Ben Aziz-Aloya, M.Sc.
Shimshon Broido, M.Sc.
Joshua Bruder
Gal Ehrlich
Dalia Ginzberg, Ph.D.
David Glick, Ph.D.
Averell Gnatt, Ph.D.
Tal Harel
Rachel Karpel, Ph.D.
Chen Keysar
Efrat Lev-Lehman, M.Sc.
Yael Loewenstein
Louis Neville, Ph.D.
Haim Ozeri
Rachael Ram
Tamar Schneider
Mikael Schwarz, Ph.D.
Tamar Schweki
Yosefa Sefton
Marianne Segal
Shlomo Seidman, M.Sc.
Michael Shapira
Hermona Soreq, Ph.D.
Meira Sternfeld
Dalia Tamir
Rina Timberg
Avraham Vilnitz
Avraham Yarom
Gil Yaron

IX. GRADUATE DEGREES RESULTING FROM GRANT SUPPORT

Doctor of Philosophy
Averell Gnatt, 1990
Yaron Lapidot-Lifson, 1992

Doctor of Philosophy, about to be granted
Revital Ben-Aziz Aloya, 1993
Gal Ehrlich, 1993

Master of Science
Efrat Lev-Lehman, 1990
Rachael Beeri, 1990

X. PUBLICATIONS RESULTING FROM GRANT SUPPORT

peer-reviewed publications

1 Ben Aziz-Aloya R, Seidman S, Timberg R, Sternfeld M, Zakut H, Soreq H (1993) Expression of a human acetylcholinesterase promoter-reporter construct in developing neuromuscular junctions of *Xenopus* embryos. Proc. Natl. Acad. Sci. USA 90, 2471-2475.

2. Ben-Aziz R, Soreq H (1990) Improving poor *in vitro* transcription from GC rich genes. Nucl. Acid Res. 18, 3418.

3. Ehrlich G, Viegas-Pequignot E, Ginzberg D, Sindel L, Soreq H, Zakut H (1992) Mapping the human acetylcholinesterase gene to chromosome 7q22 by fluorescent *in situ* hybridization coupled with selective PCR amplification from a somatic hybrid cell panel and chromosome-sorted DNA libraries, Genomics 13, 1192-1197.

4. Gnatt A, Ginzberg D, Lieman-Hurwitz J, Zakut H, Soreq H (1991) Human acetylcholinesterase and butyrylcholinesterase are encoded by two distinct genes. Cell. Mol. Neurobiol. 11, 91-104.

5. Gnatt A, Loewenstein Y, Yaron A, Schwarz M, Soreq H (1994) Site-directed mutagenesis of active site residues reveals plasticity of human butyrylcholinesterase in substrate and inhibitor interactions. J. Neurochem. 62 (in press)

6. Karpel R, Ben Aziz-Aloya R, Sternfeld M, Ehrlich G, Ginzberg D, Tarroni P, Clementi F, Zakut H, Soreq H (1994) Expression of three alternative acetycholinesterase messenger RNAs in human tumor cell lines of different tissue origins, Exptl. Cell Res. 210 (in press).

7. Lapidot-Lifson Y, Patinkin D, Prody CA, Ehrlich G, Seidman S, Ben-Aziz R, Benseler F, Zakut H, Soreq H (1992) Cloning and antisense oligodeoxynucleotide inhibition of a human homolog of cdc2 required in hematopoiesis. Proc. Natl. Acad. Sci. USA 89, 579-583.

8. Lev-Lehman E, Ginzberg D, Hornreich G, Ehrlich G, Meshorer A, Eckstein F, Soreq H, Zakut H (1993) Antisense inhibition of acetylcholinesterase gene expression causes transient hematopoietic alterations *in vivo*, Gene Therapy 1,11.

9. Loewenstein Y, Gnatt A, Neville LF, Soreq H (1993) Chimeric human cholinesterase: identification of interaction sites responsible for recognition of acetyl- or butyrylcholinesterase-specific ligands. J. Mol. Biol. 234, 289-296.

10. Neville LF, Gnatt A, Loewenstein Y, Seidman S, Ehrlich G, Soreq H (1992) Intramolecular relationships in cholinesterases revealed by oocyte expression of site-directed and natural variants of human BCHE. EMBO J. 11, 1641-1649.

11. Neville LF, Gnatt A, Loewenstein Y, Soreq H (1990) Aspartate-70 to glycine substitution confers resistance to naturally occurring and synthetic anionic-site ligands on in-ovo produced human butyrylcholinesterase. J. Neurosci. Res. 27, 452-460.

12. Neville, LF, Gnatt A, Padan R, Seidman S, Soreq H (1990) Anionic site interactions in human butyrylcholinesterase disrupted by two single point mutations. J. Biol. Chem. 265, 20735-20739.

13. Seidman S, Ben Aziz-Aloya R, Timberg R, Loewenstein Y, Velan B, Shafferman A, Liao J, Norgaard-Pedersen B, Brodbeck U, Soreq H (1994) Overexpressed monomeric human acetylcholinesterase induces subtle ultrastructural modifications in developing neuromuscular junctions of *Xenopus leavis* embryos, J. Neurochem. 62 (in press).

14. Soreq H, Ben-Aziz R, Prody CA, Seidman S, Gnatt A, Neville L, Lieman-Hurwitz J, Lev-Lehman E, Ginzberg D, Lapidot-Lifson Y, Zakut H (1990) Molecular cloning and construction of the coding region for human acetylcholinesterase reveals a G+C rich attenuating structure. Proc. Natl. Acad. Sci. USA 87, 9688-9692.

15. Soreq H, Gnatt A, Loewenstein Y, Neville LF (1992) Excavations into the active site-gorge of cholinesterases. Trends Biochem. Sci. 17, 353-358.

16. Velan B, Kronman C, Grosfeld H, Leitner M, Gozes Y, Flashner Y, Sery T, Cohen S, Ben-Aziz R, Seidman S, Shafferman A, Soreq H (1991) Recombinant human acetylcholinesterase is secreted from transiently transfected 293 cells as a soluble globular enzyme. Cell. Mol. Neurobiol. 11, 143-156.

17. Zakut H, Ehrlich G, Ayalon A, Prody CA, Malinger G, Seidman S, Ginzberg D, Kehlenbach R, Soreq H (1990) Acetylcholinesterase and butyrylcholinesterase genes coamplify in primary ovarian carcinomas. J. Clin. Invest. 86, 900-908.

18. Zakut H, Lapidot-Lifson Y, Beeri R, Ballin A, Soreq H (1992) *In vivo* gene amplification in non-cancerous cells: cholinesterase genes and oncogenes amplify in thrombocytopenia associated with lupus erythematosus, Mutat. Res. 276, 275-284.

submitted for publication

19. Ehrlich G, Ginzberg D, Loewenstein Y, Glick D, Kerem B, Ben-Ari S, Zakut H, Soreq H, Population diversity and distinct haplotype ferqeuncies associated with ACHE and BCHE genes of Israeli Jews from trans-Caucasian Georgia and from Europe

non-reviewed publications

20. Ben-Aziz R, Gnatt A, Prody C, Lev-Lehman E, Neville L, Seidman S, Ginzberg D, Soreq H, Lapidot-Lifson Y, Zakut H (1991) Differential codon usage and distinct surface probabilities in human acetylcholinesterase and butyrylcholinesterase. In: Cholinesterases: Structure, Function, Mechanism, Genetics, and Cell Biology, Massoulies J, Bacou F, Barnard E, Chattonet A, Doctor BP, Quinn DM, eds., ACS Books, Washington, pp. 172-178.

21. Soreq H, Neville LF, Gnatt A, Ben-Aziz R, Lapidot-Lifson Y, Ehrlich G, Seidman S, Lev-Lehman E, Beeri R, Ginzberg D, Zakut H (1991) Structure-function relationships, in-vivo mutageneity and gene amplification in human cholinesterases, targets for organophosphorous poisons; in Biotechnology: Binding Research and Applications, Kamely D, Chakrabarty Am, Kornguth SE, eds., Kluwer Academic Publishers, Boston.

22. Soreq H, Seidman S (1992) *Xenopus* oocyte microinjection: from gene to protein, Methods Enzymol. 207, 225-265.

23. Soreq H, Zakut H (1990) Cholinesterases genes: Multileveled regulation, Karger, Basel.

24. Soreq H, Zakut H (1993) Human cholinesterases and anticholinesterases, Academic Press, San Diego.